DEVELOPMENT OF INTELLIGENT SYSTEMS FOR EVALUATING VOLTAGE PROFILE AND COLLAPSE UNDER CONTINGENCY OPERATION

by

MAHMOUD M. MOHAMMED

M. S., Zagazig University, Egypt, 2004

AN ABSTRACT OF A DISSERTATION

submitted in partial fulfillment of the requirements for the degree

DOCTOR OF PHILOSOPHY

DEPARTMENT OF ELECTRICAL AND COMPUTER ENGINEERING
COLLEGE OF ENGINEERING

KANSAS STATE UNIVERSITY
Manhattan, Kansas

2011

Abstract

Monitoring and control of modern power systems have become very complex tasks due to the interconnection of power grids. These large-scale power grids confront system operators with a huge set of system inputs and control parameters. This work develops and compares intelligent systems-based algorithms which may be considered by power system operators or planners to help manage, process, and evaluate large amounts of data due to varying conditions within the system. The methods can be used to provide assistance in making operational control and planning decisions for the system in a timely manner. The effectiveness of the proposed algorithms is tested and validated on four different power systems.

First, Artificial Neural Network (ANN) models are developed and compared for two different voltage collapse indices and utilizing two different-sized sets of inputs. The ANNs monitor and evaluate the voltage profile of a system and generate intelligent conclusions regarding the status of the system from a voltage stability perspective. A feature reduction technique, based on the analysis of generated data, is used to decrease the number of inputs fed to the ANN, decreasing the number of physical quantities that need to be measured.

The major contribution of this work is the development of four different algorithms to control the VAR resources in a system. Four different objectives were also considered in this part of the work, namely: minimization of the number of control changes needed, minimization of the system power losses, minimization of the system's voltage deviations, and consideration of the computational time required. Each of the algorithms is iterative in nature and is designed to take advantage of a method of decoupling the load flow Jacobian matrix to decrease the time needed per iteration. The methods use sensitivity information derived from the load flow Jacobian and augmented with equations relating the desired control and dependent variables. The heuristic-sensitivity based method is compared to two GA-based methods using two different objective functions. In addition, a FL algorithm is added to the heuristic-sensitivity algorithm and compared to a PS-based algorithm.

The last part of this dissertation presents the use of one of the GA-based algorithms to identify the size of shunt capacitor necessary to enhance the voltage profile of a system. A method is presented for utilizing contingency cases with this algorithm to determine required capacitor size.

DEVELOPMENT OF INTELLIGENT SYSTEMS FOR EVALUATING VOLTAGE PROFILE AND COLLAPSE UNDER CONTINGENCY OPERATION

by

MAHMOUD M. MOHAMMED

M. S., Zagazig University, Egypt, 2004

A DISSERTATION

submitted in partial fulfillment of the requirements for the degree

DOCTOR OF PHILOSOPHY

DEPARTMENT OF ELECTRICAL AND COMPUTER ENGINEERING
COLLEGE OF ENGINEERING

KANSAS STATE UNIVERSITY
Manhattan, Kansas

2011

Approved by:

Major Professor
Shelli Starrett

Abstract

Monitoring and control of modern power systems have become very complex tasks due to the interconnection of power grids. These large-scale power grids confront system operators with a huge set of system inputs and control parameters. This work develops and compares intelligent systems-based algorithms which may be considered by power system operators or planners to help manage, process, and evaluate large amounts of data due to varying conditions within the system. The methods can be used to provide assistance in making operational control and planning decisions for the system in a timely manner. The effectiveness of the proposed algorithms is tested and validated on four different power systems.

First, Artificial Neural Network (ANN) models are developed and compared for two different voltage collapse indices and utilizing two different-sized sets of inputs. The ANNs monitor and evaluate the voltage profile of a system and generate intelligent conclusions regarding the status of the system from a voltage stability perspective. A feature reduction technique, based on the analysis of generated data, is used to decrease the number of inputs fed to the ANN, decreasing the number of physical quantities that need to be measured.

The major contribution of this work is the development of four different algorithms to control the VAR resources in a system. Four different objectives were also considered in this part of the work, namely: minimization of the number of control changes needed, minimization of the system power losses, minimization of the system's voltage deviations, and consideration of the computational time required. Each of the algorithms is iterative in nature and is designed to take advantage of a method of decoupling the load flow Jacobian matrix to decrease the time needed per iteration. The methods use sensitivity information derived from the load flow Jacobian and augmented with equations relating the desired control and dependent variables. The heuristic-sensitivity based method is compared to two GA-based methods using two different objective functions. In addition, a FL algorithm is added to the heuristic-sensitivity algorithm and compared to a PS-based algorithm.

The last part of this dissertation presents the use of one of the GA-based algorithms to identify the size of shunt capacitor necessary to enhance the voltage profile of a system. A method is presented for utilizing contingency cases with this algorithm to determine required capacitor size.

Table of Contents

List of Figures

List of Tables

Acknowledgements

After the completion of this work, I would like to thank God for helping me finishing this humble work.

I would like to express my sincere gratitude to Professor Shelli Starrett, my major supervisor, for guiding me to do the research on the right track. I also deeply thank her for providing me with the necessary software at all times. I am very grateful to her, for her valuable suggestions and especially, for her great effort in reading the manuscript and giving me a valuable feedbacks.

I would like to thank Professor Medhat M. Morcos for his continuous help and support during the completion of my research. Also I would like to thank all my supervisory committee members, Dr. Shelli Starrett, Dr. Medhat M. Morcos, Dr. Ruth Douglas Miller, Dr. Hayder Rasheed, and Dr. Brett Esry, for being flexible in scheduling the final exam.

I would also like to express my gratitude to the Department of Electrical and Computer Engineering at Kansas State University for providing a friendly and healthy working environment.

Last but not least, I would like to express my ultimate gratitude to my parents, for their endless prayers and their outstanding support. Heartfelt thanks go to my wife, and our kids Moustafa, Arwa, Youssif, and Jena. Thanks to my wife for her continuous encouragement and support

Dedication

Dedicated to:

My parents, my wife, and our kids, Moustafa, Arwa, Youssif, and Jena

Chapter 1 Introduction

1.1 Overview

Deregulation has forced electric utilities to make better use of the available transmission facilities of their power systems. This has resulted in increased power transfers, reduced transmission margins and, at the same time, diminished voltage security margins [1].

Today, power systems are often interconnected, forming very large power pools. Operation of such power systems becomes increasingly complicated due to rapid growth of loads without a corresponding increase in transmission capability. The real and reactive power control generally plays a major role in Energy Management Systems (EMS). These systems are required to maintain operation requirements and quality of supply (constant voltage magnitude, constant frequency and low cost). Efficient on-line dispatch for real and reactive power depends on the proper off-line calculations for the active and reactive power scheduling. Any improper and incomplete off-line analysis may result in a maintenance problem, complicated on-line operation, or even a blackout [2]. Unlike the active power control problem, the reactive power control problem is generally difficult because of the large scale and non-linear characteristics in power systems. During the past two decades there has been growing concern in power systems about reactive power operation and planning [2]. The VAR planning problem is basically a nonlinear optimization problem. Reactive power control is achieved through complicated coordination between switchable shunt compensators (capacitors or inductors), transformer taps and generator voltage setting. Reactive power management and control is a significant factor to support the system security and reliability. In a deregulated electricity market, active power has generally become a commodity, and reactive power has been treated as an ancillary service. Many of the deregulated electricity markets have established financial compensation mechanisms for reactive power services [3]. The voltage stability margin is a key concept in power system planning and operation. The continuous development of interconnected power systems, and consumer's power demand as well as economical and environmental constraints cause this problem to be very complex. Voltage collapse typically occurs on power systems which are heavily stressed [4]. In day-to-day operation of power systems, reactive power dispatch is the control of all controllable reactive power sources in the

system in a coordinated manner to improve the system voltage profile and to minimize a suitable objective function.

1.2 Objective of the Thesis

The major objective of the research done in this thesis is to develop intelligent tools to aid in the evaluation and control of modern power systems characterized by complexity due to the interconnection of power grids.

The first part of this thesis applied ANN as an intelligent tool to monitor and evaluate the voltage profile of the power system and generate intelligent decisions regarding the system status from voltage stability prospective. The most important goal of such intelligent tools is to help the system operators prepare ahead of time for imminent voltage instability and voltage collapse. Based on the status of the power system, the system operator is required to make the correct decision in order to get the system back to an acceptable operating state.

The second part of this thesis concerns with the development of algorithms in order to control the VAR resources in a power system under abnormal and/or contingency operation to maintain the voltage at all buses within acceptable limits. Four different objectives were considered in this part, namely minimization of the number of control actions needed, minimization of active power losses, minimization of the sum of voltage deviations, and consideration of the computational time required. Each of the algorithms is iterative in nature and is designed to take advantage of a method of decoupling the load flow Jacobian matrix to decrease the time needed per iteration. The methods use sensitivity information derived from the load flow Jacobian and augmented with equations relating the desired control and dependent variables.

The third and last part of this thesis applied a GA-based optimization technique to identify the optimal size of a shunt capacitor required to keep the system stable under contingency operation.

1.3 Outline of the Dissertation

The dissertation is composed of nine chapters, the organization of these chapters as follows.

Chapter 2 is a survey of literature review related to voltage stability, voltage collapse indices and voltage control under abnormal and/or contingency operation.

Chapter 3 introduces Genetic Algorithm and Pattern Search optimization techniques that are employed to solve the voltage control problems in Chapters 6, 7, and 8.

Chapter 4 provides a contingency analysis of four different power systems to identify the critical lines and buses in these systems. All (N-1) contingencies are ranked according to their severity. This information is to be used later in Chapters 6, 7, and 8.

Chapter 5 presents the application of an Artificial Neural Network (ANN) for voltage collapse prediction in a power system to guide the operator in an Energy Control Center (ECC) to take the necessary control action. In this chapter a feature reduction technique based on the analysis of the generated data is used to decrease the number of inputs fed to ANN and so, decrease the number of physical quantities need to be measured. A comparison between the performances of two different ANN-based voltage collapse indices is investigated. Those voltage collapse indices are minimum singular value decomposition (MSV) and voltage stability index *L*.

Chapter 6 presents three different algorithms for solving the reactive power control problem. The first method has the objective of minimizing the number of control actions, i.e., the number of controllers that may be changed in order to achieve a satisfactory voltage profile. The second and third methods are based on the reactive power optimization using Genetic Algorithms (GA). The objective function for the second algorithm is minimizing the system power losses (P_L), while the objective function for the third algorithm is minimizing the summation of the squares of the voltage magnitude deviations at the load buses (V_d). All three algorithms employ linearized sensitivity relationships of the power system to establish the objective function and the system performance sensitivities relating dependent and control variables. The goal of each is to satisfy constraints for both control and dependent variables.

Chapter 7 presents the use of Fuzzy Logic (FL) for voltage and reactive power control. This method of control makes use of the sensitivities relating the dependent and control variables in order to minimize the number of the VAR resource changes in the system. The objective is to provide a solution which does both voltage improvement, and if possible loss reduction, for any practical power system. The proposed fuzzy model uses two inputs, the voltage deviation level of load bus and the controlling ability of the controlling device. The output is the change in the

controlling device. A sensitivity coefficient matrix relating the control variables and the dependent variables is used to calculate the control ability of every controller for each dependent variable. Also an optimal VAR control method suitable for online application, the direct search or pattern search (PS) method, is introduced in this chapter.

Chapter 8 presents the use of GA-based optimal reactive power control, to identify the optimal size of a shunt capacitor necessary to improve the overall voltage profile of a power system under contingency operation. The location of the shunt capacitor is defined based on the critical bus or buses in the system, which can be identified as shown in Chapter 4.

Chapter 9 provides a set of conclusions related to the work done in the dissertation and suggestions of possible future work that can be carried out.

Additionally, the dissertation includes four different appendices, each one giving the complete data for one of the tested power systems.

Chapter 2 Literature Review and Background

2.1 Introduction

In recent years, power systems, worldwide have grown markedly in size and complexity. The interconnections between individual utilities have increased, and many power elements have been required to operate at their maximum limits for long periods of time. Deregulation in the power industry forced electric utilities to make better use of the available transmission facilities of their power systems. This resulted in increased power transfer, reduced transmission margins, and diminished voltage stability margin. In addition, the most economic sites for generation plants are often remote from load centers and so, the power has to be transmitted over long distances. Due to these complexities of modern power systems, they are facing many challenges in their operation and control. Recently power system voltage instability has become one of the power utility problems gaining a great attention due to its direct or indirect impact on recent blackout incidents

Power system planning and operation has to deal with a significant degree of uncertainty about time and location [5]. With the increased loading of existing power transmission systems, the problem of voltage stability has become a major concern in power system planning and operation. In recent years reactive power optimization has gained more importance. Planning of reactive power compensation in power systems has to be comprehensive to maintain all voltages within acceptable limits during both light and heavy load conditions. During light load the system may need a decrease in the voltage by adding a reactor, on the other hand, during heavy load conditions, the system might need capacitive reactive power support.

The transmission system is one of the major components of electric power industry. Conventionally power system planning, including generation expansion planning and transmission expansion planning, is performed solely by the system operator, and is therefore known as centralized planning [6]. The worldwide trend for deregulation of electric generation and transmission industries has led to dramatic changes in system operation and planning procedures [7]. Electric power planning is now often classified into transmission planning, and generation planning. Transmission networks play a critical role in providing access to all

participants in a competitive market for supply and delivery of electric power. A more robust transmission system would bring in economic competition from far away and eliminate market pockets in which dominant generators can exercise market power due to the transmission restraints [8]. The main objective of an electric power system and its operation is to maintain the system security while respecting certain constraints imposed on the system [9].

2.2 Power System Terminology

2.2.1 Power System Adequacy

Adequacy: is the ability of a power system to supply consumers' electric power and energy requirements at all times. (NERC)

2.2.2 Power System Reliability

Reliability: is the degree to which the performance of an electrical system results in power being delivered to consumers within accepted standards and desired amounts. (NERC)

2.2.3 Power System Security

Power system security: is the ability of a power system to withstand sudden disturbances [10].

2.2.4 Smart Grid

Smart grid: is a new aspect of the power grid which highly integrates advanced information techniques, communication techniques, computer science mathematical methods and power electronics. It has many advantages, such as improving energy efficiency, reducing the impact to the environment, enhancing the security and reliability of power supply, and reducing the power losses of the electric transmission network [11]. The objectives of smart grid are:

- Fully satisfy customer requirements for electrical power
- Optimize resource allocation
- Ensure the security, reliability and economic of power supply
- Satisfy environmental protection constraints
- guarantee power quality, and
- adapt to power market development

2.2.5 Blackout

A blackout: is a condition where a major portion or all of an electrical network is de-energized as a result of major disturbances [12].

2.2.6 Power System Stability

Power System Stability: is the ability of an electric power system, for a given initial operating condition, to regain a state of operating equilibrium after being subjected to a physical disturbance, with system variables bounded so that system integrity is preserved [13]. According to the time frames of dynamics, power system stability can be divided into: steady-state, dynamic or small signal, transient or rotor angle, and long-term stability.

2.2.7 Steady State Stability

The stability of an electric power system is a property of the system motion around an equilibrium set, i.e., the initial operating condition [13]. Steady-state analysis consists of assessing the existence of the steady-state operating points of a power system.

2.2.8 Dynamic Stability

Dynamic stability or small signal stability studies consider when a system is subjected to small aperiodic disturbances [13]. The time frame of dynamics in small signal stability is up to one second. Linear system models are used in this analysis.

2.2.9 Transient Stability

Transient stability studies consider conditions under which a system is subjected to large aperiodic disturbances [13]. The time frame of transient stability is up to ten seconds and the nonlinearities of the system are included. In the study of power systems, transient stability is normally considered a part of angle stability. Angle stability is concerned with the ability of interconnected synchronous machines in a power system to remain in synchronism after being subjected to a disturbance from a given initial operating condition [13].

2.2.10 Voltage stability

Voltage stability: is the ability of a power system to maintain acceptable voltage levels at all buses under normal operating conditions and after the occurrence of disturbances [14]. Voltage stability analysis can also be divided into steady state, small signal, and transient studies.

2.2.11 Voltage Collapse

Voltage collapse: is the process by which the sequence of events accompanying voltage instability leads to a blackout or abnormally low voltages in a significant part of the power system [15]

2.2.12 Loading Margin

Loading margin: is the distance in MW between the current operating point and the maximum loading point (nose point) as shown in Figure (2.1).

2.2.13 P-V curve

P-V curve: is a relation between the active power and the voltage magnitude at a PV bus as shown in Figure (2.1).

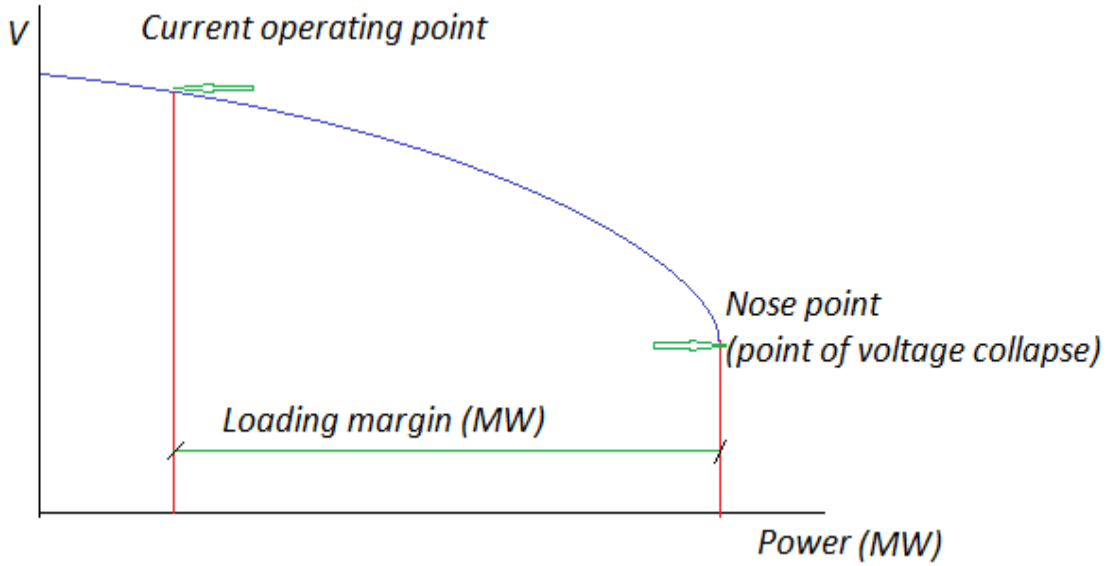

Figure 2.1: PV curve

2.3 Operating States of Power System

Power system operating conditions can be classified into five different states [13]:

1. normal
2. alert
3. emergency
4. extreme emergency, and
5. restorative

Figure (2.2) describes these states and the ways in which transition can occur from one state to another. The operation of a power system is in a normal state most of the time, this normal state is characterized by:

- Voltage and frequency of the system are within normal range
- No equipment is overloaded
- The system able to withstand any single contingency without limit violation

The alert state is similar to the normal state except that the above conditions cannot be met in the case of a disturbance. The system transits into the alert state if the security level falls below a certain limit or if the possibility of a disturbance increases. A control action, such as: generation rescheduling, increase of reserve, voltage control, etc., should be used to restore the system back to a normal state. If this does not succeed, the system stays in the alert state. The second part of this dissertation presents four different algorithms to control the controllers of a power system, namely: generator terminal voltages, tap setting of transformers, and switchable shunt capacitors . These algorithms aim to get the system back to a normal state before transiting to the emergency state.

The system transits into the emergency state if a disturbance occurs when the system is in the alert state. Many system variables are out of normal range or equipment loading exceeds short-term rating in this state. Emergency control actions more powerful than control actions related to the alert state are designed to restore the system to an alert state.

The extreme emergency state is a result of the occurrence of an extreme disturbance or action of incorrect or ineffective emergency control actions. The system is in a state where

cascading outages and shutdown of a major part of the power system might happen. The system is in an unstable or close to unstable state. The control actions needed in this state must be powerful. Usually load shedding of most unimportant loads and separation of the system into small independent parts are required in order to transit the system into a restorative state. The aim of the control actions is to save as much of the system as soon as possible from a wide area blackout. If these actions do not succeed, the result is total blackout of the system.

The restorative state is a transition state between the extreme emergency and normal or alert states. It is important to restore the power system as fast and securely as possible in order to limit the social and economic consequences for the population and economy.

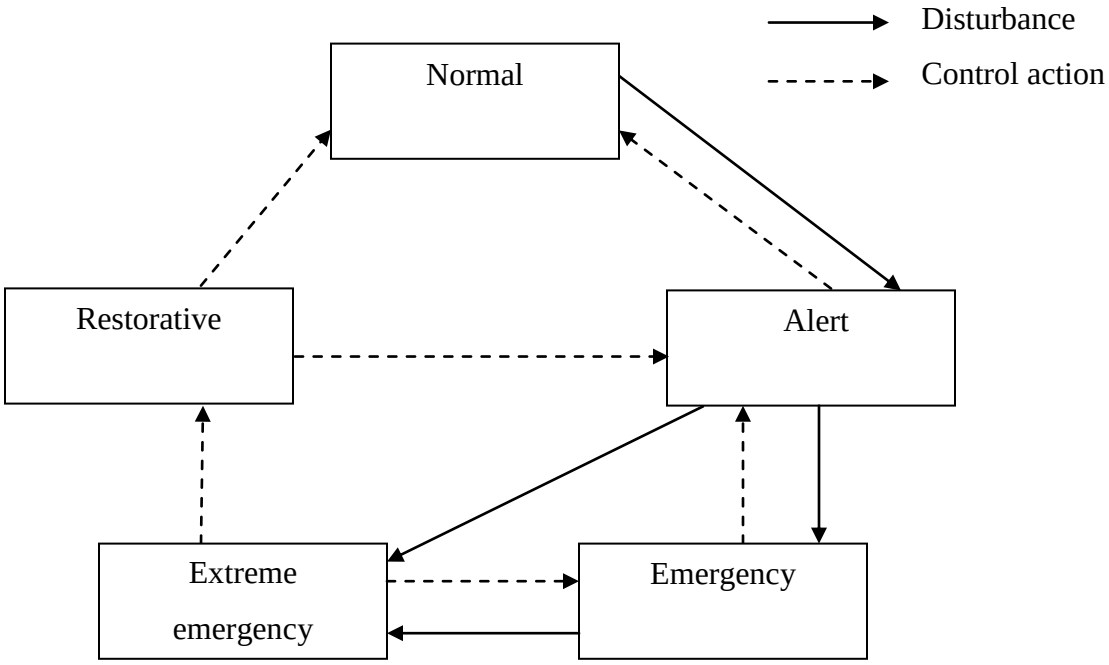

Figure 2.2: Power system operating states [13]

2.4 Contingency Analysis

Contingency analysis analyzes the power system response to an outage of a component or multiple components. An outage of a single device per contingency is commonly referred to as (N-1) contingency analysis where the system consists of N devices and analysis is performed

with the loss of one device. Contingencies consisting of multiple outages can be handled in a similar fashion. Contingency analysis is historically broken up into two distinct types:

1. dynamic contingency analysis, and
2. steady-state contingency analysis.

Contingency selection, or screening, is a technique which attempts to identify contingencies that are most threatening to system operation and only conduct analysis on this limited set of cases. Inherently this is a subset of all system contingencies. If this subset can be identified with a degree of accuracy, then only a small number of actual contingencies are required to be computed for security purposes. This results in a substantial savings of computation.

Ranking all possible contingencies based on their impact on the system voltage profile will help the operators in choosing the most suitable remedial actions before the system moves toward voltage collapse [16-18]. Contingencies such as unexpected line outages often contribute to voltage collapse blackouts. These contingencies generally reduce or even eliminate the voltage stability margin [19]. Since the contingency causes the nose point to move to a lower loading, the loading margin is reduced. If the loading margin is thought of as a smooth function of the line admittance, then the sensitivity of the loading margin with respect to changes in the line admittance can be calculated at the nominal nose point [20]**.**

Wei Gu et al. [21] proposed a contingency based approach for improving, through practical assumptions, the stability of power systems subjected to large disturbances. The proposed method is composed of two steps, solved iteratively. The first step solves an optimal bifurcation control problem that guarantees the small-signal stability of the equilibrium point. The proposed optimal bifurcation control addresses saddle-node and Hopf bifurcations. The second step is an (N-1) contingency analysis computed through time domain simulations. The second step guarantees the large-disturbance stability of the equilibrium point.

Ronnapa Paosateanpun et al [22] analyzed the P-Q curve as a rotated parabola. In the region inside the line P-Q curve, a power system can operate normally, but in the outside the system operation is impossible. The line voltage collapse coefficient is determined by using the concept of the line P-Q curve. This coefficient can be used to find weak lines in the power

system. It relates to the minimal distance of the P-Q boundary curve, the probability of safe load transmission and the probability of positive bus influence on load transmission. The probability of positive bus influence on load transmission is given from the exact post-contingency analysis with a P-V curve. The lower the values of line voltage collapse coefficient, the weaker the transmission line.

Christie and Talukdar [23] proposed the integration of a conventional algorithmic approach for contingency evaluation with expert systems for contingency selection and results interpretation. But due to an inadequate knowledge base, execution was too slow to fit into on-line environment. A rule-based system was presented in [24**]** for contingency screening designed partly on human operator expertise and partly from simulation model findings. The feasibility of the approach is demonstrated on moderate size system by monitoring 17 lines.

Niebur and Germond [25] used Kohonen neural network classifier to assess the static security of the system, where an input vector, corresponding to an operating state was mapped on a two-dimensional grid consisting of 49 nodes. Although its training is unsupervised and hence fast compared to back propagation network, the number of inputs to be handled at system level becomes too large for moderate size systems.

Sobajic and Paon [26] proposed the use of neural networks for dynamic security assessment of large-scale systems. The system is split into small subsystems and each one is handled with separate ANN. The basic principal here is to classify the system by exploiting pattern recognition capability of ANN.

Sidhu and Cui [27] proposed the use of multilayer perceptron model for contingency screening using fast Fourier transform for feature selection. An approach using query-based learning for the neural network to solve the static security problem is reported in [28]. To further enhance the performance of the neural network, a genetic algorithm is used to initialize its connection weights to near optimal values.

Lo and Ping [29] presented the use of a counter propagation network to identify the secure and insecure regions of operation with a feature selector in supervised mode. Since an operating point may be secure to one contingency but at the same time may be insecure for other contingencies, feature selection becomes more complex and vulnerable to misclassification under supervised mode.

In [30], a modified counter propagation network (CPN) with neuro-fuzzy (NF) feature selector is used for real power contingency ranking of the transmission system. The CPN is trained to estimate the severity of a series of contingencies for given pre-contingencies line-flows. But for larger size system it becomes rather difficult to cope with the increased size of input pattern and network as well. This adversely affected the performance of the network and computational overhead. The proposed NF feature selector prunes the size of input pattern by exploring the individual power of features to characterize/discriminate different clusters. The reduced set of discriminating inputs not only ensures saving in training time but also improves estimation accuracy and execution time. These are the deciding parameters in evaluating the performance of a particular contingency ranking technique

A sensitivity analysis framework for voltage contingency ranking has been presented [31]. The proposed sensitivity analysis is a combination of linear sensitivities and eigenvalue analysis. The sensitivity analysis framework can determine the voltage stability status of the power system due to the occurrence of each contingency. Moreover, stability margin or instability depth of the post-contingency state is determined in the framework. In other words, a severity index is obtained for each voltage contingency and so the contingencies can be ranked. The proposed method can also evaluate islanding contingencies as well as the non-islanding ones. Moreover, the method can consider the generator contingencies in addition to the branch contingencies in a unique framework**.**

Musirin and Abudel Rahman [32] presented a voltage stability index called fast voltage stability index (FVSI). The authors used the values of the line indices to indicate the voltage stability condition and to rank the line outage contingency in the system. The information from the contingency ranking denotes the severity of the voltage stability condition in the power system due to line outage. Several indices are proposed for contingency analysis suitable for online application [33-35].

2.5 Voltage Stability Monitoring and control

The voltage instability process is characterized by a monotonic voltage drop, which is slow at first and becomes abrupt after some time. Voltage collapse occurs when the system is unable to meet reactive power demand. Voltage collapse is also characterized by the loss of the ability to control voltage levels in a power system. Voltage instability and even voltage collapse

situations have become more likely to occur, imposing important limitations to power systems operation [36].

Voltage control system is an important segment of the hierarchical voltage control in power systems. Although voltage control schemes have both continuous voltage regulators, such as generators and static VAR compensators, and discrete voltage regulators, such as ULTC, shunt capacitors, and shunt reactors, traditional voltage control only considers continuous voltage regulators [37].

Voltage collapse in general can be caused by one of the following types of system disturbances: load disturbances, contingencies, or a combination of them. The knowledge of the reactive power reserve condition is very important in the operation of a transmission network and will strongly affect the reliability of power systems [38].

Voltage stability essentially is a dynamic phenomenon. However, the analysis based on static approaches illustrates some practical advantages over the dynamical approaches [39]. Analysis based on static approaches has been widely used, since it provides results with acceptable accuracy and little computational effort. These features are desirable in restrictive environments from the computational effort standpoint, such as in a real-time operation environment. The methods adopted in this dissertation are based on static analysis.

2.5.1 Voltage Stability Analysis

The voltage stability analysis can be classified according to the method of analysis into two different methods:

1. Static stability analysis methods
    a) sensitivity indices
    b) voltage-active power curve (P-V curve)
    c) modal analysis
    d) minimum singular value
    e) local voltage phasor approach
    f) voltage stability *L* indicator
    g) loading margin
    h) voltage stability indicator (Z_{th}/Z_l)

2. Dynamic stability analysis methods
    a) numerical integration simulations

Taylor [40] proposed some sensitivity indices to identify the critical buses in the system as follows:

- $\Delta V/\Delta P$: represents the change in voltage magnitude at a bus with respect to the change in the active power loading at the same bus
- $\Sigma\Delta Q_g/\Delta P$: represents the sum of the net change in the reactive power injections from all generators with respect to the change in the active power injection at the a certain load bus
- $\Delta V/\Delta Q$: represents the change in voltage magnitude at a bus with respect to the change in reactive power loading at *the same bus*
- $\Sigma\Delta Q_g/\Delta Q$: represents the sum of the net change in the reactive power injections from all generators with respect to the change in the reactive power injection at the a certain load bus

Sensitivity techniques are presented [41] to determine the voltage stability margins, which can be given in terms of MW, MVAR or MVA

Van Cutsem et al [42] show that voltage stability security margins must be determined in operational planning and real-time operation in order to best utilize the available system components. Finding a voltage stability index has become an important task for many voltage stability studies. Many voltage stability indices are proposed [43] based on information about the proximity to voltage collapse.

Ajjarapu et al [44] introduce a method of determining the minimum amount of shunt reactive power (VAR) support which indirectly maximizes the real power transfer before voltage collapse takes place. The proposed method depends on predictor corrector optimization technique to obtain a voltage stability index to measure the proximity to voltage collapse.

Several reports have pointed out that the use of voltage magnitudes only may not give a good indication of the proximity to the static voltage stability limit, as discussed in [45]. The use of the minimum singular value of the Jacobian is proposed as a security index against voltage

collapse [46]. The minimum singular values of Jacobian matrix together with the total generated reactive power may also be calculated as indicators of stability margin [47].

Venikov et al [48] proposed the use of load flow calculations to estimate the steady state stability at a certain operating condition. The sign of the determinant of the Jacobian matrix is used to determine if the system under study is stable or not. The minimum singular value of the power flow Jacobian matrix has earlier been proposed as a static voltage stability index (i.e., a voltage collapse security index) by Thomas and Tiranuchit [49]. The minimum singular value is used to indicate the distance between the studied operating point and the steady state voltage stability limit (point of voltage collapse).

Lof et al [50] presented the use of static voltage stability indices based on a singular value decomposition of the power flow Jacobian matrix and matrices derived from the Jacobian matrix. They concluded that the magnitude of the smallest singular value is a measure of the proximity to the steady state voltage stability limit.

Gao et al [51] discussed the voltage stability analysis of large power system using a modal analysis technique. The method applies a steady state system model to compute a specified number of the smallest eigenvalues and the associated eigenvectors of a reduced Jacobian matrix. The eigenvalues, each of which is associated with a mode of voltage/reactive power variation, provide a relative measure of proximity to voltage instability. The eigenvectors are used to describe the mode shape and to provide information about the network elements and generators which participate in each mode.

Two different static methods i.e. modal analysis technique and reactive reserve margin approach are implemented [52] to find the zones which push the system into voltage collapse or voltage instability. In the modal analysis method weak zones are identified by monitoring the participation factor of the buses in the critical modes. In the reactive power reserve method, reactive power reserves of the zones are monitored for single line outages, generator outages, and double line outages and the zones that have exhausted their reactive power reserves are identified as critical. The critical contingencies resulting in the smallest stability margins are also computed, and are ranked in the order of severity.

A phasor concept of voltage collapse proximity determination is presented [53]. An adequate voltage proximity index is calculated based on the voltage phasor values only. The voltage phasors contain sufficient information to determine voltage collapse proximity. This

information makes the proposed algorithm able to detect the network transmission paths to the load nodes which are prone to voltage collapse due to additional real or reactive loading.

A voltage collapse proximity indicator is proposed [54]. The proposed indicator can be applied at the load points of a power system and is based on the optimal impedance solution at maximum power transfer to the load bus under consideration. The maximum power transfer occurs when the magnitude of the load impedance (Z_l) becomes equal to the magnitude of the driving point impedance (Z_{th}), as seen from the bus under consideration. The stability margin is obtained as the distance of this indicator from unity.

Phadke et al [55] presented a new method of estimating the voltage stability margin which uses local measurements and calculates an index which is based on the basic definition of voltage stability. The proposed technique is very simple and straightforward. This technique uses the information about the current operating point and determines the voltage stability margin. The proposed method can accurately predict the proximity to voltage collapse at each bus. The method is computationally efficient and suitable for on-line monitoring of voltage stability margin.

Zalapa and Cory [56] proposed a methodology in steady state to determine the outputs of existing VAR/voltage control devices, so that the allocation of reactive reserves guarantees that the system does not move towards voltage collapse as demand changes, and that it will handle credible contingency conditions. The method is used to identify the weak circuit in the system by using “Q-distances” proximity indicators

A method proposed in [57] deals with the diagnosis of voltage collapse situations, following large disturbances and/or load increases. The proposed method is used to identify the set of buses where load restoration is responsible for the collapse and to determine the corresponding corrective actions. It has been implemented in a fast voltage stability simulator, using sensitivity techniques.

Nizam, Mohamed, and Hussain [58] introduced an indicator called power transfer stability index (PTSI). The PTSI is calculated from Equation (2.1). The value of PTSI will fall between 0 and 1. When the value of PTSI reaches 1, this means that the voltage collapse has occurred. The formula of that indicator can be described as;

$$PTSI = \frac{2S_L Z_{th}(1+\cos(\beta-\alpha))}{E_{th}^2} \quad (2.1)$$

where:

S_L: is load power at a bus

β: is the phase angle of Thevenin impedance at Thevenin bus

Z_{th}: is Thevenin impedance

α: is the phase angle of load bus

E_{th}: is Thevenin voltage

A neural network-based method is proposed in [59] for monitoring on-line voltage security of electric power systems using a dynamic model of the system. The voltage stability is measured totally, considering a suitable stability index for the whole system, and locally, by defining appropriate voltage margins for detecting the area of the system where the instability phenomenon arises.

Jinquan et al [60] present a preventive control method for mitigating the voltage instability problem. The preventive control problem is decomposed into two sub-problems and solved iteratively. The first sub-problem is that the stability nose points in contingency parameter space are calculated by using the continuation power flow. The other sub-problem is that a sensitivity based linear programming is used to obtain the preventive control actions.

Iba et al [61] introduced a method for calculating power systems' P-V curves and critical loading conditions. In this method, the P-V curve, which denotes the relationship between total load and system voltages, is calculated by a method based on a continuation load flow method.

A method for the online testing of a power system is proposed in [62] which is aimed at the detection of voltage instabilities based on an indicator *L*. The method depends on the results of load flow. Many authors [20, 63, 64, 65, 66, 67, 68] introduce the use of continuation load flow methods to find the maximum loadability point (nose point). Performance indexes are presented to determine the load margin, and the amount of load demand that the system can withstand before collapse [69, 70]

2.5.2 Voltage Collapse and Blackouts

When voltages in certain areas of the power system are significantly lower than normal, cascading events can occur accompanied by voltage collapse. Voltage collapse normally takes place when a power system is heavily loaded and/or has limited reactive power to support the load. The limiting factors could be the inadequate reactive power supply (SVC and generators hit limits) or the inability to transmit reactive power through the transmission lines [52].

Voltage collapse is a major interrelated phenomenon that occurs when the system is under stress. Many voltage collapse incidents [71-76] have been reported in which the system experiences excessive voltage drop after one or more severe faults. High loading conditions on system components cause them to trip, leading to cascading events of tripping.

Many power plants all over the world have been exposed to major blackout [40, 77]. Several analyses and investigations of recent major power system disturbances [73, 77, 78] illustrated that voltage collapse is the root cause of these major disturbances

According to [79] voltage collapse is a system instability that involves several power system components simultaneously. It typically occurs on power systems that are heavily loaded, faulted and/or have reactive power shortages. When the reactive power demands of loads cannot be met due to constraints and limitations on the generation and transmission of reactive power, voltage collapse may occur.

Yakout Mansour et al [80] presented a tool based on the determination of critical modes. Critical modes are computed by studying the system modes in the vicinity of the point of voltage collapse. System participation factors for the critical mode are used to determine the most suitable sites for system reinforcement.

Successful implementation of electric power deregulation requires the determination of the available transfer capability of a power system. The available transfer capability indicates the amount by which inter-area bulk power transfers can be increased without compromising system security [81]. According to [82] available transfer capability (ATC) is a measure of the transfer capability remaining in the physical transmission network for further commercial activity over and above already committed uses.

A method to compute the reactive power margin, the difference between the maximum reactive load and the corresponding base case value, at a given set of load buses of a power system is presented [83]. This margin aims to assess the system robustness with respect to

voltage collapse. The corresponding collapse point can be obtained from the solution of an optimization problem with the load increase as the objective, and the generator reactive limits as inequality constraints. So, the voltage collapse can be applied to compute the maximum loadability for a power system.

Claudio et al [84] proposed detailed steady-state models with controls of two flexible AC transmission system (FACTS) controllers, namely, static VAR compensators (SVCs) and thyristor controlled series capacitors (TCSCs), to study their effect on voltage collapse phenomena in power systems. Based on results at the point of collapse, design strategies are proposed for these two controllers, so that their location, dimensions and controls can be optimally defined to increase system stability margin.

Vourns et al [85] describe the on-line voltage security assessment environment developed within the framework of the EU-sponsored OMASES project, as well as its application to the Greek Interconnected Power System. The authors used a time-domain computation method to analyze the security of the power system with respect to power transfers under critical conditions or power consumption in load areas. They investigated the system security under secure operation and under contingency operation. A simple approach is presented in [86] to identify the point of voltage collapse by simulation of a power system using a slightly modified transient stability program. The system is stressed by progressively increasing the system load through a multiplier k. Total system voltage collapse was observed after the disturbance. They concluded that collapse coincides with the singularity of the sub-matrix J_R, of the load flow Jacobian matrix corresponding to load buses.

2.5.3 Mitigation of Voltage Stability Problems

The following methods can be used to mitigate voltage stability problems [87]:

- **Must-run generation:** operate uneconomic generators to provide voltage support during emergencies.
- **Generation rescheduling:** generation rescheduling is an effective method to alleviate network overload.
- **Phase shifting transformers:** phase shifting transformers can be used to control the power flow through the line in which they are connected by changing the phase angle.

- **Series capacitors:** use series capacitors to effectively shorten long lines, thus, decreasing the net reactive loss. In addition, the compensated line can deliver more reactive power from a strong system at one end to weak system that has a reactive shortage at the other end.
- **Shunt capacitors:** shunt capacitors can solve the voltage stability problem by providing local sources of reactive power.
- **Static compensators (SVCs and STATCOMs):** static compensators are effective in controlling voltage and preventing voltage collapse.
- **Operate at higher voltages:** operating at higher voltage may not increase reactive reserves, but it does decrease reactive demand. This can help keep generators away from reactive power limits.
- **Line switching**: switching in or out of lines or transformers can be effective method to control the voltage profile under light and heavy load conditions
- **Under voltage load shedding:** A small load reduction, even 5% to 10%, can make the difference between collapse and survival.

Midicherla et al [88, 89] presented algorithms to solve the problem of alleviating line overloads in a power system by generation rescheduling and load shedding. The techniques developed can be used to determine the generation rescheduling and load curtailment pattern to alleviate line overloads. The approaches presented help in determining the system security. Generation rescheduling has been proven to be one of the most effective control methods to alleviate the network overloading [88-93].

Sallam and Khafaga [94] suggested an algorithm for controlling voltage stability of power system by load shedding using fuzzy technique as a fuzzy controller. The fuzzy logic and fuzzy set theory are applied to the problem formulated on the study system.

Well designed power systems usually have adequate transmission lines. If some of these lines are standby, then by switching them in, the overload problem can be alleviated. Line switching is presented in [95, 96] as an effective tool to alleviate line overload.

2.6 Reactive Power Planning and Control

One major aspect of voltage stability is the capability of a system to transfer reactive power from generation stations to load centers under steady operating conditions. One of the

most effective ways to improve the power transfer capability and voltage stability of a power system is the compensation of reactive power. Reactive power management in power systems has attracted utility planners to consider the growing importance of reactive power planning [97].

Optimal power flow based on optimization techniques has been presented [91, 92, 98]. The optimal power flow is an effective tool in minimizing the active power losses, and keeping the voltage magnitude at all buses within acceptable limits. Improvement of voltage stability is achieved while maintaining acceptable system performance in terms of limits on generator active and reactive power outputs, limits on outputs of reactive power compensating devices, limits of tap changing transformers, and limits on voltage magnitude at all system buses.

The main task of energy control centers (ECC) is to keep all the voltages at all buses within acceptable operating limits, while, at the same time, satisfying certain optimization problems such as: minimum losses, maximum reactive power reserve, or minimum number of control actions. According to the current voltage profile of the power system, the power system operator makes the decision on how many controllers should be rescheduled in order to get the system back within acceptable operating limits. Several numerical optimization techniques have been proposed [99-101].

A method of finding the network constrained reactive power control presented in [102]. A linear programming (LP) technique is used to solve the problem by giving priorities to generators in the system. The main purpose of this method is to find the values of control variables which would cause the dependent variables to remain within a pre-specified limit.

Mamandur and Chenoweth [103] proposed a mathematical formulation of the optimal reactive power flow. The model minimizes the real power losses in the system under the constraints of: reactive power limits of the generators, limits on the load bus voltages, and the operating limits of the control variables. The algorithm employs linearized sensitivity relationships of power systems to establish both the objective function for minimizing the system losses and the system performance sensitivities relating dependent and control variables. Then a dual linear programming technique is used to determine the optimal adjustments to the control variables, simultaneously satisfying all constraints. The results showed that this technique is suitable to improve voltage profiles and to minimize system losses under operating conditions.

Soman et al [104] address the problem of curtailing the number of control actions and minimizing controller movements for real-time voltage and reactive power control. The

proposed algorithms are used to identify the most effective subset of control actions and to minimize controller movements. An algorithmic objective function suitable for the treatment of system security and economy is also proposed. A single parameter decides the priority between movement of controls and gains in security as well as loss reduction.

An approach using fuzzy set theory for voltage and reactive power control of power systems is presented in [105-107]. The approach is used to enhance voltage security of an electric power system. The violation bus voltage and the controlling variables are translated into fuzzy set notations to formulate the relation between voltage violation level and controlling ability of controlling devices. A feasible solution set is first attained using the min- operation of fuzzy sets, then the optimal solution is fast determined employing the max- operation.

Qiu and Shahidehpour [108] proposed an algorithm for minimizing transmission line losses and improving voltage profile in a given power system by adjusting control variables: tap setting of transformers and reactive power injection of VAR sources. Line losses are considered as a function of voltage increments. Linear programming technique is used to calculate the voltage increments which minimize the transmission losses. The required adjustments of control variables are obtained by a modified Jacobian matrix.

Menezes et al [109] proposed a method that provides a solution for the pre-dispatch problem considering the evaluation and improvement of the voltage stability margin by optimizing reactive power injections by generators and synchronous condensers. Modal participation factors are used to define penalty indices for all generators, which are then added to the optimal power flow objective function. This identifies the most adequate reactive power injection for each generator or synchronous condenser, to maximize voltage stability margins.

Zhang and Ren [110] proposed a mathematical model for optimal reactive power dispatch whose objective function is to minimize the active power losses. The simulation demonstrated that the proposed model reflects the principle of profit maximization and can decrease active power loss and avoid excessive controls simultaneously.

William et al [111] presented a rule based approach for decentralized voltage control. A network decomposition technique is used to alleviate bus voltage limit violations using the most effective voltage control device available locally.

A fuzzy linear programming approach is proposed as a method for the steady-state reactive power and voltage control in [112]. Multiple objectives and soft constraints are

modeled using fuzzy sets in a fuzzy linear programming approach to the reactive power and voltage control problem.

An approach to the optimal reactive dispatch problem with the objective of minimization of real power losses, based on an augmented Lagrangian function of the original problem is presented in [113]. The authors used Newton Raphson method to solve optimality problem.

Marques et al [114] presented a knowledge-based system for supervision and control of a regional voltage profile and security using fuzzy logic. In this work, the control strategies are defined by the system operators based on their experience and also based on off-line studies which are translated into rules of a hierarchical fuzzy inference system.

Ghafouri et al [115] present the application of a fuzzy logic controlled static compensator (STATCOM) to improve the stability of power system. The authors used different input variables to design the controller. Parameters of the proposed controller are adjusted by means of Neural Network techniques to improve performance of the system. Proposed controller is implemented on a single machine infinite bus system to confirm the performance of the controller.

An on-line voltage stability assessment has been presented [116] for the identification of voltage control areas and reactive power reserves requirement to ensure voltage stability under contingency operation. The authors defined voltage control areas as: regions in a power system that under specific conditions are prone to voltage instability.

Chapter 3 Genetic Algorithm and Pattern Search

3.1 What Is the Genetic Algorithm?

The genetic algorithm (GA) is a search technique used to find exact or approximate solutions for both constrained and unconstrained optimization problems. The GA repeatedly modifies a population of individual solutions. At each step, the GA selects individuals at random from the current population to be parents and uses them to produce the children for the next generation. Successive generations are generated randomly seeking for an optimal solution. GA can be applied to solve a variety of optimization problems that are not well suited for conventional optimization algorithms, including problems in which the objective function is discontinuous, non differentiable, stochastic, or highly nonlinear. GA can search several possible solutions simultaneously without any prior knowledge or special properties of the objective function [117].

The GA uses three main types of rules at each step to create the next generation from the current population, these generations are subjected the fitness function and its constraints:

- Selection rules select the individuals, called parents, which contribute to the population at the next generation.
- Crossover rules combine two parents to form children for the next generation.
- Mutation rules apply random changes to individual parents to form children.

3.2 Genetic Algorithm Terminology

3.2.1 Fitness Functions

The fitness function is the function to be optimized. For traditional optimization algorithms, this is known as the objective function.

3.2.2 Individuals

An individual is any data point to which the fitness function can be applied. The value of the fitness function for system condition is its score. An individual is sometimes referred to as a genome and the vector entries that describe the properties of the system as genes.

3.2.3 Populations and Generations

A population is an array of individuals. For example, if the size of the population is *m* and the number of variables in the fitness function is *n*, the population array can be represented by a (*m* x *n*) matrix. The same individual can appear more than once in the population. At each iteration, the GA performs a series of computations on the current population to produce a new population. Each successive population is called a new generation.

3.2.4 Diversity

Diversity refers to the average distance between individuals in a population. A population has high diversity if the average distance is large; otherwise it has low diversity. Figure (3.1) indicates the population of twenty individuals for a two variables fitness function. On the left hand side the population has high diversity, while the population on the right hand side has low diversity. Diversity is essential to the GA because it enables the algorithm to search a larger region of the space.

3.2.5 Reproduction

Reproduction is a process by which current individuals are put together to move to a new generation. Fitness of parents is used to determine characteristics passed to children. At each step, the GA uses the current population to create the children that make up the next generation. The algorithm selects a group of individuals in the current population, called parents, who contribute their genes (the entries of their data vectors) to their children. The algorithm usually selects individuals that have better fitness values as parents. The GA creates three types of children for the next generation as follow:

- Elite children are the individuals in the current generation with the best fitness values. These individuals automatically survive to the next generation.
- Crossover children are created by combining the vectors of a pair of parents.

- Mutation children are created by introducing random changes, or mutations, to a single parent.

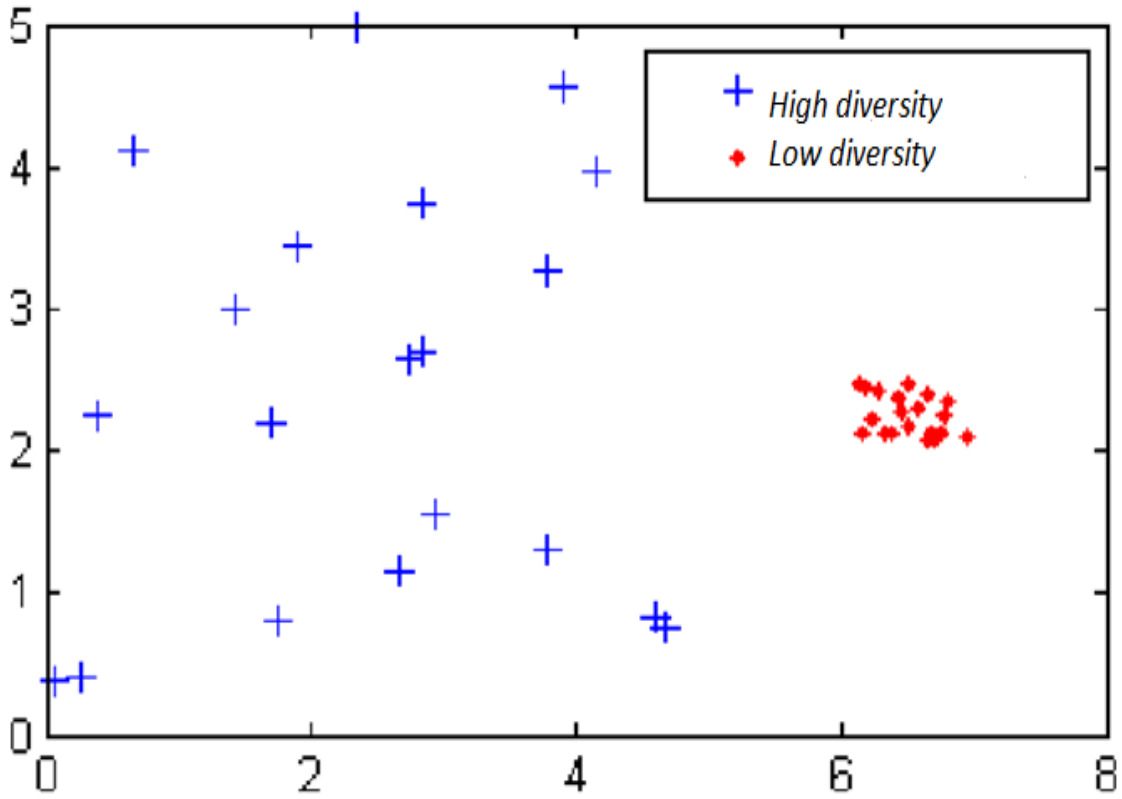

Figure 3.1: The diversity of population of 20 individuals for a two variables fitness function

3.3 How the Genetic Algorithm Works

The following outline summarizes how the genetic algorithm works:

1. The algorithm begins by creating a random initial population.
2. The algorithm then creates a sequence of new populations. At each step, the algorithm uses the individuals in the current generation to create the next population. To create the new population, the algorithm performs the following steps:

a. Scores each member of the current population by computing its fitness value.
b. Scales the raw fitness scores to convert them into a more usable range of values.
c. Selects members, called parents, based on their fitness.
d. Some of the individuals in the current population that have lower fitness are chosen as elite. These elite individuals are passed to the next population.
e. Produces children from the parents. Children are produced either by making random changes to a single parent (mutation) or by combining the vector entries of a pair of parents (crossover).
f. Replaces the current population with the children to form the next generation.

3. The algorithm stops when one of the stopping criteria is met.

3.4 Stopping Conditions for the GA

The genetic algorithm uses the following conditions to determine when to stop:

- Generations**:** The algorithm stops when the number of generations reaches a pre-specified value.
- Time limit**:** The algorithm stops after running for pre-specified time.
- Stall time limit: The algorithm stops if there is no improvement in the objective function during a pre-specified interval of time.
- Function Tolerance: The algorithm stops if the change in the fitness function value over a pre-specified number of generations is less than a given tolerance.

The algorithm stops as soon as any one of the above conditions is met.

3.5 What Is Direct Search?

Direct search is a method for solving optimization problems that does not require any information about the gradient of the objective function. Unlike more traditional optimization methods that use information about the gradient [117] or higher derivatives to search for an optimal point, a direct search algorithm searches a set of points around the current point, looking for one where the value of the objective function is lower than the value at the current point. You can use direct search to solve problems for which the objective function is not differentiable, or

is not even continuous. Pattern search algorithm computes a sequence of points that approach an optimal point. At each step, the algorithm searches a set of points, called a "mesh", around the current point, the point computed at the previous step of the algorithm. The mesh is formed by adding the current point to a scalar multiple of a set of vectors called a "pattern". If the pattern search algorithm finds a point in the mesh that defines better value to the objective function than the current point, the new point becomes the current point at the next step of the algorithm.

3.5.1 Patterns

A pattern is a set of vectors (v_i) that the pattern search algorithm uses to determine which points to search at each iteration. The set (v_i) is defined by the number of independent variables (control variables) in the objective function, N. Two commonly used sets in pattern search algorithms are 2N vectors, and N+1vectors. For example, if there are three independent variables in the optimization problem, the default for a 2N set consists of the following pattern vectors:

v_1=(1 0 0) v_2=(0 1 0) v_3=(0 0 1) v_4=(-1 0 0) v_5=(0 -1 0) v_6=(0 0 -1)

While the default for an N+1 set consists of the following default pattern vectors.

v_1= (1 0 0) v_2= (0 1 0) v_3= (0 0 1) v_4= (-1 -1 -1)

3.5.2 Meshes

At each step, a pattern search method searches a set of points, called a mesh, for a point that improves the objective function. Pattern search forms the mesh by

1. Generating a set of vectors (d_i) by multiplying each pattern vector (v_i) by a scalar Δ^m. Δ^m is called the mesh size.
2. Adding each (d_i) to the current point (the point with the best objective function value found at the previous step).

For example, suppose that an objective function with two independent variables has a current point of (1.6 3.4). The pattern for a 2N positive basis consists of the following pattern vectors:

v_1 = (1 0)
v_2 = (0 1)
v_4 = (-1 0)
v_5 = (0 -1)

If the current mesh size Δ^m is 4. The algorithm multiplies the pattern vectors by 4 and adds them to the current point to obtain the following mesh.

(1.6 3.4) + 4*(1 0) = (5.6 3.4)
(1.6 3.4) + 4*(0 1) = (1.6 7.4)
(1.6 3.4) + 4*(-1 0) = (-2.4 3.4)
(1.6 3.4) + 4*(0 -1) = (1.6 -0.6)

The pattern vector that produces a mesh point is called its direction.

3.5.3 Polling

At each step, the algorithm polls the points in the current mesh by computing their objective function values. There are two types of polling as follow:

1. Incomplete poll: in which the algorithm stops polling the mesh points as soon as it finds a point whose objective function value is less than that of the current point. If this occurs, the poll is called successful and the point it finds becomes the current point at the next iteration. The algorithm only computes the mesh points and their objective function values up to the point at which it stops the poll. If the algorithm fails to find a point that improves the objective function, the poll is called unsuccessful and the current point stays the same at the next iteration.

2. Complete poll: in which the algorithm computes the objective function values at all mesh points. The algorithm then compares the mesh point with the smallest objective function value to the current point. If that mesh point has a smaller value than the current point, the poll is successful.

3.5.4 Expanding and Contracting

After polling, the algorithm changes the value of the mesh size Δ^m. The default is to multiply Δ^m by 2 after a successful poll and by 0.5 after an unsuccessful poll.

3.6 Stopping Conditions for the Pattern Search

The algorithm stops when any of the following conditions occurs:

- The mesh size is less than the pre-specified mesh tolerance.
- The maximum number of iterations is violated.
- The maximum number of objective function calculations is reached
- The algorithm runs until it reaches a pre-specified time.

Chapter 4 Contingency Analysis

This chapter discusses the effect of single level contingencies (N-1) on the static voltage stability of power systems. A ranking scheme is proposed for screening contingencies based on the mega Watt margin (MWM), which is the distance measured in MW from the base load operating point to the point of voltage collapse (nose point of P-V curve). The MWM corresponding to each contingency case is compared with the MWM of the system without contingency. By ranking the contingencies, the system operator is able to reduce the number of contingencies out of all possible contingencies that need to be considered for voltage stability analysis. The proposed method is applied on four different systems in order to identify critical buses and lines in these systems and rank all (N-1) contingency according to their impact on the voltage stability margin. The results of contingency analysis for these systems will be used in the following chapters as a guide for controlling and planning of power systems. .

4.1 Introduction

Any failure in the power system, such as loss of transmission lines, generators, or transformers, will change the network configuration that in turn results in a smaller MWM for the specific system failures. For an ideal condition when the system experiences no failure and all of the components in the system are working properly, the system is capable of providing the maximum margin of MW. In a real large-scale power system, many possible contingencies are encountered and different contingencies may have different impacts on the system stability and also its loading margin. The main reason for low voltage profile and therefore smaller load margin for some contingency is the insufficient reactive power in the vicinity of the low voltage buses. There are some severe contingencies with very low load margin that are only a small fraction of the maximum margin, while for some other contingencies the load margins is close to its maximum.

Due to deregulation and the fact that many systems have not expanded their transmission and generation capacity in recent years, many utilities are operating closer to their maximum capacity. For a system with smaller margin, more contingencies are considered as severe contingencies, and the system is exposed to more frequent voltage collapses [118]. Many power systems are now experiencing voltage problems more frequently and voltage studies have gained

increasing attention from operating and planning points of views. It is vital, then, for the electric utility planners and operators to know the impact of every contingency on the voltage profile. Ranking all possible contingencies based on their impact on the system voltage profile will help the operators in choosing the most suitable remedial actions before the system moves toward voltage collapse. To maintain the system reliability, it is desirable to study the impact of the contingency on the load margin, and to categorize them based on the ratio of their load margin to its maximum load margin without any contingency [18]. For contingencies with zero or negative margin an immediate operating action is strongly needed.

4.2 Overview of Contingency Analysis

Contingency Analysis (CA) is a "what if" scenario simulator that provides, evaluates and prioritizes the impacts on an electric power system when problems occur. Evaluation of power system security is necessary in order to develop ways to maintain system operation when one or more elements fail [119]. A power system is secure when it can withstand the loss of one or more elements and still continue operation without major problems. Contingency Analysis (CA) is one of the security analysis applications in a power system control center that differentiates an Energy Management System (EMS) from a less complex SCADA system [119]. Its purpose is to analyze the power system to identify the overloads and predict problems that can occur due to a contingency. In other words, single level contingency analysis is used to evaluate the effects of removing an element from a power system.

After a contingency event, the power system may suffer from one of the following problems [13]:

- None: when the power system can be rebalanced after a contingency, without causing overloads to any element.
- Severe: when several elements such as lines and transformers become overloaded and at risk of damage.
- Critical: when the power system becomes unstable and will go to collapse.

A robust power system must be able to withstand and recover from most of the N-1 contingencies. Therefore CA is one of the tools used primarily by power system planners and

engineers to test the power system for its strengths and weaknesses. CA has always been an important part of electric utility system planning and operations. By analyzing the effects of contingency events in advance, problems and unstable situations can be identified, critical (unacceptable) configurations can be recognized, and then operating constraints and limits can be applied, and corrective actions can be planned. CA is also used for scheduling the withdrawal of power system equipment for periodic or restorative maintenance. According to [84] Contingency cases can be classified based on their impact on the voltage collapse as seen in Figure (4.1):

- Acceptable: Contingencies with more than 80% of the MWM without contingency.
- Significant: contingencies with 0% to 80% of the MWM without contingency.
- Unacceptable: Contingencies that result in negative MWM.

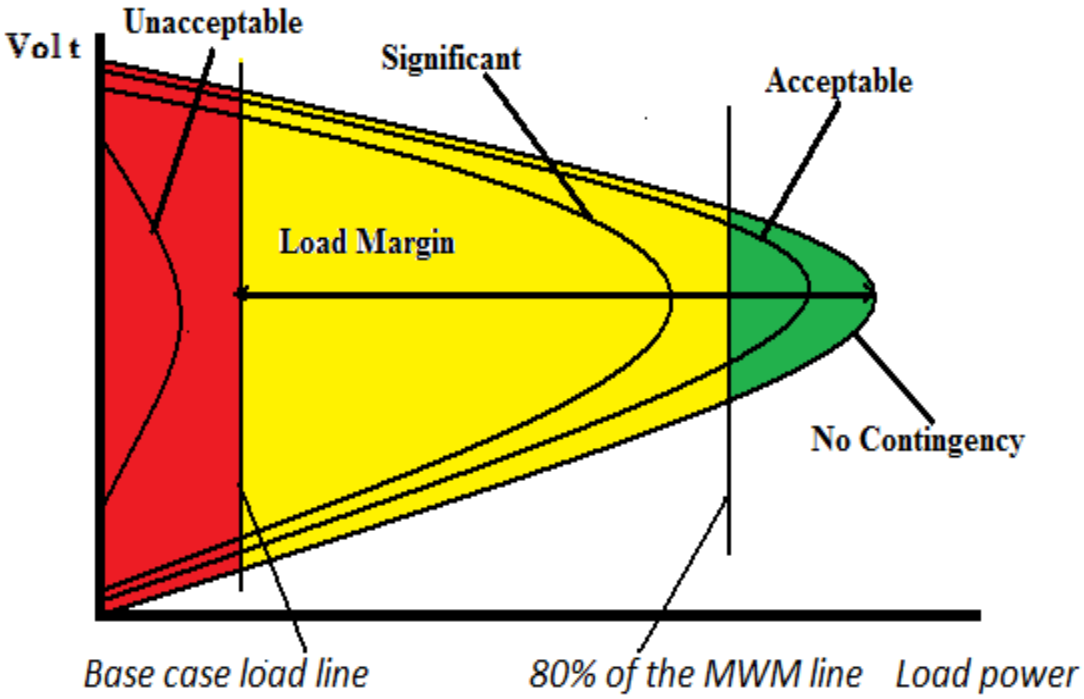

Figure 4.1: Contingency classifications according to their severity

4.3 Methodology

1. Perform a series of load flow runs while increasing the system load with a step of 1% of the base case load keeping constant power factor (P/Q=constant) until the load flow program fails to converge. Failure to converge means that the system under study reached its maximum allowable load (i.e. load after which the system will go to voltage collapse).
2. Calculate the maximum loading, loading margin, and the ratio of the maximum load to the base load without any contingency.
3. Repeat steps 1 and 2 for all possible (N-1) contingencies.
4. Tabulate the values of maximum loading, loading margin, and the ratio of the maximum load to the base load.
5. Calculate the ratio of the maximum loading with single level contingency to the maximum loading without contingency.
6. Classify contingencies based on their impact on the voltage collapse.
7. Rank load buses based on their voltage magnitudes at the point of voltage collapse.

4.4 Simulation Results

4.4.1 Case1: 6 Generator System

The one line diagram of the 6 generator system is shown in Figure (4.2), while a complete data set for the system can be found in Appendix A. The system has 6 generators, 21 buses, and 30 lines. In the base case (without contingency) the total system load is 5.06 pu, the swing bus (bus number 1) generates real power of 0.4454 pu, while the remaining five generators produce real power of 4.8 pu, the minimum voltage magnitude is at bus number 16 with 0.9501 pu, and the voltage collapse occurs at a total system load of 6.9828 pu, giving a base case load margin of 1.9228 pu. As shown in Figure (4.2), the most robust buses in the 6 generator system, buses 7, and 14 are circled with a green circle and the weakest buses, 16, 15, and 17 are circled with a red one. On the other hand, the buses circled with a yellow circle refer to moderate buses between the weakest and strongest areas in the same system.

The load flow program of power system toolbox (PST) [120] is modified in order to do a continuation load flow to be used in producing P-V curves as part of this work.

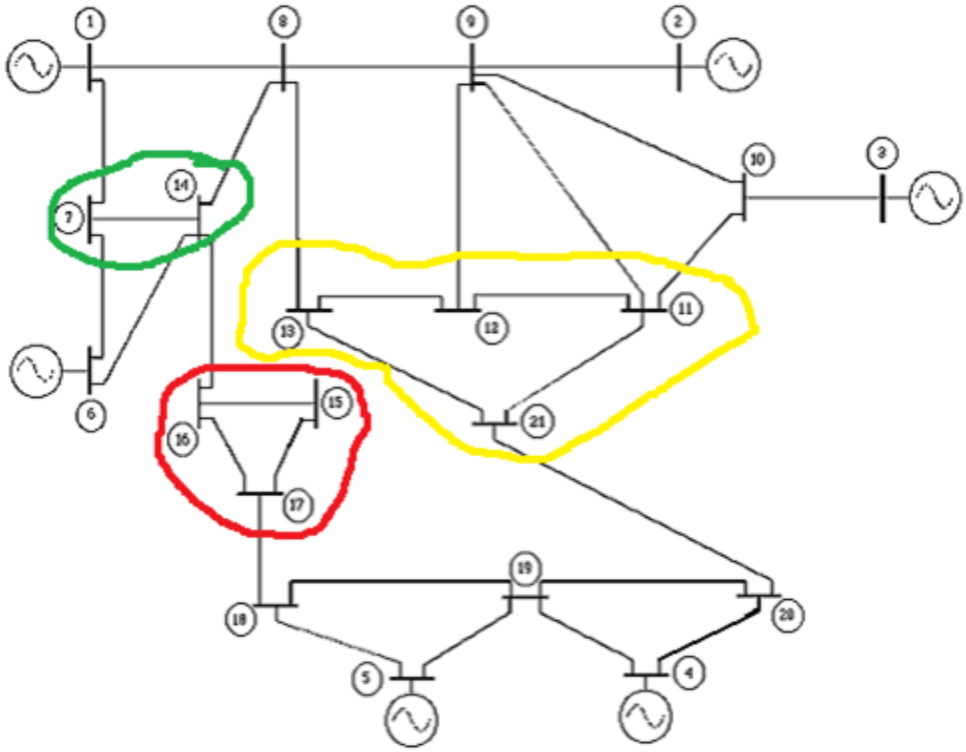

Figure 4.2: Single line diagram for the 6 generator system

Figure (4.3) shows the P-V curves at all load buses without contingency; every curve represents the relation between a bus voltage magnitude and the corresponding bus real power as a fraction of base case load. This figure shows that the voltage collapse will start from bus 16 that has the lowest voltage at 1.38 loading factor and also shows that the voltage magnitudes at buses 7 and 14 almost remain constant at all loading factors. Figure (4.4) gives P-V curves at bus 16 which represents the weakest bus in the system without contingency and under selected contingencies. Finally Figure (4.5) presents P-V curves at bus 7 which represents the strongest bus in the system without contingency and under selected contingencies. From Figures (4.4), and (4.5) it can be noticed that there is no post-contingency load flow solution in the two cases, outage of the generator at bus 5, and outage of line connecting buses 19, and 20, while outage of the generator at bus number 4 is very critical because it has zero load margin. On the other hand, outage of the line between buses 12, and 13 almost has no effect on the system.

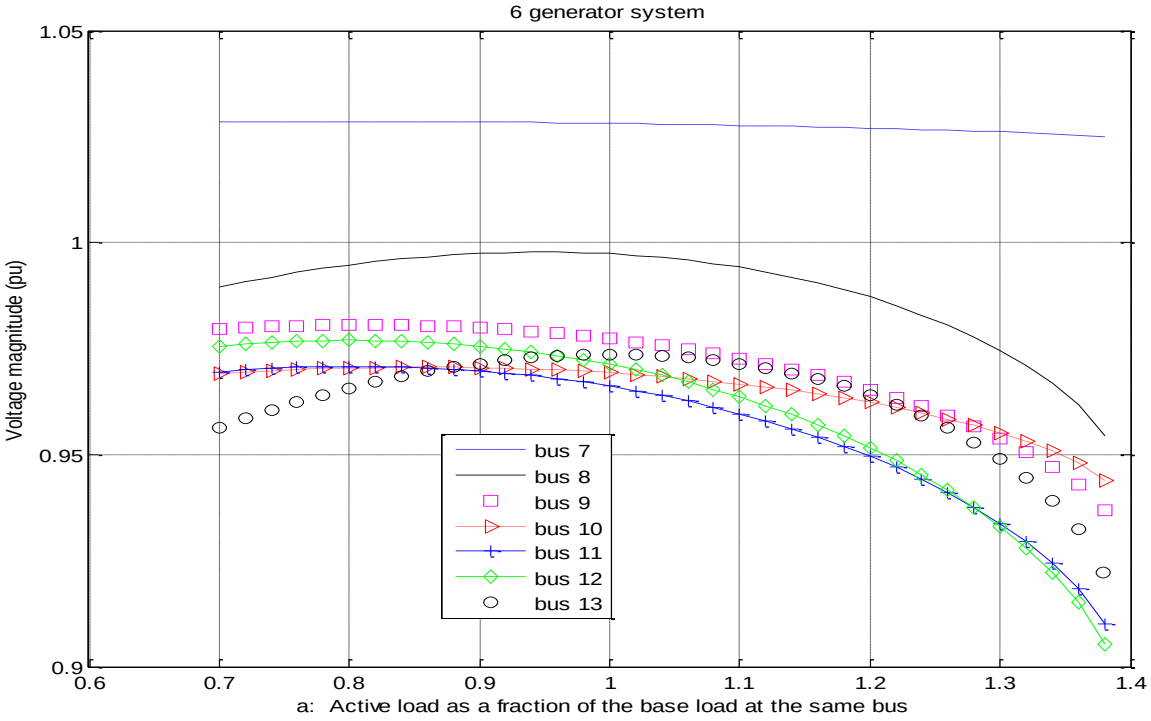

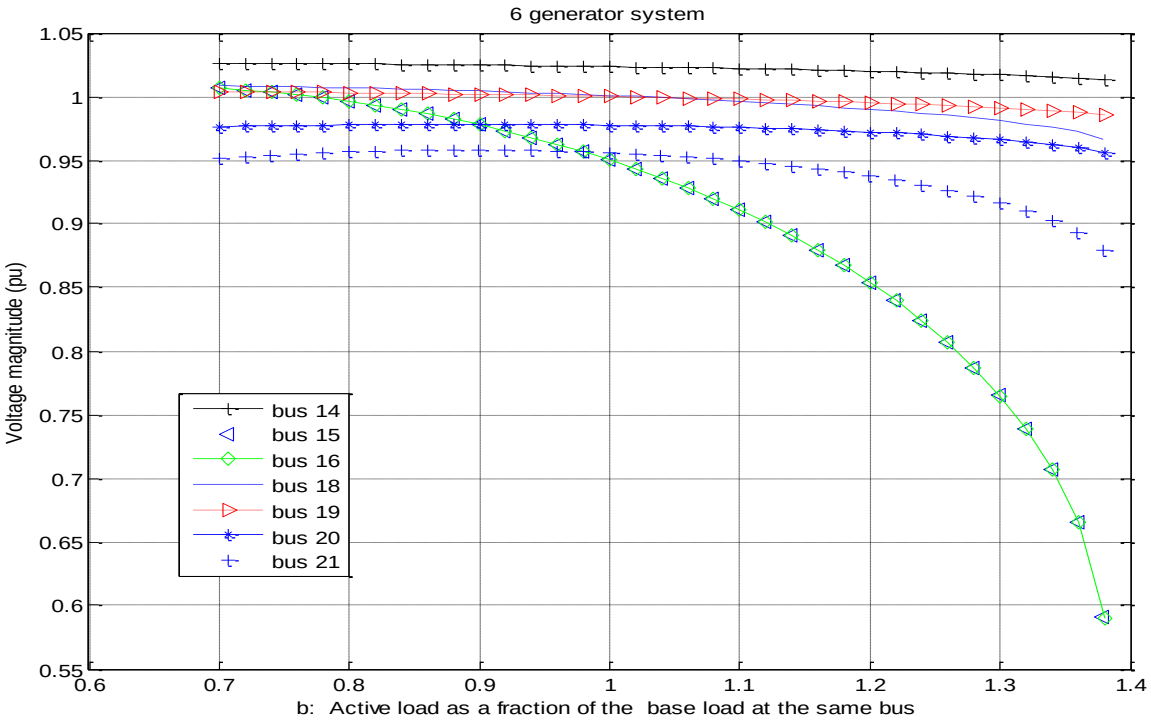

Figure 4.3: P-V curves without contingency

a: Buses 7, 8, 9, 10, 11, 12, 13 b: Buses 14, 15, 16, 18, 19, 20, 21

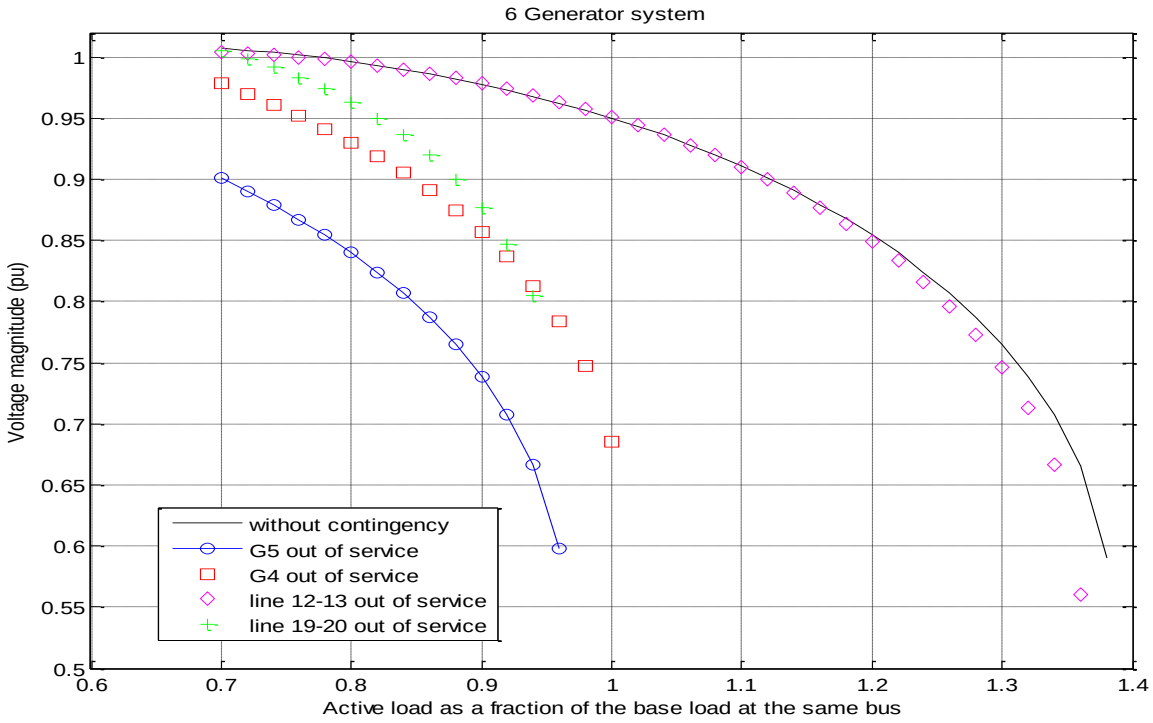

Figure 4.4: P-V curves at bus 16, the weakest bus in the system

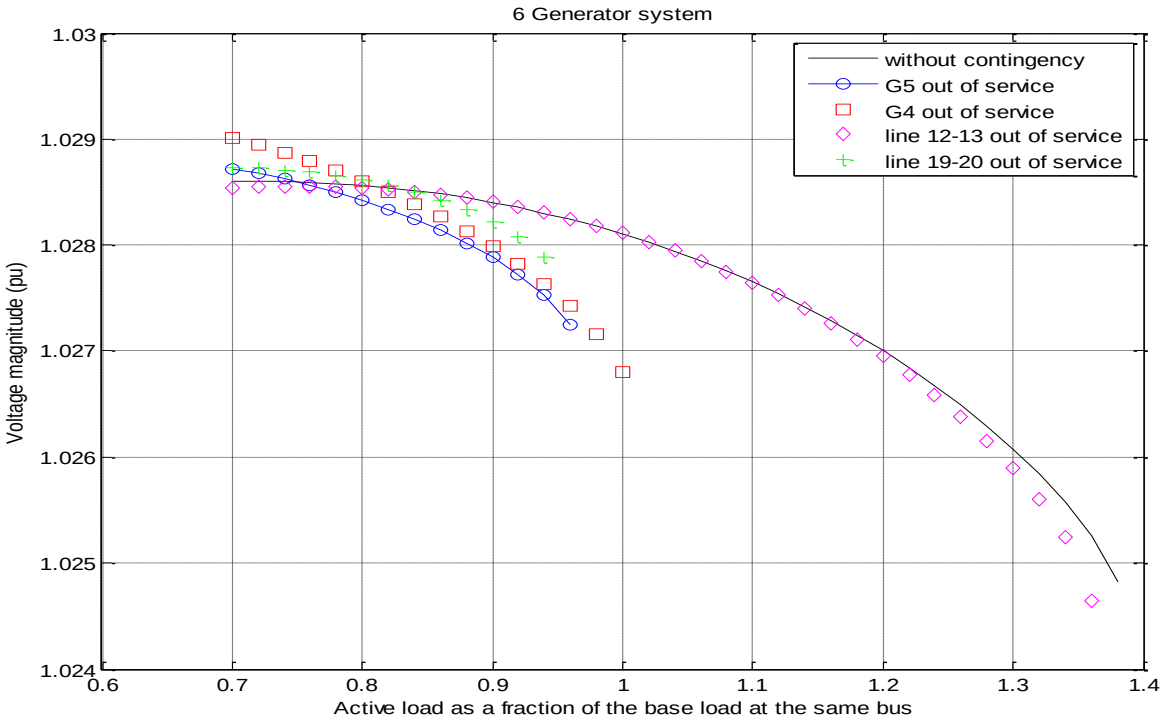

Figure 4.5: P-V curves at bus 7, the strongest bus in the system

The results related to the 6 Generator system, for the base case, all single level (N-1) contingencies, and the ranking of load buses are tabulated in Table (4.1) and Table (4.2). In Table (4.1) all contingencies are ranked according to their impact on the voltage collapse into three categories as follows:

1. Acceptable: cases from 15 to 36 in Table (4.1).
2. Significant: cases from 4 to 14 in Table (4.1).
3. Unacceptable: cases from 1 to 3 in Table (4.1).

Negative load margin (P_{max} less than base case load without contingences) means that no post-contingency load flow solution exists for that contingency. In such cases the load has to be shed immediately to avoid voltage collapse in the system.

Out of the three types of contingencies "Acceptable, Significant, Unacceptable" the Unacceptable and Significant contingencies are more important contingencies, because they need more analysis and planning to find the most appropriate solution to prevent any voltage instability problems.

Table (4.2) ranks all the load buses according to their weakness, such that the lowest number represents the weakest bus, while the largest number represents the strongest bus in the system.

Table 4.1: Ranking of (N-1) Contingencies for 6 generator system

Case #	Contingency		Pmax (pu)	Load Margin (pu)	Load Margin % Of the load Margin at base load	P_{max} / P_{base}
	Line Outage					
	From bus	To bus				
1	20	21	Does not CONVERGE AT ALL			
2	19	20	4.7564	-0.3036	-0.0312	0.94
3	G5	--	4.8576	-0.2024	-0.0208	0.96
4	G4	--	5.0600	zero	zero	1.00
5	G2	--	5.1106	0.0506	2.63	1.01

Continuation of Table 4.1: Ranking of (N-1) Contingencies for 6 generator system

6	17	18	5.2624	0.2024	10.53	1.04
7	14	16	5.4142	0.3542	18.42	1.07
8	8	13	5.7684	0.7084	36.74	1.14
9	1	8	6.2744	1.2144	63.16	1.24
10	G1	--	6.3250	1.2650	65.78	1.25
11	G3	--	6.3250	1.2650	65.78	1.25
12	13	21	6.3756	1.3156	68.42	1.26
13	3	10	6.5274	1.4674	76.32	1.29
14	5	19	6.5274	1.4674	76.32	1.29
15	2	9	6.6286	1.5686	81.58	1.31
16	4	20	6.6286	1.5686	81.58	1.31
17	10	11	6.8816	1.6216	84.34	1.36
18	6	--	6.7804	1.7204	89.47	1.34
19	6	14	6.8310	1.7710	92.11	1.35
20	8	14	6.8310	1.7710	92.11	1.35
21	12	13	6.8816	1.8216	94.74	1.36
22	11	21	6.8816	1.8216	94.74	1.36
23	4	19	6.8816	1.8216	94.74	1.36
24	18	19	6.8816	1.8216	94.74	1.36
25	9	12	6.9322	1.8722	97.36	1.37
26	8	9	6.9322	1.8722	97.36	1.37
27	5	18	6.9322	1.8722	97.36	1.37
28	15	16	6.9828	1.9228	100	1.38
29	9	10	6.9828	1.9228	100	1.38
30	9	11	6.9828	1.9228	100	1.38
31	11	12	6.9828	1.9228	100	1.38
32	7	14	6.9828	1.9228	100	1.38
33	6	7	6.9828	1.9228	100	1.38
34	16	17	6.9828	1.9228	100	1.38
35	15	17	6.9828	1.9228	100	1.38
36	1	7	6.9828	1.9228	100	1.38
37	NO CONTINGENCY		6.9828	1.9228	100	1.38

Acceptable: contingencies with load margin more than 80% of the load margin at base load.

Significant: contingencies with load margin from 0% to 80% of the load margin at base load.

Unacceptable: contingencies with negative load margin.

Table 4.2: Ranking of load buses for 6 generator system

Load bus number	Bus order (Smallest = weakest)
7	15 (strongest)
8	10
9	8
10	9
11	6
12	5
13	7
14	14
15	2
16	1 (weakest)
17 (no load)	3
18	12
19	13
20	11
21	4

4.4.2 Case 2: Ward and Hale system

The complete description of this system [121] can be found in Appendix B. The system has 2 generators, 6 buses, 2 under load tap changing transformers, and 5 lines. In the base case (without contingency) the total system load is 1.35 pu, the swing bus (bus number 1) generates real power of 0.966 pu, while the second generator produces 0.5 pu real power. The minimum voltage magnitude for Ward and Hale system is at bus number 3 with 0.8554 pu, and the voltage collapse occurs at a total load of 2.0925 pu, results in a load margin of 0.7425 pu. All the load buses are ranked according to their weakness in Table (4.3). As seen in Table (4.3) bus 4 is the strongest bus in the system and bus 3 is the weakest bus in the system. Table (4.4) shows the results for base case, and all single level (N-1) contingencies. All contingencies are categorized according to their impact on the voltage collapse into the three categories as follows:

1. Acceptable: None.
2. Significant: cases from 6 to 9 in Table (4.4).
3. Unacceptable: cases from 1 to 5 in Table (4.4).

Table 4.3: Ranking of load buses for Ward and Hale system

Load bus number	Bus order (Smallest =weakest)
3	1 (weakest)
4(No load)	4 (strongest)
5	2
6	3

Table 4.4: Ranking of (N-1) Contingencies for Ward and Hale system

Case #	Contingency		Pmax (PU)	Load margin (PU)	Load margin % of the load margin at base load	P_{max}/P_{base}
	Line outage					
	From Bus	To bus				
1	G1	--	Cannot meet the power requirement			
2	3	4	0.6480	-0.7020	-94.55	0.4800
3	1	4	1.1704	-0.1796	-24.19	0.8670
4	1	6	1.3081	-0.0419	-05.64	0.9690
5	G2	--	1.3203	-0.0297	-4.00	0.9780
6	2	5	1.3905	0.0405	5.45	1.0300
7	2	3	1.8360	0.4860	65.45	1.3600
8	5	6	1.8495	0.4995	67.27	1.3700
9	4	6	1.9035	0.5535	74.55	1.4100
10	No Contingency		2.0925	0.7425	100	1.5500

Figure (4.6) shows the P-V curves for Ward and Hale system at all load buses without contingency. This figure shows that bus number 4 is the strongest bus in the system, while bus 3 that has the lowest voltage at the collapse point is the weakest bus in the system. Figure (4.7) gives the P-V curves, with and without contingency, at bus 3, the weakest bus in the system. This figure shows that the outage of the generator at bus number 4, and the outage of line connecting buses 1, and 4, have no post-contingency load flow solution, while the outage of the element between buses 2, and 3 and the element between buses 5, and 6 cases a significant contingency.

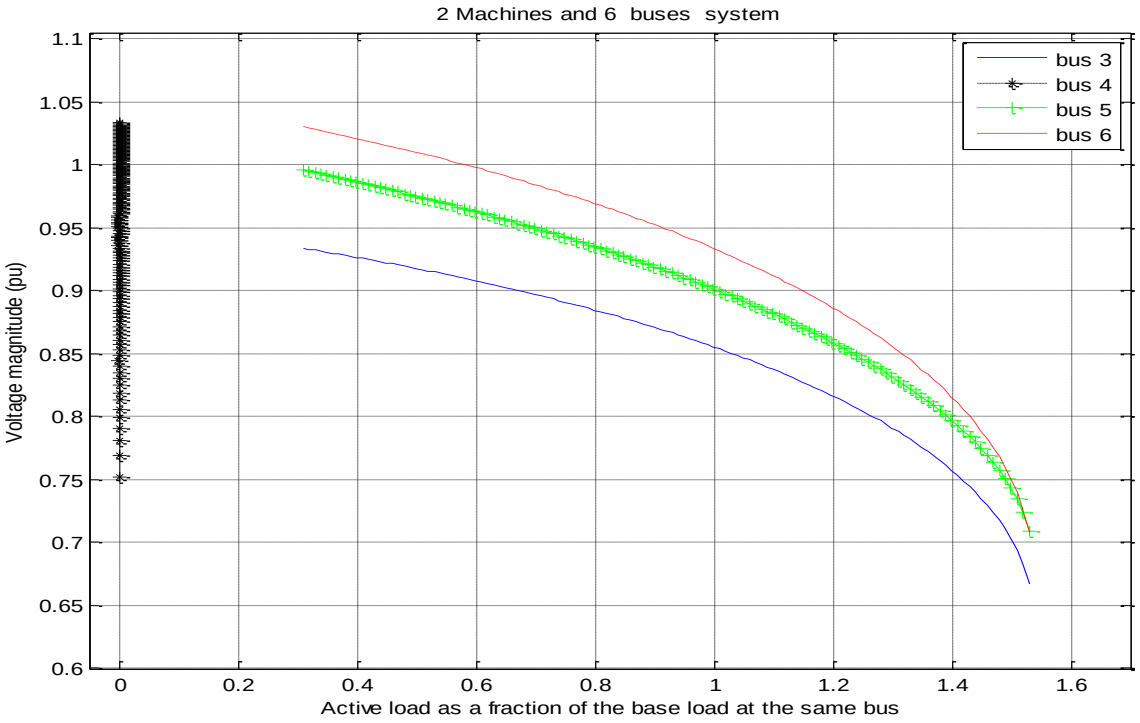

Figure 4.6: P-V curves without contingency

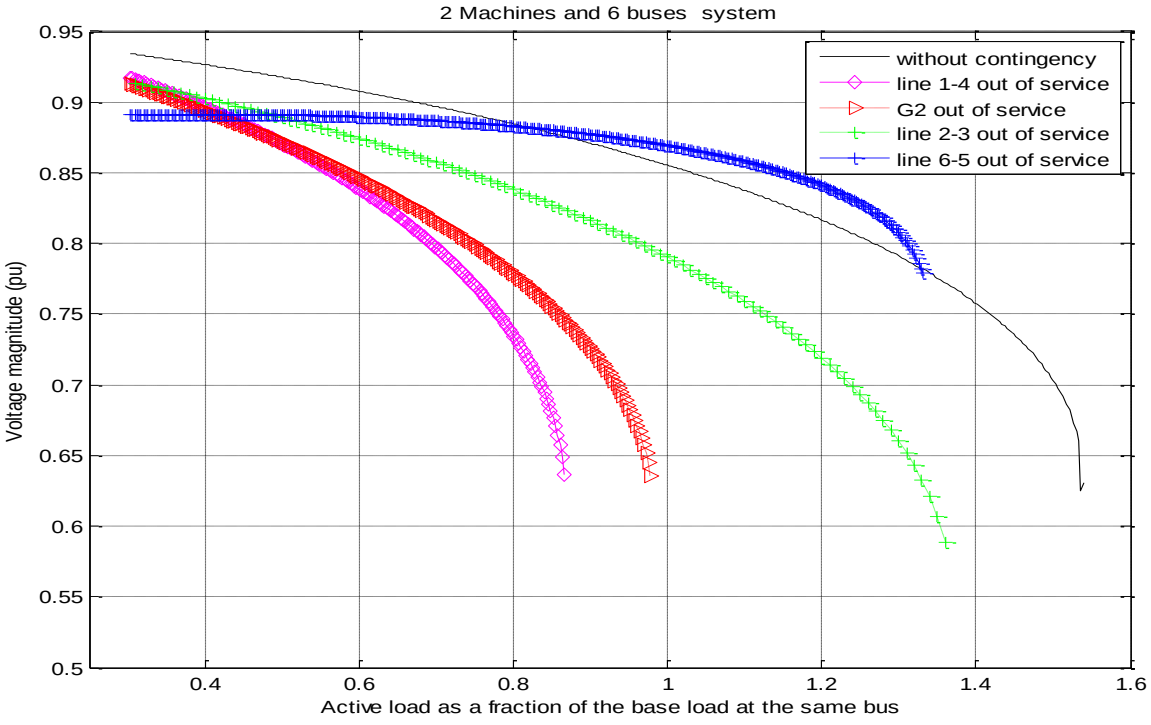

Figure 4.7: P-V curves at bus 3, the weakest bus in the system

4.4.3 Case 3: IEEE 14 bus System

The complete description of this system can be found in Appendix C. The system has 5 generators, 14 buses, 3 under load tap changing transformers, and 18 lines. In the base case the total system load is 2.59 pu, the swing bus generates real power of 2.3265 pu, while the other generators produce 0.4 pu real power. The minimum voltage magnitude is at bus number 14 with 0.9837 pu, the voltage collapse occurs at a total load of 4.4548 pu, giving a load margin of 1.8648 pu.

Figure (4.8) shows the P-V curves for all load buses without contingency, for the IEEE 14 bus system. The results shown in this figure indicate that bus number 14, the weakest bus in the system, has the lowest voltage at the point of collapse. On the other hand, the voltage at bus number 5, the strongest bus in the system, has the highest voltage at the collapse point.

Figure (5.9) gives P-V curves at bus 14, the weakest bus in the IEEE 14 bus system, without contingency and under some selected contingencies. On the other hand in the other side, Figure (4.10) presents P-V curves at bus 5, the strongest bus in the system, without contingency and under the same selected contingencies. Figures (4.9) and (4.10) show that there is no considerable change in the load margin when the line connecting buses 13, and 14 is out of service, while the outage of lines connecting buses (1, and 5), (1, and 2), and (2, and 4) decreases the load margin to be 50 %, 69.4 %, and 76.4 % of the base case load margin respectively

Table (4.5) shows the results for base case, and all single level (N-1) contingencies, all contingencies are categorized as follows:

1. Acceptable: cases from 11 to 26 in Table (4.5).
2. Significant: cases from 2 to 10 in Table (4.5).
3. Unacceptable: case number 1 in Table (4.5).

On the other hand Table (4.6) shows the ranking of the load buses of IEEE 14 bus system according to weakness. Bus number 14 is the weakest bus in the system, while bus 5 is the strongest bus in the system.

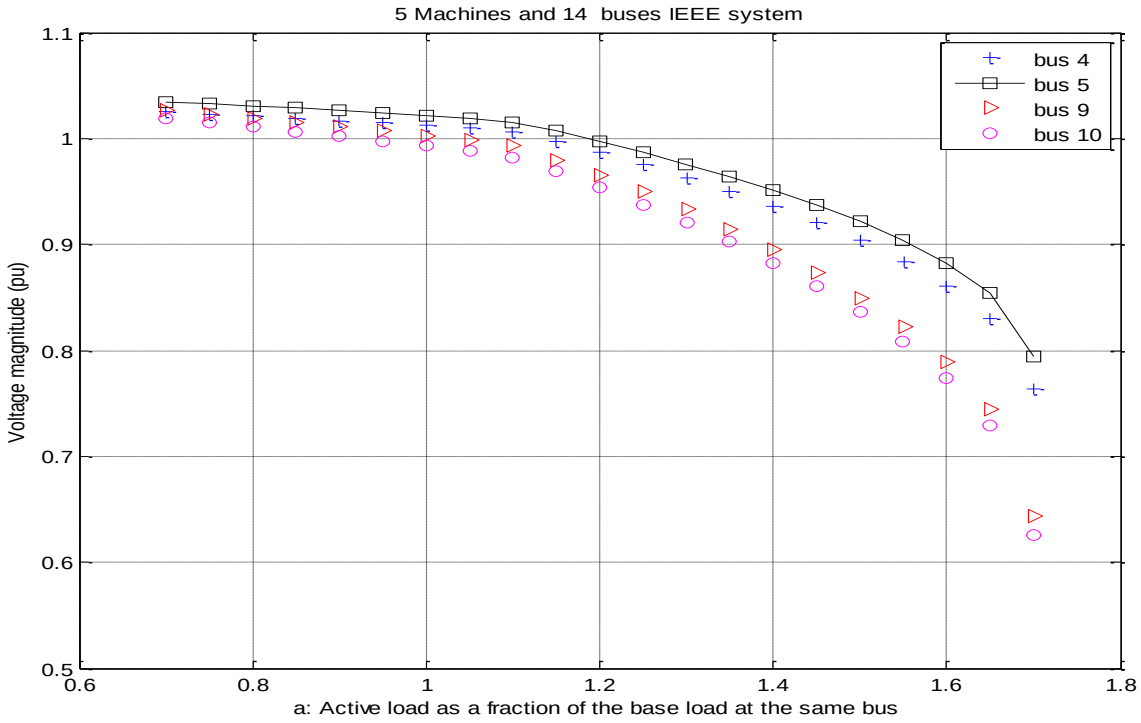

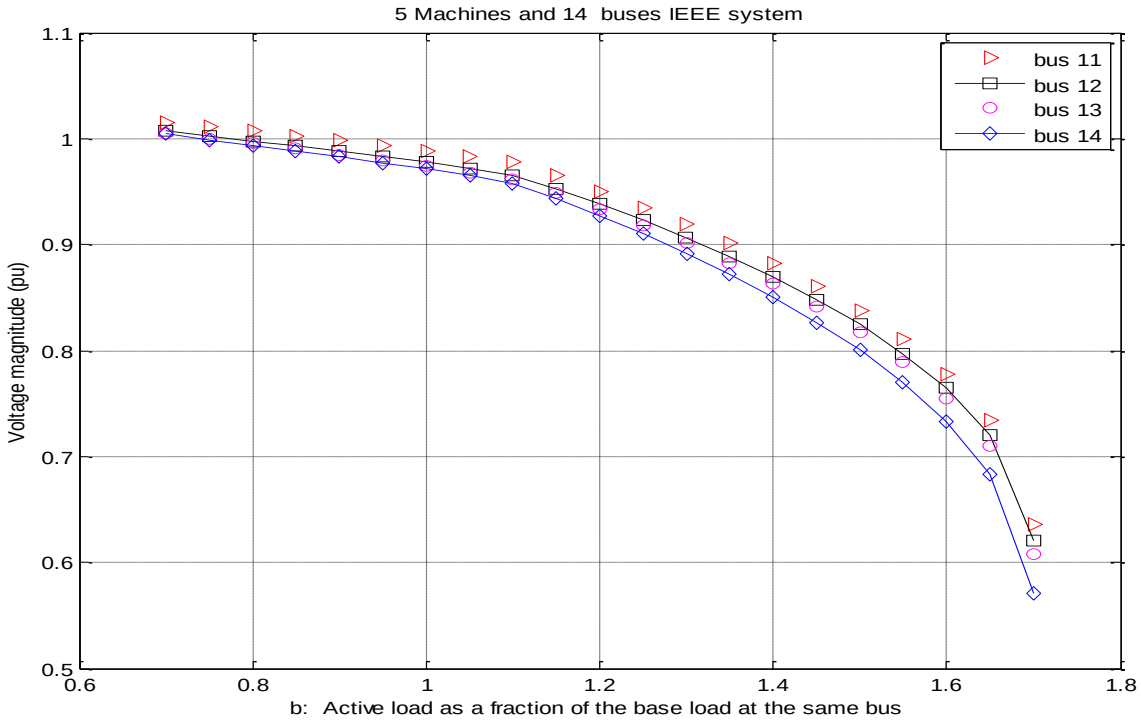

Figure 4.8: P-V curves without contingency

a: Buses 3, 4, 9, 10 b: Buses 11, 12, 13, 14

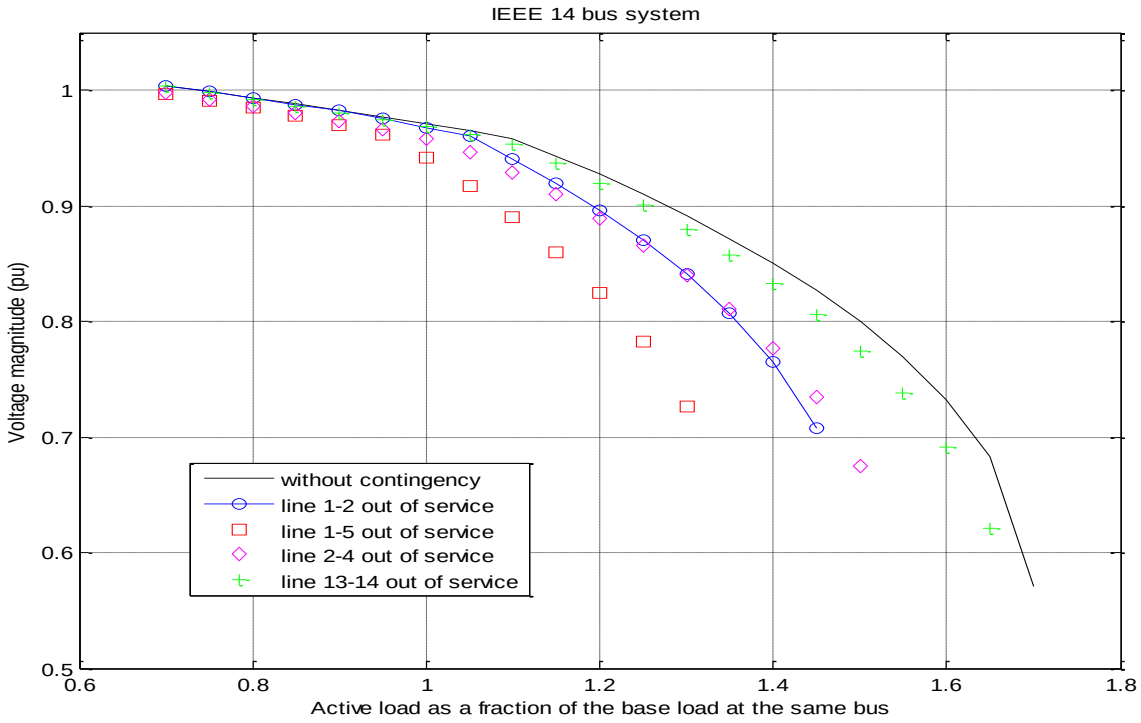

Figure 4.9: P-V curves at bus 14, the weakest bus in the system

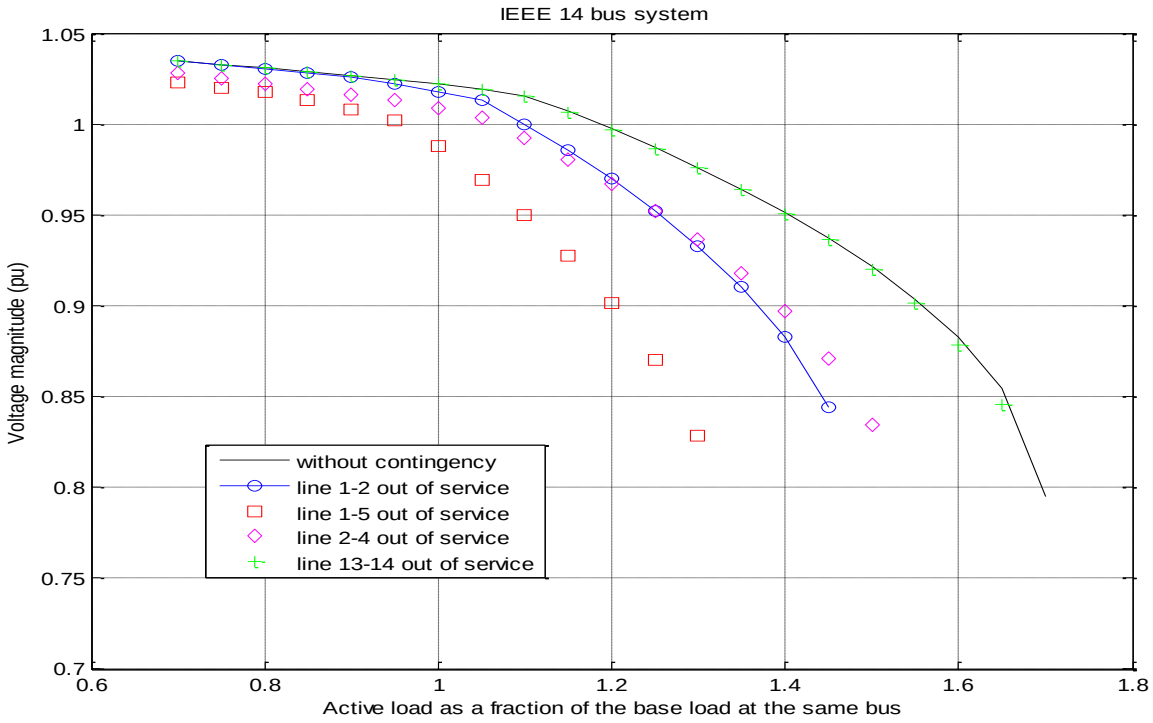

Figure 4.10: P-V curves at bus 5, the strongest bus in the system

Table 4.5: Ranking of (N-1) Contingencies for IEEE 14 bus system

Case #	Contingency		Pmax (PU)	Load margin (PU)	Load margin % of the load margin at base case load	P_{max}/P_{base}
	Line outage					
	From bus	To bus				
1	G1	--	The system cannot meet the power required			
2	2	3	3.3152	0.7252	38.9	1.2800
3	6	5	3.3670	0.7770	41.7	1.3000
4	1	5	3.5224	0.9324	50	1.3600
5	7	9	3.6519	1.0619	56.9	1.4100
6	4	7	3.9368	1.3468	72.2	1.5200
7	1	2	3.8850	1.2950	69.4	1.5000
8	4	5	4.0145	1.4245	76.4	1.5500
9	9	14	4.0145	1.4245	76.4	1.5500
10	2	4	4.0145	1.4245	76.4	1.5500
11	6	13	4.1440	1.5540	83.3	1.6000
12	G6	--	4.1699	1.5799	84.7	1.6100
13	2	5	4.1958	1.6058	86.1	1.6200
14	4	9	4.2217	1.6317	87.5	1.6300
15	G3	--	4.2217	1.6317	87.5	1.6300
16	7	8	4.2217	1.6317	87.5	1.6300
17	G8	--	4.2217	1.6317	87.5	1.6300
18	2G	--	4.2476	1.6576	88.9	1.6400
19	9	10	4.3253	1.7353	93.1	1.6700
20	Cap9	--	4.3512	1.7612	94.4	1.6800
21	3	4	4.3512	1.7612	94.4	1.6800
22	6	12	4.3771	1.7871	95.8	1.6900
23	6	11	4.4030	1.8130	97.2	1.7000
24	13	14	4.4030	1.8130	97.2	1.7000
25	10	11	4.4548	1.8648	100	1.7200
26	11	12	4.4548	1.8648	100	1.7200
27	No Contingency		4.4548	1.8648	100	1.7200

Table 4.6: Ranking of load buses for IEEE 14 bus system

Load bus number	Bus order (smallest = weakest)
4	8
5	9 (strongest)
7	7
9	6
10	4
11	5
12	3
13	2
14	1 (weakest)

4.4.4 Case 4: IEEE 30 bus System

The complete description of this system can be found in [122]. The system has 6 Generators, 30 buses, 4 under load tap changing transformers, and 37 lines. In the base case the total system load is 2.834 pu, the swing bus (bus number 1) generates real power of 2.6098 pu, while the other generators generate 0.4 pu real power. The minimum voltage magnitude is at bus number 30 with 0.9886 pu, and the voltage collapse occurs at a total load of 4.336 pu, with a load margin of 1.502 pu.

Table (4.7) gives the ranking of the load buses of IEEE 30 bus system according to weakness. It shows that bus 30 is the weakest bus, while bus3 is the strongest bus. Table (4.8) lists contingency results for the base case, and all single level (N-1) contingencies according to their impact on the voltage collapse in the same three categories as follows:

1. Acceptable: cases from 12 to 49 in Table (4.8).
2. Significant: cases from 2 to 11 in Table (4.8).
3. Unacceptable: case number 1 in Table (4.8).

The P-V curves at all load buses without contingency, for IEEE 30 bus system, are shown in Figure (4.11). The results given in this figure indicate that bus number 30, the weakest bus in the system, has the lowest voltage at a 1.53 loading factor. This loading factor is the point at which a voltage collapse may occur. On the other hand, the voltage at bus number 3, the strongest bus in the system, has the highest voltage at the same loading factor.

Figure (4.12) gives P-V curves at bus 30, the weakest bus in this system, without contingency and under some selected contingencies. Figure (4.13) shows the P-V curves at bus 3, the strongest bus in the system, without contingency and under the same selected contingencies.

Table 4.7: Ranking of load buses for IEEE 30 bus system

Load bus number	Bus order (smallest = weakest)
3	24 (strongest)
4	23
6	21
7	18
9	20
10	15
12	21
14	17
15	14
16	16
17	13
18	9
19	6
20	8
21	10
22	11
23	7
24	4
25	5
26	2
27	12
28	19
29	3
30	1 (weakest)

Table 4.8: Ranking of (N-1) Contingencies for IEEE 30 bus system

Case #	Contingency		Pmax (PU)	Load margin (PU)	Load margin % of the load margin at base case load	P_{max}/P_{base}
	Line outage					
	From Bus	To Bus				
1	G1	--	The system cannot meet the power requirement			
2	2	5	3.2138	0.3798	25.2863	1.1340
3	1	3	3.4603	0.6263	41.6977	1.2210
4	3	4	3.4858	0.6518	43.3955	1.2300
5	28	27	3.5198	0.6858	45.6591	1.2420
6	4	12	3.6133	0.7793	51.8842	1.2750
7	1	2	3.8259	0.9919	66.0400	1.3500
8	4	6	3.9024	1.0684	71.1318	1.3770
9	6	7	3.9194	1.0854	72.2636	1.3830
10	2	6	3.9194	1.0854	72.2636	1.3830
11	9	10	3.9364	1.1024	73.3955	1.3890
12	27	30	4.0810	1.2470	83.0226	1.4400
13	G8	--	4.0810	1.2470	83.0226	1.4400
14	2	4	4.0980	1.2640	84.1545	1.4460
15	6	9	4.1065	1.2725	84.7204	1.4490
16	G5	--	4.1150	1.2810	85.2863	1.4520
17	12	13	4.1320	1.2980	86.4181	1.4580
18	G13	--	4.1320	1.2980	86.4181	1.4580
19	9	11	4.1490	1.3150	87.5499	1.4640
20	G11	--	4.1490	1.3150	87.5499	1.4640
21	G2	--	4.1575	1.3235	88.1158	1.4670
22	27	29	4.1745	1.3405	89.2477	1.4730
23	6	8	4.2085	1.3745	91.5113	1.4850
24	12	15	4.2085	1.3745	91.5113	1.4850
25	6	28	4.2340	1.4000	93.2091	1.4940
26	10	6	4.2425	1.4085	93.7750	1.4970

Continuation of table 4.8: Ranking of (N-1) Contingencies for IEEE 30 bus system

27	10	20	4.2425	1.4085	93.7750	1.4970
28	Cap10	--	4.2510	1.4170	94.3409	1.5000
29	10	21	4.2595	1.4255	94.9068	1.5030
30	25	27	4.2850	1.4510	96.6045	1.5120
31	22	24	4.2850	1.4510	96.6045	1.5120
32	19	20	4.2850	1.4510	96.6045	1.5120
33	29	30	4.2850	1.4510	96.6045	1.5120
34	15	23	4.2935	1.4595	97.1704	1.5150
35	15	18	4.3020	1.4680	97.7364	1.5180
36	12	14	4.3020	1.4680	97.7364	1.5180
37	12	16	4.3020	1.4680	97.7364	1.5180
38	5	7	4.3105	1.4765	98.3023	1.5210
39	10	17	4.3105	1.4765	98.3023	1.5210
40	10	22	4.3190	1.4850	98.8682	1.5240
41	8	28	4.3190	1.4850	98.8682	1.5240
42	Cap24	--	4.3190	1.4850	98.8682	1.5240
43	23	24	4.3275	1.4935	99.4341	1.5270
44	18	19	4.3275	1.4935	99.4341	1.5270
45	16	17	4.3275	1.4935	99.4341	1.5270
46	25	26	4.3360	1.5020	100.0000	1.5300
47	24	25	4.3360	1.5020	100.0000	1.5300
48	14	15	4.3360	1.5020	100.0000	1.5300
49	21	22	4.3360	1.5020	100.0000	1.5300
50	No Contingency		4.3360	1.5020	100.0000	1.5300

The P-V curves in Figures (4.12) and (4.13) show that the outage of lines connecting buses (6, and 7), and (23, and 24) almost has no effect on the load margin. On the other hand the outage of the generator at bus 2 will decrease the load margin to be 88.1158 %, of the base case load margin.

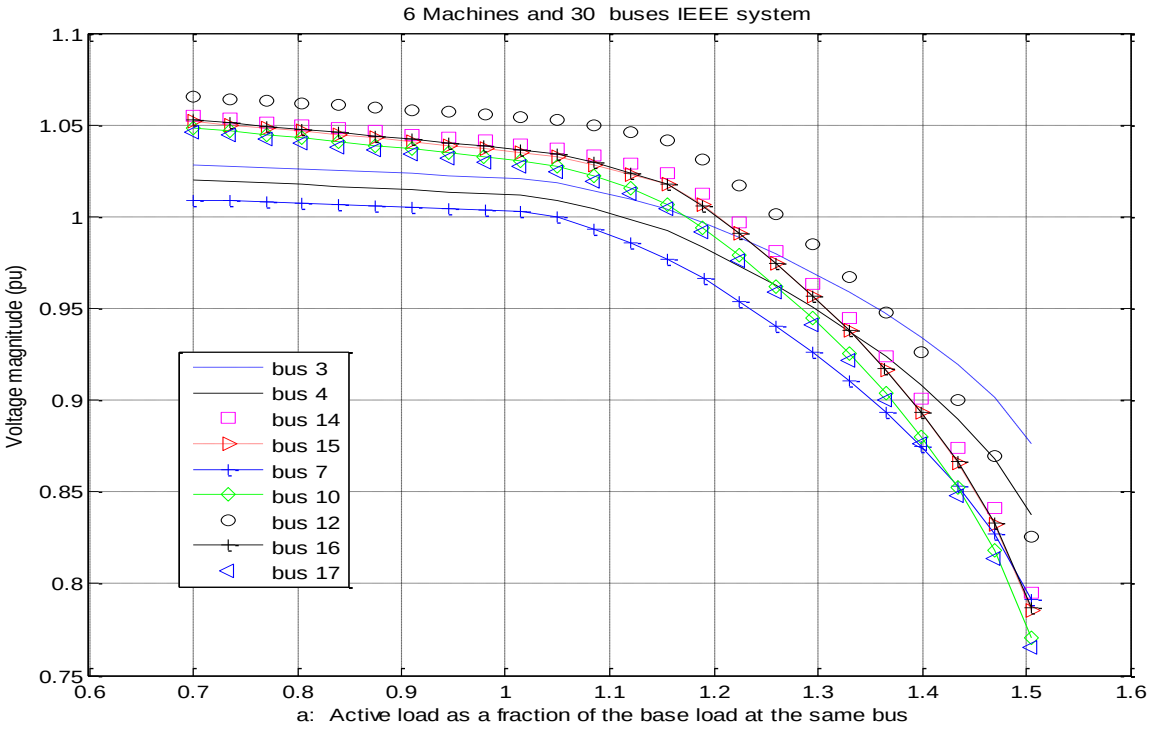

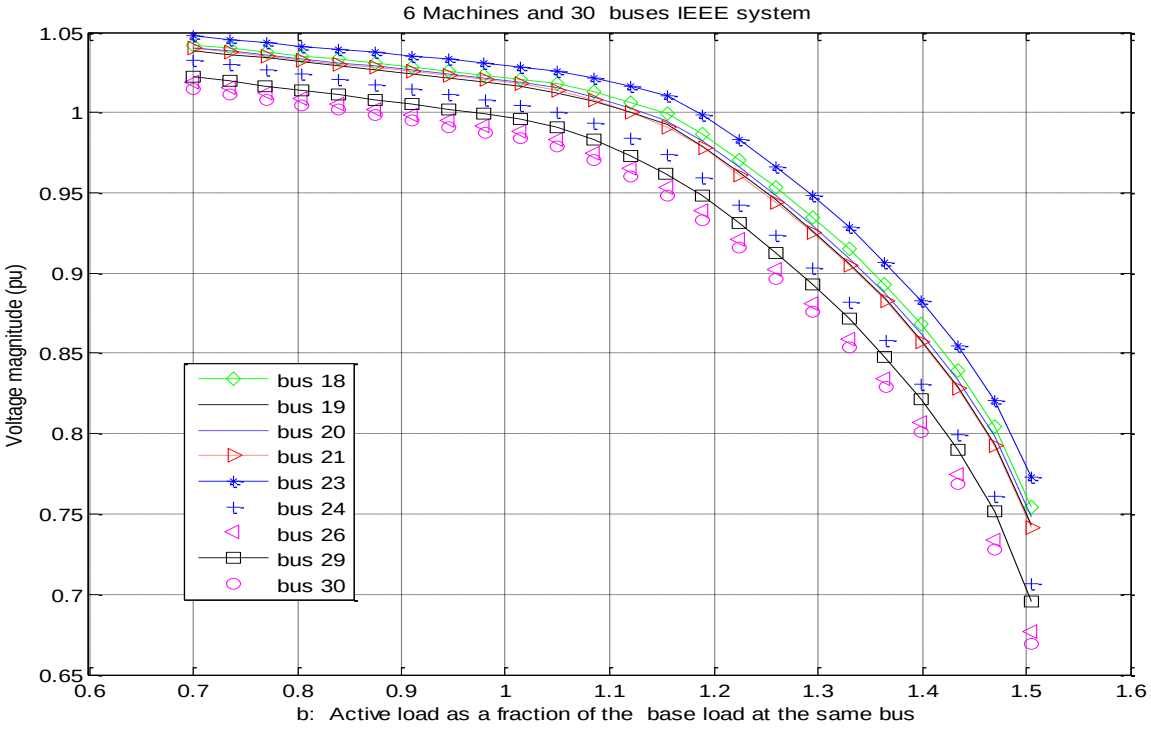

Figure 4.11: P-V curves without contingency

a: Buses 3, 4, 7, 10, 12, 14, 15, 16, 17 b: Buses 18, 19, 20, 21, 23, 24, 26, 29, 30

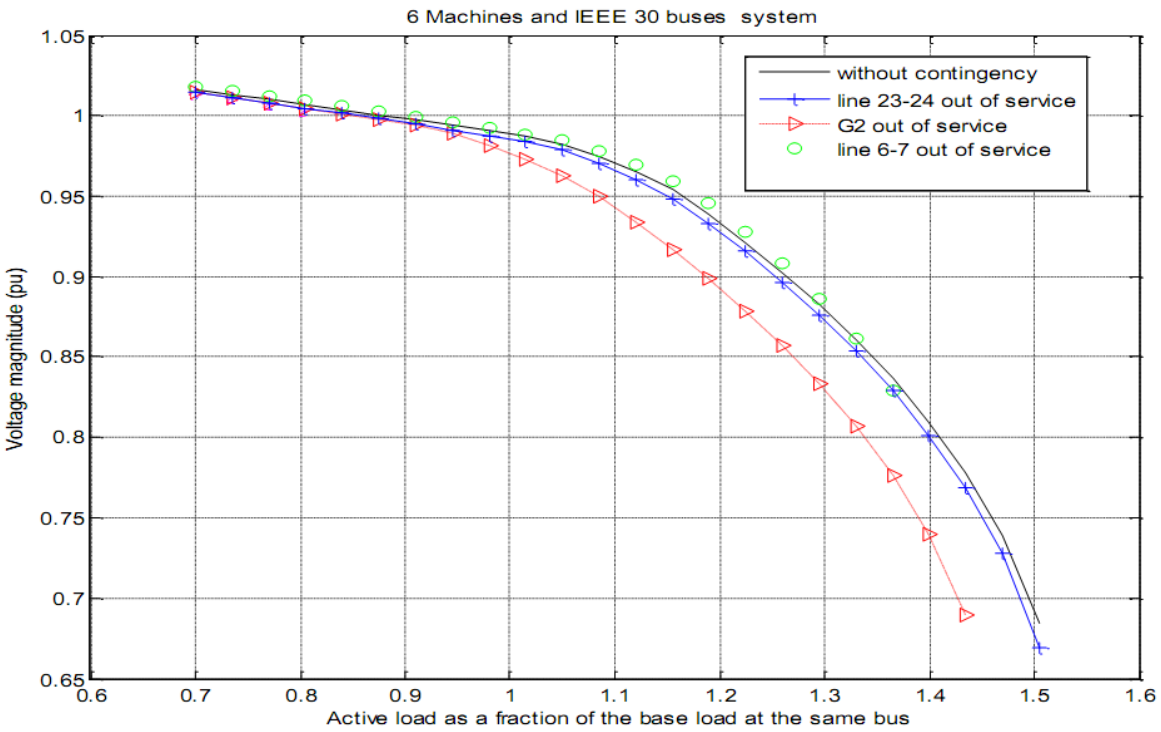

Figure 4.12: P-V curves at bus 30, the weakest bus in the system

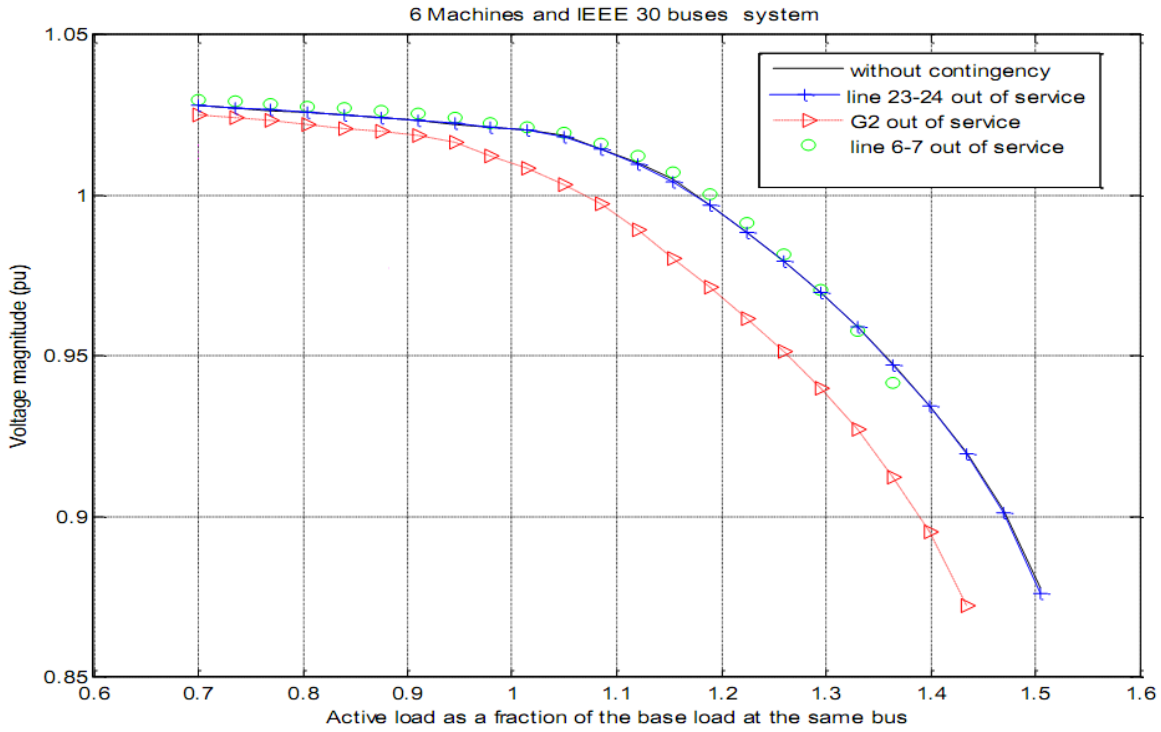

Figure 4.13: P-V curves at bus 3, the strongest bus in the system

4.5 Discussion of Results

4.5.1 Case 1: 6 generator system

All the results for this case indicate that buses 16, 15, and 17 are the weakest buses in the system respectively, so reactive compensation devices should be located at these buses to enhance the system voltage stability.

The system fails to work at all without line 20-21, and has a negative MWM without generator number 5, and line number 19-20, so a lot of concerns and monitoring must be given to those elements.

Generators at buses number 5 and 2 have the largest reactive load in the system 0.33, 0.25 pu respectively, so failure of either one of them causes voltage instability due to the fact that local reactive power support is better.

4.5.2 Case 2: Ward and Hale system

The results for this case indicate that more than 50% of the (N-1) contingencies are unacceptable and the system cannot carry the full load because of those contingencies. The best way to keep the system operational is to do immediate load shedding.

4.5.3 Case 3: IEEE 14 buses system

The results for this system show that out of 26 (N-1) contingencies only one case (loss of swing bus) results in the system being unable to meet its power requirement. Ten cases counted as significant, and the remaining cases are acceptable.

4.5.4 Case 4: IEEE 30 buses system

The results for this system show that out of 49 (N-1) contingencies only one case (loss of swing bus) results in the system being unable to meet its power requirement. Out of 49 cases, 10 cases are significant, the rest are acceptable.

Chapter 5 Artificial Neural Network-Based Voltage Collapse Monitoring

This chapter presents the application of Artificial Neural Networks (ANN) for voltage collapse prediction in a power system to guide the operator in an Energy Control Center (ECC) to prepare ahead of time for imminent voltage stability problems, and take the necessary control action. In this study, a feature reduction technique based on the analysis of the generated data is used to decrease the number of inputs fed to ANNs, and so decrease the number of physical quantities need to be measured. In this research, a comparison between the performances of two different voltage collapse indices is investigated, namely: minimum singular value decomposition (MSV) and voltage stability *L* index for use with ANNs. The effectiveness of the proposed algorithm is tested under a large number of different operating conditions on the IEEE 14 bus system. The results show that the proposed feature reduction algorithm gives encouraging results.

5.1 Introduction

With the increased loading and exploitation of the power transmission system, the problem of voltage stability and voltage collapse is attracting more and more attention. Voltage collapse can take place in systems or subsystems and can appear quite abruptly, which requires improved continuous monitoring of the system state.

The problem of voltage collapse may be simply explained as an inability of the power system to supply reactive power or as an excessive absorption of reactive power by the system itself. It is to be understood as a reactive power problem, and it is strongly affected by the load behavior. Voltage instability is one phenomenon that could happen in a power system due to its stressed condition. The result may be the occurrence of voltage collapse which may lead to total blackout of the whole system. Therefore voltage collapse prediction is very important in power system planning and operation so that the occurrence of voltage collapse may be avoided. Artificial Neural Networks (ANN) are emerging as an Artificial Intelligence (AI) tool which give fast and acceptable solutions in real time as they mostly use parallel processing techniques for computation.

5.2 Voltage Stability Indicators

5.2.1 Voltage Stability Index L

A static voltage stability index *L* for online application based on normal load flow solution, has been proposed by Kessel and Glavitsch [62], the aim of this method is to detect the voltage instabilities in the power system. The authors have shown that the value of this index *L* must lie within a unit circle, with a range *L*=0 (no load on the system) to *L*=1 (voltage collapse point). The value of *L* is computed for each load bus in the system. The bus having the maximum value of the *L* index, is the weakest bus in the system and is taken as the point from which the voltage collapse usually starts. The stability margin for the system in this case is obtained as the distance of maximum *L* from a unit value, i.e., (*1-L*). This method has the advantage of very simple calculations, and the values of *L* for all individual load buses are useful in identifying the most critical buses in the system.

For a power system with a total number of busses equal to n, and the number of generator buses equal to g, the number of the load buses is equal to (n-g). At a given operating condition for a power system, the bus voltage and power flow data can be obtained from a load flow program, otherwise these results are available from the output of an on-line state estimator. Using these load flow results, the *L* index is computed as follow:

$$L_j = \left|1 - \sum_{i=1}^{g} F_{ji} \frac{V_i}{V_j}\right| \tag{5.1}$$

where:

i: Represents any generator bus in the system *i*=1,…,g.

j: Represents any load bus in the system *j* =g+1, ..., n.

V_i: Represents the voltage as a complex value at a generator bus number *i*.

V_j: Represents the voltage as a complex value at a load bus number *j*.

F_{ji}: These values are obtained from the Y bus matrix as follows:

$$\begin{bmatrix} I_i \\ I_j \end{bmatrix} = \begin{bmatrix} Y_{ii} Y_{ij} \\ Y_{ji} Y_{jj} \end{bmatrix} \begin{bmatrix} V_i \\ V_j \end{bmatrix} \tag{5.2}$$

where:

I_i, I_j and V_i, V_j: represent currents and voltages at the generator and load buses .

Y_{ii}: is a sub-matrix with dimension (g x g).

Y_{ij}: is a sub-matrix with dimension (g x (n-g)).

Y_{jj}: is a sub-matrix with dimension ((n-g) x (n-g)).

Y_{ji}: is a sub-matrix with dimension ((n-g) x g).

Rearranging Equation (5.2) in order to separate V_j, and I_i in the LHS, we get

$$\begin{bmatrix} V_j \\ I_i \end{bmatrix} = \begin{bmatrix} Z_{jj} F_{ji} \\ K_{ij} Y_{ii} \end{bmatrix} \begin{bmatrix} I_j \\ V_i \end{bmatrix} \tag{5.3}$$

where:

$Z_{jj}=[Y_{jj}]^{-1}$: is a sub-matrix with dimension ((n-g) x (n-g)).

$K_{ij}=[Y_{ij}][Y_{jj}]^{-1}$: is a sub-matrix with dimension (g x (n-g)).

$[Yii]=[Yii]-[Yij][Yjj]^{-1}[Yji]$: is a sub-matrix with dimension (g x g).

$[F_{ji}] = -[Y_{jj}]^{-1}[Y_{ji}]$: is a sub-matrix with dimension ((n-g) x g), and represents the matrix to be substituted into Equation (5.1).

The *L* indices for a given load condition are computed for all load busses, and must be bounded between 0 (no load condition) and 1 (the point of voltage collapse) for any stable system, the overall stability of the system can be found from the maximum value of the L_j which represents the *L* index at the weakest bus in the system.

An *L* index value away from 1 and close to zero indicates improved system security. For a given network, as the load/generation increases, the voltage magnitude and angles change. For near maximum power transfer conditions, the voltage stability indices, L_j, for load buses tend to approach 1, indicating that the system is close to voltage collapse. The stability margin is obtained as the distance of maximum *L* from a unit value i.e. (*1-L*).

5.2.2 Minimum Singular Value (MSV)

The minimum singular value of the power flow Jacobian matrix, obtained from a full singular value decomposition of the power flow Jacobian matrix, was proposed as a measure of the static voltage stability of the power system as indicated in the literature. At the point of voltage collapse there is no possibility of getting a physical load flow solution, where the load flow Jacobian matrix will become singular. At an operating point, the distance of the minimum singular value from zero is the measure of proximity to voltage collapse, and so the proximity to voltage collapse can be traced by monitoring of the minimum singular value (σ_n) from zero.

For a power system with a total number of equations in the Jacobian matrix (J) equal to n, the Jacobian matrix is (n x n), and the singular value decomposition is given by:

$$J = U \sum V^T = \sum_{i=1}^{n} u_i \sigma_i v_i^T \tag{5.4}$$

where, U and V are $(n \times n)$ orthonormal matrices whose ith columns are the singular vectors u_i and v_i, respectively, and Σ is a diagonal matrix of positive real singular values σ_i such that $\sigma_1 \geq \sigma_2 \geq \ldots \geq \sigma_n$. Based on the singular value decomposition of the power flow Jacobian matrix, the smallest singular value, σ_n, is an indicator of the proximity to the steady state stability limit.

An important property of the singular value decomposition which is worth noticing is that by adding a column to the studied matrix, the largest singular value will increase and the smallest singular value will diminish. This important in this work because the size of the power flow Jacobian matrix will increase with one row and one column each time a generator bus (PV bus) hits its limitation for the reactive power capability and changes into a load bus (PQ bus). This change in dimension of the matrix will, as described above, reduce the numerical value of the minimum singular value for the studied matrix. The matrix under consideration in this case is the power flow Jacobian matrix (J) which is expressed as;

$$\begin{bmatrix} \Delta P \\ \Delta Q \end{bmatrix} = \begin{bmatrix} J_1 & J_2 \\ J_3 & J_4 \end{bmatrix} \begin{bmatrix} \Delta \delta \\ \Delta v \end{bmatrix} \tag{5.5}$$

The MSV of the different sub-matrices (J_1, J_4 and J_{4R}) can be also used as an indicator. MSV of sub-matrices can be analyzed in real practice because it can save computing burden of computing MSV of J, while still providing meaningful sensitivity information. J_4 and J_{4R} provide sensitivity information between reactive power injection and voltage at buses (Q-V sensitivity). J_{4R} considers further the weak coupling between reactive power and angle (by assuming ΔP in Equation (5.5) equal to zero) where, $J_{4R} = J_4 - J_3 J_1^{-1} J_2$.

5.3 Proposed ANN- Based Methods

5.3.1 Data generation

Training, validation and testing data sets for the ANNs are generated using the power system toolbox (PST) [120] and MATLAB Neural Network Toolbox [123]. Two types of data sets are generated as follows:

1. Increasing both real and reactive power in 1% steps from base case at all load buses at constant power factor until the system collapses.
2. Increasing the active and reactive power in 10% steps from base case at a particular load bus, until the system collapses, with the load at the other load at other buses remaining constant. This process is repeated at every load bus.

The corresponding voltage stability indicators, MSV and L-index are calculated at every step.

5.3.2 Back Propagation-ANN

A multi-layered feed-forward neural network has been proved suitable for most power system problems [124]. The architecture of the ANN used in this paper consists of an input layer, two hidden layers and an output layer. The number of inputs depends on the number features used. The number of output neurons is equal to the number of load buses for the L index-based method and equal to one for MSV-based method. After many trials, the sigmoid activation function (logsig) is chosen for the hidden layers, while the linear activation function (purelin) is chosen for the output layer. The number of neurons in hidden layers is variable based on the best results. The ANNs are trained by the back propagation algorithm using Lavenberg-

Marquartdt (LM) optimization. Validation technique is applied to improve ANN generalization by preventing the training from over-fitting the problem. In the context of neural networks, over-fitting is also known as overtraining where further training will not result in better generalization. The error of the validation set is periodically monitored during the training process. The training error usually decreases as the number of iterations grows, and so does the validation error. When the overtraining starts to occur, the validation error typically tends to increase. Therefore, it is useful and time saving to stop the training after the validation has increased for some specified number of iterations [123].

5.4 Methodology

The Matlab PST is used to simulate the IEEE 14 bus system. Figure (5.1) shows the IEEE 14 bus system.

The steps in this study are carried out as follows:

1. Input bus and line data which include generation active and reactive power, load active and reactive power, and line parameters.
2. Run load flow at base case and calculate the MSV and L-index for every load bus.
3. Run load flow for all generated data and calculate the MSV and L-index for every load bus.
4. Create a data base for the input vector based on the selected features and for the target vector based on the selected index.
5. Normalize the input vectors.
6. Divide input data into training, validation and testing sets.
7. Select ANN parameters to train the network.
8. Compute the validation error periodically.
9. Check if the validation error starts to increase or not.
10. Stop the training if the validation error starts to increase.
11. Test the ANN, if the results are satisfied, go to step 12. Else repeat Steps from 6 to 11.
12. Calculate the ANN estimation error and stop.

5.5 Results and Discussions

In order to test the ability and effectiveness of the proposed ANN in predicting voltage instability in a power system, the standard IEEE 14 bus system is used. It consists of five PV buses, buses (1, 2, 3, 6 and 8), and nine PQ or load buses. In this study, active and reactive load power were increased at constant power factor with a constant step size until the collapse is reached. At every step the power flow program was run. The voltage magnitude (V) and angle (δ) , active and reactive power demand (P_l, Q_l) and active and reactive power generation (P_g,Q_g) at every bus were obtained. A total of 84 features for that system (14 bus x 6 measurements for every bus) can be used as element of the input vector for the neural network. 1309 different cases were generated, 60% of them were used for training, 20% for validation and the final 20% were used for testing the generalization of the neural network. The simulation result at base case load flow shows that bus 14 is the most critical load bus, while bus 5 is the strongest load bus in IEEE 14 bus system.

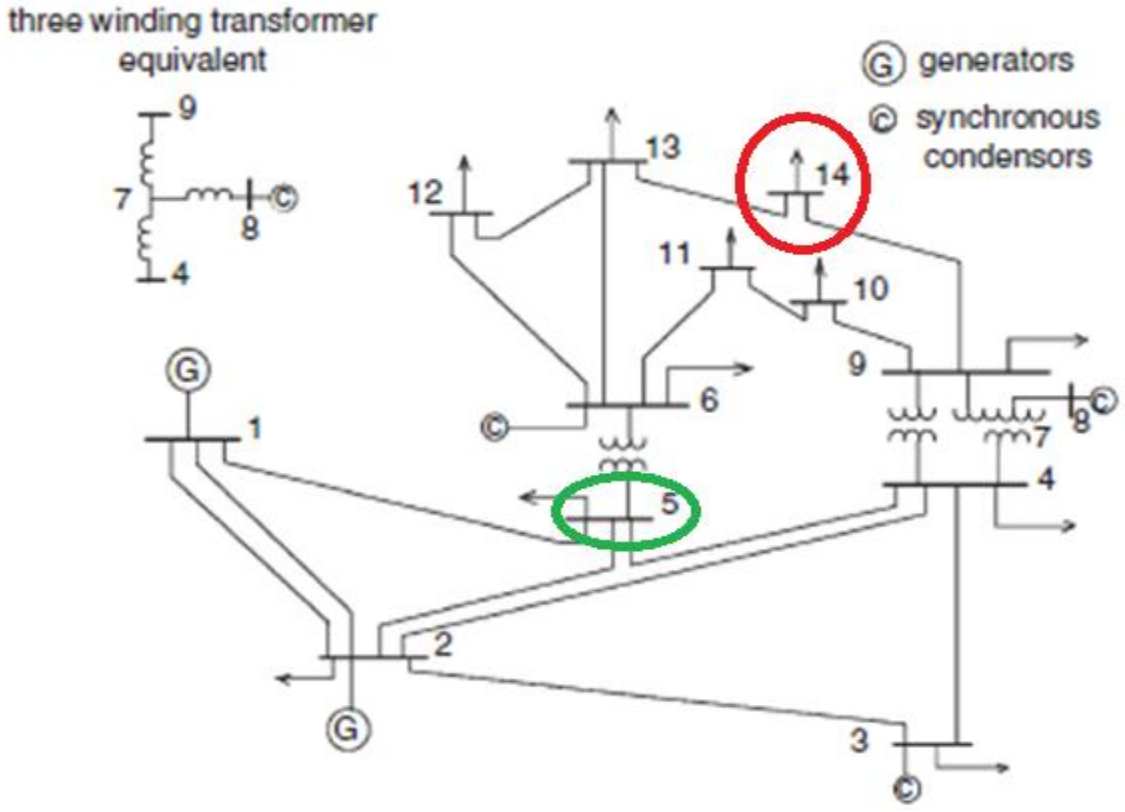

Figure 5.1: IEEE 14 bus system

In this work there are four different neural networks, two for MSV index and two for L-index. Two different numbers of features were used; one has 53 inputs which represent all the measurable variables in the system while the other used 12 inputs selected after studying the results of power flow simulation. These 12 inputs are Pl_3, V_3, Pl_{10}, V_{10}, Pl_{11}, V_{11}, Pl_{12}, V_{12}, Pl_{13}, V_{13}, Pl_{14}, and V_{14}. The details of the four different neural networks are shown in Table (5.1). The first number in the ANN architecture refers to the number of inputs, the second number is the number of neurons in the first hidden layer, the third number shows the number of neurons in the second hidden layer, and the last number refers to the number of outputs.

Many trials were done for every network until reaching the best results which were confirmed by testing their generalization. Figures (5.2), (5.3) and (5.4) show the MSV ANN results at different loading levels for both the target and neural network output using 53 input features under three different scenarios. These scenarios are: load increase at all load buses simultaneously, load increase at bus 14 only (the weakest bus) and load increase at bus 5 only (strongest bus), respectively. Figures (5.5), (5.6) and (5.7) show the MSV ANN results at different loading levels for both the target and neural network output using 12 input features under the same three scenarios respectively. The MSV ANN, estimated absolute error and the percentage error with 12 different scenarios for the whole system with 53 and 12 input features are shown in Figures (5.8) and (5.9), respectively. The results for the L-index ANN for two different networks with 53 and 12 input features are shown in Figures (5.10) and (5.11), respectively. Each figure has nine curves, and every curve represents the results for one load bus.

In the MSV case as shown in Figures (5.8) and (5.9), the absolute error is less than 0.02 for 53 inputs and less than 0.1 for 12 inputs. While in the L-index ANN case, as shown in Figures (5.10) and (5.11), the absolute error is almost the same in both cases and is less than 0.007, this means that using 12 inputs only, rather than 53 almost gives comparable results. Thus the proposed feature reduction method is highly recommended to be used in order to decrease the number of inputs (the number of monitored variables).

Figures (5.2) through (5.7) show that the absolute error for the MSV indicator occurs when the system is far away from instability. This means that this small error will not affect the decision of the power system operator.

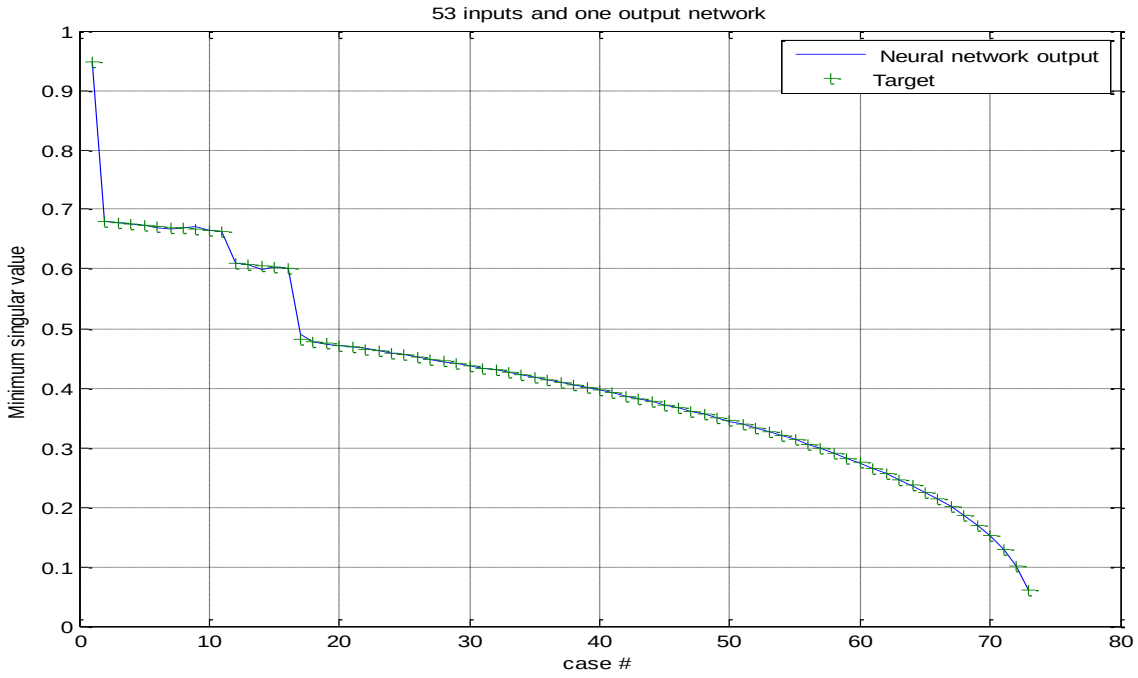

Figure 5.2: Minimum singular value for 53 input features network with load increase at all load buses simultaneously

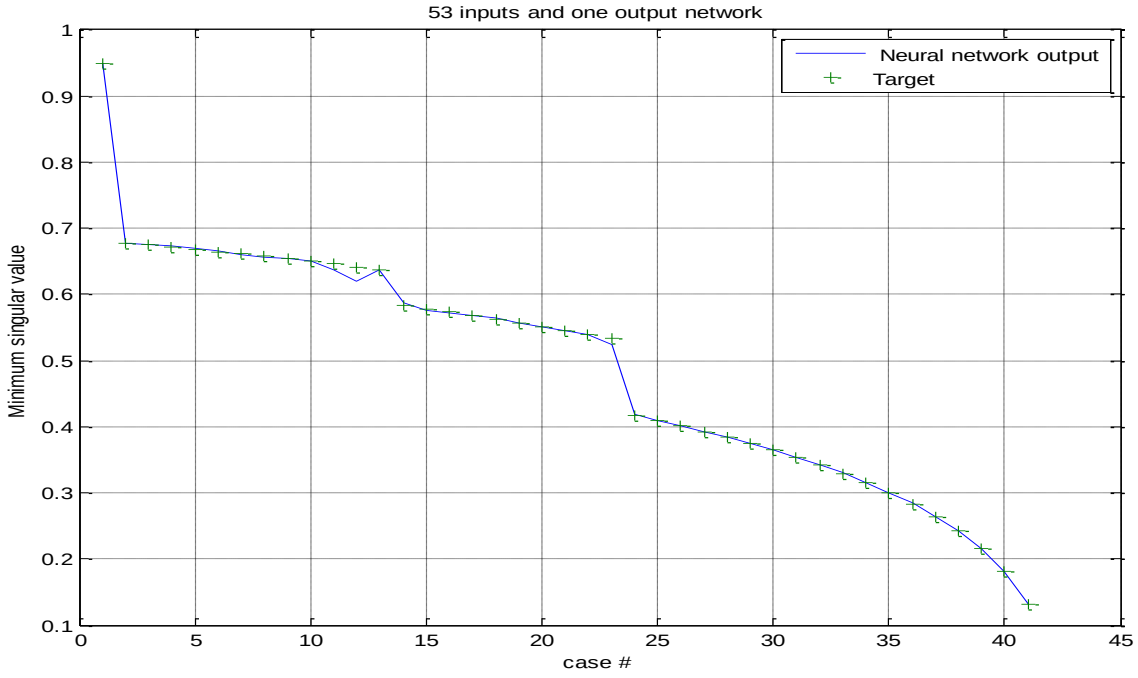

Figure 5.3: Minimum singular value for 53 input features network with load increase at bus 14 (weakest bus) only

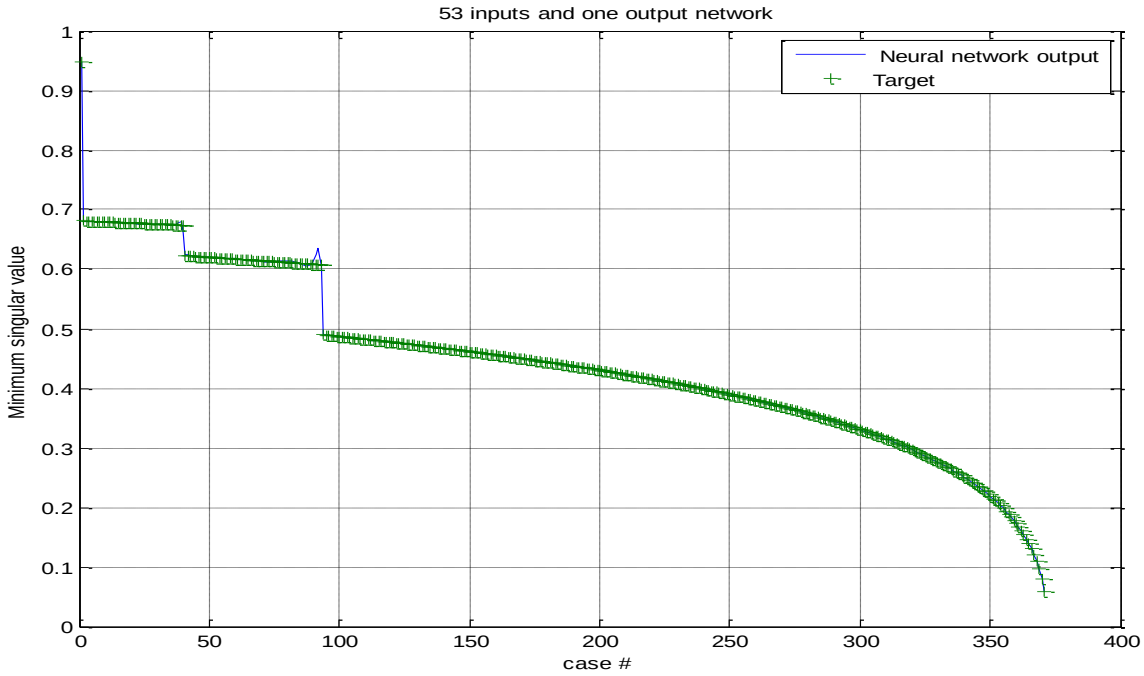

Figure 5.4: Minimum singular value for 53 input features network with load increase at bus 5 (strongest bus) only

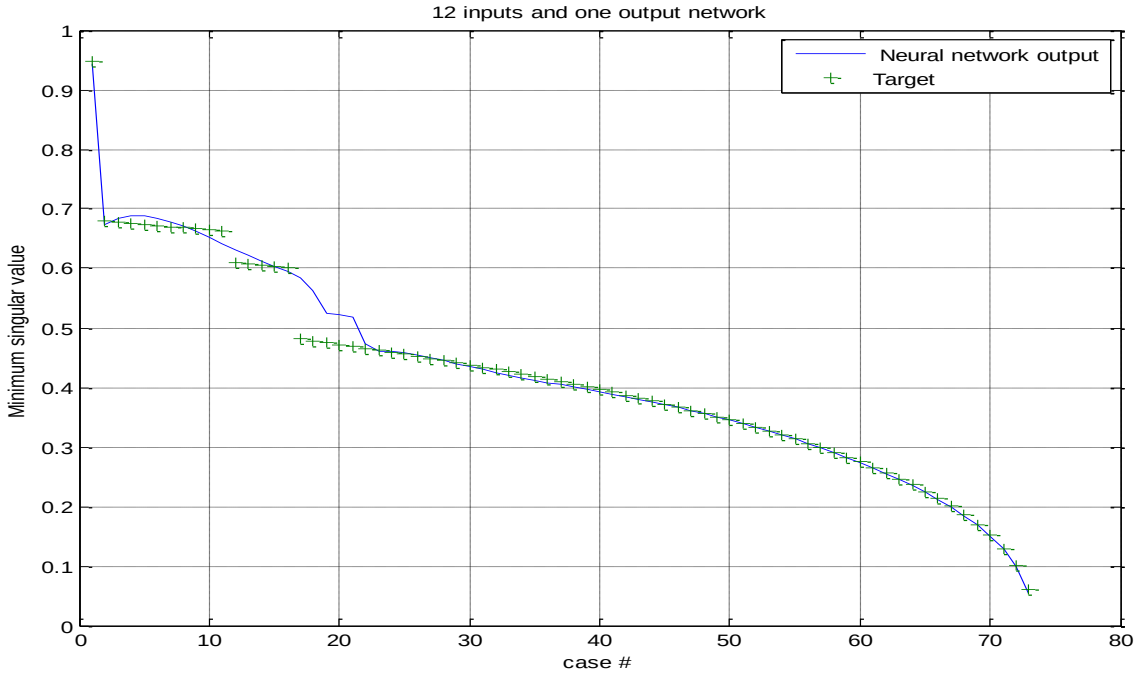

Figure 5.5: Minimum singular value for 12 input features network with load increase at all the load buses simultaneously

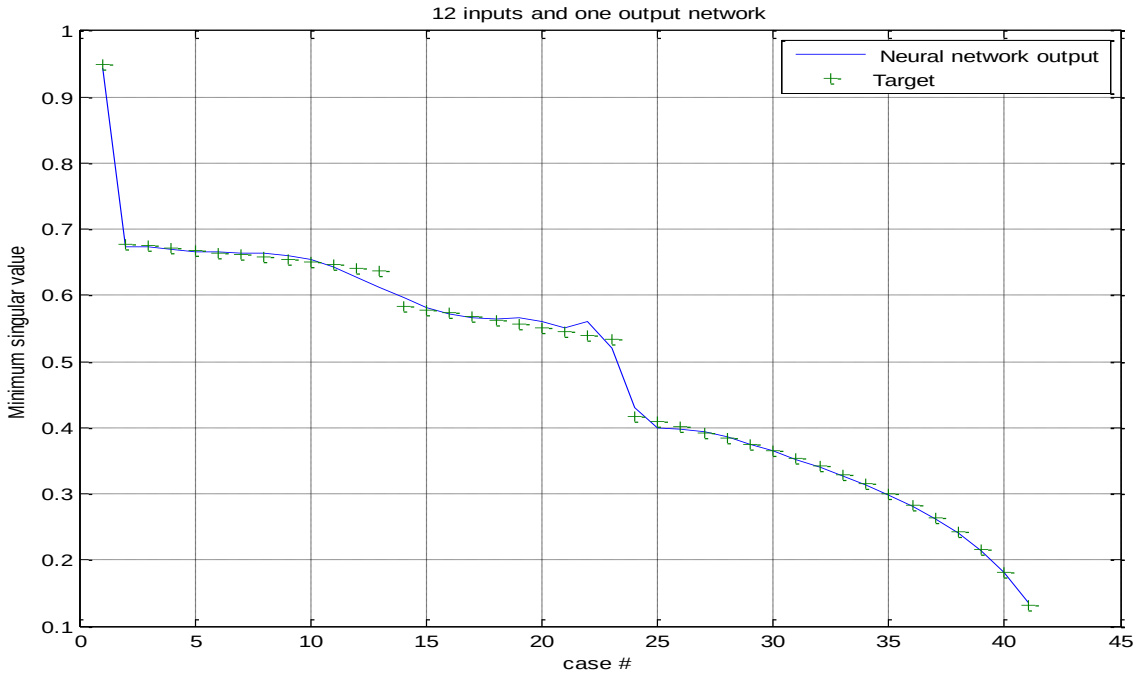

Figure 5.6: Minimum singular value for 12 input features network with load increase at bus 14 (weakest bus) only

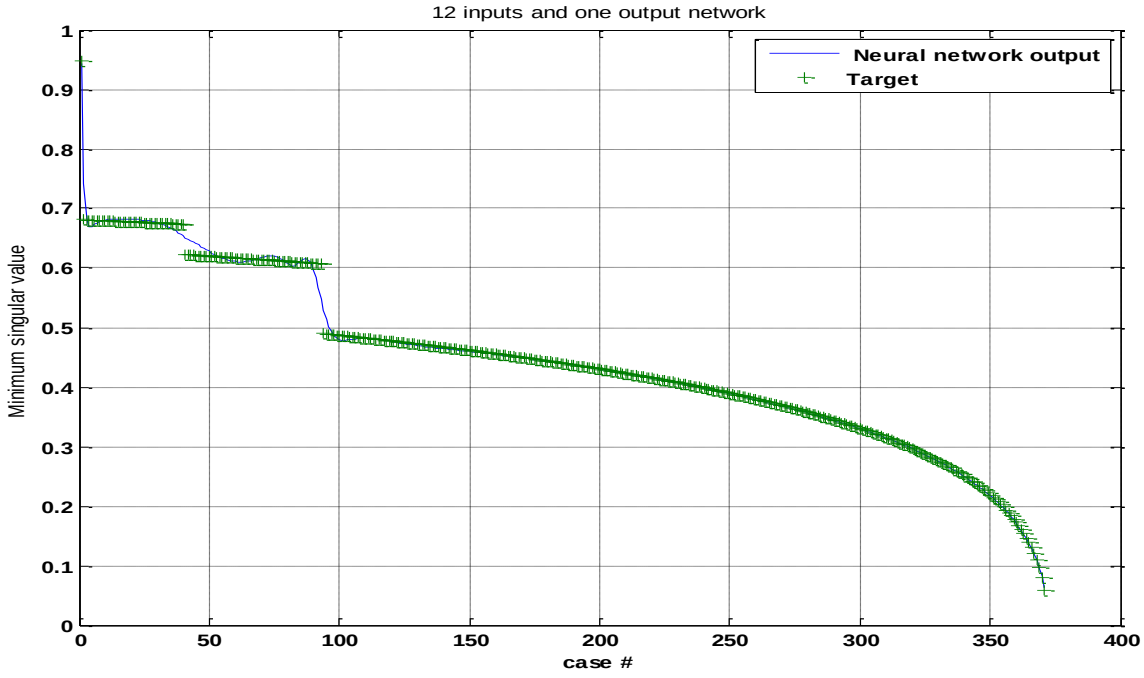

Figure 5.7: Minimum singular value for 12 input features network with load increase at bus 5 (strongest bus) only

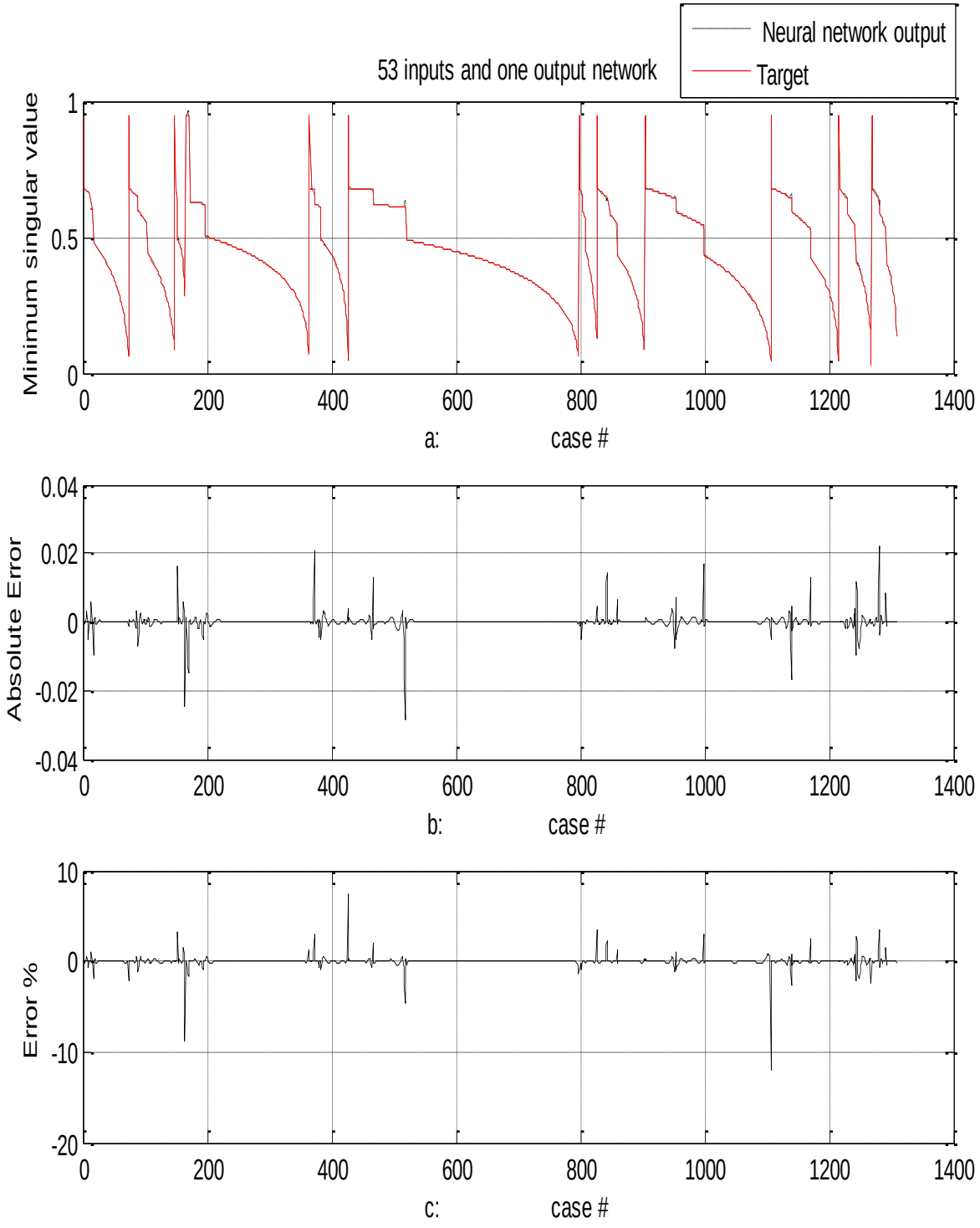

Figure 5.8: Minimum singular value estimation error for 53 input features network

a) Minimum singular value b) Absolute error c) Percentage error

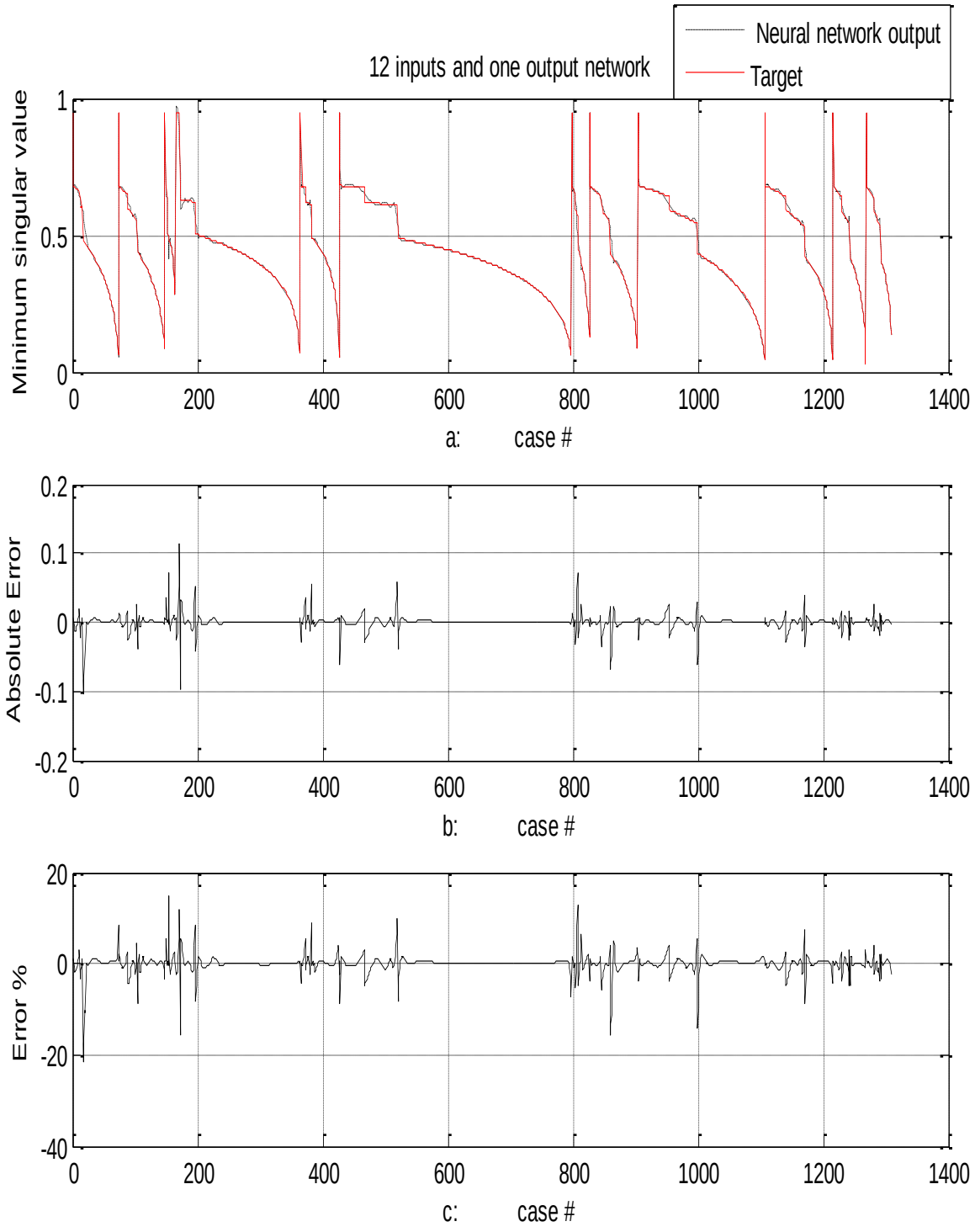

Figure 5.9: Minimum singular value estimation error for 12 input features network

a) Minimum singular value b) Absolute error c) Percentage error

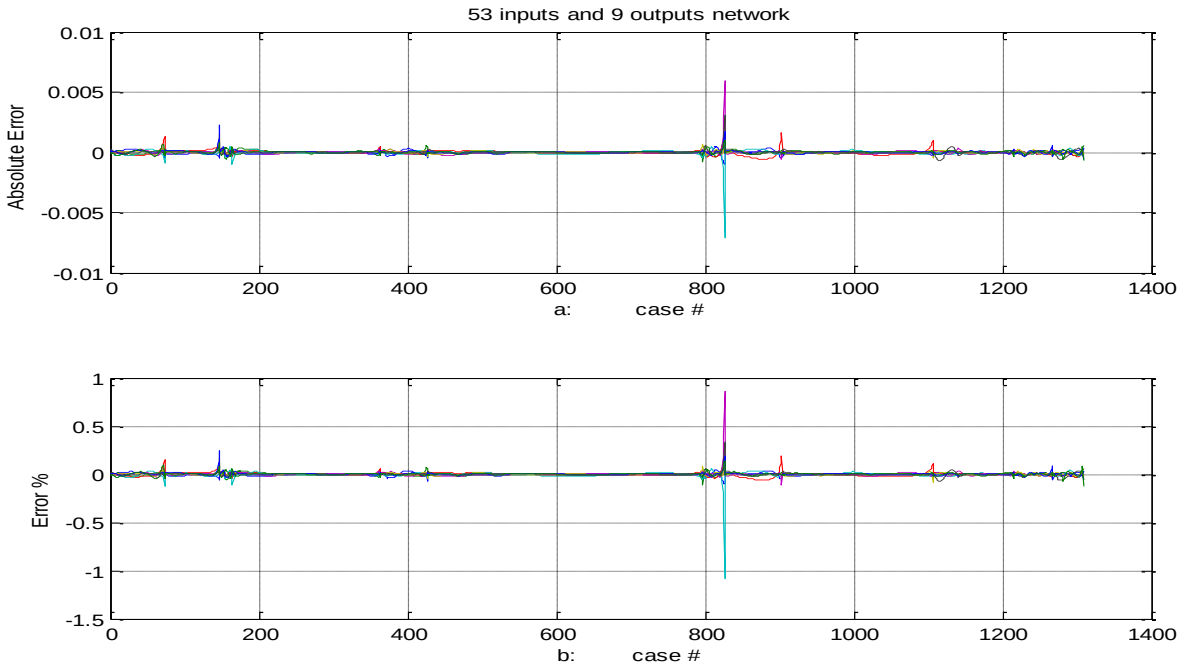

Figure 5.10: L-index estimation error for 53 input features network

a) Absolute error b) Percentage error

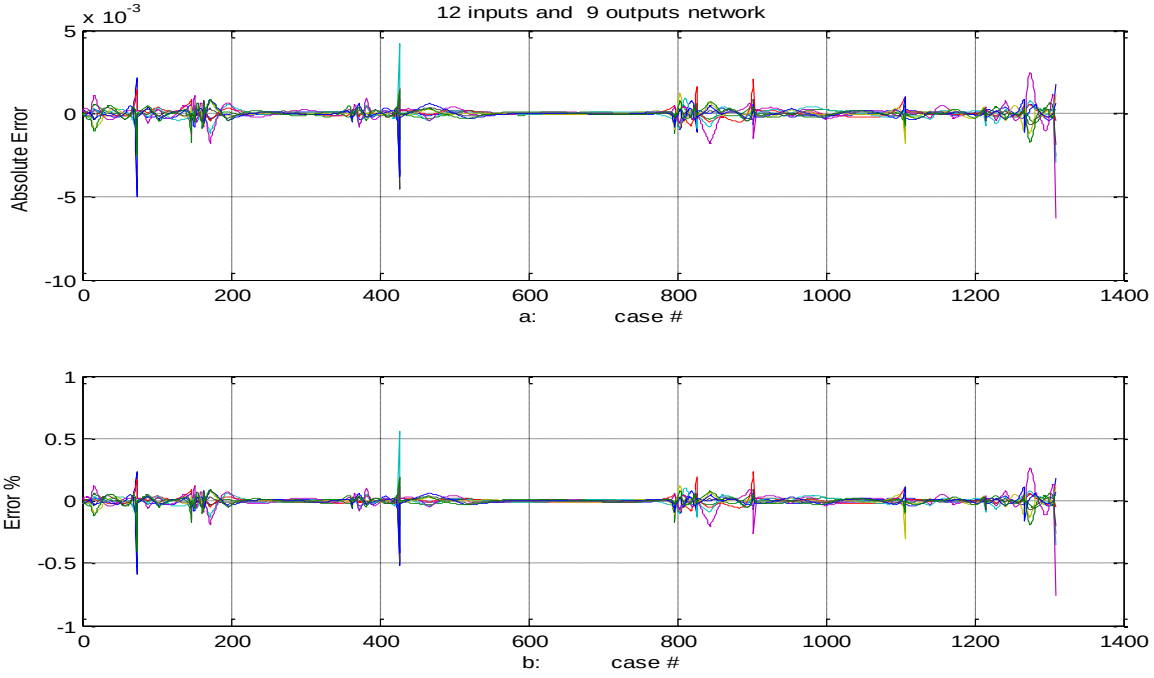

Figure 5.11: L-index estimation error for 12 input features network

a) Absolute error b) Percentage error

Table 5.1: Comparison of Four Different ANNs

No. of features	MSV network architecture	L-index network architecture
53	53:18:7:1	53:18:8:9
12	12:18:8:1	12:18:10:9

5.6 Conclusion

In this study an ANN approach is proposed to predict voltage instability proximity. The proposed algorithm is fast, reliable, accurate, and strongly suitable for on-line application. In this work two different indicators are used, MSV and L-index, to predict the proximity of voltage collapse, both MSV and L-index networks are used to predict the proximity of voltage collapse on IEEE 14 bus system.

One objective of this study is to compare different number of input features; the other objective is to compare two different indicators of voltage collapse proximity. Regarding the number of input features, the 53 input features network gave better results but still comparable to the results of 12 input features network with the MSV indicator. On the other hand the time consumed in 12 input networks is almost one forth that of 53 input networks. Based on this fact the 12 inputs network is more suitable for online application. The two networks almost have the same absolute error with the *L* indicator

The adopted MVS ANN algorithm gives information about the status of the whole system, while L-index ANN algorithm gives information about each load bus individually. The obtained results for voltage instability proximity from the proposed four networks are very close to the actual value of both of the indicators, but the two 12 input networks respond faster than the two 53 input networks.

The proposed approach can be applied for real world application to help the power system operator taking the suitable control action regarding the status of the system.

Chapter 6 Fast and Optimal Reactive Power Control

This chapter proposes three different algorithms for solving the reactive power control problem. The first method has the objective of minimizing the number of control actions, i.e., the number of controllers that must be changed in order to achieve a satisfactory voltage profile for the controlled system, under the constraints of: reactive power limits of the generators, voltage magnitude limits at all load buses, and the operating limits of the control variables. The control variables used are: generator terminal voltages, transformer tap setting, and switchable reactive power resources. The second and third methods perform reactive power optimization by using genetic algorithms. The objective function for the second algorithm is designed to minimize the system power losses (P_L), while the objective function for the third algorithm is selected to minimize the sum of the squares of the voltage magnitude deviations at the load buses (V_d). All the three algorithms employ linearized sensitivity relationships of the power system variables to establish the objective functions, and system performance sensitivities relating dependent and control variables. This is achieved while satisfying constraints for both control and dependent variables. The three algorithms mentioned above have been tested on the Ward and Hale 6 bus system, the modified IEEE 14 bus system, and the modified IEEE 30 bus system, the results showed that each method was successful on each of the three systems

6.1 Introduction

Maintaining the voltage profile within specified limits for high quality of services at each consumer load point is one of the most important operating tasks of a power utility operator. As the power system becomes more complicated and the number of voltage regulating facilities installed in the system increases, the voltage control problem tends to be more complex and more difficult to handle. The variations in load and generation profiles during normal and abnormal operating states of a power system may worsen the voltage profile at different nodes. This is so, because sustained or intermittent over-voltages ultimately lead to equipment insulation failure. On the other hand, under-voltages adversely impact the system voltage stability margin and bulk power carrying capacity of transmission lines which, if left unchecked, can lead to steady state or dynamic voltage collapse phenomenon. Consequently, the power utility operator in the energy control center must re-dispatch the reactive power control devices such as generators, tap

positions of under-load tap changer of transformers, static shunt capacitors, shunt reactors, and FACT in order to maintain system voltage stability.

Over the years, many useful studies [102, 125, 126, 127] based on traditional techniques for solving the reactive power dispatch problem have been carried out. This includes successive linear programming (LP), nonlinear programming (NLP), mixed integer programming, Newton, and quadratic techniques. Most of these approaches can be classified as constrained optimization techniques. Undoubtedly, the reactive power control problem is essentially a global optimization problem with several local minima. The first obvious problem is the case where a local minimum is returned instead of a unique global minimum. The second difficulty is the inherent integer (not continuous) nature of the problem. Most control devices (transformer tap positions, shunt capacitor, and reactor banks) have pre-specified discrete state values. Thus no matter the accuracy of the continuous solution, it is impossible, without making some reasonable approximations, to assign these values directly to the physical control devices.

6.2 Problem Statement

Any changes to the power system configuration or in power demands can result in higher or lower voltages in the system. After those changes, redistribution of the available reactive power generation is necessary for the system voltage profile to be maintained within the pre-specified limits. Reactive power distributions in the system can be controlled by the system operators by suitably adjusting the following controllable variables:

- generator terminal voltage magnitude set point
- taps of the under-load tap changing transformers.
- Set points of switchable shunt capacitors and inductors

These control variables each has upper and lower limits. Any change in one of these control variables has the effect of changing the reactive power output of generators, the system voltage profile, and the system losses. The operators control of these control variables is indirectly limited by the constraints of the dependent variables, i.e., limits of the voltage magnitudes at all load buses, the reactive power limits of all the generators in the system, and the thermal limits of the other components in the power system. So, the problem that faces the

operator in the energy control center is to find a set of adjustments to the available control variables that satisfies the power system performance constraints and the limiting constrains for both control and dependent variables. This is to be done while simultaneously minimizing the overall power losses in the system. Minimizing the power losses in the power system will increase revenue, and so any small percentage of savings in power losses will increase the profits due to the fact that the total power generated is on the order of thousands of megawatts.

6.3 Effect of Control Variables on the Power System Performance

The IEEE 14 bus system at full load level is used to study the effect of the nine control variables on the power system performance. In this system, there are three tap changing transformers, t_{65}, t_{47}, and t_{49}, one capacitor at bus nine, in addition to the terminal voltage magnitudes of the five generators (at buses 1, 2, 3, 6, and 8). All these control variables were used in order to enhance the system performance after being subjected to any disturbance, such as load change, and/or N-1 contingency, using many methods in this chapter and Chapter 7.

In order to investigate the effect of any change in these control variables on the power system performance, such as active power losses, reactive power losses, minimum singular variable, the active power generated from the swing bus, and the reactive power generated from the swing bus. The status of each control variable was varied from its lower limit value to its upper limit value in increments equal to 0.01, assuming that is the defined step for all the controllers. After every change in one control variable, keeping the other eight at their pre-specified values, a load flow was performed using the Newton Raphson method to calculate the system performance. All the results are plotted in the following fifteen figures.

6.3.1 Effect of Tap Setting of Transformers on Power System Performance

The effect of any change of a transformer tap setting on the power system performance is indicated in Figures (6.1) through (6.5).

Figure (6.1) shows the nonlinear variation of power system losses in MW with a change in the tap setting of transformers t_{65}, t_{47}, and t_{49} from 0.9 to 1.1. This reflects that the power loss sensitivities with respect to a change in the tap setting of a transformer are not constant through the whole range defined by their operating limits. However these curves can be linearized over one step change.

Figure (6.2) indicates the nonlinearity of the reactive power losses as a function of tap setting of a transformer, and Figure (6.3) shows how a tap setting change affects the MSV. The curve for t_{65} has a sudden increase at t =1.05, because generator G6 switched back to be a PV bus due to the generated reactive power decrease from 24 MVAR (max VAR limit) to 21.77 MVAR. This change decreases the dimension of the Jacobian matrix, and so it increases the MSV. At t =1.06, the curve starts to decrease again because of generator G2 with a max VAR limit of 50 MVAR, switches to a PQ bus. For transformer $t_{47,}$ at t = 0.91, generator G3 switches to a PV bus, which is reflected by a sudden increase in MSV. At t =0.94, generator G2 switched to a PV bus, which caused another increase in MSV, while at t =1.0, generator G8 switched to a PQ bus causing sudden decrease in MSV. For transformer $t_{49,}$ at t = 1.04, generator G8 switched to a PQ bus, which is reflected by the sudden decrease of the MSV.

Figures (6.4) and (6.5) indicate the active power generated by the swing bus, and the reactive power generated by the swing bus respectively. A comparison of Figures (6.1), and (6.4) shows that both figures are identical in shape, but with different scale, that is due to the fact that the power losses are in proportion to the power generated by the swing bus.

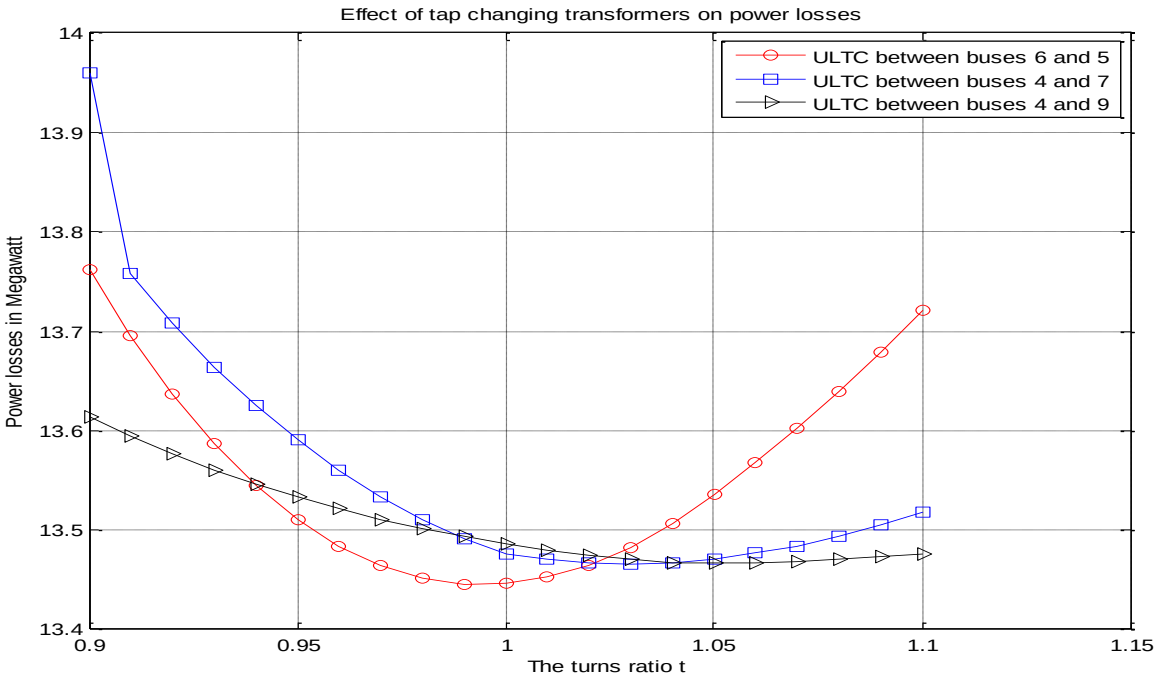

Figure 6.1: Effect of tap changing transformers on power losses

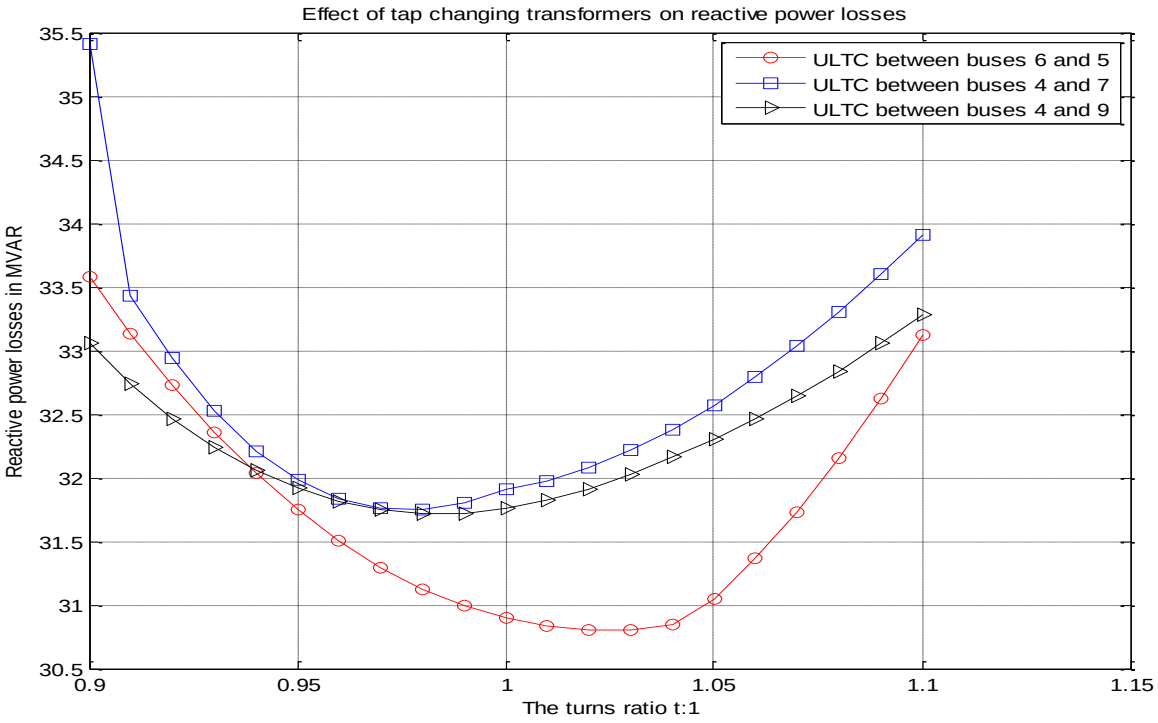

Figure 6.2: Effect of tap changing transformers on reactive power losses

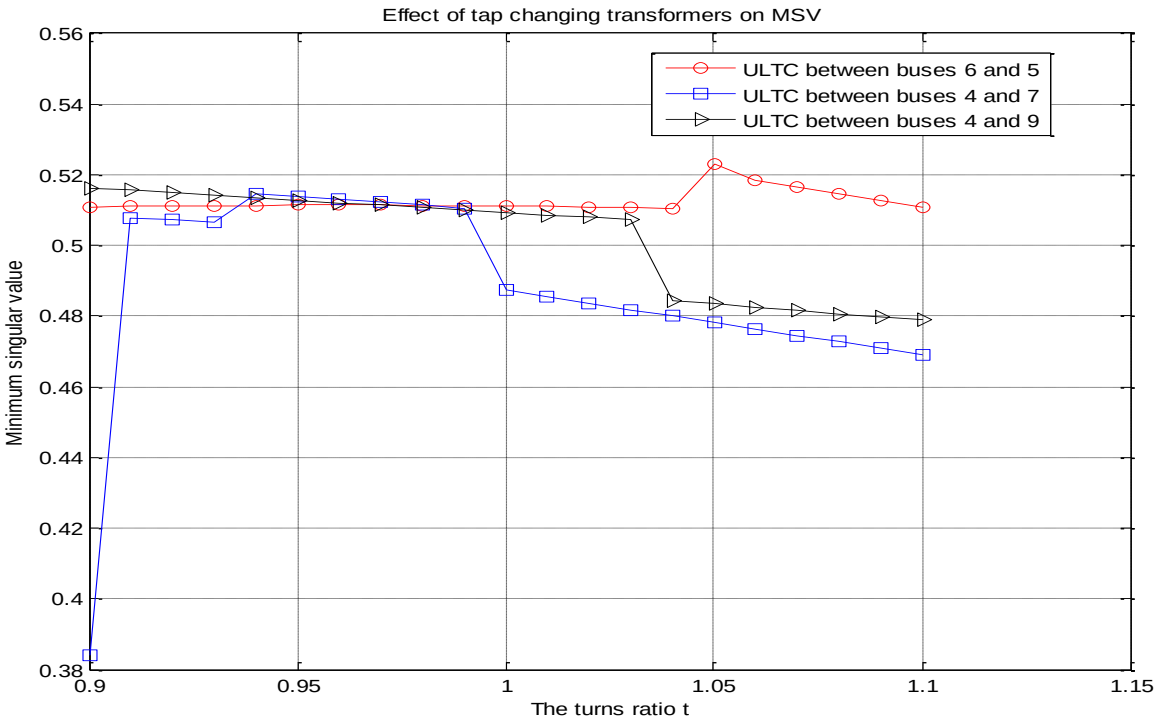

Figure 6.3: Effect of tap changing transformers on MSV

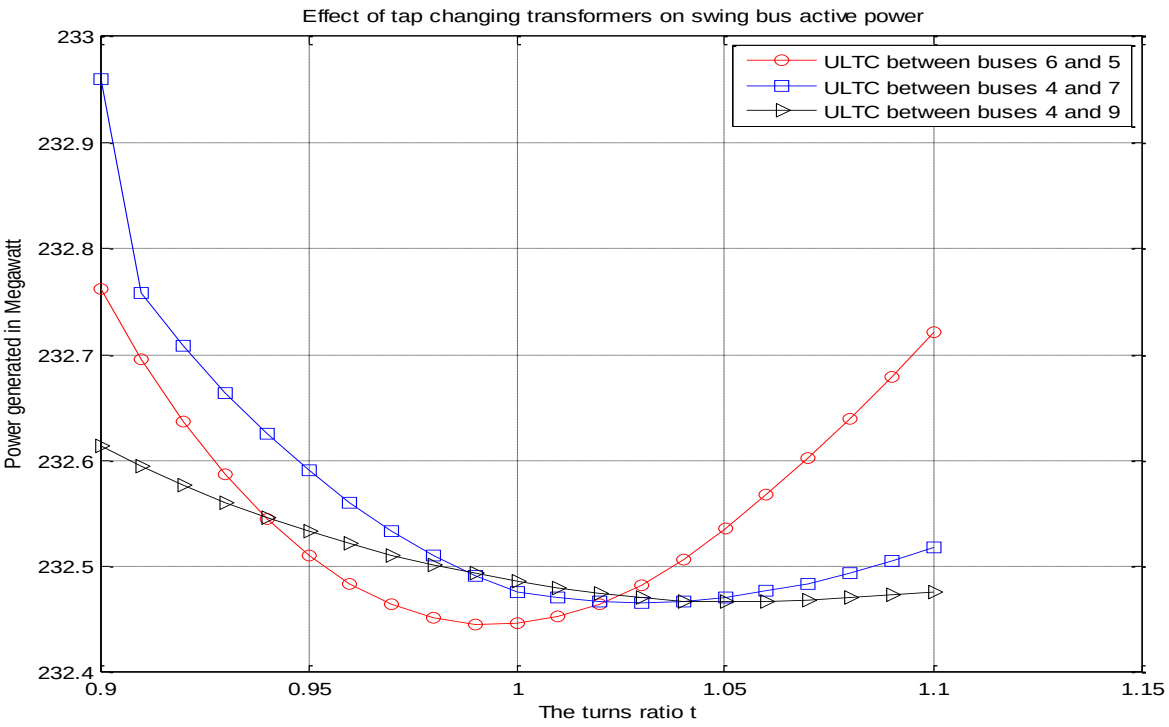

Figure 6.4: Effect of tap changing transformers on swing bus active power

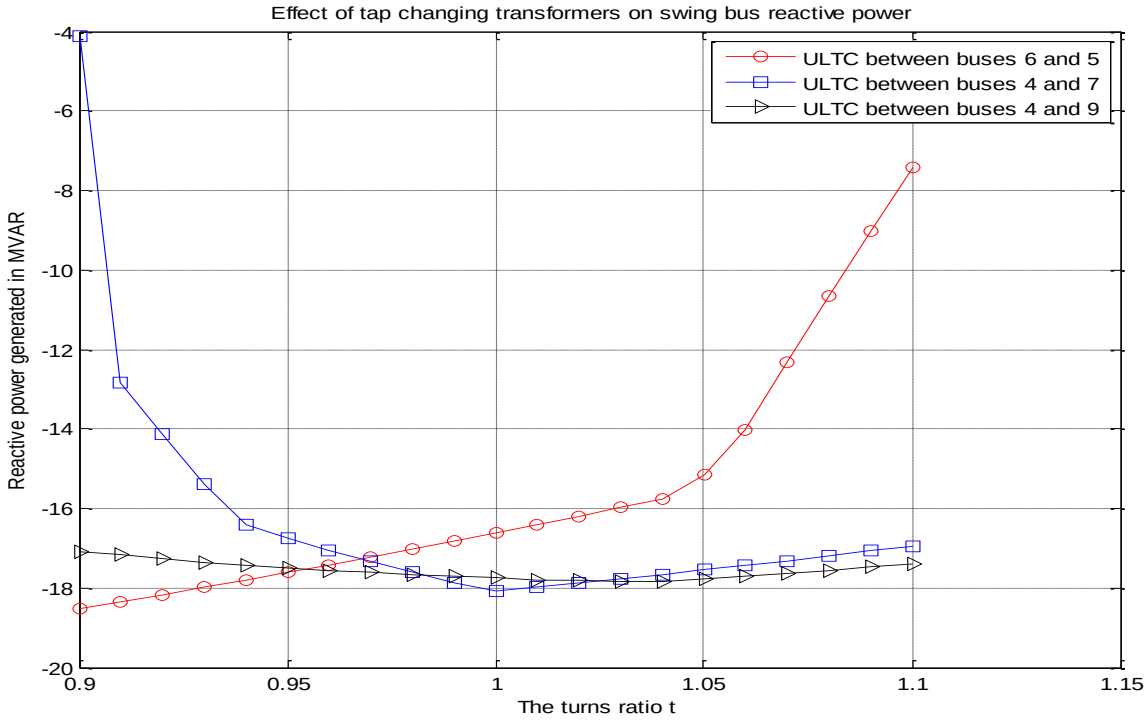

Figure 6.5: Effect of tap changing transformers on swing bus reactive power

6.3.2 Effect of Capacitor Rating on Power System Performance

The effects of changes of capacitor ratings on the power system performance are indicated in Figures (6.6) through (6.10).

Figure (6.6) shows the nonlinear variation of power system losses in MW with a change in the capacitor rating in MVAR from 0.0 to 25 MVAR at bus number 9. Note there is no change in Jacobian matrix dimension for this case. The power loss sensitivities with respect to a change in the capacitor ratings are not constant through the whole range defined by its operating limits, however this curve can be linearized over one step change. The minimum active power losses of 13.5045 MW occur at Q_c = 12 MVAR.

Figure (6.7) indicates the nonlinearity of the reactive power losses as a function of capacitor rating in MVAR. Figure (6.8) reflects how a change in the capacitor rating affects the MSV of the whole system. From this figure it can be seen that there is a linear relation between the MVAR of the capacitor at bus number 9 and the MSV of the system.

Figures (6.9) and (6.10) indicate the active power generated by the swing bus, and the reactive power generated by the swing bus respectively as a function of the capacitor rating in MVAR.

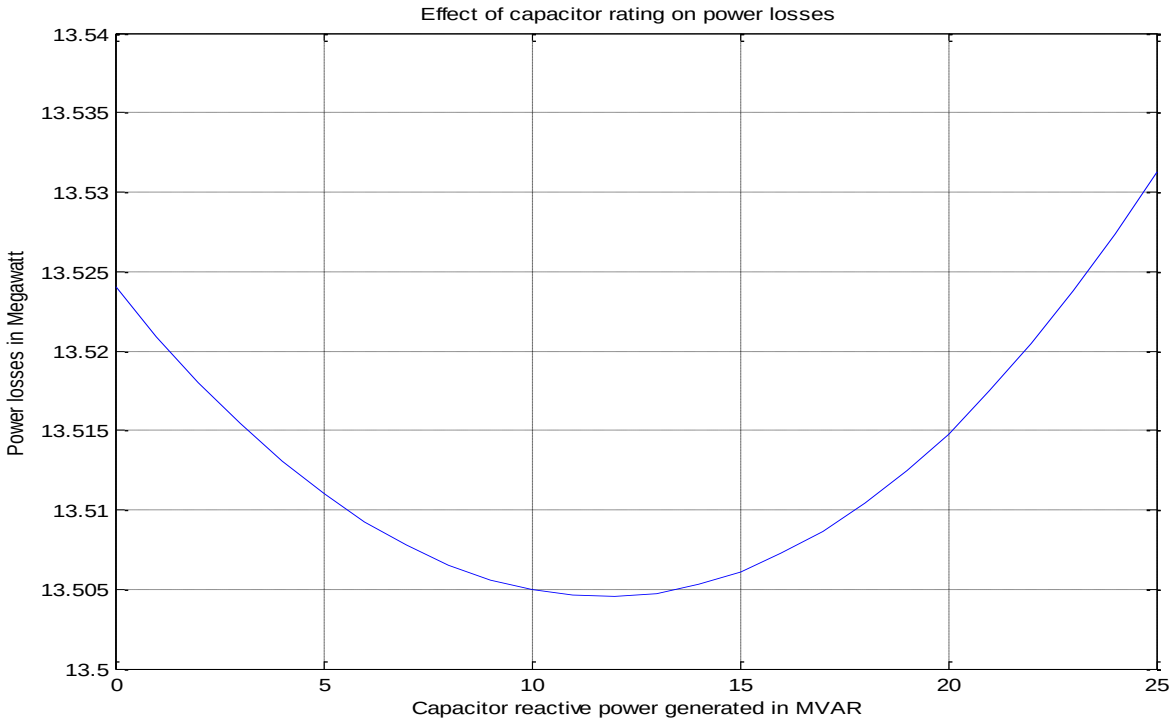

Figure 6.6: Effect of capacitor rating on power losses

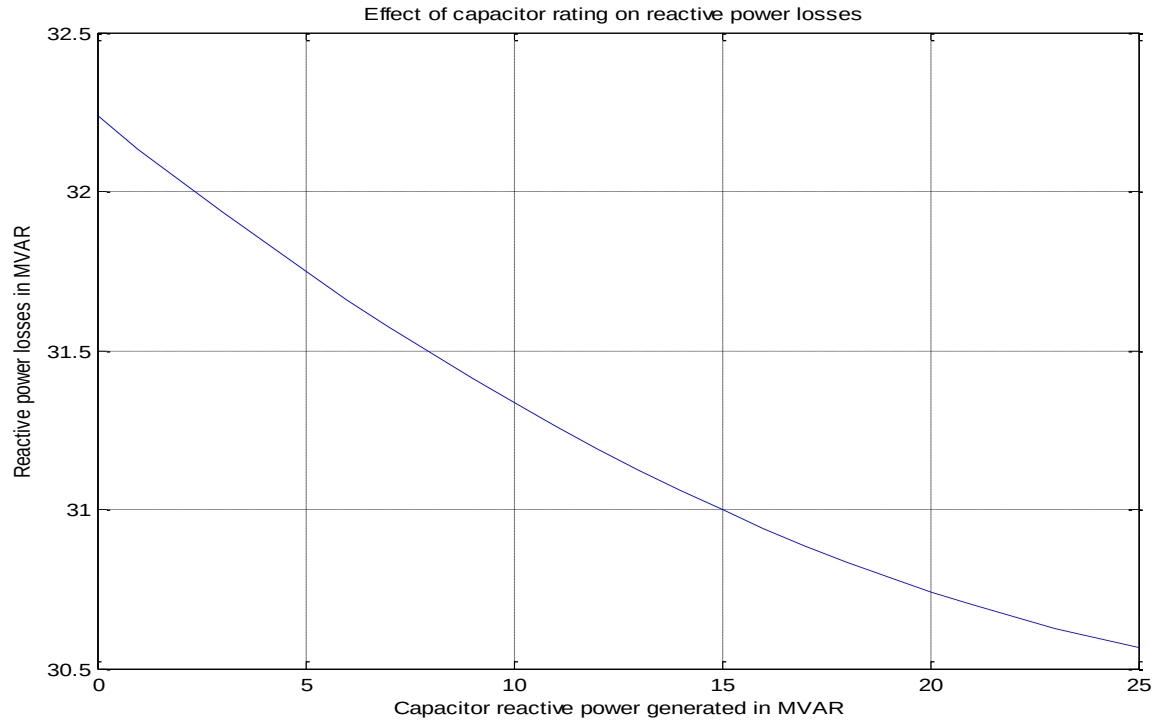

Figure 6.7: Effect of capacitor rating on reactive power losses

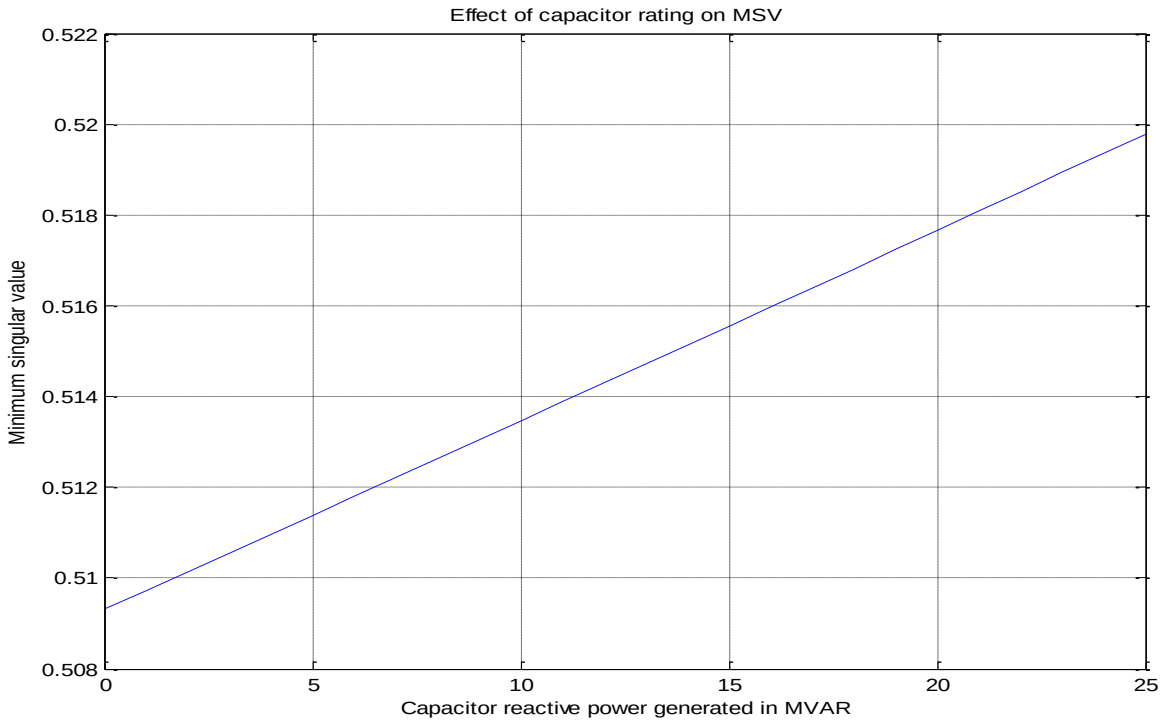

Figure 6.8: Effect of capacitor rating on MSV

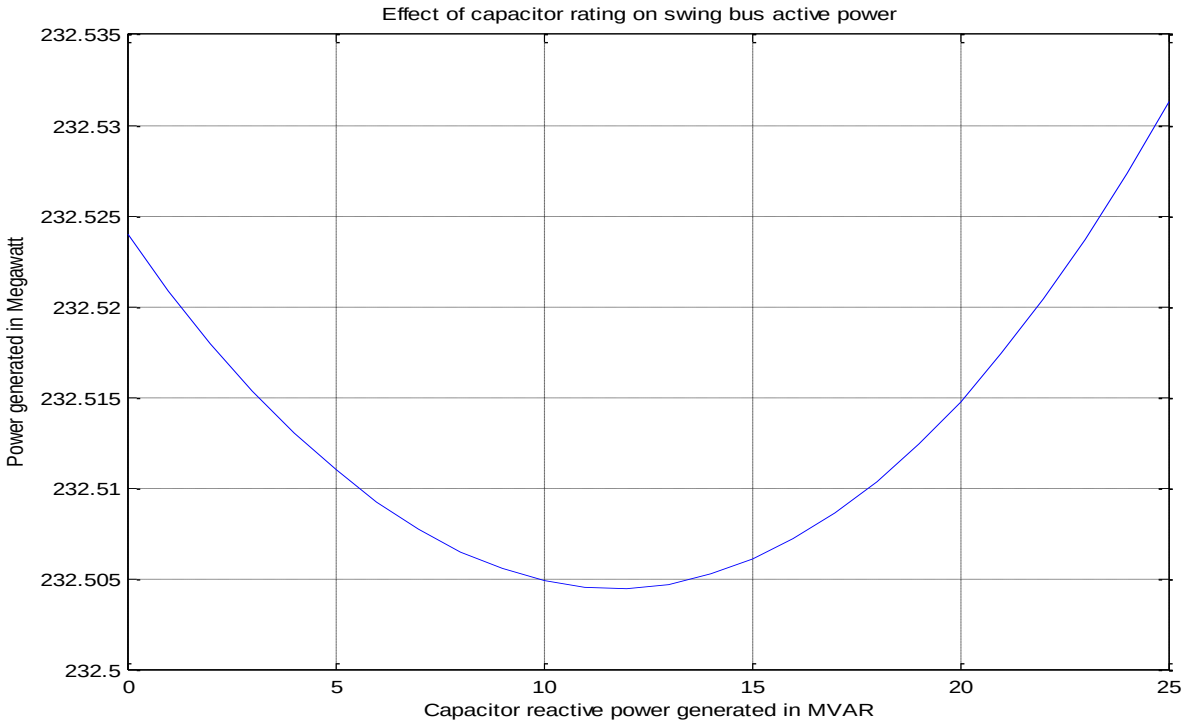

Figure 6.9: Effect of capacitor rating on swing bus active power generated

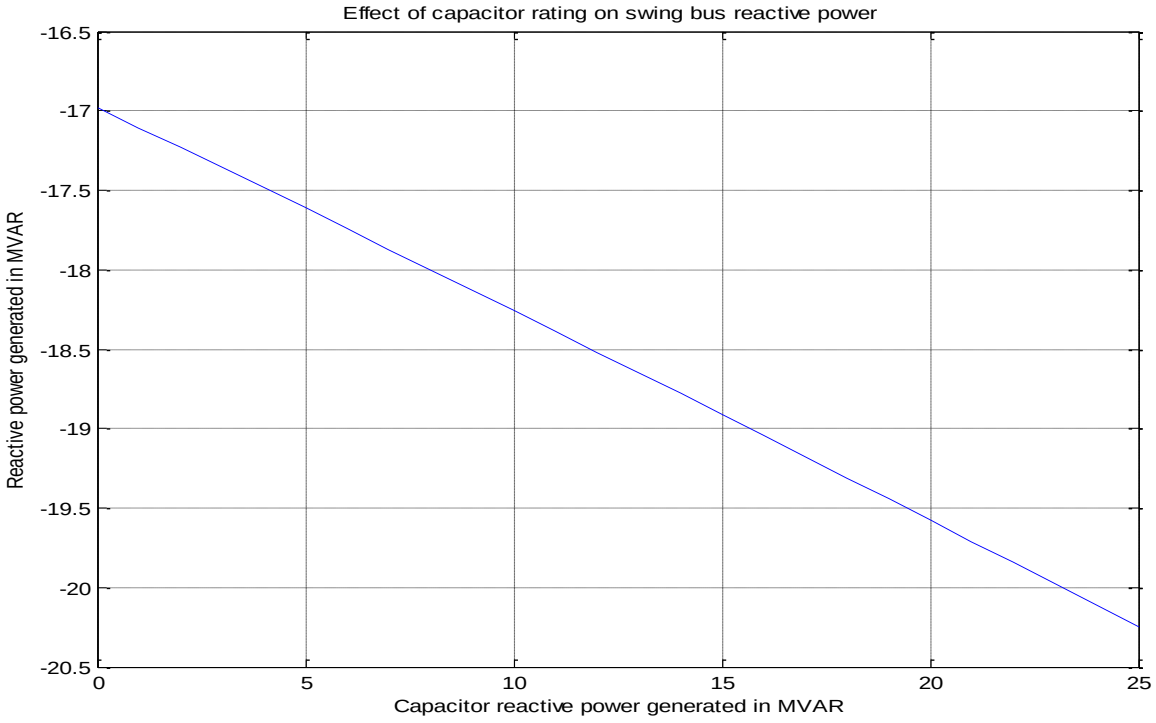

Figure 6.10: Effect of capacitor rating on swing bus reactive power generated

6.3.3 Effect of Generator Terminal Voltages on Power System Performance

The effects of changes of generator terminal voltages on the power system performance are indicated in Figures (6.11) through (6.15).

Figure (6.11) shows the nonlinear variation of power system losses in MW with a change in the generator terminal voltage in pu from 1.0 to 1.1 pu. This figure shows that the power loss sensitivities with respect to a change in the generator terminal voltage are not constant through the whole ranges defined by their operating limits. However these curves can be linearized over one step change.

Figure (6.12) indicates the nonlinearity of the reactive power losses as a function of generator terminal voltage in pu, while Figure (6.13) shows how a change in the generator terminal voltage affects the MSV of the whole system.

Figures (6.14) and (6.15) indicate the active power generated by the swing bus and the reactive power generated by the swing bus respectively, as a function of the generator terminal voltage in pu. Changing the terminal voltage of generator G1 from 1.0 pu to 1.1 pu causes switching of generators at buses 8, 3, and 2 from PQ buses to PV buses at terminal voltages of 1.04, 1.05, and 1.06 respectively. This can be seen as a sudden increase of the MSV of the system in the curve generated by a change of the terminal voltage of generator G1. The curve of MSV, which is generated by changing the terminal voltage of the generator at bus number 2, has three sudden changes at terminal voltages of 1.03, 1.04, and 1.05.

At a terminal voltage of 1.03, generator G2 switched as a PV bus, at the same time, the generator G8 switched to a PV bus. At a terminal voltage of 1.04, the generator G3 switched to a PV bus, while at a terminal voltage of 1.05 the generator G2 hit the upper limit and switched back to a PQ bus.

As the terminal voltage of the generator at bus number 3 changes from 1.0 pu to 1.1 pu, the generator at bus number 2 switched to a PV bus at a terminal voltage of 1.01 pu, while the generator at bus number 3 hits the upper limit and switched to a PQ bus at a terminal voltage of 1.03 pu.

Changing the terminal voltage of the generator at bus number 6 does not affect the case of any other generator. In the case of changing the terminal voltage of the generator at bus number 8, the generator at bus number 2 switched to PV bus at terminal voltages of 1.04. The generator at bus number 8 switched to a PV bus at a terminal voltage of 1.01 after reaching the

lower limit and switched back to a PQ bus after hitting the upper limit at a terminal voltage of 1.08.

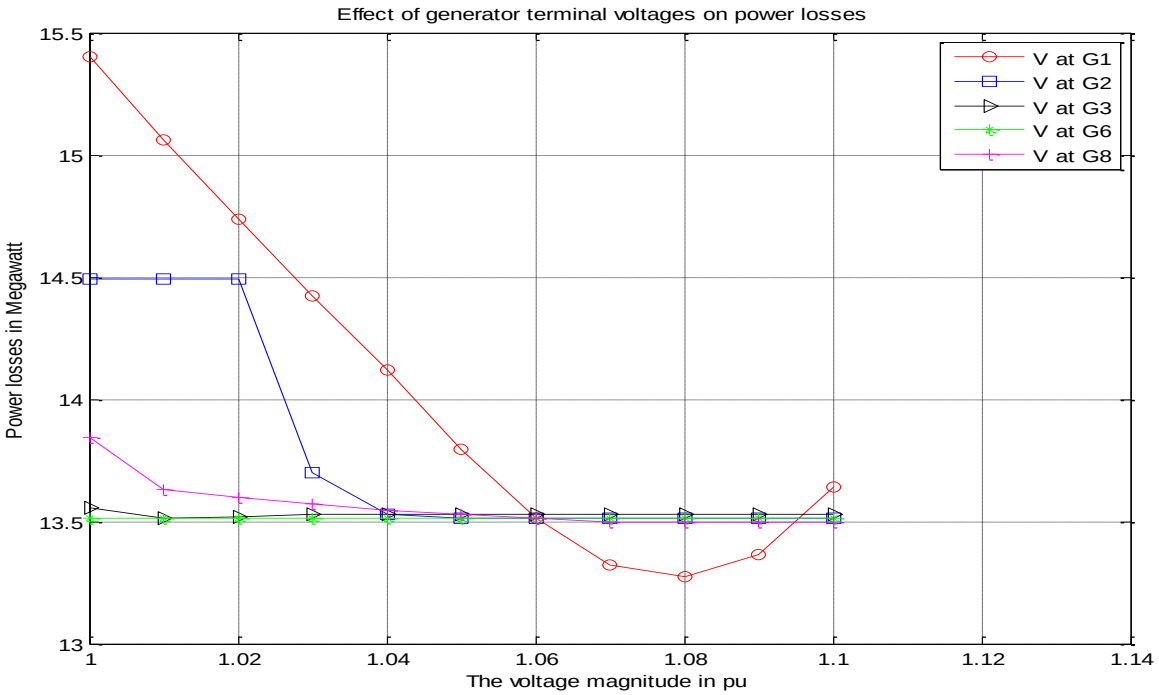

Figure 6.11: Effect of generator terminal voltages on power losses

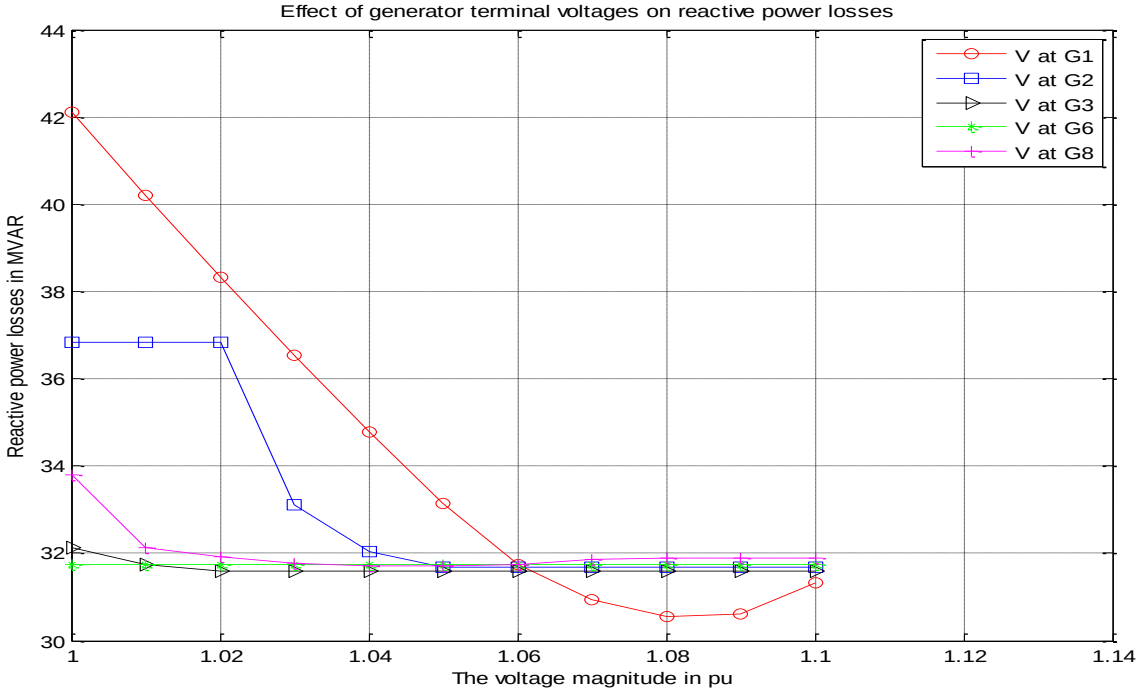

Figure 6.12: Effect of generator terminal voltages on reactive power losses

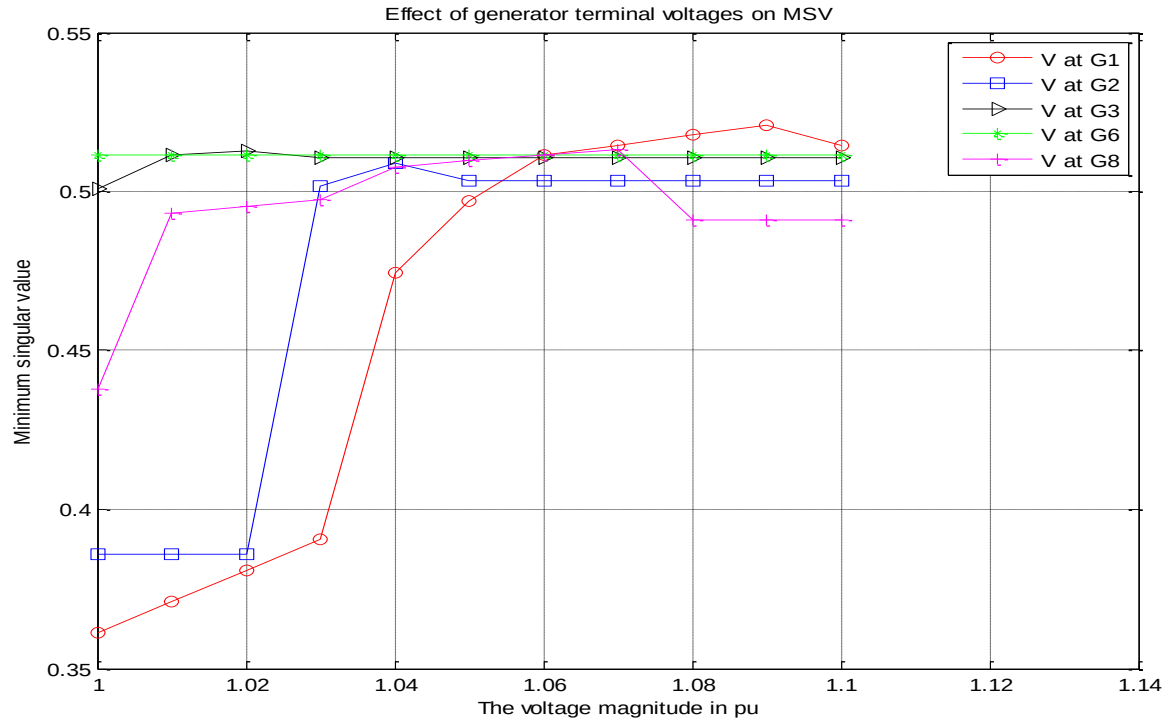

Figure 6.13: Effect of generator terminal voltages on MSV

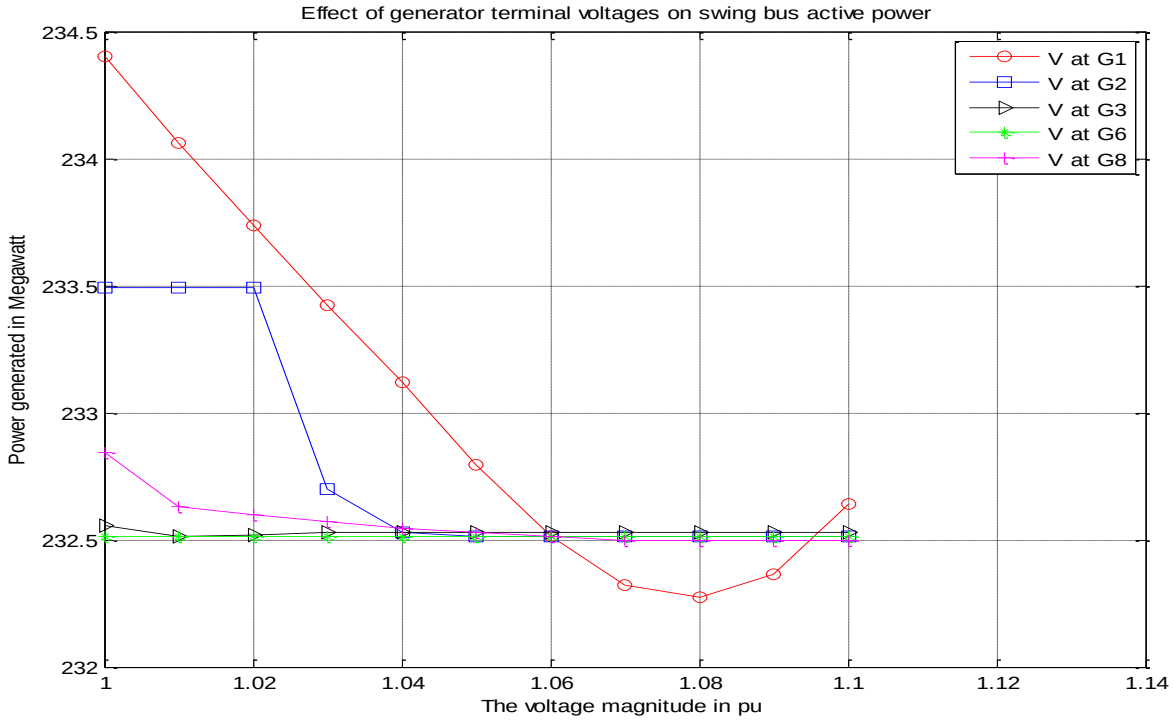

Figure 6.14: Effect of generator terminal voltages on swing bus active power

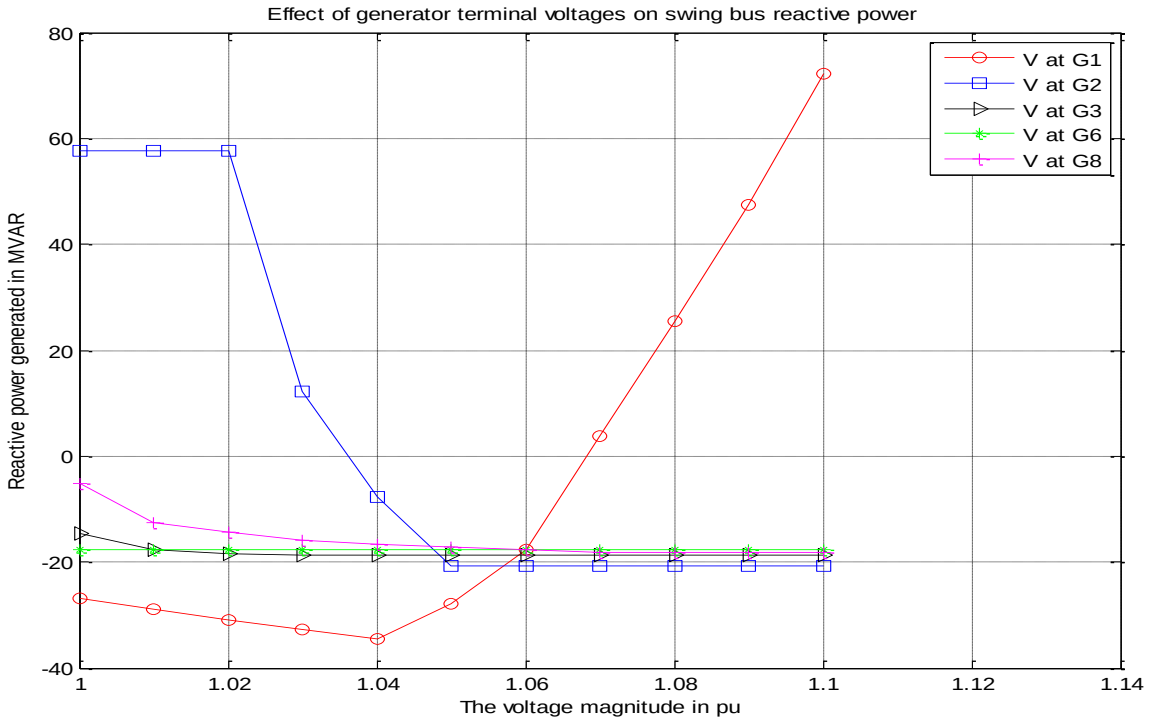

Figure 6.15: Effect of generator terminal voltages on swing bus reactive power

6.4 Proposed Objective Functions

As stated earlier three methods for optimizing reactive power control were used and compared:

Method 1. Minimizing the number of controllers.

Method 2. Minimizing the power losses (P_L). The objective function used:

$$P_L = \sum_{j=1}^{n} P_j \tag{6.1}$$

where:

n: is the total number of buses

P_j: is the active power injected at bus j

P_L: is the total power loss.

Method 3. Minimizing the sum of the squares of the voltage deviations (V_d). The objective function used:

$$V_d = \sum_{j=g+1}^{n} (V_j^{actual} - V_j^{norm})^2 \quad (6.2)$$

where:

n: is the total number of buses

g: is the total number of generators

V_j^{actual}: is the voltage magnitude at j bus from load flow

V_j^{norm}: is the nominal value of voltage magnitude at bus j, usually equal to 1 pu

V_d: is the sum of the squares of voltage deviations

The goal for each of the three objective functions is to: minimize the number of controllers, minimize the power losses (P_L), and minimize the sum of the squares of the voltage deviations (V_d). This is done by controlling the generators terminal voltages, transformer taps, and switchable shunt capacitors. Since all the three algorithms use a linearized formulation, the objective functions must be linearized, to minimize changes in active power losses, and voltage deviations (ΔP_L, and ΔV_d) rather than P_L, and V_d values.

The constraints on these objective functions are:

- limits on the control variables
- limits on the dependent variables

6.5 General Form of the Optimization Problem

The general form of any optimization problem is as follows:

Minimize: objective function = c*u* (6.3)

Subjected to:

Dependent variable constraints $x_i^{min} \le x_i \le x_i^{max}$ for i=1, 2, …., n (6.4)

Control variable constraints $u_m^{min} \le u_m \le u_m^{max}$ for m = 1, 2, …, g + t + cap (6.5)

$$x = Su \quad (6.6)$$

where:

c: is a row vector of the linearized objective function sensitivity coefficients

u: is a column vector of linearized control variables and can be written as:

$$u = \left[\Delta(t_{jk})_1, \Delta(t_{jk})_2, \dots, \Delta(t_{jk})_t, \Delta V_1, \Delta V_2, \dots, \Delta V_g, \Delta Q_1, \Delta Q_2, \dots, \Delta Q_{cap}\right]^T$$

u^{min}, u^{max}: are the lower and upper limits on the control variables

x: is a column vector of linearized dependent variables and can be written as:

$$x = \left[\Delta Q_1, \Delta Q_2, \dots, \Delta Q_g, \Delta V_{g+1}, \Delta V_{g+2}, \dots, \Delta V_n\right]^T$$

x^{min}, x^{max}: are the lower and upper limits on the dependent variables, and

S: is a linearized sensitivity matrix relating the dependent and control variables

6.5.1 Constraints on the Dependent Variables

These constraints represent the limits for the reactive power generation of the generators, and the limits for the voltage magnitudes of all load buses, these limits are as follow:

$$Q_i^{min} \le Q_i \le Q_i^{max} \quad \text{for } i = 1, 2, \dots, g \quad (6.7)$$

$$V_j^{min} \le V_j \le V_j^{max} \quad \text{for } j = g+1, g+2, \dots, n \quad (6.8)$$

The inequalities (6.7) and (6.8) can be rewritten in a linearized form as

$$\Delta Q_i^{min} \le \Delta Q_i \le \Delta Q_i^{max} \quad \text{for } i = 1, 2, \dots, g \quad (6.9)$$

$$\Delta V_j^{min} \le \Delta V_j \le \Delta V_j^{max} \quad \text{for } j = g+1, g+2, \dots, n \quad (6.10)$$

where:

$$\Delta Q_i^{min} = Q_i^{min} - Q_i$$
$$\Delta Q_i^{max} = Q_i^{max} - Q_i$$
$$\Delta V_j^{min} = V_j^{min} - V_j$$
$$\Delta V_j^{max} = V_j^{max} - V_j$$

These linearized constraints of the dependent variables depend on the current values of $Q_i, V_j,$ and their upper and lower limits ($Q_i^{max}, V_j^{max}, Q_i^{min}, V_j^{min}$)

6.5.2 Constraints on the Control Variables

These constraints represent the limits for the generator terminal voltages, the limits for the transformer taps, and those for the switchable shunt capacitors, these limits in linearized form are:

$$\Delta t_{jk}^{min} \leq \Delta t_{jk} \leq \Delta t_{jk}^{max} \quad \text{j, k buses connecting transformers} \quad (6.11)$$
$$\Delta V_i^{min} \leq \Delta V_i \leq \Delta V_i^{max} \quad \text{for } i = 1, 2, \ldots, g \quad (5.12)$$
$$\Delta Q_k^{min} \leq \Delta Q_k \leq \Delta Q_k^{max} \quad \text{for } k = g+1, g+2, \ldots, g + cap \quad (6.13)$$

where:

Cap: is the number of switchable shunt capacitors

t: is the number of tap changing transformers

$$\Delta t_{jk}^{min} = t_{jk}^{min} - t_{jk}$$
$$\Delta t_{jk}^{max} = t_{jk}^{max} - t_{jk}$$
$$\Delta V_i^{min} = V_i^{min} - V_i$$
$$\Delta V_i^{max} = V_i^{max} - V_i$$
$$\Delta Q_k^{min} = Q_k^{min} - Q_k$$
$$\Delta Q_k^{max} = Q_k^{max} - Q_k$$

Again these linearized constraints of the control variables depend on the current values of $t_{jk}, V_i, Q_k,$ and their upper and lower limits (t_{jk}^{max} , V_i^{max} , $Q_k^{max}, t_{jk}^{min}. V_i^{min}, Q_k^{min}$)

6.6 Tap Changing Transformer Model

The tap ratio of a transformer can be changed by adding turns to or subtracting turns from either the primary or the secondary winding using an under-load tap-changer (ULTC). The ULTC can be located at the primary or the secondary side of the transformer. The representation of a transformer equipped with an ULTC and its equivalent circuit is shown in Figure (6.16). Notation *I*, *V*, and *y* in this figure are complex values which indicate current, voltage and transformer admittance, respectively, while t_{jk}, *j* and *k* indicate transformer turn ratio, tap side and non tap side of the transformer, respectively.

From Figure (6.16) the relation between currents and voltages can be written in matrix form as follows:

$$\begin{bmatrix} I_j \\ I_k \end{bmatrix} = \begin{bmatrix} \frac{y}{t^2} & \frac{-y}{t} \\ \frac{-y}{t} & y \end{bmatrix} \begin{bmatrix} V_j \\ V_k \end{bmatrix} \tag{6.14}$$

The complex power injected at bus j can be written as:

$$S_j = P_j + jQ_j = V_j I_j^* \tag{6.15}$$

From Equation (6.15), $P_j \; and \; Q_j, \; with \; y = g + jb, \; and$ $the \; phase \; angles \; of \; V_j, \; and \; V_k \; are \; \theta_j$, and θ_k respectively, can be written as:

$$P_j = g\frac{V_j^2}{t_{jk}^2} - \left(\frac{V_j V_k}{t_{jk}}\right)[gcos(\theta_j - \theta_k) + bsin(\theta_j - \theta_k)] \tag{6.16}$$

$$Q_j = -b\frac{V_j^2}{t_{jk}^2} - \left(\frac{V_j V_k}{t_{jk}}\right)[gsin(\theta_j - \theta_k) - bcos(\theta_j - \theta_k)] \tag{6.17}$$

Similarly, $P_k \; and \; Q_k$ can be written as:

$$P_k = gV_k^2 - \left(\frac{V_j V_k}{t_{jk}}\right)[gcos(\theta_j - \theta_k) - bsin(\theta_j - \theta_k)] \tag{6.18}$$

$$Q_k = -bV_k^2 + \left(\frac{V_j V_k}{t_{jk}}\right)[gsin(\theta_j - \theta_k) + bcos(\theta_j - \theta_k)\,] \tag{6.19}$$

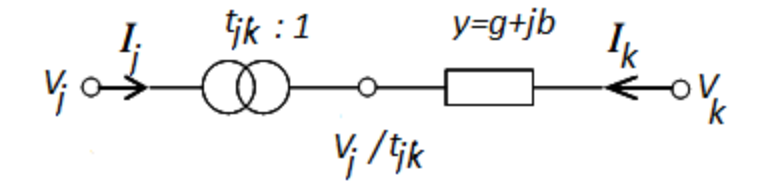

a

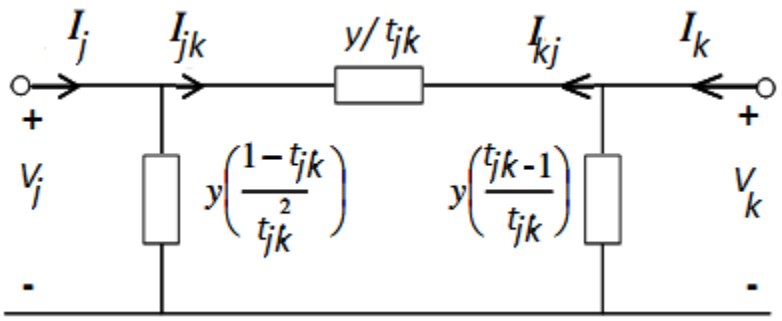

b

Figure 6.16: Representation of a transformer equipped with an ULTC
a: UTCT representation b: Equivalent circuit

The derivatives of Equations (6.16), (6.17), (6.18), and (6.19) can be found as:

$$\frac{\partial P_j}{\partial t_{jk}} = -2g\frac{V_j^2}{t_{jk}^3} + \left(\frac{V_j V_k}{t_{jk}^2}\right)[g\cos(\theta_j - \theta_k) + b\sin(\theta_j - \theta_k)] \tag{6.20}$$

$$\frac{\partial Q_j}{\partial t_{jk}} = 2b\frac{V_j^2}{t_{jk}^3} + \left(\frac{V_j V_k}{t_{jk}^2}\right)[g\sin(\theta_j - \theta_k) - b\cos(\theta_j - \theta_k)] \tag{6.21}$$

$$\frac{\partial P_k}{\partial t_{jk}} = \left(\frac{V_j V_k}{t_{jk}^2}\right)[g\cos(\theta_j - \theta_k) - b\sin(\theta_j - \theta_k)] \tag{6.22}$$

$$\frac{\partial Q_k}{\partial t_{jk}} = -\left(\frac{V_j V_k}{t_{jk}^2}\right)[g\sin(\theta_j - \theta_k) + b\cos(\theta_j - \theta_k)] \tag{6.23}$$

The complex power through branch jk in Figure (6.16 b) can be written as:

$$S_{jk} = P_{jk} + jQ_{jk} = V_j I_{jk}^* \tag{6.24}$$

From Equation (6.24), $P_{jk}\ and\ Q_{jk}$ can be written as:

$$P_{jk} = g\frac{V_j^2}{t_{jk}} - \left(\frac{V_jV_k}{t_{jk}}\right)[gcos(\theta_j - \theta_k) + bsin(\theta_j - \theta_k)] \quad (6.25)$$

$$Q_{jk} = -b\frac{V_j^2}{t_{jk}} - \left(\frac{V_jV_k}{t_{jk}}\right)[gsin(\theta_j - \theta_k) - bcos(\theta_j - \theta_k)] \quad (6.26)$$

Similarly, $P_{kj}\ and\ Q_{kj}$ can be written as:

$$P_{kj} = g\frac{V_k^2}{t_{jk}} - \left(\frac{V_jV_k}{t_{jk}}\right)[gcos(\theta_j - \theta_k) - bsin(\theta_j - \theta_k)] \quad (6.27)$$

$$Q_{kj} = -b\frac{V_k^2}{t_{jk}} + \left(\frac{V_jV_k}{t_{jk}}\right)[gsin(\theta_j - \theta_k) + bcos(\theta_j - \theta_k)] \quad (6.28)$$

The derivatives of Equations (6.25), (6.26) , (6.27), and (6.28) can be found as:

$$\frac{\partial P_{jk}}{\partial t_{jk}} = -g\frac{V_j^2}{t_{jk}^2} + \left(\frac{V_jV_k}{t_{jk}^2}\right)[gcos(\theta_j - \theta_k) + bsin(\theta_j - \theta_k)] \quad (6.29)$$

$$\frac{\partial Q_{jk}}{\partial t_{jk}} = b\frac{V_j^2}{t_{jk}^2} + \left(\frac{V_jV_k}{t_{jk}^2}\right)[gsin(\theta_j - \theta_k) - bcos(\theta_j - \theta_k)] \quad (6.30)$$

$$\frac{\partial P_{kj}}{\partial t_{jk}} = -g\frac{V_k^2}{t_{jk}^2} + \left(\frac{V_jV_k}{t_{jk}^2}\right)[gcos(\theta_j - \theta_k) - bsin(\theta_j - \theta_k)] \quad (6.31)$$

$$\frac{\partial Q_{kj}}{\partial t_{jk}} = b\frac{V_k^2}{t_{jk}^2} - \left(\frac{V_jV_k}{t_{jk}^2}\right)[gsin(\theta_j - \theta_k) + bcos(\theta_j - \theta_k)] \quad (6.32)$$

These derivatives will be used later to determine the sensitivity of active power losses (P_L) with respect to transformer tap setting t_{jk}.

6.7 Sensitivity Matrix Calculation

Forming the Newton Raphson (NR) load flow equations assuming that the system has only one swing bus, the set of these equations in matrix form is as follows:

$$\begin{bmatrix} \Delta P_2 \\ \vdots \\ \vdots \\ \Delta P_n \\ \Delta Q_2 \\ \vdots \\ \vdots \\ \Delta Q_n \end{bmatrix} = \begin{bmatrix} \frac{\partial P_2}{\partial \theta_2} & \cdots & \frac{\partial P_2}{\partial \theta_n} & \frac{\partial P_2}{\partial V_2} & \cdots & \frac{\partial P_2}{\partial V_n} \\ \vdots & \ddots & \vdots & \vdots & \ddots & \vdots \\ \frac{\partial P_n}{\partial \theta_2} & \cdots & \frac{\partial P_n}{\partial \theta_n} & \frac{\partial P_n}{\partial V_2} & \cdots & \frac{\partial n}{\partial V_n} \\ \frac{\partial Q_2}{\partial \theta_2} & \cdots & \frac{\partial QP_2}{\partial \theta_n} & \frac{\partial Q_2}{\partial V_2} & \cdots & \frac{\partial Q_2}{\partial V_n} \\ \vdots & \ddots & \vdots & \vdots & \ddots & \vdots \\ \frac{\partial Q_n}{\partial \theta_2} & \cdots & \frac{\partial Q_n}{\partial \theta_n} & \frac{\partial Q_n}{\partial V_2} & \cdots & \frac{\partial Q_n}{\partial V_n} \end{bmatrix} \begin{bmatrix} \Delta\theta_2 \\ \vdots \\ \vdots \\ \Delta\theta_n \\ \Delta V_2 \\ \vdots \\ \vdots \\ \Delta V_n \end{bmatrix} \tag{6.33}$$

The active and reactive power injected at the swing bus and the power flow equations for transformers with controllable tap settings are augmented to the load flow equations in Equation (6.33) to get a new set of equations:

$$\begin{bmatrix} \Delta P_1 \\ \vdots \\ \vdots \\ \Delta P_n \\ \Delta P_{jk} \\ \Delta Q_1 \\ \vdots \\ \vdots \\ \Delta Q_n \end{bmatrix} = \begin{bmatrix} \frac{\partial P}{\partial \theta} & \frac{\partial P}{\partial t_{jk}} & \frac{\partial P}{\partial V} \\ \frac{\partial P_{jk}}{\partial \theta} & \frac{\partial P_{jk}}{\partial t_{jk}} & \frac{\partial P_{jk}}{\partial V} \\ \frac{\partial Q}{\partial \theta} & \frac{\partial Q}{\partial t_{jk}} & \frac{\partial Q}{\partial V} \end{bmatrix} \begin{bmatrix} \Delta\theta_1 \\ \vdots \\ \vdots \\ \Delta\theta_n \\ \Delta t_{jk} \\ \Delta V_1 \\ \vdots \\ \vdots \\ \Delta V_n \end{bmatrix} \tag{6.34}$$

where:

n: The total number of buses.

t: The total number of tap changing transformers

$\frac{\partial P}{\partial \theta}$: is (n x n) sub-matrix

$\frac{\partial P}{\partial t_{jk}}$: is (n x t) sub-matrix

$\frac{\partial P}{\partial V}$: is (n x n) sub-matrix

$\frac{\partial P_{jk}}{\partial \theta}$: is (t x n) sub-matrix

$\frac{\partial P_{jk}}{\partial t_{jk}}$: is (t x t) sub-matrix

$\frac{\partial P_{jk}}{\partial V}$: is (t x n) sub-matrix

$\frac{\partial Q}{\partial \theta}$: is (n x n) sub-matrix

$\frac{\partial Q}{\partial t_{jk}}$: is (n x t) sub-matrix, and

$\frac{\partial Q}{\partial V}$: is (n x n) sub-matrix

Equation (6.34) can be divided into three Equations (6.35), (6.36) and (6.37) as follows:

$$\begin{bmatrix} \Delta P_1 \\ \vdots \\ \vdots \\ \Delta P_n \end{bmatrix} = \begin{bmatrix} \frac{\partial P}{\partial \theta} & \frac{\partial P}{\partial t_{jk}} & \frac{\partial P}{\partial V} \end{bmatrix} \begin{bmatrix} \Delta\theta_1 \\ \vdots \\ \vdots \\ \Delta\theta_n \\ \Delta t_{jk} \\ \Delta V_1 \\ \vdots \\ \vdots \\ \Delta V_n \end{bmatrix} \tag{6.35}$$

$$\begin{bmatrix} \Delta P_{jk} \end{bmatrix} = \begin{bmatrix} \frac{\partial P_{jk}}{\partial \theta} & \frac{\partial P_{jk}}{\partial t_{jk}} & \frac{\partial P_{jk}}{\partial V} \end{bmatrix} \begin{bmatrix} \Delta\theta_1 \\ \vdots \\ \vdots \\ \Delta\theta_n \\ \Delta t_{jk} \\ \Delta V_1 \\ \vdots \\ \vdots \\ \Delta V_n \end{bmatrix} \tag{6.36}$$

$$\begin{bmatrix} \Delta Q_1 \\ \vdots \\ \vdots \\ \Delta Q_n \end{bmatrix} = \begin{bmatrix} \frac{\partial Q}{\partial \theta} & \frac{\partial Q}{\partial t_{jk}} & \frac{\partial Q}{\partial V} \end{bmatrix} \begin{bmatrix} \Delta\theta_1 \\ \vdots \\ \vdots \\ \Delta\theta_n \\ \Delta t_{jk} \\ \Delta V_1 \\ \vdots \\ \vdots \\ \Delta V_n \end{bmatrix} \tag{6.37}$$

Assuming that a small change in the phase angle of the bus voltage ($\Delta\theta$) does not change the reactive power injection, (i.e., $\frac{\partial Q}{\partial \theta} \cong 0$), Equation (6.37) can be rewritten as:

$$\begin{bmatrix} \Delta Q_1 \\ \vdots \\ \vdots \\ \Delta Q_n \end{bmatrix} = \begin{bmatrix} \frac{\partial Q}{\partial t_{jk}} & \frac{\partial Q}{\partial V} \end{bmatrix} \begin{bmatrix} \Delta t_{jk} \\ \Delta V_1 \\ \vdots \\ \vdots \\ \Delta V_n \end{bmatrix} \tag{6.38}$$

The total number of buses in a power system (n) can be divided into three categories as follow:

- generator buses (g)
- switchable VAR compensator buses (cap)
- load buses without any source of VAR compensation (l)

where: n = g + cap + l

Equation (6.38) can be rewritten as:

$$\begin{bmatrix} \Delta Q_1 \\ \vdots \\ \Delta Q_g \\ \Delta Q_{g+1} \\ \vdots \\ \Delta Q_{g+cap} \\ \Delta Q_{g+cap+1} \\ \vdots \\ \Delta Q_n \end{bmatrix} = \begin{bmatrix} J_{g\_t} & J_{g\_g} & J_{g\_cap} & J_{g\_l} \\ J_{cap\_t} & J_{cap\_g} & J_{cap\_cap} & J_{cap\_l} \\ J_{l\_t} & J_{l\_g} & J_{l\_cap} & J_{l\_l} \end{bmatrix} \begin{bmatrix} (\Delta t_{jk})_1 \\ \vdots \\ (\Delta t_{jk})_t \\ \Delta V_1 \\ \vdots \\ \Delta V_g \\ \Delta V_{g+1} \\ \vdots \\ \Delta V_{g+cap} \\ \Delta V_{g+cap+1} \\ \vdots \\ \Delta V_n \end{bmatrix} \tag{6.39}$$

where:

$J_{g\_t} = \frac{\partial Q_g}{\partial t_{jk}}$ is (g x t) sub-matrix

$J_{g\_g} = \frac{\partial Q_g}{\partial V_g}$ is (g x g) sub-matrix

$J_{g\_cap} = \frac{\partial Q_g}{\partial V_{cap}}$ is (*g x cap*) sub-matrix

$J_{g\_l} = \frac{\partial Q_g}{\partial V_l}$ is (*g x l*) sub-matrix

$J_{cap\_t} = \frac{\partial Q_{cap}}{\partial t_{jk}}$ is (*cap x t*) sub-matrix

$J_{cap\_g} = \frac{\partial Q_{cap}}{\partial V_g}$ is (*cap x g*) sub-matrix

$J_{cap\_cap} = \frac{\partial Q_{cap}}{\partial V_{cap}}$ is (*cap x cap*) sub-matrix

$J_{cap\_l} = \frac{\partial Q_{cap}}{\partial V_l}$ is (*cap x l*) sub-matrix

$J_{l\_t} = \frac{\partial Q_l}{\partial t_{jk}}$ is (*l x t*) sub-matrix

$J_{l\_g} = \frac{\partial Q_l}{\partial V_g}$ is (*l x g*) sub-matrix

$J_{l\_cap} = \frac{\partial Q_l}{\partial V_{cap}}$ is (*l x cap*) sub-matrix, and

$J_{l\_l} = \frac{\partial Q_l}{\partial V_l}$ is (*l x l*) sub-matrix

The sub-matrices $J_{g\_t}, J_{cap\_t},$ and J_{l_t} in Equation (6.39) can be calculated from Equation (6.21) at the tap side bus of ULTC transformer and Equation (6.23) at the non tap side bus of the transformer. For any bus not connected to a transformer, the value of $\frac{\partial Q}{\partial t_{jk}}$ is equal to zero. The other sub-matrices in Equation (6.39) can be found directly from the Jacobian matrix by assuming that all buses are load buses.

In order to get the sensitivity matrix (S), a modified Jacobian matrix, which is a relation between the control and the dependent variables, we have to separate the control variables to the right side and the dependent variables to the left side. The reactive power distribution in any power system can be controlled by the control system operator by suitable adjustment of the following controllers:

- The transformer tap settings (Δt_{jk})
- The generator output voltage (ΔV_i), and
- The switchable VAR source values (ΔQ_k)

These control variables (state variables) have their upper and lower permissible limits. Any changes to these state variables have the effect of changing the system voltage profiles and the reactive power output of generators and the system losses. Thus, the operator's control on these state variables is indirectly limited by the system response constraints, i.e., by the permissible limits of the voltages at the load buses, reactive power ratings of the generators. These constraints are referred to as network performance constraints.

The dependent variables are:

- The reactive power of the generators (ΔQ_i).
- The voltage magnitude at all load buses switchable VAR controller buses and load buses without any VAR resources (ΔV_j).

Let

$$S_1 = [J_{g\_t} \quad J_{g\_g}] \tag{6.40}$$

$$S_2 = [J_{g\_cap} \quad J_{g\_l}] \tag{6.41}$$

$$S_3 = \begin{bmatrix} J_{cap\_t} & J_{cap\_g} \\ J_{l\_t} & J_{l\_g} \end{bmatrix} \tag{6.42}$$

$$S_4 = \begin{bmatrix} J_{cap\_cap} & J_{cap\_l} \\ J_{l\_cap} & J_{l\_l} \end{bmatrix} \tag{6.43}$$

Knowing the control and dependent variables, Equation (6.39) can be divided into the following two equations:

$$\begin{bmatrix} \Delta Q_1 \\ \vdots \\ \Delta Q_g \end{bmatrix} = S_1 \begin{bmatrix} (\Delta t_{jk})_1 \\ \vdots \\ (\Delta t_{jk})_t \\ \Delta V_1 \\ \vdots \\ \Delta V_g \end{bmatrix} + S_2 \begin{bmatrix} \Delta V_{g+1} \\ \vdots \\ \Delta V_{g+cap} \\ \Delta V_{g+cap+1} \\ \vdots \\ \Delta V_n \end{bmatrix} \tag{6.44}$$

$$\begin{bmatrix} \Delta Q_{g+1} \\ \vdots \\ \Delta Q_{g+cap} \\ \Delta Q_{g+cap+1} \\ \vdots \\ \Delta Q_n \end{bmatrix} = S_3 \begin{bmatrix} (\Delta t_{jk})_1 \\ \vdots \\ (\Delta t_{jk})_t \\ \Delta V_1 \\ \vdots \\ \Delta V_g \end{bmatrix} + S_4 \begin{bmatrix} \Delta V_{g+1} \\ \vdots \\ \Delta V_{g+cap} \\ \Delta V_{g+cap+1} \\ \vdots \\ \Delta V_n \end{bmatrix} \tag{6.45}$$

Rearranging Equation (6.45):

$$\begin{bmatrix} \Delta V_{g+1} \\ \vdots \\ \Delta V_{g+cap} \\ \Delta V_{g+cap+1} \\ \vdots \\ \Delta V_n \end{bmatrix} = (S_4)^{-1} \begin{bmatrix} \Delta Q_{g+1} \\ \vdots \\ \Delta Q_{g+cap} \\ \Delta Q_{g+cap+1} \\ \vdots \\ \Delta Q_n \end{bmatrix} - (S_4)^{-1}(S_3) \begin{bmatrix} (\Delta t_{jk})_1 \\ \vdots \\ (\Delta t_{jk})_t \\ \Delta V_1 \\ \vdots \\ \Delta V_g \end{bmatrix} \tag{6.46}$$

Substituting (6.46) into (6.44) for $\begin{bmatrix} \Delta V_{g+1} \\ \vdots \\ \Delta V_{g+cap} \\ \Delta V_{g+cap+1} \\ \vdots \\ \Delta V_n \end{bmatrix}$ we get

$$\begin{bmatrix} \Delta Q_1 \\ \vdots \\ \Delta Q_g \end{bmatrix} = (S_1 - (S_2)(S_4)^{-1}(S_3)) \begin{bmatrix} (\Delta t_{jk})_1 \\ \vdots \\ (\Delta t_{jk})_t \\ \Delta V_1 \\ \vdots \\ \Delta V_g \end{bmatrix} + S_2(S_4)^{-1} \begin{bmatrix} \Delta Q_{g+1} \\ \vdots \\ \Delta Q_{g+cap} \\ \Delta Q_{g+cap+1} \\ \vdots \\ \Delta Q_n \end{bmatrix} \tag{6.47}$$

Equation (6.47) can be rewritten as:

$$\begin{bmatrix}\Delta Q_1\\ \vdots \\ \Delta Q_g\end{bmatrix} = (S_1\text{-}(S_2)(S_4)^{-1}(S_3))\begin{bmatrix}(\Delta t_{jk})_1\\ \vdots \\ (\Delta t_{jk})_t \\ \Delta V_1 \\ \vdots \\ \Delta V_g\end{bmatrix} + S_2(S_4)^{-1}\begin{bmatrix}I_{(cap\ x\ cap)}\\ 0_{(l\ x\ cap)}\end{bmatrix}\begin{bmatrix}\Delta Q_{g+1}\\ \vdots \\ \Delta Q_{g+cap}\end{bmatrix} + S_2(S_4)^{-1}$$

$$*\begin{bmatrix}I_{(l\ x\ l)}\\ 0_{(cap\ x\ l)}\end{bmatrix}\begin{bmatrix}\Delta Q_{g+cap+1}\\ \vdots \\ \Delta Q_n\end{bmatrix} \qquad (6.48)$$

The last term in Equation (6.48) is zero since the change in the reactive power at any load bus without VAR resource due to change in any control variable is` zero. So Equation (6.48) can be rewritten as:

$$\begin{bmatrix}\Delta Q_1\\ \vdots \\ \Delta Q_g\end{bmatrix} = (S_1\text{-}(S_2)(S_4)^{-1}(S_3))\begin{bmatrix}(\Delta t_{jk})_1\\ \vdots \\ (\Delta t_{jk})_t \\ \Delta V_1 \\ \vdots \\ \Delta V_g\end{bmatrix} + S_2(S_4)^{-1}\begin{bmatrix}I_{(cap\ x\ cap)}\\ 0_{(l\ x\ cap)}\end{bmatrix}\begin{bmatrix}\Delta Q_{g+1}\\ \vdots \\ \Delta Q_{g+cap}\end{bmatrix} \qquad (6..49)$$

Similarly Equation (6.46) can be rewritten as:

$$\begin{bmatrix}\Delta V_{g+1}\\ \vdots \\ \Delta V_{g+cap} \\ \Delta V_{g+cap+1} \\ \vdots \\ \Delta V_n\end{bmatrix} = \text{ - }(S_4)^{-1}(S_3)\begin{bmatrix}(\Delta t_{jk})_1\\ \vdots \\ (\Delta t_{jk})_t \\ \Delta V_1 \\ \vdots \\ \Delta V_g\end{bmatrix} + (S_4)^{-1}\begin{bmatrix}I_{(cap\ x\ cap)}\\ 0_{(l\ x\ cap)}\end{bmatrix}\begin{bmatrix}\Delta Q_{g+1}\\ \vdots \\ \Delta Q_{g+cap}\end{bmatrix} \qquad (6.50)$$

Augmenting Equations (6.49) and (6.50) in one equation to get the whole system sensitivity:

$$\begin{bmatrix} \Delta Q_1 \\ \vdots \\ \Delta Q_g \\ \Delta V_{g+1} \\ \vdots \\ \Delta V_{g+cap} \\ \Delta V_{g+cap+1} \\ \vdots \\ \Delta V_n \end{bmatrix} = [S] \begin{bmatrix} (\Delta t_{jk})_1 \\ \vdots \\ (\Delta t_{jk})_t \\ \Delta V_1 \\ \vdots \\ \Delta V_g \\ \Delta Q_{g+1} \\ \vdots \\ \Delta Q_{g+cap} \end{bmatrix} \quad (6.51)$$

where:

$$[S] = \begin{bmatrix} (S_1 - (S_2)(S_4)^{-1}(S_3)) & (S_2)(S_4)^{-1} \begin{bmatrix} I_{(cap\ x\ cap)} \\ 0_{(l\ x\ cap)} \end{bmatrix} \\ -(S_4)^{-1}(S_3) & (S_4)^{-1} \begin{bmatrix} I_{(cap\ x\ cap)} \\ 0_{(l\ x\ cap)} \end{bmatrix} \end{bmatrix} \quad (6.52)$$

where:

I: Is the unity matrix

0: Is a zero matrix

6.8 Method 1: Minimizing the Number of Control Variables

6.8.1 Relation between Dependent and Control Variables

Consider a power system with *n* buses, with buses 1 to *g* as a generator buses, buses *g+1* to *n* as load buses, and the first generator is counted as the swing bus, the system has a number of tap changing transformers equal to t, and a number of buses with a switchable shunt capacitor equal to cap. By adjusting the controlling device at load bus *j*, the voltage improvement at bus *i* can be found by Equation (6.53) as:

$$\Delta V_i = S_{ij}.\Delta U_j \quad \text{for } i = g+1, g+2, \ldots, n \quad \text{and} \quad j = 1,2, \ldots, t + g + cap \quad (6.53)$$

where:

ΔV_i: is the voltage change at load bus *i*

ΔU_j: is the adjustment of the controlling device *j*

S_{ij}: is the sensitivity coefficient of the controlling device *j* on voltage at load bus *i*

The adjustment of the controlling devices is constrained with the upper and lower limits as:

$$\Delta U^{min} \leq \Delta U \leq \Delta U^{max} \tag{6.54}$$

where:

$$\Delta U = \left[(\Delta t_{jk})_1, \dots, (\Delta t_{jk})_t, \Delta V_1, \dots, \Delta V_g, \Delta Q_{g+1}, \dots, \Delta Q_{g+cap}\right]^{\mathrm{T}}$$

$$\Delta U^{min} = \left[\Delta(t_{jk})_1^{min}, \dots, \Delta(t_{jk})_t^{min}, \Delta V_1^{min}, \dots, \Delta V_g^{min}, \Delta Q_{g+1}^{min}, \dots, \Delta Q_{g+cap}^{min}\right]^{\mathrm{T}}$$

$$\Delta U^{max} = \left[\Delta(t_{jk})_1^{max}, \dots, \Delta(t_{jk})_t^{max}, \Delta V_1^{max}, \dots, \Delta V_g^{max}, \Delta Q_{g+1}^{max}, \dots, \Delta Q_{g+cap}^{max}\right]^{\mathrm{T}}$$

The objective in this work is to keep the load bus voltage deviation within $\pm 5\%$ of the nominal voltage which is 1 pu i.e.,

$$0.95 \leq V_i \leq 1.05 \qquad \text{for } i = g+1, g+2, \dots, n \tag{6.55}$$

The controlling ability of the controlling devices on load buses can be found as:

$$C = S_{vc} M \tag{6.56}$$

where:

C: is a matrix of dimension ((n-g)x(t+g+cap)) represents the controlling ability of the controlling devices on voltage magnitude at all load buses. This column vector represents the change in voltage magnitude at all load buses

M: is a diagonal matrix of dimension ((t+g+cap)x((t+g+cap)). The diagonal elements represent the controlling margins of the controlling devices.

S_{vc}: is the sensitivity matrix (a modified Jacobian matrix) of dimension ((n-g)x(t+g+cap)) represents derivatives of voltage magnitude at all load buses with respect each control variable. This matrix shows the effect of any change in one control variable on all the dependent variables.

Based on the upper and lower limits for every controller the controlling ability for each controller can be divided into two, one for the positive margin and the other for the negative margin as follows:

$$C^+ = S_{vc} M^+ \tag{6.57}$$

$$C^- = S_{vc} M^- \tag{6.58}$$

where:

M^+: is a diagonal matrix of dimension ((t+g+cap)x((t+g+cap)). The diagonal elements represent positive margins of the controlling devices based on the current operating point and equal to $(U^{max} - U)$

M^-: is a diagonal matrix of dimension ((t+g+cap)x((t+g+cap)). The diagonal elements represent negative margins of the controlling devices based on the current operating point and equal to $(U^{min} - U)$

6.8.2 Methodology

The details of the solution process for minimum control action algorithm (Method 1) are given below. Figure (6.17) is a corresponding flow chart.

1. Perform base case load flow solution.
2. Check the system performance for voltage magnitudes at load buses. If voltage profile improvement is needed proceed to Step 3, otherwise, stop.
3. Calculate the sensitivity matrix (S_{vc}), M^+, M^-, C^+, and C^-.
4. Find the minimum voltage magnitude (V_{min}) and the maximum voltage magnitude (V_{max}) within the set of system voltages.
5. Find the load bus with the most voltage violation by comparing the absolute values of (1- V_{min}) and (1- V_{max}). If the value of absolute value of (1- V_{min}) is greater than the absolute value of (1- V_{max}), then proceed to Step 6, otherwise go to Step 8.
6. Find the maximum value of augmented matrix, [C^+ C^-], in the row corresponding to the bus with the minimum voltage magnitude to be C_i^{max}. Find the element S_{ij} corresponding to load bus *i* and controlling device *j*.
7. Calculate the value of (1- V_{min})/S_{ij}. Store this value in A. Find the max value of [C^+ C^-] / S_{ij}. Store this value in B, then go to Step 10.

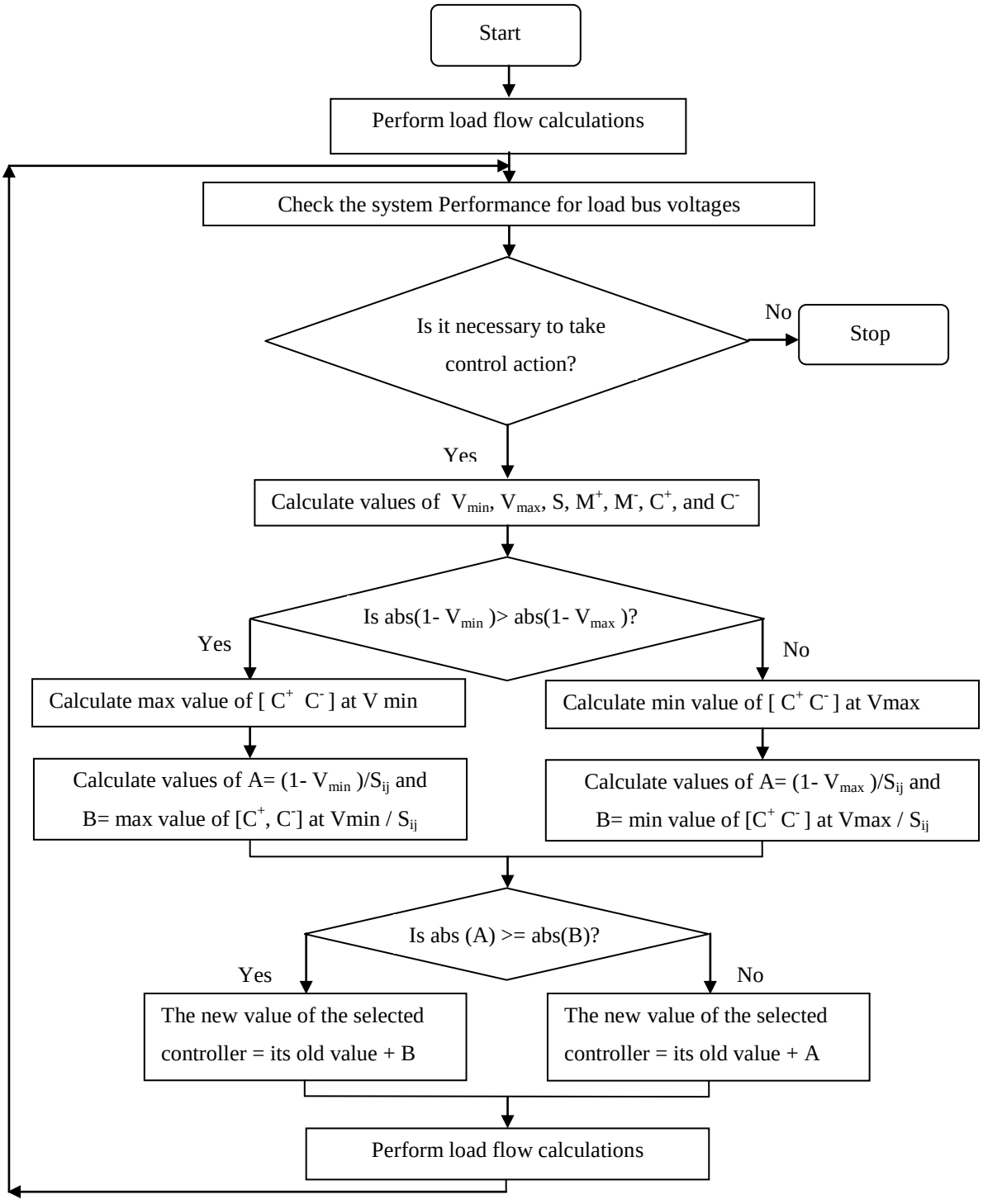

Figure 6.17: Flow chart for minimum control action algorithm

8. Find the minimum value of the matrix [C^+ C^-] in the row corresponding to the bus with the maximum voltage magnitude. Find the element S_{ij} corresponding to load bus *i* and controlling device *j*.
9. Calculate the value of (1- V_{min})/S_{ij}. Store this value in A. Find the min value of [C^+ C^-]/ S_{ij}. Store this value in B.
10. If the absolute value of A is greater than the absolute value of B, proceed to Step 11. Else go to step 12
11. Get the new setting of the controller = the old setting + B, and go to step 13
12. Get the new setting of the controller = the old setting + A.
13. Perform load flow calculations and go back to Step 2.

6.9 Method 2: Minimizing the Power Losses (P_L)

6.9.1 Mathematical Statement of the Minimizing Power Losses Problem

The objective of this method is to minimize ΔP_L of Equation (6.59) below which subjected to inequality constrains of equations from Equation (6.9) to Equation (6.13)

$$\Delta P_L = \left[\frac{\partial P_L}{\partial (t_{jk})_1} \dots \frac{\partial P_L}{\partial (t_{jk})_t} \quad \frac{\partial P_L}{\partial V_1} \dots \frac{\partial P_L}{\partial V_g} \quad \frac{\partial P_L}{\partial Q_{g+1}} \dots \frac{\partial P_L}{\partial Q_{g+cap}}\right] \begin{bmatrix} (\Delta t_{jk})_1 \\ \vdots \\ (\Delta t_{jk})_t \\ \Delta V_1 \\ \vdots \\ \Delta V_g \\ \Delta Q_{g+1} \\ \vdots \\ \Delta Q_{g+cap} \end{bmatrix} \tag{6.59}$$

A method of finding the sensitivities of the system losses with respect to the control variables starts by calculating the sensitivities of the losses with respect to the real and reactive power injections at all the buses except the swing bus. The equation dealing with the development of these variables is developed in [128], and can be written as:

$$\begin{bmatrix} \frac{\partial P_L}{\partial \theta_2} \\ \vdots \\ \frac{\partial P_L}{\partial \theta_n} \\ \frac{\partial P_L}{\partial V_2} \\ \vdots \\ \frac{\partial P_L}{\partial V_n} \end{bmatrix} = \begin{bmatrix} \frac{\partial P_2}{\partial \theta_2} & \cdots & \frac{\partial P_n}{\partial \theta_2} & \frac{\partial Q_2}{\partial \theta_2} & \cdots & \frac{\partial Q_n}{\partial \theta_2} \\ \vdots & \ddots & \vdots & \vdots & \ddots & \vdots \\ \frac{\partial P_2}{\partial \theta_n} & \cdots & \frac{\partial P_n}{\partial \theta_n} & \frac{\partial Q_2}{\partial \theta_n} & \cdots & \frac{\partial Q_n}{\partial \theta_n} \\ \frac{\partial P_2}{\partial V_2} & \cdots & \frac{\partial P_n}{\partial V_2} & \frac{\partial Q_2}{\partial V_2} & \cdots & \frac{\partial Q_n}{\partial V_2} \\ \vdots & \ddots & \vdots & \vdots & \ddots & \vdots \\ \frac{\partial P_2}{\partial V_n} & \cdots & \frac{\partial P_n}{\partial V_n} & \frac{\partial Q_2}{\partial V_n} & \cdots & \frac{\partial Q_n}{\partial V_n} \end{bmatrix} \cdot \begin{bmatrix} \frac{\partial P_L}{\partial P_2} \\ \vdots \\ \frac{\partial P_L}{\partial P_n} \\ \frac{\partial P_L}{\partial Q_2} \\ \vdots \\ \frac{\partial P_L}{\partial Q_n} \end{bmatrix} \tag{6.60}$$

Equation (6.60) can be decoupled into two equations as follow:

$$\begin{bmatrix} \frac{\partial P_L}{\partial \theta_2} \\ \vdots \\ \frac{\partial P_L}{\partial \theta_n} \end{bmatrix} = \begin{bmatrix} \frac{\partial P_2}{\partial \theta_2} & \cdots & \frac{\partial P_n}{\partial \theta_2} \\ \vdots & \ddots & \vdots \\ \frac{\partial P_2}{\partial \theta_n} & \cdots & \frac{\partial P_n}{\partial \theta_n} \end{bmatrix} \cdot \begin{bmatrix} \frac{\partial P_L}{\partial P_2} \\ \vdots \\ \frac{\partial P_L}{\partial P_n} \end{bmatrix} \tag{6.61}$$

$$\begin{bmatrix} \frac{\partial P_L}{\partial V_2} \\ \vdots \\ \frac{\partial P_L}{\partial V_n} \end{bmatrix} = \begin{bmatrix} \frac{\partial Q_2}{\partial V_2} & \cdots & \frac{\partial Q_n}{\partial V_2} \\ \vdots & \ddots & \vdots \\ \frac{\partial Q_2}{\partial V_n} & \cdots & \frac{\partial Q_n}{\partial V_n} \end{bmatrix} \cdot \begin{bmatrix} \frac{\partial P_L}{\partial Q_2} \\ \vdots \\ \frac{\partial P_L}{\partial Q_n} \end{bmatrix} \tag{6.62}$$

From Equation (6.1) the elements of $\partial P_L/\partial \theta$ and $\partial P_L/\partial V$ can be found as follows:

$$\frac{\partial P_L}{\partial \theta_i} = \frac{\partial P_1}{\partial \theta_i} + \frac{\partial P_2}{\partial \theta_i} + \cdots + \frac{\partial P_n}{\partial \theta_i} \qquad \text{for } i = 2, 3, \ldots, n \tag{6.63}$$

$$\frac{\partial P_L}{\partial V_i} = \frac{\partial P_1}{\partial V_i} + \frac{\partial P_2}{\partial V_i} + \cdots + \frac{\partial P_n}{\partial V_i} \qquad \text{for } i = 2, 3, \ldots, n \tag{6.64}$$

Knowing the Jacobian matrix (J), Equation (6.35) can be used to find the elements $\partial P/\partial \theta$, and $\partial P/\partial V$ can be determined. Then by substituting Equations (6.63) and (6.64) into Equations (6.61), and (6.62) the values of $\partial P_L/\partial P$ and $\partial P_L/\partial Q$ at all buses except the swing bus can be found.

6.9.2 Power Losses Sensitivities With Respect to Transformer Tap position

For a transformer connecting buses *j* and *k*, with tap side on bus *j*, the power injections into buses *j* and k are P_j, Q_j, P_k and Q_k, respectively, as shown in Figure (6.18). Calculation of

the sensitivity with respect to transformer tap setting depends on the approximation that these power injections into end buses *j* and *k* do not change with the transformer tap setting.

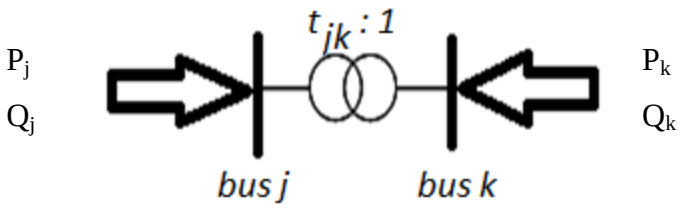

Figure 6.18: Representation of a transformer with tap side at bus j

A small change in the tap setting, Δt_{jk}, of transformer jk, will cause an incremental power flow in the transformer, changing the power injections into end buses as indicated in Figure (6.19). These changes in power injections are to be eliminated by suitably injecting incremental powers of opposite sign. This modification in power injections is the key to determine the sensitivities of the injected active and reactive power at the transformer end buses with respect to the change in transformer tap setting.

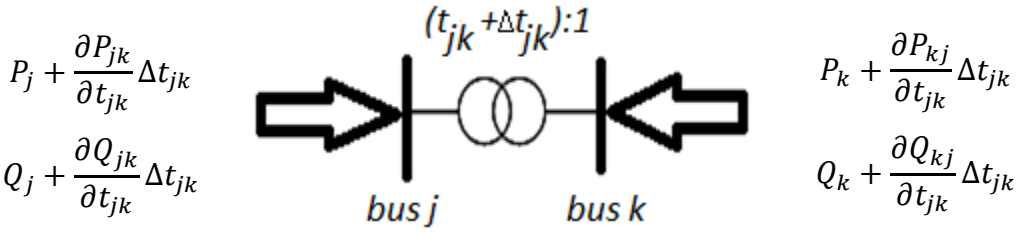

Figure 6.19: Representation of a transformer with incremental power injection errors

The real and reactive power injection errors at tap side bus (*j*) are:

$$\Delta P_j = P_j^{scheduled} - P_j^{calculated} = P_j - (P_j + \frac{\partial P_{jk}}{\partial t_{jk}} \Delta t_{jk}) = -\frac{\partial P_{jk}}{\partial t_{jk}} \Delta t_{jk} \quad (6.65)$$

$$\Delta Q_j = Q_j^{scheduled} - Q_j^{calculated} = Q_j - (Q_j + \frac{\partial Q_{jk}}{\partial t_{jk}} \Delta t_{jk}) = -\frac{\partial Q_{jk}}{\partial t_{jk}} \Delta t_{jk} \quad (6.66)$$

Similarly at the non tap side bus (*k*) those values are:

$$\Delta P_k = P_k^{scheduled} - P_k^{calculated} = P_k - (P_k + \frac{\partial P_{kj}}{\partial t_{jk}} \Delta t_{jk}) = -\frac{\partial P_{kj}}{\partial t_{jk}} \Delta t_{jk} \quad (6.67)$$

$$\Delta Q_k = Q_k^{scheduled} - Q_k^{calculated} = Q_k - (Q_k + \frac{\partial Q_{kj}}{\partial t_{jk}} \Delta t_{jk}) = -\frac{\partial Q_{kj}}{\partial t_{jk}} \Delta t_{jk} \quad (6.68)$$

From Equations (6.65), (6.66), (6.67), and (6.68), ΔP_L for a transformer *jk* can be written as:

$$\Delta P_L = \frac{\partial P_L}{\partial P_j} \Delta P_j + \frac{\partial P_L}{\partial Q_j} \Delta Q_j + \frac{\partial P_L}{\partial P_k} \Delta P_k + \frac{\partial P_L}{\partial Q_k} \Delta Q_k \quad (6.69)$$

From (6.63), (6.64), (6.65), and (6.66) into (6.67), ΔP_L can be rewritten as:

$$\Delta P_L = \{\frac{\partial P_L}{\partial P_j}\left(-\frac{\partial P_{jk}}{\partial t_{jk}}\right) + \frac{\partial P_L}{\partial Q_j}\left(-\frac{\partial Q_{jk}}{\partial t_{jk}}\right) + \frac{\partial P_L}{\partial P_k}\left(-\frac{\partial P_{kj}}{\partial t_{jk}}\right) + \frac{\partial P_L}{\partial Q_k}\left(-\frac{\partial Q_{kj}}{\partial t_{jk}}\right)\}\Delta t_{jk} \quad (6.70)$$

Assuming that

$$\frac{\Delta P_L}{\Delta t_{jk}} = \frac{\partial P_L}{\partial t_{jk}} \quad (6.71)$$

From (6.70) into (6.71), $\partial P_L / \partial t_{jk}$ can be expressed as:

$$\frac{\partial P_L}{\partial t_{jk}} = \{\frac{\partial P_L}{\partial P_j}\left(-\frac{\partial P_{jk}}{\partial t_{jk}}\right) + \frac{\partial P_L}{\partial Q_j}\left(-\frac{\partial Q_{jk}}{\partial t_{jk}}\right) + \frac{\partial P_L}{\partial P_k}\left(-\frac{\partial P_{kj}}{\partial t_{jk}}\right) + \frac{\partial P_L}{\partial Q_k}\left(-\frac{\partial Q_{kj}}{\partial t_{jk}}\right)\} \quad (6.72)$$

The values of $\partial P_L / \partial P_j$, $\partial P_L / \partial Q_j$, $\partial P_L / \partial P_k$, and $\partial P_L / \partial Q_k$ can be obtained from Equation (6.60), while the values of $\partial P_{jk} / \partial t_{jk}$, $\partial Q_{jk} / \partial t_{jk}$, $\partial P_{kj} / \partial t_{jk}$, and $\partial Q_{kj} / \partial t_{jk}$ can be determined from Equations (6.29), (6.30), (6.31), and (6.32) respectively. Thus Equation (6.72) can be used to find the sensitivity of power losses with respect to the change in the tap setting of a transformer.

6.9.3 Power Losses Sensitivities With Respect to Generator Terminal Voltage

By changing the excitation voltage of a generator, the reactive power injection at that bus will be modified. Sensitivity of the power losses with respect to generator terminal voltage can be found form the equation below.

$$\frac{\partial P_L}{\partial V_i} = \frac{\partial P_L}{\partial Q_i}\frac{\partial Q_i}{\partial V_i} \qquad \text{i} = 2, 3, \ldots, \text{g} \tag{6.73}$$

where, *i* represents any generator bus except the swing bus. The term $\partial P_L/\partial Q_i$ can be calculated from Equation (6.62) while the term $\partial Q_i/\partial V_i$ can be found from Equation (6.37). Finally Equation (6.73) can be used to find the sensitivity of the power losses with respect to any generator terminal voltage except the swing bus.

6.9.4 Power Losses Sensitivities With Respect to Swing Bus Terminal Voltage

Changing the terminal voltage of the swing bus results in changing the reactive power injection at remaining generators in the system, and at the same time it will affect the reactive power at all load busses connected to the swing bus. This is based on this fact the sensitivity of the power losses with respect to the swing bus voltage can be expressed as:

$$\frac{\partial P_L}{V_1} = \frac{\partial P_L}{\partial Q_2}\frac{\partial Q_2}{\partial V_1} + \frac{\partial P_L}{\partial Q_3}\frac{\partial Q_3}{\partial V_1} + \cdots + \frac{\partial P_L}{\partial Q_g}\frac{\partial Q_g}{\partial V_1} + \sum_u \frac{\partial P_L}{\partial Q_u}\left(\frac{-\partial Q_u}{\partial V_1}\right) \tag{6.74}$$

where, u represents any load bus connected to the swing bus (bus1). The terms $\partial P_L/\partial Q_2, \partial P_L/\partial Q_3, \ldots, \partial P_L/\partial Q_g$ and $\partial P_L/\partial Q_u$ can be calculated from Equation (6.62), while the terms $\partial Q_2/\partial V_1, \partial Q_3/\partial V_1, \ldots,$ and $\partial Q_g/\partial V_1$ can be determined directly from the sensitivity matrix (S) in Equation (6.52), and finally the value of $\partial Q_u/\partial V_1$ comes from Equation (6.37).

6.9.5 Power Losses Sensitivities With Respect to Reactive Power of Switchable Shunt Capacitor Bus

Here m represents any bus which has a switchable shunt capacitor. The values of sensitivities with respect to reactive power of switchable shunt capacitor bus ($\partial P_L/\partial Q_m$), can be calculated directly from Equation (6.62), where, m= 1,2,….., cap.

6.10 Method 3: Minimizing the Summation of the Squares of the Voltage Deviations

6.10.1 Mathematical Statement of the Minimizing Voltage Deviation Problem

The voltage deviations of all the load buses can be found from the following equation:

$$V_d = \sum_{j=g+1}^{n} \left(V_j - V_j^{norm}\right)^2 \tag{6.75}$$

After linearization, the objective of this method is to minimize ΔV_d of Equation (6.76) below which subjected to inequality constrains of equations from Equation (6.9) to Equation (6.13)

$$\Delta V_d = \begin{bmatrix} \frac{\partial V_d}{\partial (t_{jk})_1} & \cdots & \frac{\partial V_d}{\partial (t_{jk})_t} & \frac{\partial V_d}{\partial V_1} & \cdots & \frac{\partial V_d}{\partial V_g} & \frac{\partial V_d}{\partial Q_{g+1}} & \cdots & \frac{\partial V_d}{\partial Q_{g+cap}} \end{bmatrix} \begin{bmatrix} (\Delta t_{jk})_1 \\ \vdots \\ (\Delta t_{jk})_t \\ \Delta V_1 \\ \vdots \\ \Delta V_g \\ \Delta Q_{g+1} \\ \vdots \\ \Delta Q_{g+cap} \end{bmatrix} \tag{6.76}$$

6.10.2 Voltage Deviation Sensitivities With Respect to Transformer Tap position

For a system with a total number of tap changing transformers equal to *t* , the sensitivities of voltage deviation with respect to change in the tap setting can be determined as:

$$\frac{\partial V_d}{(\partial t_{jk})_m} = \sum_{j=g+1}^{n} 2\left(V_j - V_j^{norm}\right)\left(\frac{\partial V_j}{(\partial t_{jk})_m}\right) \tag{6.77}$$

where, m = 1, 2, …, t. The value of V_j can be found from load flow results, while the value of $\partial V_j/(\partial t_{jk})_m$ can be determined from Equation (6.52). By knowing these values, the sensitivity

of the voltage deviation with respect to transformer tap setting can be evaluated using Equation (6.77).

6.10.3 Voltage Deviation Sensitivities With Respect to Generator Terminal Voltages

For a system with total number of generators equal to *g*, the sensitivities of voltage deviation with respect to change in generator terminal voltage can be determined as:

$$\frac{\partial V_d}{\partial V_k} = \sum_{j=g+1}^{n} 2\left(V_j - V_j^{norm}\right)\left(\frac{\partial V_j}{\partial V_k}\right) \tag{6.78}$$

where, k = *t + 1, t + 2, …, t + g*. The value of V_j can be found from load flow results, while the value of $\partial V_j / \partial V_k$ can be determined from Equation (6.52), by knowing these values, the sensitivity of the voltage deviation with respect to generator terminal voltages can be determined using Equation (6.78).

6.10.4 Voltage Deviation Sensitivities With Respect to Reactive Power of Switchable Shunt Capacitor Bus

For a system with total number of switchable shunt capacitors equal to *cap*, the sensitivities of voltage deviation with respect to change in the reactive power of switchable shunt capacitors can be determined as:

$$\frac{\partial V_d}{\partial Q_k} = \sum_{j=g+1}^{n} 2\left(V_j - V_j^{norm}\right)\left(\frac{\partial V_j}{\partial Q_k}\right) \tag{6.79}$$

where, k = *t + g + 1, t + g + 2, …, t + g + cap*. The value of V_j can be found from load flow results, while the value of $\partial V_j / \partial Q_k$ can be determined from Equation (6.52). By knowing these values, the sensitivity of the voltage deviation with respect to change in the reactive power of switchable shunt capacitors can be determined using Equation (6.79).

6.11 General Methodology for Method 2(Minimum P_L) and Method 3 (Minimum V_d) Algorithms Using GA Optimization Technique

The steps of the solution process for methods 2 and 3 are given below.

1. Perform a base case load flow solution.
2. Check the system performance. If improvement of the voltage profiles or minimization of the objective function, or both, is necessary then proceed to Step 3, otherwise, stop.
3. Calculate the sensitivity matrix (S) relating the dependent variables, Δx, and the control variables, Δu as explained in the previous sections.
4. Find the dependent variables' lower and upper limits, $\Delta x^{min}, \Delta x^{max}$ and the control variables' lower and upper limits, $\Delta u^{min}, \Delta u^{max}$.
5. Calculate the coefficients of the objective function using the derivative of the objective function with respect to all the control variables, u, as indicated in the previous sections.
6. Solve the optimization problem using the Genetic Algorithm (GA) [117] to evaluate the required adjustments to the control variables (Δu).
7. Update the values of the control variables from the output of the GA optimization technique. $u_{\text{new}} = u_{\text{old}} + \Delta u$.
8. Perform a load flow solution after the adjustments in the control variables and go back to Step 2.

6.12 Results and Analysis

The proposed methods have been tested on three different systems: the Ward and Hale 6 bus system, the modified IEEE 14 bus system, and the modified IEEE 30 bus system. The results and analysis for some cases, including some contingencies, are following.

6.12.1 Case 1: Modified IEEE 14 Bus System with Loading Factor = 1.4

The single line diagram and the data of a modified IEEE 14 system can be found in appendix C. At a loading factor equal to 1.4 the system has a total active load of 362.60 MW, and a total reactive load of 102.90MVAR. As shown in Figure (6.20) the minimum voltage magnitude before any control action, is 0.8504 pu at bus number 14, the most critical bus in the system. This voltage improved to 0.9891 pu with the objective function of minimum number of controllers, to 0.9513 pu with the objective function of minimum power losses, and to 0.9797 pu

using the objective function of minimum voltage deviations. Before compensation, 10 buses out of fourteen violated the lower voltage limit. After compensation all the buses, their voltages came back to be within acceptable operating limits as shown in Figure (6.20).

The minimum number of control actions algorithm for the this case uses three controllers as indicated in Table (6.1) to improve the voltage profiles of the system. On the other hand, the other two methods, minimum power losses and minimum voltage deviations, use five controllers in order to remove any voltage violation in the system. The required adjustments for all controllers for the three different methods are indicated in Table (6.1).

Figure (6.21) shows that bus number 14, most critical bus in the system, has the minimum value (0.4303) of the *1-L* indicator. This value improved to be 0.6801 after adjusting the controllers using minimum number of control action, to be 0.7260 with minimum power losses method, and to be 0.6776 with minimum voltage deviation method. Figure (6.22) indicates that all the three methods managed to increase the stability margin of the system.

A review of Table (6.2) indicates that the MSV improved from 0.2666 to 0.4185 with the first method, to 0.4688 using minimum power losses method, and to 0.4155 with minimum voltage deviation method. The real power losses are decreased from 31.87 MW to 28.96 MW with a percentage reduction of 9.13 %, and the reactive power losses are improved from 109.64 MVAR to 94.49 MVAR with a percentage reduction of 13.82 % using the method of minimum number of control action. When applying minimum power losses method, the real power losses changed to 28.41 MW with a percentage reduction of 10.86 %, and the reactive power losses are improved to 93.46 MVAR with a percentage reduction of 14.76 %. By using the method of minimum voltage deviations, the real and reactive power losses are reduced to 28.34 MW and 93.14 MVAR respectively. The corresponding percentage reductions are 11.08 % and 15.05 % respectively.

The time taken to get the required control actions with Intel core i5 PC computer of 2.27GHz is 6.727 seconds with minimum number of control actions, 22.833 seconds using minimum power losses method, and 19.467 seconds with minimum voltage deviation method.

Table 6.1: Change in controllers for IEEE 14 bus system at 1.4 loading factor

Algorithm / Controller name	Minimum control action	Minimum power losses	Minimum voltage deviations
Δt_{6-5}	0.15	0.02	0.12
Δt_{4-7}	-0.08	-0.07	-0.04
Δt_{4-9}	0	0.10	0.11
ΔV_1	0.04	0.04	0.03
ΔV_2	0	0	0
ΔV_3	0	0	0
ΔV_6	0	0	0
ΔV_8	0	0	0
ΔQ_{c9}	0	0.20	0.20

Table 6.2: IEEE 14 bus system performance at 1.4 loading factor

Algorithm / Parameter	Without compensation	Using minimum control action	Using minimum power losses	Using minimum voltage deviations
Power losses	31.87 MW	28.96 MW	28.41 MW	28.38 MW
Reactive power losses	109.64 MVAR	94.49 MVAR	93.46 MVAR	93.14 MVAR
MSV	0.2666	0.4185	0.4688	0.4155

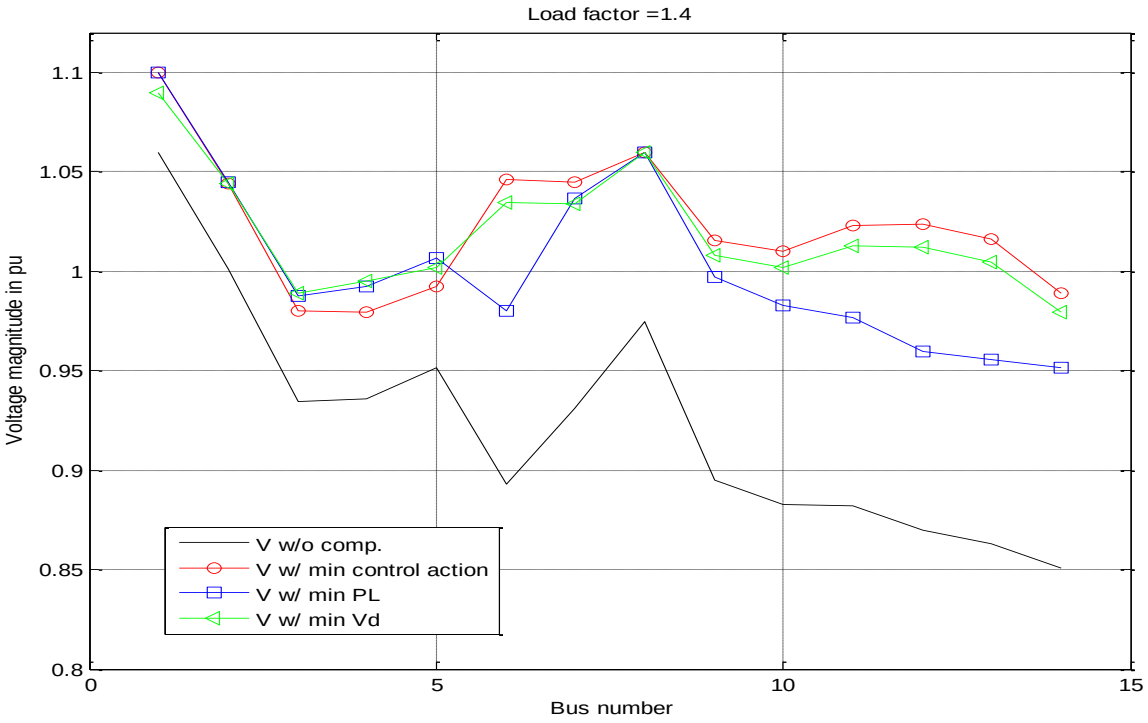

Figure 6.20: Voltage profile at 1.4 loading factor for the modified IEEE 14 bus

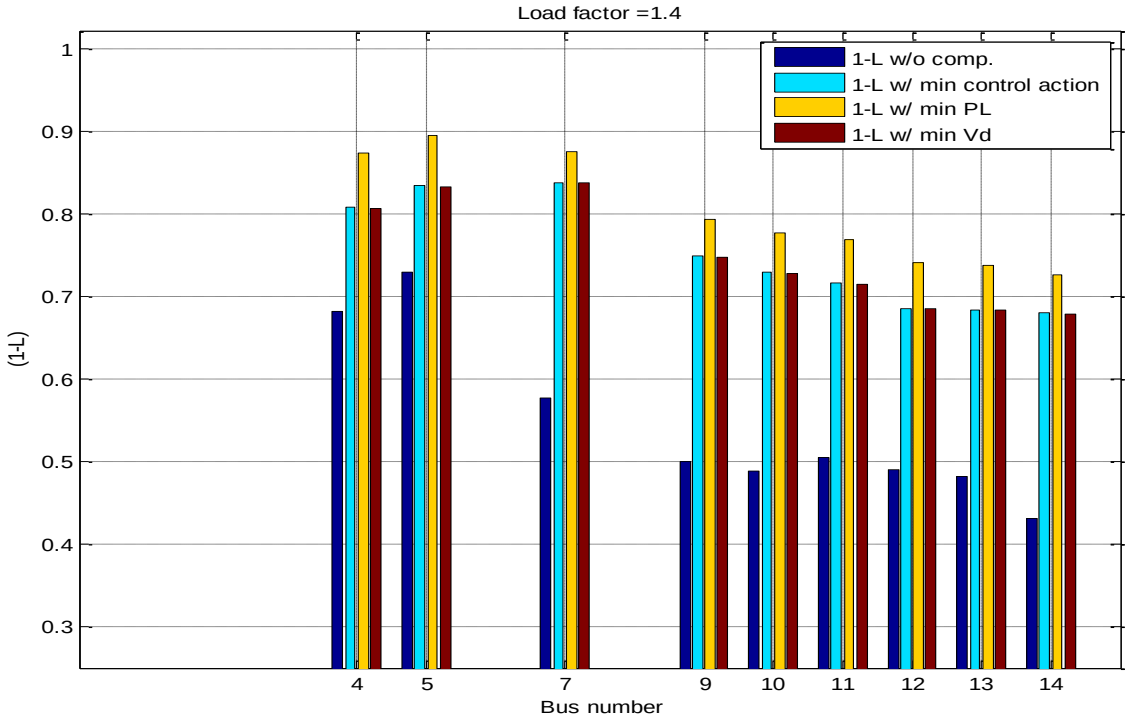

Figure 6.21: *1-L* index at 1.4 loading factor for the modified IEEE 14 bus

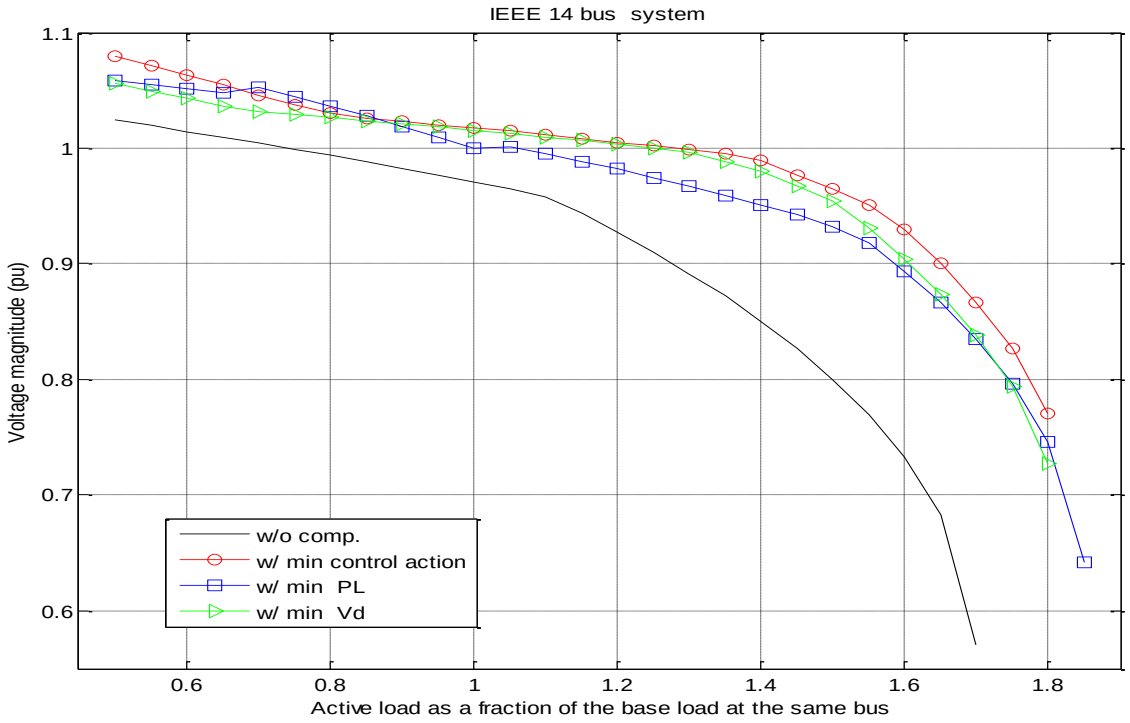

Figure 6.22: PV curves at bus 14 at 1.4 loading factor for the modified IEEE 14 bus

6.12.2 Case 2: Modified IEEE 14 Bus System with Transformer t65 Out of Service

The modified IEEE 14 bus system at full load with transformer t_{65} out of service has a total active load of 259 MW, and a total reactive load of 73.50 MVAR. In this case, only two buses violate the voltage limits, bus 12 and bus 13 as shown in Figure (6.23). The minimum voltage magnitude before taking any control action is 0.9459 pu at bus number 12. This voltage enhanced to be 0.9877 pu with the objective function of minimum number of controllers, to be 0.9984 pu with the objective function of minimum power losses, and to be 0.9883 pu using the objective function of minimum voltage deviations. Figure (6.23) also indicates that after compensation all the buses are within acceptable operating limits.

As indicated in Table (6.3), the minimum number of control action algorithm for this case uses only one controller to improve the voltage profiles of the system. On the other hand, the other two methods, minimum power losses and minimum voltage deviations, use three and

four controllers respectively in order to remove any voltage violation in the system. The required adjustments for these controllers are indicated in Table (6.3).

As indicated in Figure (6.24), bus number 12 has the minimum value (0.6680) of the *1-L* indicator. This value improved to be 0.6906 after the adjustment of the controller of minimum number of control action method, to be 0.6962 with minimum power losses method, and to be 0.6913 with minimum voltage deviation method. Figure (6.25) shows that the stability margin at all buses including bus number 12 has been increased.

Table (6.4) indicates that the MSV improved from 0.2401 to 0.2583 with the first method, to 0.2622 using minimum power losses method, and to 0.2587 with minimum voltage deviation method. The real power losses are decreased from 16.86 MW to 16.50 MW with a percentage reduction of 2.14 %, and the reactive power losses are improved from 48.20 MVAR to 45.19 MVAR with a percentage reduction of 6.24 % using the method of minimum number of control action. By using the method of minimum power losses, the real power losses changed to 16.43 MW with a percentage reduction of 2.55 %, and the reactive power losses are improved to 46.93 MVAR with a percentage reduction of 2.63 %. Finally, the real and reactive power losses are reduced to 16.28 MW and 46.69 MVAR respectively by using the method of minimum voltage deviation. The corresponding percentage reductions are 3.44 % and 3.13 % respectively.

Table 6.3: Change in controllers for IEEE 14 bus system at full load and w/o t_{65}

Algorithm / Controller name	Minimum control action	Minimum power losses	Minimum voltage deviations
Δt_{4-7}	0	0.04	0.05
Δt_{4-9}	0	-0.07	-0.06
ΔV_1	0	0	0.01
ΔV_2	0	0	0
ΔV_3	0	0	0
ΔV_6	0	0	0
ΔV_8	0	0	0
ΔQ_{c9}	0.20	0.20	0.18

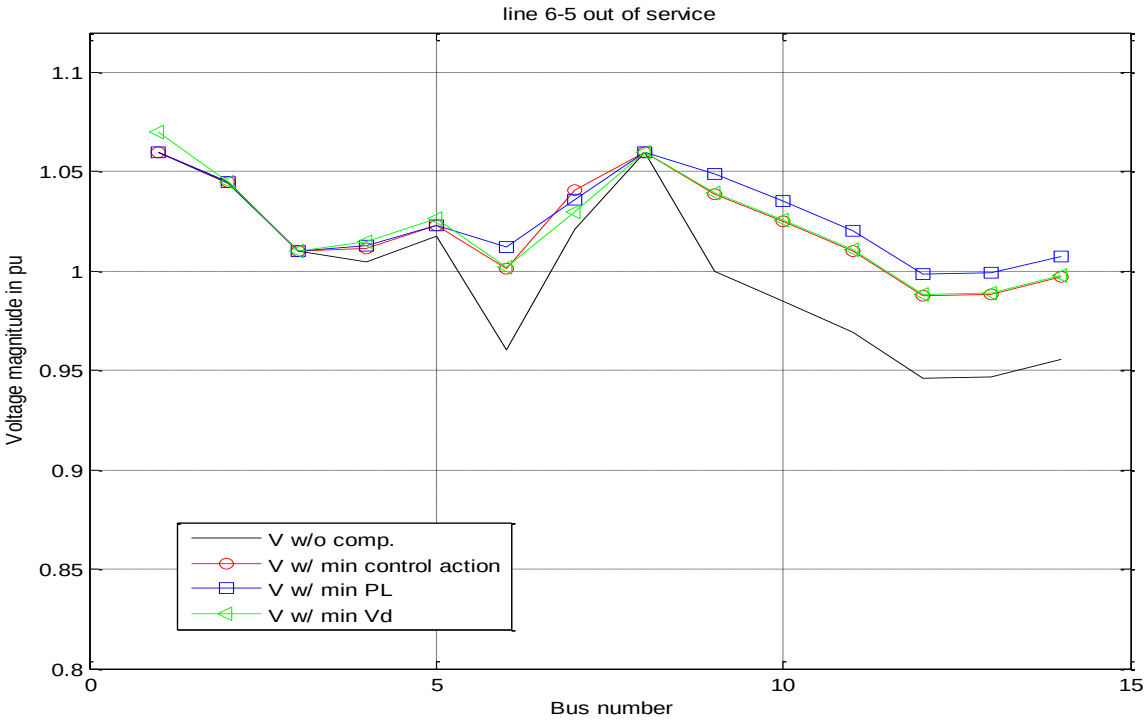

Figure 6.23: Voltage profile at full load and t_{65} out for the modified IEEE 14 bus

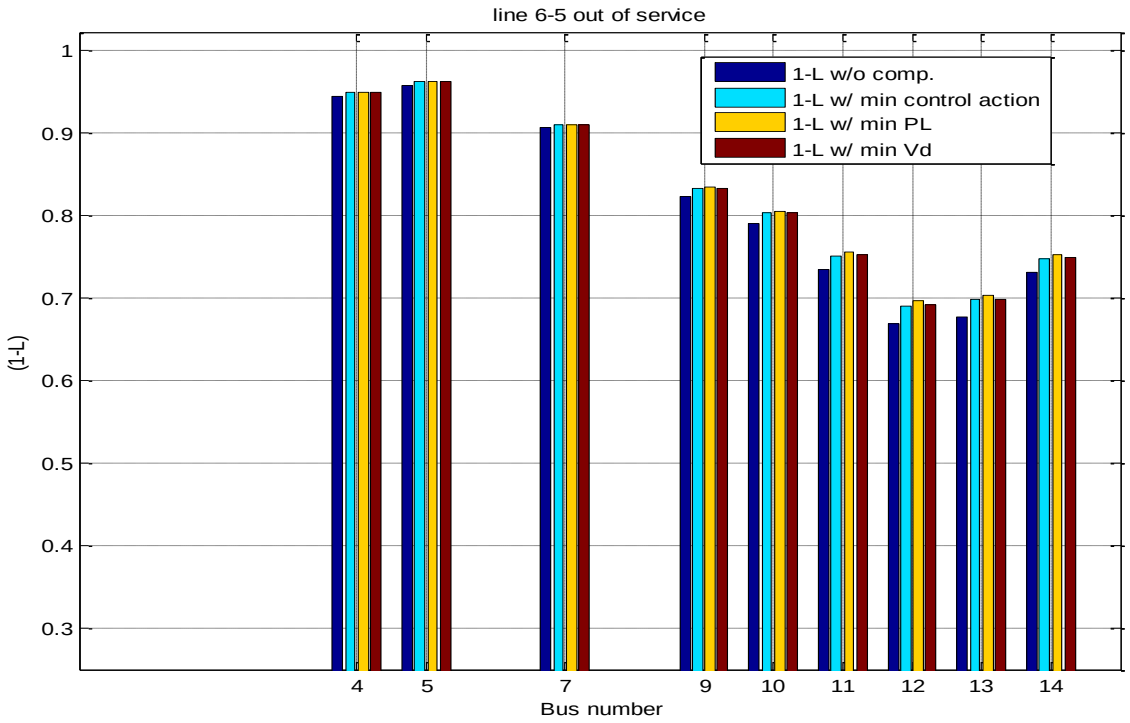

Figure 6.24: *1-L* index at full load and t_{65} out for the modified IEEE 14 bus

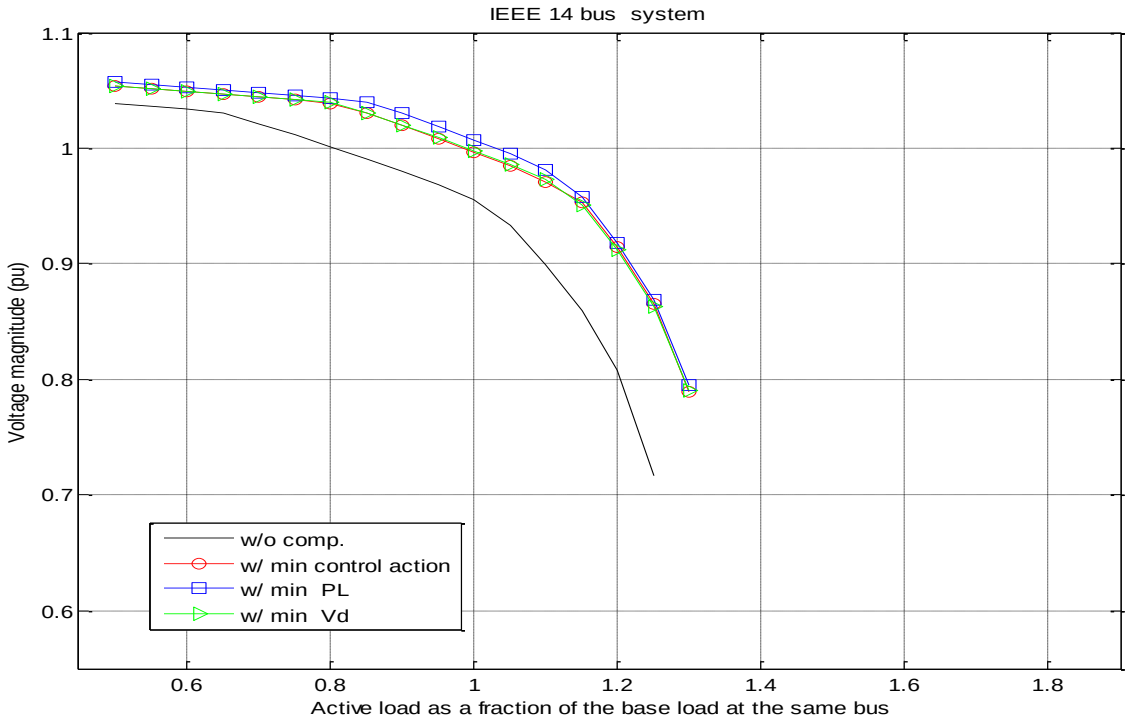

Figure 6.25: PV curves at bus 14 at full load and t_{65} out for the modified IEEE 14 bus

Table 6.4: IEEE 14 bus system performance at full load and w/o t_{65}

Algorithm / Parameter	Without compensation	Using minimum control action	Using minimum power losses	Using minimum voltage deviations
Power losses	16.86 MW	16.50 MW	16.43 MW	16.28 MW
Reactive power losses	48.20 MVAR	45.19 MVAR	46.93 MVAR	46.69 MVAR
MSV	0.2401	0.2583	0.2622	0.2587

6.12.3 Case 3: Modified IEEE 30 Bus System with Loading Factor = 1.3

The data and single line diagram for the modified IEEE 30 system can be found in appendix D. At a loading factor equal to 1.3 the system has a total active load of 343.33 MW, and a total reactive load of 162.50 MVAR. As shown in Figure (6.26) the minimum voltage magnitude before any control action, is 0.9012 pu at bus number 30, the most critical bus in the

system. This voltage improved to 0.9667 pu with the objective function of minimum number of controllers, to 1.0277 pu with the objective function of minimum power losses, and to 1.0219 pu using the objective function of minimum voltage deviations. Before compensation, 9 buses out of thirty violated the lower voltage limit. Figure (6.26) indicates that all the three methods succeeded to remove any voltage violation in the system.

As shown in Table (6.5), the method of minimum number of control actions for this case uses two controllers to improve the voltage profiles of the system. On the other hand, the other two methods, minimum power losses and minimum voltage deviations, use fourteen and fifteen controllers respectively in order to remove any voltage violation in the system. All the required adjustments for these controllers are indicated in Table (6.5).

Figure (6.27) shows that bus number 30 has the minimum value (0.7559) of the *1-L* indicator. This value improved to be 0.7697 after the adjustment of the controllers of minimum number of control action method, to be 0.7996 with minimum power losses method, and to be 0.7901 with minimum voltage deviation method. Also the stability margin at all buses including bus number 30, the most critical bus, has been increased as shown in Figure (6.28).

As shown in Table (6.6), the MSV improved from 0.2191 to 0.2221 with the first method, to 0.2364 using minimum power losses method, and to 0.2331 with minimum voltage deviation method. The same table indicates that the real power losses are decreased from 6.11 MW to 5.92 MW with a percentage reduction of 3.11 %, and the reactive power losses are improved from 29.90 MVAR to 28.95 MVAR with a percentage reduction of 3.18 % using the method of minimum number of control action. By using the method of minimum power losses, the real power losses decreased to 4.60 MW with a percentage reduction of 24.71 %, and the reactive power losses are improved to 23.58 MVAR with a percentage reduction of 21.14 %. Finally, the real and reactive power losses are reduced to 4.78 MW and 25.35 MVAR respectively by using the method of minimum voltage deviation. The corresponding percentage reductions are 21.77 % and 15.22 % respectively.

Table 6.5: Change in controllers for IEEE 30 bus system at 1.3 loading factor

Algorithm / Controller name	Minimum control action	Minimum power losses	Minimum voltage deviations
$\Delta t_{12\text{-}4}$	0	0	0.02
$\Delta t_{9\text{-}6}$	0	0	-0.05
$\Delta t_{10\text{-}6}$	0	0	0
$\Delta t_{27\text{-}28}$	0	0	0
ΔV_1	0	-0.01	-0.02
ΔV_2	0	0	0
ΔV_5	0	0.05	0.05
ΔV_8	0	0.03	0.01
ΔV_{11}	0	0.05	0
ΔV_{13}	0	0.03	0.05
ΔQ_{c10}	0	-0.02	0.02
ΔQ_{c12}	0	0.08	0.02
ΔQ_{c15}	0	0.09	0.02
ΔQ_{c17}	0	0.10	0.10
ΔQ_{c20}	0	0.03	0.02
ΔQ_{c21}	0	0.08	0.08
ΔQ_{c24}	0	0.03	0.09
ΔQ_{c26}	0.03	0.03	0.02
ΔQ_{c30}	0.08	0.08	0.09

Table 6.6: IEEE 30 bus system performance at 1.3 loading factor

Algorithm / Parameter	Without compensation	Using minimum control action	Using minimum power losses	Using minimum voltage deviations
Power losses	6.11 MW	5.92 MW	4.60 MW	4.78 MW
Reactive power losses	29.90 MVAR	28.95 MVAR	23.58 MVAR	25.35 MVAR
MSV	0.2191	0.2221	0.2364	0.2331

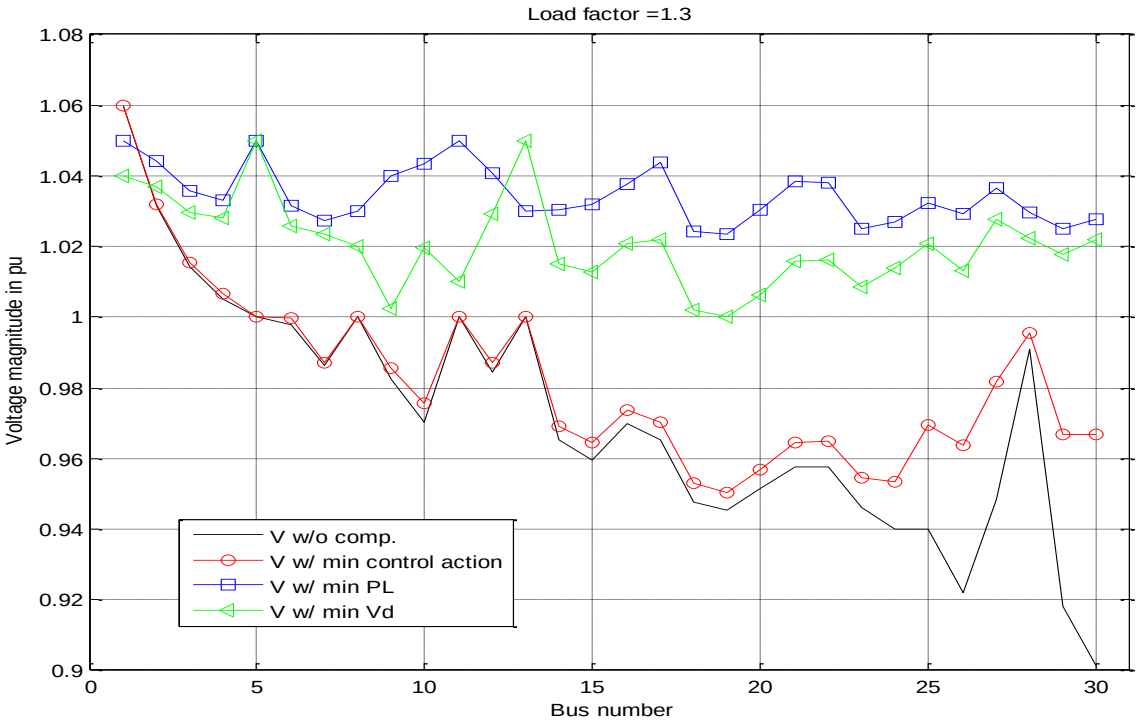

Figure 6.26: Voltage profile at 1.3 loading factor for the modified IEEE 30 bus

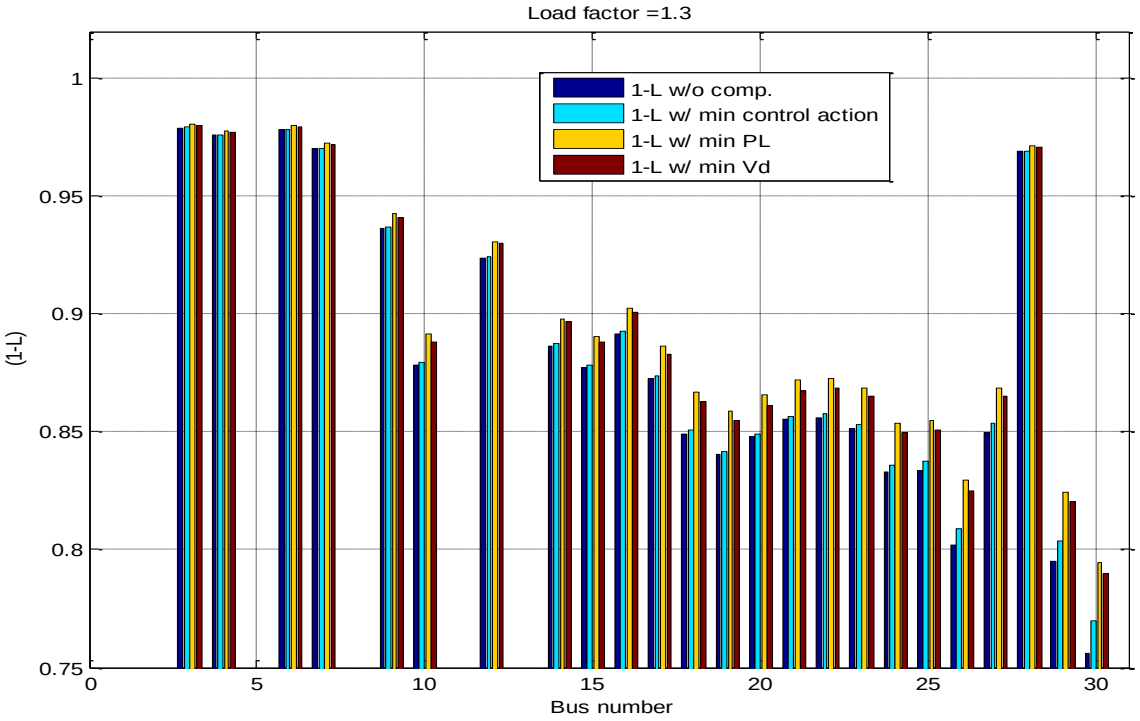

Figure 6.27: *1-L* index at 1.3 loading factor for the modified IEEE 30 bus

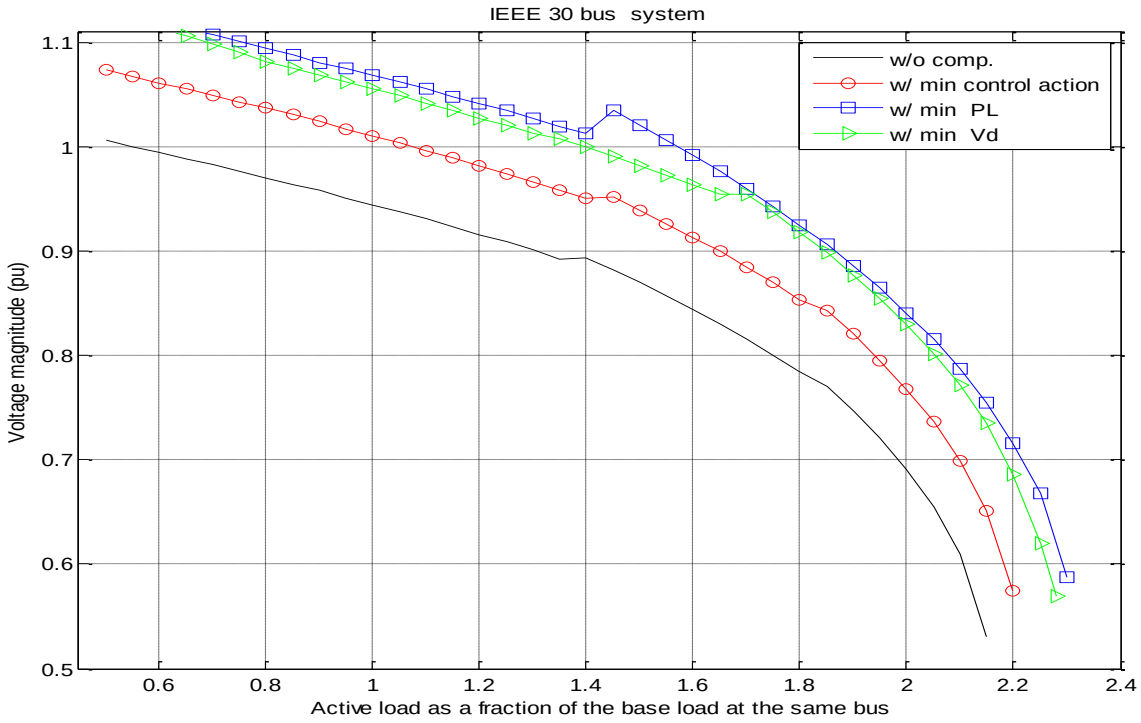

Figure 6.28: PV curves at bus 30 at 1.3 loading factor for the modified IEEE 30 bus

6.12.4 Case 4: Modified IEEE 30 Bus System with The Line 2-5 Out of Service

The modified IEEE 30 bus system at full load with line 2-5 out of service has a total active load of 264.10 MW, and a total reactive load of 125 MVAR. As indicated in Figure (6.29), the minimum voltage magnitude is at bus number 30 with 0.9460 pu, and this is the only bus that violates the voltage limits in this case. This voltage improved to 0.9670 pu with the objective function of minimum number of controllers, to 0.9865 pu with the objective function of minimum power losses, and to 0.9926 pu using the objective function of minimum voltage deviations. After compensation with any method, all the buses became within acceptable operating limits as indicated in Figure (6.29).

Table (6.7) shows that the method of minimum number of control actions for this case uses only one controller to improve the voltage profiles of the system. On the other hand, the other two methods, minimum power losses and minimum voltage deviations, use sixteen and fourteen controllers respectively in order to remove any voltage violation in the system. All the required adjustments for these controllers are indicated in Table (6.7).

As indicated in Figure (6.30), bus number 30 has the minimum value (0.8298) of the *1-L* indicator. This value improved to be 0.8326 after the adjustment of the controller of minimum number of control action method, to be 0.8421 with minimum power losses method, and to be 0.8436 with minimum voltage deviation method. Figure (6.31) indicates that the stability margin at all buses including bus number 30, the most critical bus, has been increased a little bit.

As shown in Table (6.8), the MSV improved from 0.2180 to 0.2187 with the first method, to 0.2192 using minimum power losses method, and to 0.2214 with minimum voltage deviation method. The same table indicates that the real power losses are decreased from 5.54 MW to 5.51 MW with a percentage reduction of 0.54 %, and the reactive power losses are improved from 26.39 MVAR to 26.24 MVAR with a percentage reduction of 0.57 % using the method of minimum number of control action. By using the method of minimum power losses, the real power losses decreased to 4.38 MW with a percentage reduction of 20.94 %, and the reactive power losses are improved to 21.60 MVAR with a percentage reduction of 18.15 %. Finally, the real and reactive power losses are reduced to 4.50 MW and 23.08 MVAR respectively by using the method of minimum voltage deviation. The corresponding percentage reductions are 18.77 % and 12.54 % respectively.

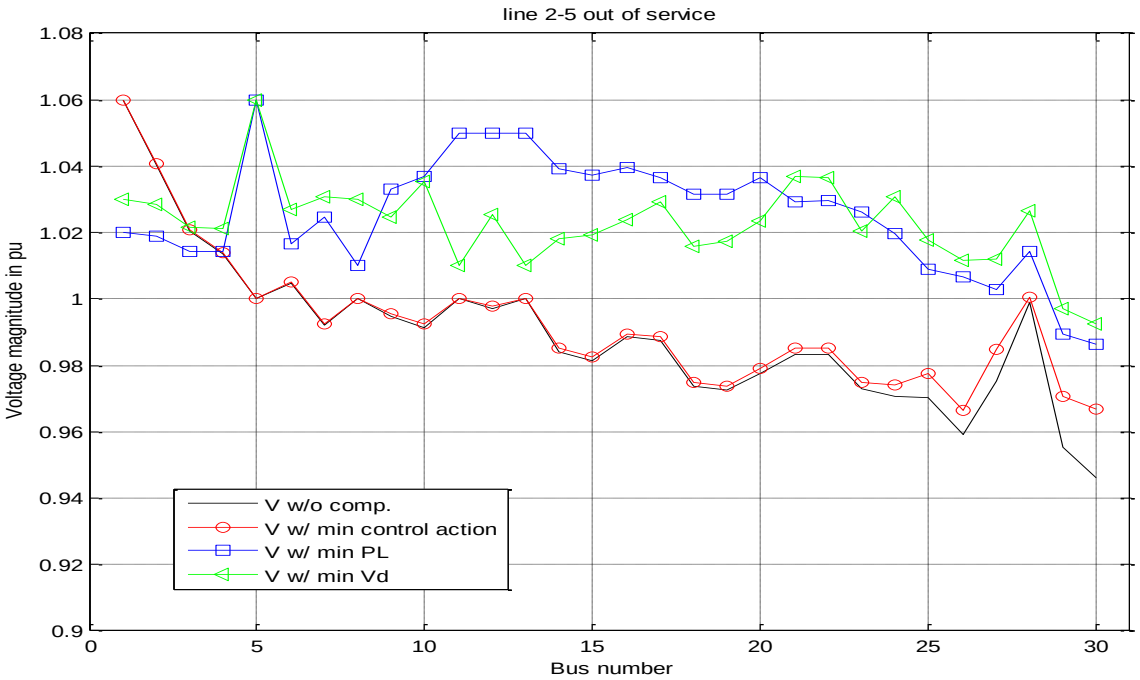

Figure 6.29: Voltage profile at full load and line 2-5 out for the modified IEEE 30 bus

Table 6.7: Change in controllers for IEEE 30 bus system at full load and w/o line 2-5

Algorithm / Controller name	Minimum control action	Minimum power losses	Minimum voltage deviations
Δt_{12-4}	0	0	0.04
Δt_{9-6}	0	-0.01	0
Δt_{10-6}	0	0	0
Δt_{27-28}	0	-0.03	-0.02
ΔV_1	0	-0.04	-0.03
ΔV_2	0	0	0
ΔV_5	0	0.06	0.06
ΔV_8	0	0.01	0.03
ΔV_{11}	0	0.05	0.01
ΔV_{13}	0	0.05	0.01
ΔQ_{c10}	0	0.02	0
ΔQ_{c12}	0	0.03	-0.06
ΔQ_{c15}	0	0.03	0.02
ΔQ_{c17}	0	0.02	0
ΔQ_{c20}	0	0.06	0.02
ΔQ_{c21}	0	-0.02	0.13
ΔQ_{c24}	0	0.02	0.11
ΔQ_{c26}	0	0.02	0.01
ΔQ_{c30}	0.03	0.03	0.02

Table 6.8: IEEE 30 bus system performance at full load and w/o line 2-5

Algorithm / Parameter	Without compensation	Using minimum control action	Using minimum power losses	Using minimum voltage deviations
Power losses	5.54 MW	5.51 MW	4.38 MW	4.50 MW
Reactive power losses	26.39 MVAR	26.24 MVAR	21.60 MVAR	23.08 MVAR
MSV	0.2180	0.2187	0.2192	0.2214

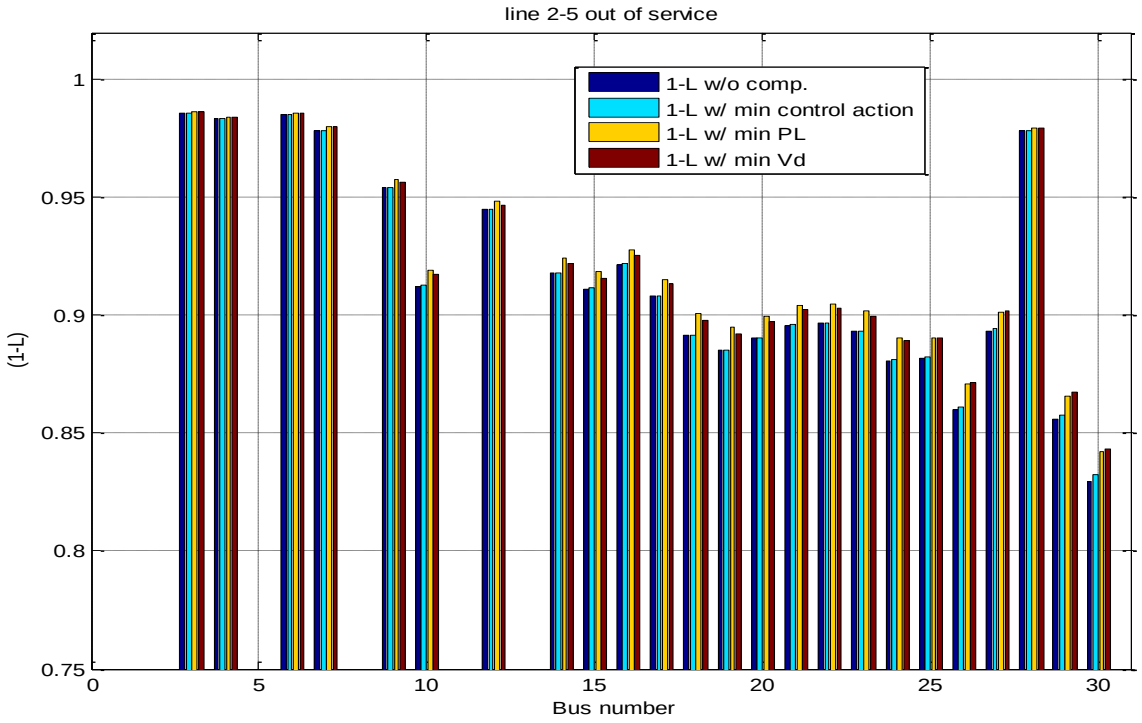

Figure 6.30: *1-L* index at full load and line 2-5 out for the modified IEEE 30 bus

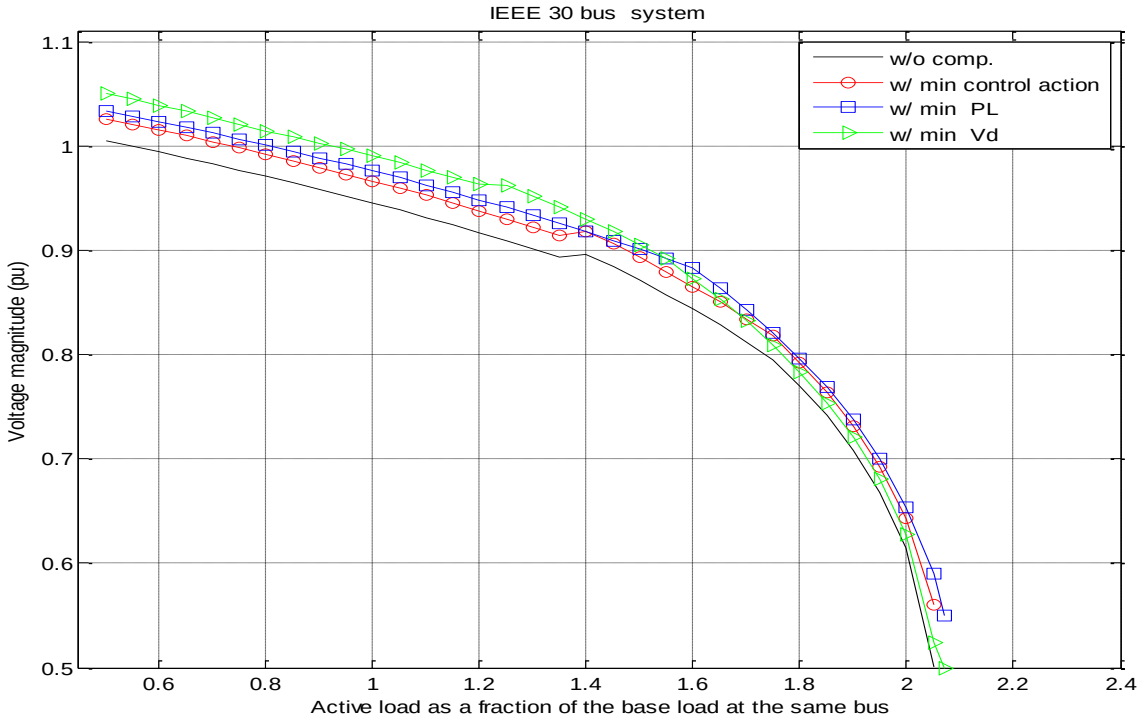

Figure 6.31: PV curves at bus 30 at full load and line 2-5 out for the modified IEEE 30 bus

6.12.5 Case 5: Ward and Hale System with Loading Factor = 0.7

The single line diagram and data of Ward and Hale system can be found in appendix B, At a loading factor equal to 0.7 the system has a total active load of 94.50 MW, and a total reactive load of 25.20 MVAR. As shown in Figure (6.32) the minimum voltage magnitude before any control action, is 0.8923 pu at bus number 5.. This voltage improved to 0.9828 pu with the objective function of minimum number of controllers, to 0.9613 pu with the objective function of minimum power losses, and to 0.9803 pu using the objective function of minimum voltage deviations. Before compensation, there were 3 buses out of six violated the lower voltage limit. After compensation all the buses, became within acceptable operating limits as shown in Figure (6.32).

The minimum number of control action algorithm for the this case uses three controllers as indicated in Table (6.9) to improve the voltage profiles of the system. On the other hand, the other two methods, minimum power losses and minimum voltage deviations, use five and six controllers respectively in order to remove any voltage violation in the system. The required adjustments for all controllers for the three different methods are indicated in Table (6.9).

Figure (6.33) indicates that bus number five has the minimum value (0.8010) of the *1-L* indicator. This value improved to be 0.8377 after adjusting the controllers using minimum number of control action, to be 0.8267 with minimum power losses method, and to be 0.8280 with minimum voltage deviation method. Figure (6.34) indicates that all the three methods managed to increase the stability margin of the system.

A review of Table (6.10) shows that the MSV improved from 0.6474 to 0.7393 with the first method, to 0.6962 using minimum power losses method, and to 0.7182 with minimum voltage deviation method. The real power losses are decreased from 7.54 MW to 6.35 MW with a percentage reduction of 15.78 %, and the reactive power losses are improved from 21.18 MVAR to 18.14 MVAR with a percentage reduction of 14.35 % using the method of minimum number of control action. With minimum power losses method, the real power losses changed to 6.11 MW with a percentage reduction of 18.97 %, and the reactive power losses are improved to 16.07 MVAR with a percentage reduction of 24.13 %. By using the method of minimum voltage

deviations, the real and reactive power losses are reduced to 6.28 MW and 17.25 MVAR respectively. The corresponding percentage reductions are 16.71 % and 18.58 % respectively.

Table 6.9: Change in controllers for Ward and Hale system at 0.7 loading factor

Algorithm / Controller name	Minimum control action	Minimum power losses	Minimum voltage deviations
Δt_{43}	0	0	-0.01
Δt_{65}	-0.10	0.01	-0.03
ΔV_1	0.05	0.01	0.03
ΔV_2	0.10	0.09	0.07
ΔQ_{c4}	0	0.03	0.04
ΔQ_{c6}	0	0.05	0.05

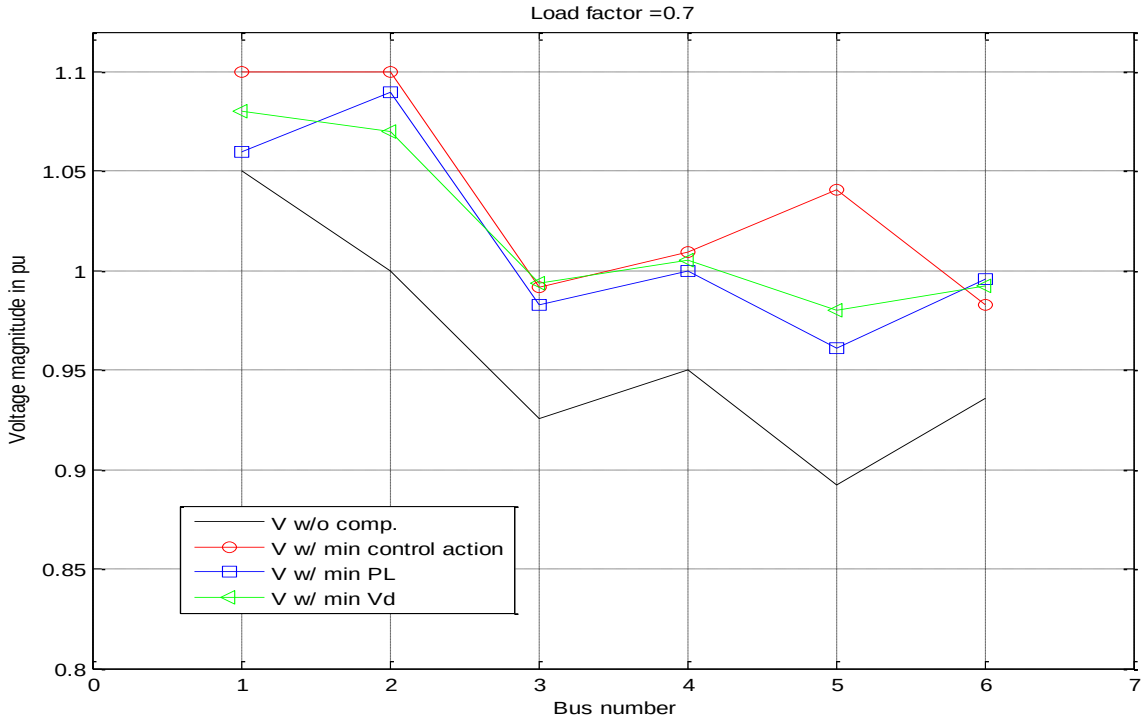

Figure 6.32: Voltage profile at 0.7 loading factor for the Ward and Hale system

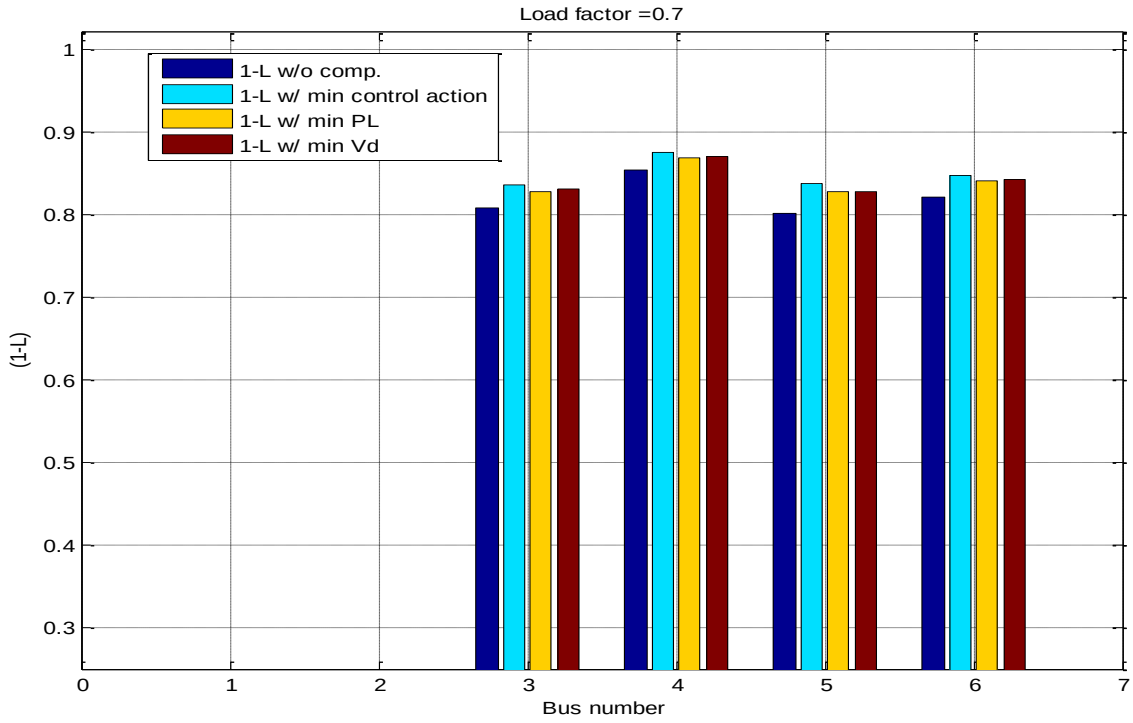

Figure 6.33: *1-L* index at 0.7 loading factor for the Ward and Hale system

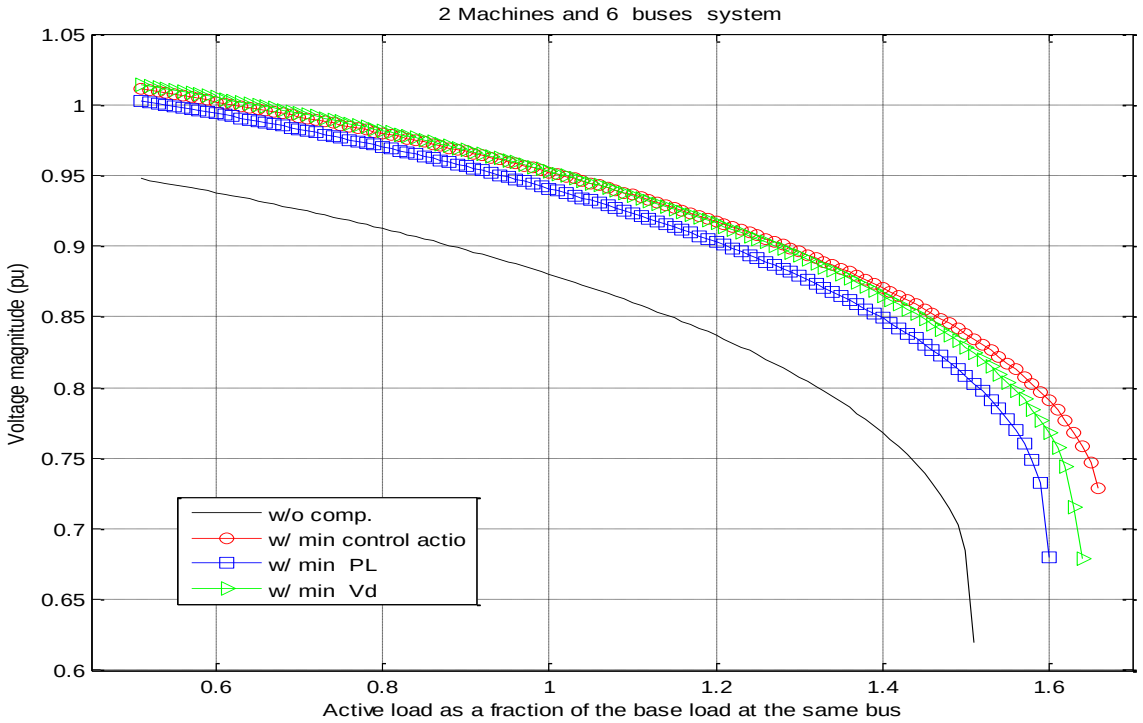

Figure 6.34: PV curves at bus 3 at 0.7 loading factor for the Ward and Hale system

Table 6.10: Ward and Hale system performance at 0.7 loading factor

Algorithm / Parameter	Without compensation	Using minimum control action	Using minimum power losses	Using minimum voltage deviations
Power losses	7.54 MW	6.35 MW	6.11 MW	6.28 MW
Reactive power losses	21.18 MVAR	18.14 MVAR	16.07 MVAR	17.25 MVAR
MSV	0.6474	0.7393	0.6972	0.7182

6.13 Conclusions

Three different algorithms for improving the voltage profiles, decreasing the power losses, and increasing the voltage stability margin in a power system have been presented in this chapter. All the three algorithms consider all the available control variables in the system, i.e. ULTC transformer, generator excitation, and the shunt switchable capacitors. The objective of the first algorithm -minimize the number of control actions- is to improve the voltage profiles of all load buses to be within the pre-specified limits with a minimum number of control actions after being subjected to any contingency and/or load change. This method is fast and suitable for on-line application, but it does not guarantee decreasing the power losses. The study cases indicate that this algorithm is practical and useful for assisting the ECC operator in making control decisions to improve the voltage profiles.

The GA-based methods in all cases give better results regarding the active and reactive power losses, but with larger numbers of controllers, and also longer computational times.

Due to the fact that the GA-based algorithms started from a random initial point, the results of these methods depend on the selected random initial point, which makes these methods more suitable for off-line operation, like in the planning of power system.

Many runs are done in order to get the final results of the GA-based method, because the GA-based method depends on a random initial point.

The method of minimum number of controllers can be used on-line to find a fast solution to put the system within acceptable operating limits. After that GA -based methods can be applied off-line for more improvements in the system active and reactive losses.

Chapter 7 On-Line Voltage/Reactive Power Control

This chapter proposes the use of fuzzy logic for voltage and reactive power control of power systems using as few as possible of the available VAR resources in the system. The objective is to provide a solution, which does both voltage improvement and if possible loss reduction for any practical power system. The proposed fuzzy model uses two inputs: the voltage deviation level of load buses, and the controlling ability of the controlling devices, such as generators terminal voltages, tap changing transformers, and the switchable shunt capacitors. The output is the change in the controlling device. A sensitivity coefficient matrix relating the control variables and the dependent variables is used to calculate the control ability of every controller for each dependent variable. In addition, an optimal control method suitable for on-line application, which is the direct search (also called pattern search (PS)) method is introduced in this chapter and compared to the fuzzy logic method. The idea is that these methods could be used in real time application. A modified IEEE 14 bus system and a modified IEEE 30 bus system are used to validate the performance of the proposed fuzzy system and direct search methods. The obtained results show that the proposed methods are reliable, fast, and practical.

7.1 Introduction

Any change in the network configuration, or perturbation in the system load, will result in voltage profile variation of the power system, in order to guarantee a fast and reliable alleviation of such variation in the voltage profile, a real time control actions must be taken by the ECC operator. In order to improve voltage security, power systems are equipped with a lot of voltage controlling devices such as:

- Generator terminal voltages
- Tap changing transformers
- Synchronous condensers
- Static VAR compensators
- Switchable shunt capacitors
- Switchable shunt reactors, and

- FACTS

Power systems under any condition are required to have an acceptable voltage profile, to keep the system stable, and to guarantee the quality of the power supplied for their consumers. After any perturbation in the system voltage profile, a fast and accurate determination of the locations and amounts of the available compensators is required in order to select those most appropriate to get the system back within voltage limits.

The available optimization techniques use all the exiting reactive power resources to optimize the power system, i.e. all the available controllers must be reset to optimize the power system. In some situations, especially for mechanically adjusted controllers, this solution is not practical because of the large number of controllers. The operator in the ECC cannot reset so many controllers within a reasonable time to catch the system before going to a voltage collapse. Due to the previous fact (difficulty to reset a large number of controllers in a reasonable time) the need to get the system back to work within the pre-specified limits using a smaller number of the available controllers becomes an urgent requirement. The fuzzy logic method is an appropriate solution to decrease the number of control actions required to correct system voltage within a reasonable time.

7.2 Problem Formulation

Any change in power system topology and/or power demand can cause a voltage violation. A permanent improvement in voltage security is essential to keep the power system secured. Optimal control of voltage and reactive power is a significant technique for voltage profile improvements of power system. By finding a set of adjustments to the control variables, these methods optimize a certain objective function, while satisfying the power system constraints for both dependent and control variables. The objective of the fuzzy logic method is to improve the voltage profile of the power system using the least number of the available controllers. As in the rest of this dissertation, network constraints include the upper and lower limits of the voltage magnitude at all load buses, the upper and lower limits of the reactive power for all the generators, and the upper and lower limits of all the available controllers. The controllers include generator terminal voltages, tap changing transformers, and switchable shunt capacitors.

When the voltage magnitude at a load bus violates the pre-specified limits, control action must be taken by the ECC operator to alleviate the violation. As elsewhere in this work, consider a power system with *n* buses, with buses 1 to *g* as a generator buses, buses *g + 1* to *n* as load buses, and the first generator counted as the swing bus. The system has a number of tap changing transformers equal to t, and a number of buses with a switchable shunt capacitor equal to cap. By adjusting the controlling device at load bus *j*, the voltage improvement at bus *i* can be found by Equation (6.24) repeated here as Equation (7.1):

$$\Delta V_i = S_{ij}.\Delta U_j \quad \text{for } i = g+1, g+2, \ldots, n \quad \text{and} \quad j = 1,2, \ldots, t + g + cap \tag{7.1}$$

where:

ΔV_i: is the voltage change at load bus *i*

ΔU_j: is the adjustment of the controlling device *j*

S_{ij}: is the sensitivity coefficient of *the controlling device j* on voltage magnitude of the load bus *i*

The sensitivity matrix (S), a modified Jacobian matrix, is a matrix which relates the control variable and dependent variables as shown in Equation (6.51) repeated here as Equation (7.2)

$$\begin{bmatrix} \Delta Q_1 \\ \vdots \\ \Delta Q_g \\ \Delta V_{g+1} \\ \vdots \\ \Delta V_{g+cap} \\ \Delta V_{g+cap+1} \\ \vdots \\ \Delta V_n \end{bmatrix} = [S] \begin{bmatrix} (\Delta t_{jk})_1 \\ \vdots \\ (\Delta t_{jk})_t \\ \Delta V_1 \\ \vdots \\ \Delta V_g \\ \Delta Q_{g+1} \\ \vdots \\ \Delta Q_{g+cap} \end{bmatrix} \tag{7.2}$$

The adjustment of the controlling devices is constrained with the upper and lower limits as:

$$\Delta U^{min} \leq \Delta U \leq \Delta U^{max} \tag{7.3}$$

where:

$$\Delta U = \left[(\Delta t_{jk})_1, \dots, (\Delta t_{jk})_t, \Delta V_1, \dots, \Delta V_g, \Delta Q_{g+1}, \dots, \Delta Q_{g+cap}\right]^{\mathrm{T}}$$

$$\Delta U^{min} = \left[\Delta(t_{jk})_1^{min}, \dots, \Delta(t_{jk})_t^{min}, \Delta V_1^{min}, \dots, \Delta V_g^{min}, \Delta Q_{g+1}^{min}, \dots, \Delta Q_{g+cap}^{min}\right]^{\mathrm{T}}$$

$$\Delta U^{max} = \left[\Delta(t_{jk})_1^{max}, \dots, \Delta(t_{jk})_t^{max}, \Delta V_1^{max}, \dots, \Delta V_g^{max}, \Delta Q_{g+1}^{max}, \dots, \Delta Q_{g+cap}^{max}\right]^{\mathrm{T}}$$

The objective in this work is to keep the load bus voltage deviation within $\pm 5\%$ of the nominal voltage which is 1 pu i.e.,

$$0.95 \leq V_i \leq 1.05 \qquad \text{for } i = g+1, g+2, \dots, n \tag{7.4}$$

7.3 Fuzzy Logic

The concept of Fuzzy Logic (FL) was introduced by Lotfi Zadeh as a mathematical tool to describe vagueness and ambiguity in linguistics [129]. FL mimics how an expert person would make decisions, but at very high rate depending on the knowledge base. FL provides an easy way to arrive at a definite conclusion regarding a problem when there is no mathematical model for the problem, or there is a mathematical model but difficult to understand, or there is a mathematical model but it is complex to be used in real time.

7.3.1 Difference Between FL and Conventional Controllers

FL incorporates a simple, rule-based *IF X AND Y THEN Z* approach to solve a control problem rather than attempt to model the system mathematically. The FL model is empirically-based, relying on operators' experience rather than their technical understanding of the system [130]. For example instead of dealing with speed control in terms such as *Rated speed =1800 rpm, speed <1700 rpm, or speed >1900C,* terms like *IF* (motor speed is about right) *THEN* (no change in the voltage) or *IF* (motor speed is too slow) *THEN* (increase the voltage) or *IF* (motor speed is too fast) *THEN* (decrease the voltage) are used. These terms are imprecise and very descriptive of what must actually happen.

7.3.2 WHY USE FL?

FL offers several unique features that make it a particularly good choice for many control problems [131].

- FL does not require a mathematical model
- FL can control nonlinear systems that are difficult to be modeled mathematically
- FL is relatively simple, fast and adaptive
- FL is less sensitive to system fluctuations and disturbances
- FL has the ability to simulate the human experience
- FL can be incorporated in conventional methods
- FL is conceptually easy to understand.

7.3.3 Membership Functions

A membership function (MF) is a curve that defines how each point in the universe (input space) is mapped to a membership value (or degree of membership) between 0 and 1[132]. There are many types of membership functions. Each membership function has specific features as below [133].

- SHAPE: triangular and trapezoidal shapes are the most common, but there are other shapes like bell, and exponential.
- HEIGHT: the height or the maximum magnitude of a membership function is 1
- WIDTH: the width of the base of a membership function
- CENTER: the center of the membership function shape
- OVERLAP: the overlap is typically about 50% of width of membership function but can be less.

7.3.4 Mamdani Fuzzy Inference System

Figure (7.1) shows how a two inputs, two rules Mamdani fuzzy inference system drives the output based on the centroid defuzzification method.

7.3.5 Elements of Fuzzy Model

The main elements of a fuzzy model can be summarized as follows:

- Knowledge base (KB): represents fuzzy rules that explain the relations between inputs and outputs within the problem domain

- Fuzzy model: is a group of fuzzy sets that model the system variables
- Fuzzifier: converts crisp inputs into a fuzzy format suitable for processing within the fuzzy model
- Fuzzy inference system (FIS): executes all the rules in the KB that have the fuzzy input
- Defuzzifier: converts the output fuzzy set into a crisp value

Figure (7.2) shows the fuzzy logic block diagram, and the relation between the elements of fuzzy model.

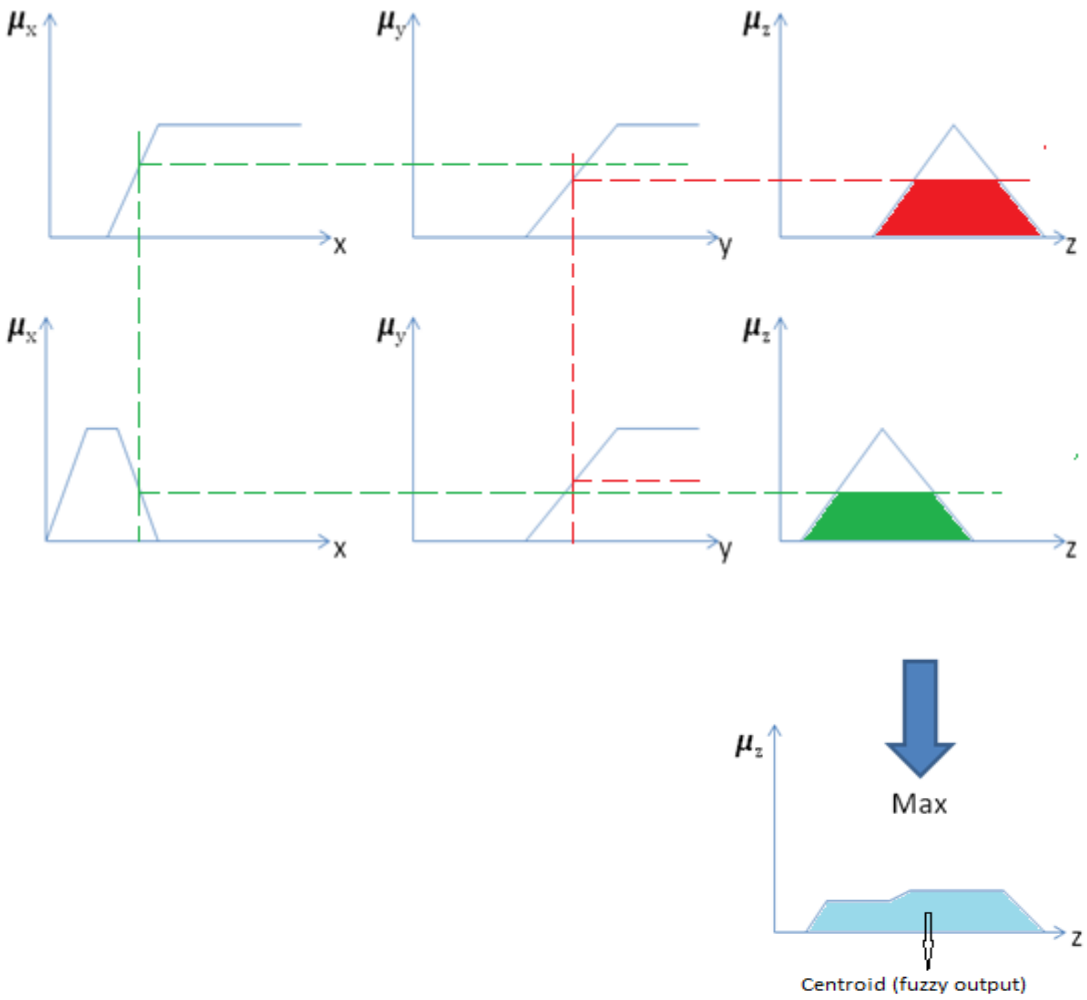

Figure 7.1: Mamdani fuzzy inference system

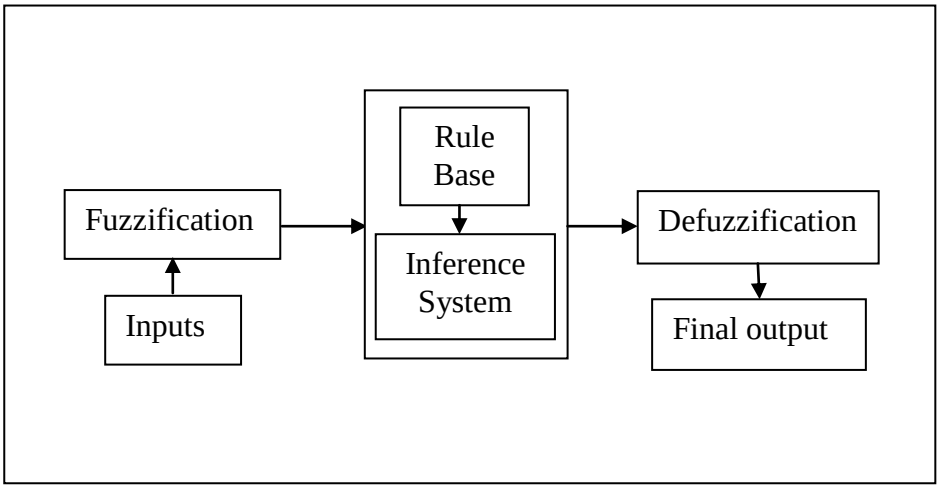

Figure 7.2: Fuzzy system block diagram

7.4 Fuzzy Modeling

The main problem of the conventional optimization algorithms, is the strict modeling of network constraints, as a result of such strict modeling, the resulting solutions of this modeling may be incapable of representing practical cases. Consequently, a more reasonable, and reliable model for the voltage magnitude control is needed. In the proposed work, fuzzy sets are used to model the objective function and network constraints. Two different variables are observed and used as two inputs to the proposed model, these inputs are:

- Load bus that has the largest voltage violation (ΔV_i)
- Controlling ability (C_{ij}) of the controlling device j that has maximum control ability on bus i, that has the largest voltage violation

The main problem is to improve the voltage profile of a power system. The largest voltage violation (ΔV_i) at a load bus is selected as one input to the proposed fuzzy logic because it is a direct measure of the severity of the problem, voltage violation. On the other hand, controlling ability (C_{ij}) is selected as a second input because it represents the ability of the available controller to fix the problem.

7.4.1 Load Bus Voltage Violation

The membership functions that represent the voltage deviations are shown in Figure (6.3). In this work, we need to control the voltage deviation at any load bus to be within $\pm$ 5% of the rated voltage magnitude. The minimum and maximum voltage deviation at a load bus can be calculated from Equations (7.5) and (7.6) respectively

$$\Delta V_i^{min} = V_i^{min} - V_i^{nominal} \tag{7.5}$$

$$\Delta V_i^{max} = V_i^{max} - V_i^{nominal} \tag{7.6}$$

where:

V_i^{min} : is the minimum accepted voltage magnitude at a load bus. In this work it is 0.95 pu

V_i^{max} : is the maximum accepted voltage magnitude at a load bus. In this work it is1.05 pu

$V_i^{nominal}$: is the rated voltage magnitude in per unit. In this work it is 1.0 pu

7.4.2 Controlling Ability of the Controller

The membership functions that represent the controlling ability of the controller are shown in Figure (7.4). In the case of an over-loaded system, the bus voltage magnitude is lower than the minimum acceptable voltage limit, and so the controller must increase the voltage magnitude to get the system back within acceptable limits. The maximum controlling ability of all the controllers on bus *i*, the bus with minimum voltage, is the maximum of Equation (7.9). On the other hand, if the system is lightly loaded, the bus voltage magnitude is larger than the maximum acceptable voltage limit. In this case, the controller should decrease the voltage magnitude to be within acceptable limits. The minimum of Equation (7.9) represents the maximum controlling ability to decrease the voltage magnitude at bus *i*, the bus that has maximum voltage. These equations are re-calculated every iteration.

$$C_i^+ = S_i M^+ \tag{7.7}$$

$$C_i^- = S_i M^- \tag{7.8}$$

$$C_i = [C_i^+ \; C_i^-] \tag{7.9}$$

where:

S_i : is a row vector corresponding to the load bus with the largest voltage violation. Its dimension is (1x(t + g + cap)). t + g + cap, represent the total number of controllers

M^+: is a diagonal matrix its diagonal element are the positive margins of the controllers = $(U^{max} - U)$

C_i^+: is a row vector represents the control ability of all controllers on bus *i* which results from positive margins. Its dimension is the same as the dimension of S_i

M^-: is a diagonal matrix its diagonal element are the negative margins of the controllers = $(U^{min} - U)$

C_i^-: is a row vector represents the control ability of all controllers on bus *i which results from negative margins*. Its dimension is the same as the dimension of S_i

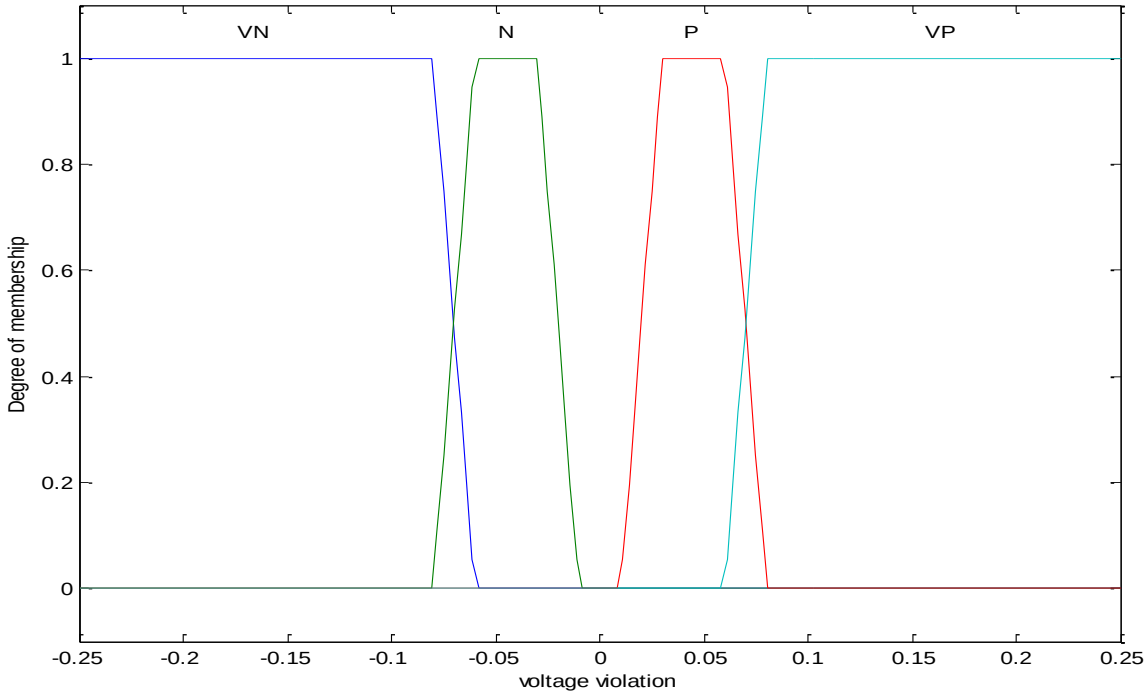

Figure 7.3: Membership function for voltage violation

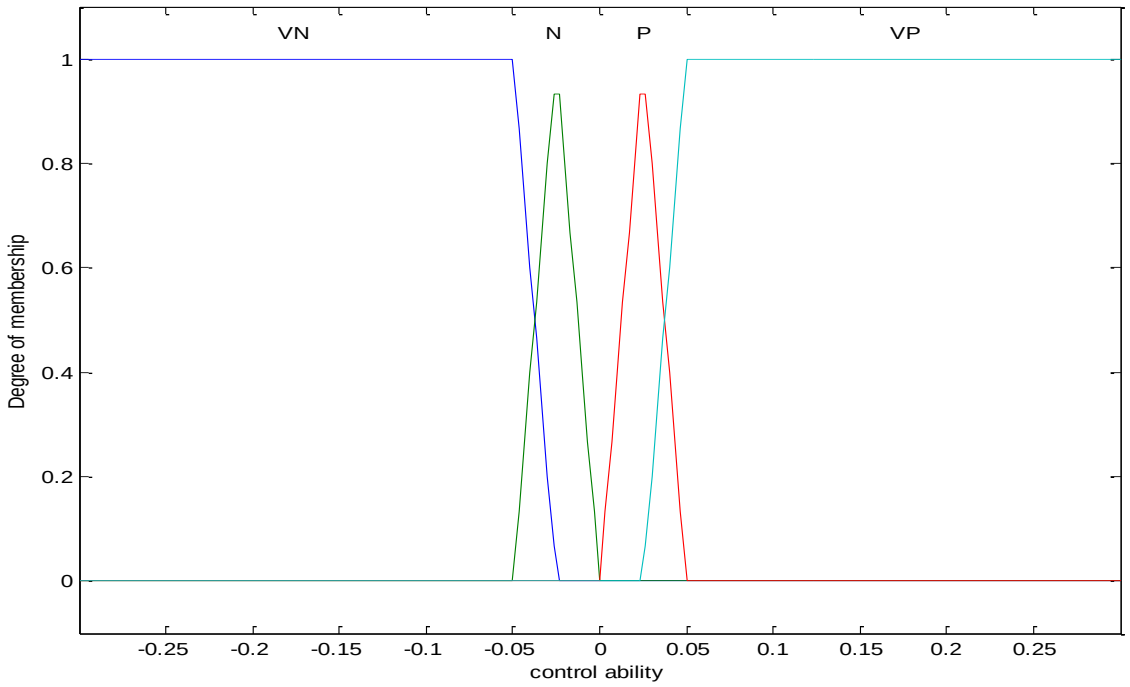

Figure 7.4 : Membership function for control ability

7.4.3 Controller Output

The load bus with the largest voltage violation is fuzzified according to the membership functions in Figure (7.3), in the same manner the control device that has the largest control ability on that bus is fuzzified using the membership functions shown in Figure (7.4). The decision taken by the controller is based on the rule base designed according to the experience with the power system. The membership functions of the controller output are depicted on Figure (7.5). The design of the membership functions completely depends on the power system under study, and may be changed from one to other according to the acceptable voltage violations. The controller uses Mamdani FIS structure method, and the defuzzification method adopted is the center of gravity method.

7.4.4 Description of Input Output Fuzzy System

After many trials, we found that four membership functions for both of the two inputs and seven membership functions for the output are sufficient to give a fast, and acceptable control action. The four membership functions for the first input (Voltage violation) are: very

negative (VN), negative (N), positive (P), and very positive (VP). These membership functions are shown in Figure (7.3). On the other hand, the four membership functions of the second input are: very negative (VN), negative (N), positive (P), and very positive (VP) as shown in Figure (7.4). While the seven membership functions for the output of the controller are: negative three steps (N3), negative two steps (N2), negative one step (N1), no control action (Z), positive one step (P1), positive two steps (P2) and positive three steps (P3) as shown in Figure (7.5).

7.4.5 Rule Base Generation

The rule base is designed based on the operator's experience using *IF (X) AND (Y) THEN (Z)*. A sample of these rules can be seen below:

IF voltage violation (ΔV_i) is VN *AND* control ability (C_{ij}) is P *THEN* controller output is P2.

The complete rule base of the designed fuzzy controller are shown in Table (7.1)

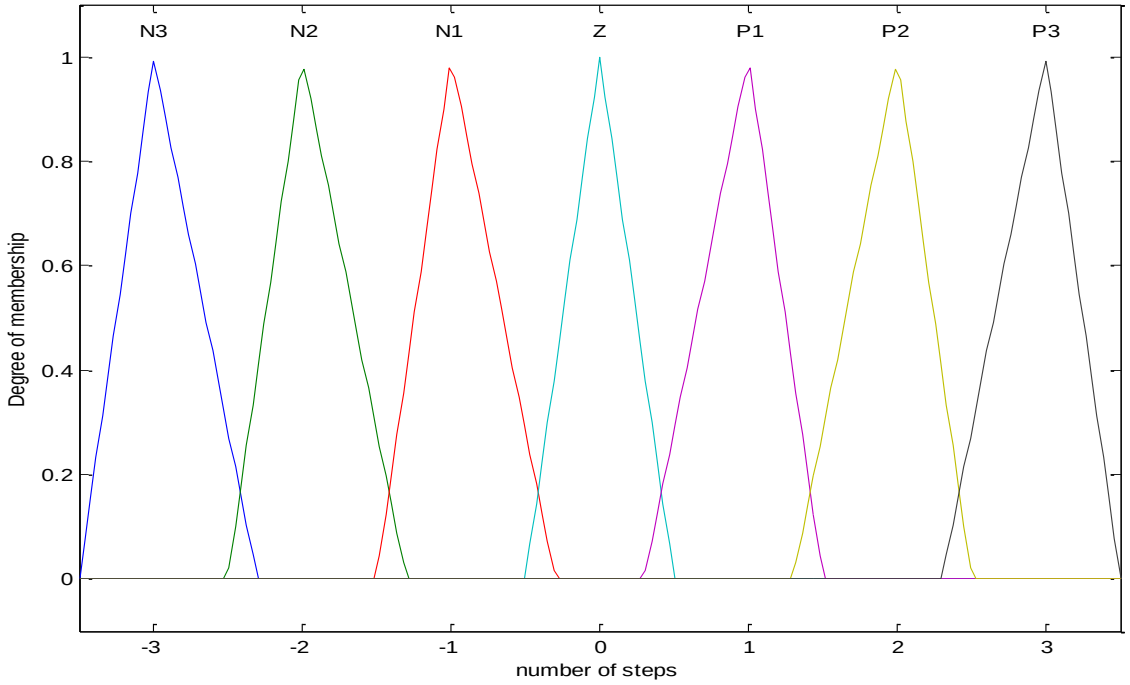

Figure 7.5: The output of the fuzzy controller

Table 7.1: Rule map of Fuzzy controller

C_{ij} / ΔV_i	VN	N	P	VP
VN	Z	Z	P2	P3
N	Z	Z	P1	P2
P	N2	N1	Z	Z
VP	N3	N2	Z	Z

7.5 Controller Algorithm

The details of the solution process for fuzzy logic controller algorithm are given below, in the same time Figure (7.6) is a corresponding flow chart.

1. Perform base case load flow solution.
2. Check the system performance for voltage magnitudes at load buses and if necessary to improve the system voltage profile, proceed to Step 3, otherwise, stop.
3. Calculate the sensitivity matrix (S), M^+, M^-.
4. Calculate the minimum voltage magnitude (V_{min}) and the maximum voltage magnitude (V_{max}).
5. Find the load bus that has the largest voltage deviation.
6. Calculate maximum value of the augmented row vector [C_i^+ C_i^-] corresponding to the bus *i* with the largest voltage violation (ΔV_i) in the case of over loaded system, otherwise calculate the minimum of [C_i^+ C_i^-].
7. Fuzzify the two inputs to the fuzzy controller [132] named voltage violation (ΔV_i) and the control ability of controller *j* on bus *i* (C_{ij}).
8. Apply the fuzzy controller to get the new setting of the controller *j*.
9. Update the setting of the controller *j*.
10. Perform load flow calculations and go back to Step 2

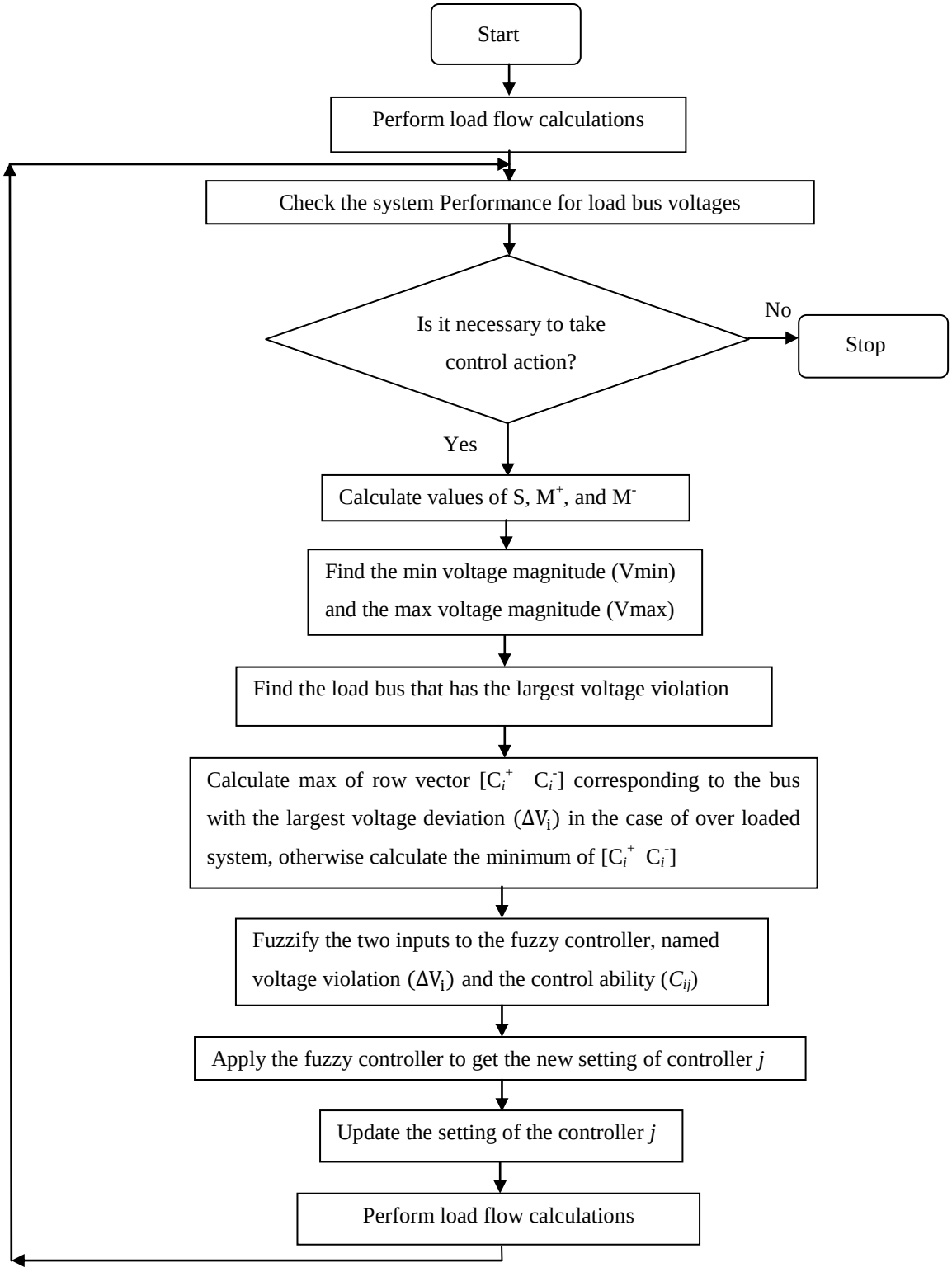

Figure 7.6: Flow chart for Fuzzy controller

7.6 Direct (Pattern) search method

In this method the objective function is chosen to minimize voltage deviations (V_d) at all load buses according to the following equation:

$$V_d = \sum_{j=g+1}^{n} \left(V_j - V_j^{norm}\right)^2 \tag{7.10}$$

where:

n: is the total number of buses

g: is the number of generator buses

V_j^{norm}: is the nominal voltage at bus *j* which is equal to 1 pu

V_j: is the actual voltage at load bus *j*

This method is used in order to get an optimal solution to the VAR control problem by applying the pattern search (PS) technique. After linearization, the objective function as mentioned before in the previous chapter is:

$$\Delta V_d = \begin{bmatrix} \frac{\partial V_d}{\partial (t_{jk})_1} & \dots & \frac{\partial V_d}{\partial (t_{jk})_t} & \frac{\partial V_d}{\partial V_1} & \dots & \frac{\partial V_d}{\partial V_g} & \frac{\partial V_d}{\partial Q_{g+1}} & \dots & \frac{\partial V_d}{\partial Q_{g+cap}} \end{bmatrix} \begin{bmatrix} (\Delta t_{jk})_1 \\ \vdots \\ (\Delta t_{jk})_t \\ \Delta V_1 \\ \vdots \\ \Delta V_g \\ \Delta Q_{g+1} \\ \vdots \\ \Delta Q_{g+cap} \end{bmatrix} \tag{7.10}$$

where:

$(\Delta t_{jk})_1 \dots, (\Delta t_{jk})_t, \Delta V_1, \dots, \Delta V_g, \Delta Q_{g+1}, \dots, \Delta Q_{g+cap}$ are the control variables

t: is the total number of tap changing transformers

g: is the total number of generators

cap: is the total number of switchable shunt capacitors

The complete solution process can be found in the previous chapter, while the steps of the solution process of the optimal VAR control problem using minimum voltage deviations (V_d) are given below.

1. Perform a base case load flow solution.
2. Check the system performance and if it is necessary to improve the voltage profiles or to minimize the objective function or both, then proceed to Step 3, otherwise, stop.
3. Calculate the sensitivity matrix (S) relating the dependent variables, Δx, and the control variables, Δu as explained in the previous chapter.
4. Find the dependent variables lower and upper limits, $\Delta x^{min}, \Delta x^{max}$ and the control variables lower and upper limits, $\Delta u^{min}, \Delta u^{max}$ using Equations (6.9) to (6.13)
5. Calculate the coefficients of the objective function using the derivative of the objective function with respect to each control variable u, as indicated in the previous chapter.
6. Solve the optimization problem by using the Pattern Search (PS) [112] to evaluate the required adjustments to the control variables.
7. Update the values of the control variables using the output of the PS optimization technique.
8. Perform a load flow solution after the adjustments in the control variables and go back to Step 2.

7.7 Results and Discussion

The proposed algorithms have been tested on two different systems under contingency operation, the two systems are the modified IEEE 14 bus system and the modified IEEE 30 bus system. The results and analysis for some cases including some contingencies are indicated in the next sections below.

7.7.1 Case 1: Modified IEEE 14 Bus System with Line 2-3 Out of Service

The complete description and data of the modified IEEE 14 system can be found in Appendix C. At full load with line 2-3 out of service the system has three buses which violate the voltage limits, namely: bus 3, bus 13, and bus 14 as shown in Figure (7.7). The minimum voltage magnitude before any control action is at bus number 3 with 0.9340 pu. The voltage magnitude at bus number 14, the most critical bus in the system, is 0.9422 pu. After

compensation, the voltage magnitude at bus 3 improved to 0.9607 pu with fuzzy logic controller, and to 0.9734pu using the objective function of minimum voltage deviation. At the same time, the voltage magnitude at bus 14 improved to 0.9671 pu with fuzzy logic controller, and to 0.9785 pu using the objective function of minimum voltage deviation. Figure (7.7) indicates the improvement in the voltage profile at all buses after compensation using both methods.

The fuzzy logic controller in this case uses two controllers, namely: terminal voltage of generator at bus 1 and the terminal voltage at generator at bus 2, to improve the voltage profiles of the system. On the other hand, the other method, minimum voltage deviation, uses seven controllers in order to remove any voltage violation in the system. The required adjustments for all controllers for the two different methods are indicated in Table (7.2).

Figure (7.8) shows that bus number 14, most critical bus in the system, has the minimum value (0.6111) of the *1-L* indicator. This value improved to be 0.7611 after adjusting the controllers using fuzzy logic controller, and to be 0.7862 with minimum voltage deviation method. The same figure indicates the improvement at all load buses after compensation. The second method, minimum voltage deviation, causes more improvement in the *1-L* indicator. Figure (7.9) shows that the two methods succeeded to increase the stability margin of the system.

Table (7.3) indicates that the MSV improved from 0.3204 to 0.4274 with fuzzy logic controller and to 0.4610 with minimum voltage deviation method. The real power losses are decreased from 25.08 MW to 23.81 MW with a percentage reduction of 5.06 %, and the reactive power losses are improved from 68.68 MVAR to 63.38 MVAR with a percentage reduction of 7.72 % using the fuzzy logic controller method. By using the method of minimum voltage deviation, the real and reactive power losses are reduced to 23.22 MW and 60.27 MVAR respectively. The corresponding percentage reductions are 7.42 % and 12.25 % respectively.

Table 7.2: Change in controllers for IEEE 14 bus system at full load and w/o line 2-3

Algorithm / Controller name	Fuzzy logic Controller	Minimum voltage deviations using PS
Δt_{6-5}	0	0.01
Δt_{4-7}	0	0.01
Δt_{4-9}	0	0.07
ΔV_1	0.02	0.03
ΔV_2	0.02	0.02
ΔV_3	0	0
ΔV_6	0	0
ΔV_8	0	-0.02
ΔQ_{c9}	0	0.19

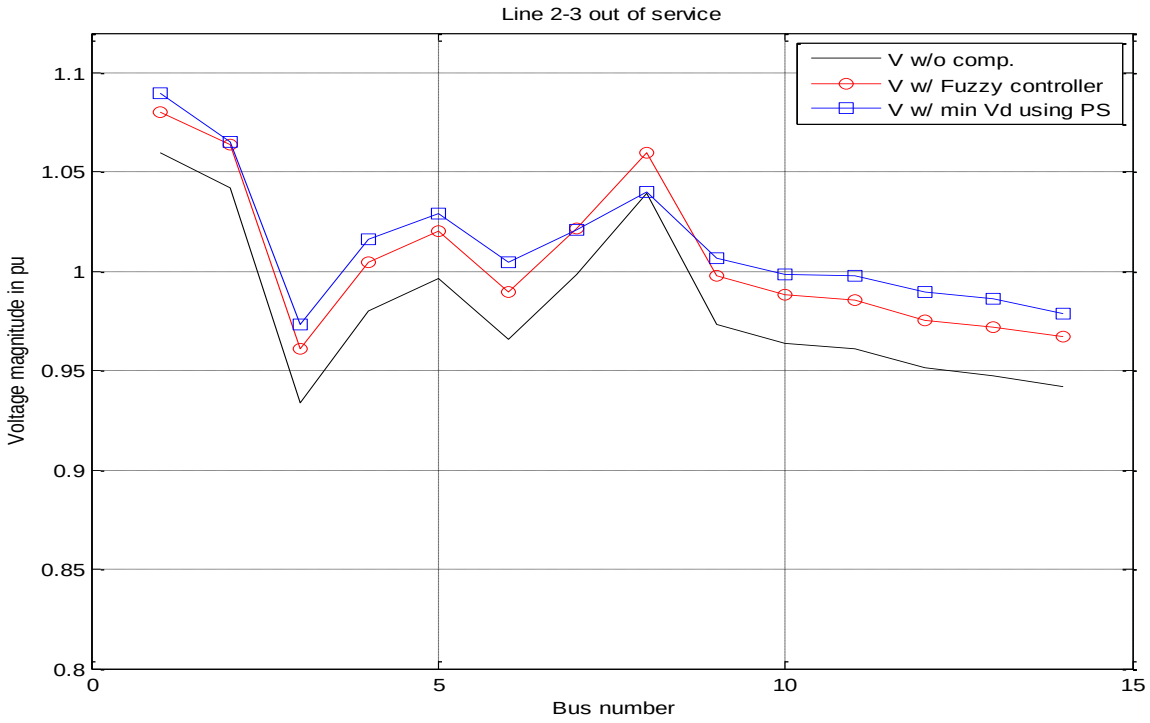

Figure 7.7: Voltage profile at full load and line 2-3 out for the modified IEEE 14 bus

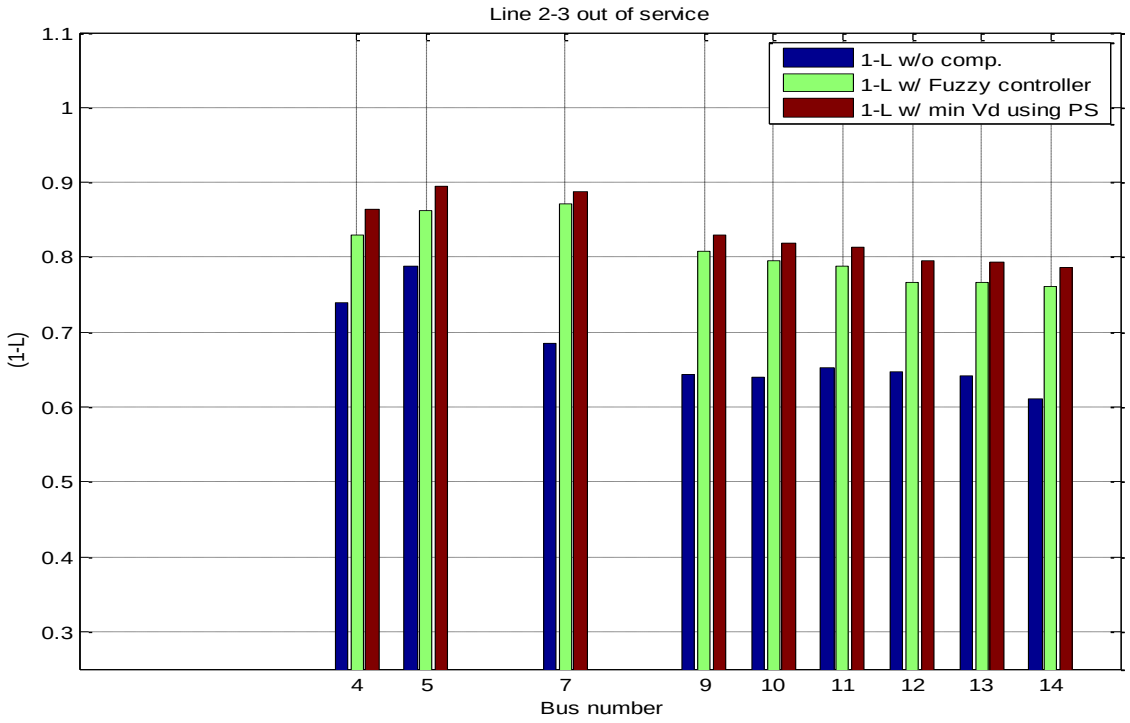

Figure 7.8: *1-L* index at full load and line 2-3 out for the modified IEEE 14 bus

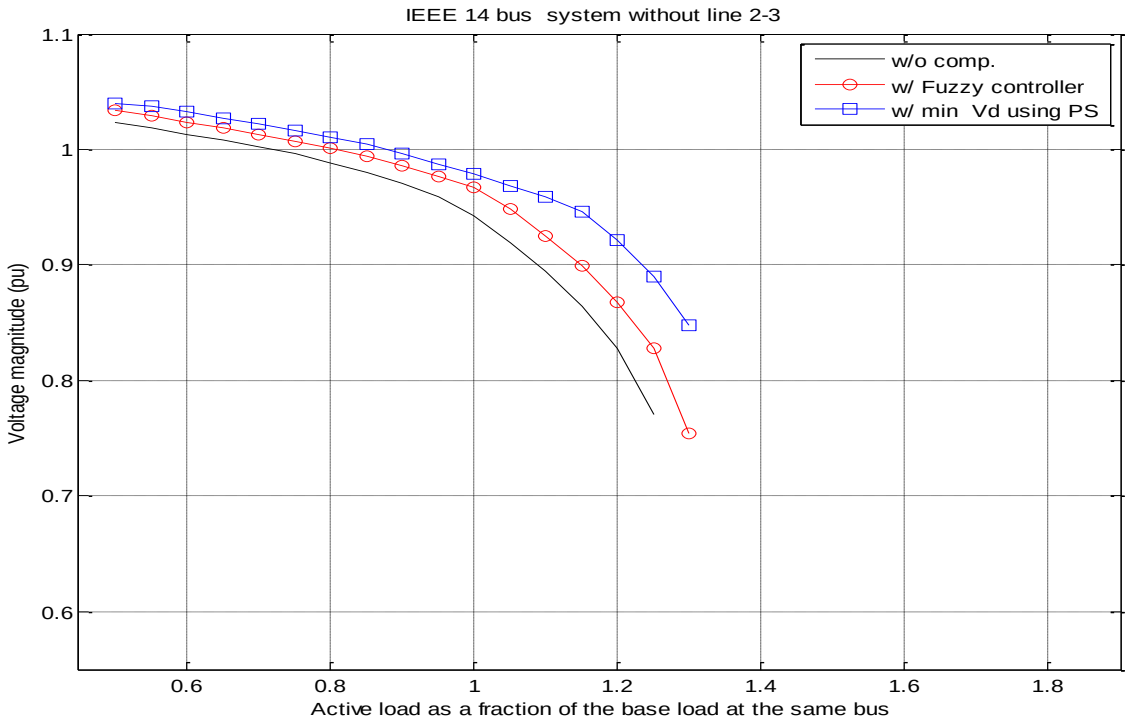

Figure 7.9: PV curves at bus 14 at full load and line 2-3 out for the modified IEEE 14 bus

Table 7.3: IEEE 14 bus system performance at full load and w/o line 2-3

Algorithm / Parameter	Without compensation	Fuzzy logic Controller	Minimum voltage deviations using PS
Power losses	25.08 MW	23.81 MW	23.22 MW
Reactive power losses	68.68 MVAR	63.38 MVAR	60.27 MVAR
MSV	0.3204	0.4274	0.4610

7.7.2 Case 2: Modified IEEE 14 Bus System with Line 1-5 Out of Service

The modified IEEE 14 bus system at full load with line 1-5 out of service has three buses which violate the voltage limits; these are bus 12, bus 13 and bus 14 as indicated in Figure (7.10). In this case, the minimum voltage magnitude before making any control action is at bus number 14 with 0.9412 pu. After Appling a control action, the voltage magnitude at bus 14 improved to 0.9781 pu with fuzzy logic controller, and to 1.0112 pu using the objective function of minimum voltage deviation. Figure (7.10) indicates the improvement in the voltage profile at all buses after compensation using both methods.

The fuzzy logic controller in this case uses two controllers, namely: tap setting of the transformer connected between buses 5 and 6, and tap setting of the transformer connected between buses 4 and 7, to improve the voltage profiles of the system. On the other hand, the other method, minimum voltage deviation, uses seven controllers to remove any voltage violation in the system. The required adjustments for all controllers for the two different methods are indicated in Table (7.4).

Figure (7.11) indicates that bus number 14, most critical bus in the system, has the minimum value (0.5582) of the *1-L* indicator. This value was enhanced to be 0.7435 after adjusting the controllers using fuzzy logic controller, and to be 0.9056 with minimum voltage deviation method. It can be seen from the same figure that both methods are able to improve the voltage profile at all load buses. The second method, minimum voltage deviation, causes better improvement in the *1-L* indicator than the fuzzy logic controller method. As shown in Figure (7.12), the two methods succeeded to increase the stability margin of the system and to remove any voltage violation in the system.

A review of Table (7.5) indicates that the MSV enhanced from 0.2597 to 0.3328 with fuzzy logic controller and to 0.3829 with minimum voltage deviation method. The real power losses are changed from 21.39 MW to 21.30 MW with a percentage reduction of 0.42 %, and the reactive power losses are improved from 60.90 MVAR to 59.78 MVAR with a percentage reduction of 1.84 % using the fuzzy logic controller method. When applying the method of minimum voltage deviation, the real and reactive power losses are reduced to 20.29 MW and 55.91 MVAR respectively. The corresponding percentage reductions are 5.14 % and 8.19 % respectively.

Table 7.4: Change in controllers for IEEE 14 bus system at full load and w/o line 1-5

Algorithm / Controller name	Fuzzy logic Controller	Minimum voltage deviations using PS
Δt_{6-5}	0.07	0.10
Δt_{4-7}	-0.02	-0.01
Δt_{4-9}	0	0.11
ΔV_1	0	0.02
ΔV_2	0	0.02
ΔV_3	0	0.02
ΔV_6	0	0
ΔV_8	0	0
ΔQ_{c9}	0	0.20

Table 7.5: IEEE 14 bus system performance at full load and w/o line 1-5

Algorithm / Parameter	Without compensation	Fuzzy logic controller	Minimum voltage deviations using PS
Power losses	21.39 MW	21.30 MW	20.29 MW
Reactive power losses	60.90 MVAR	59.78 MVAR	55.91 MVAR
MSV	0.2597	0.3328	0.3829

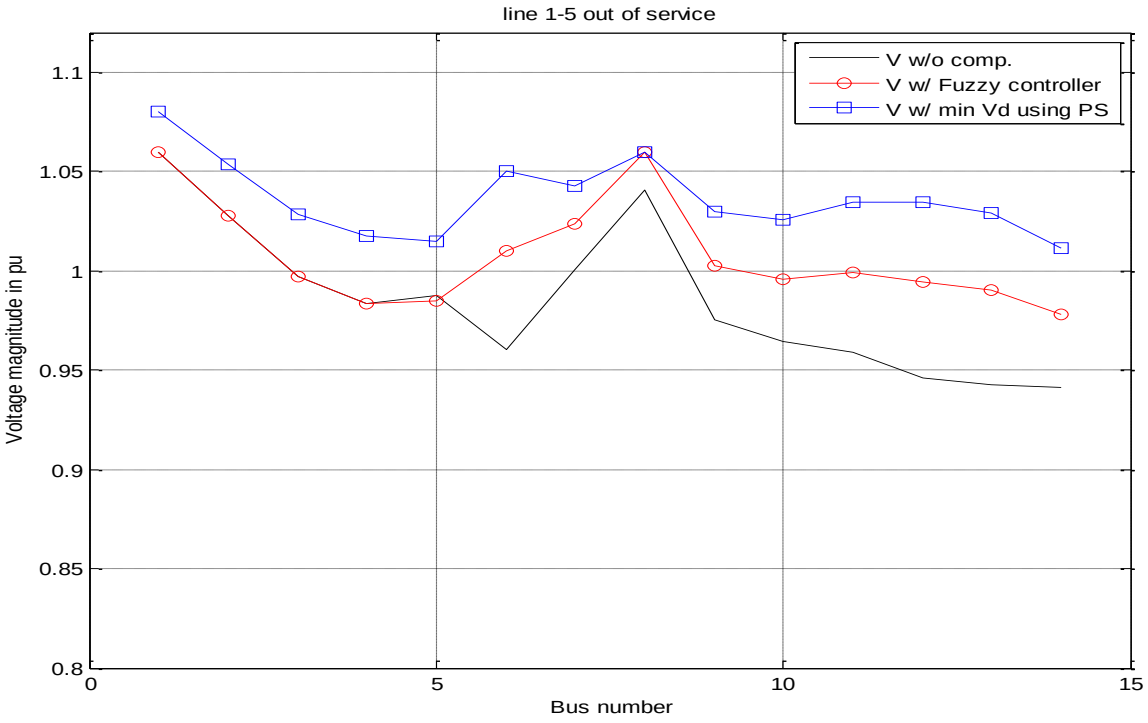

Figure 7.10: Voltage profile at full load and line 1-5 out for the modified IEEE 14 bus

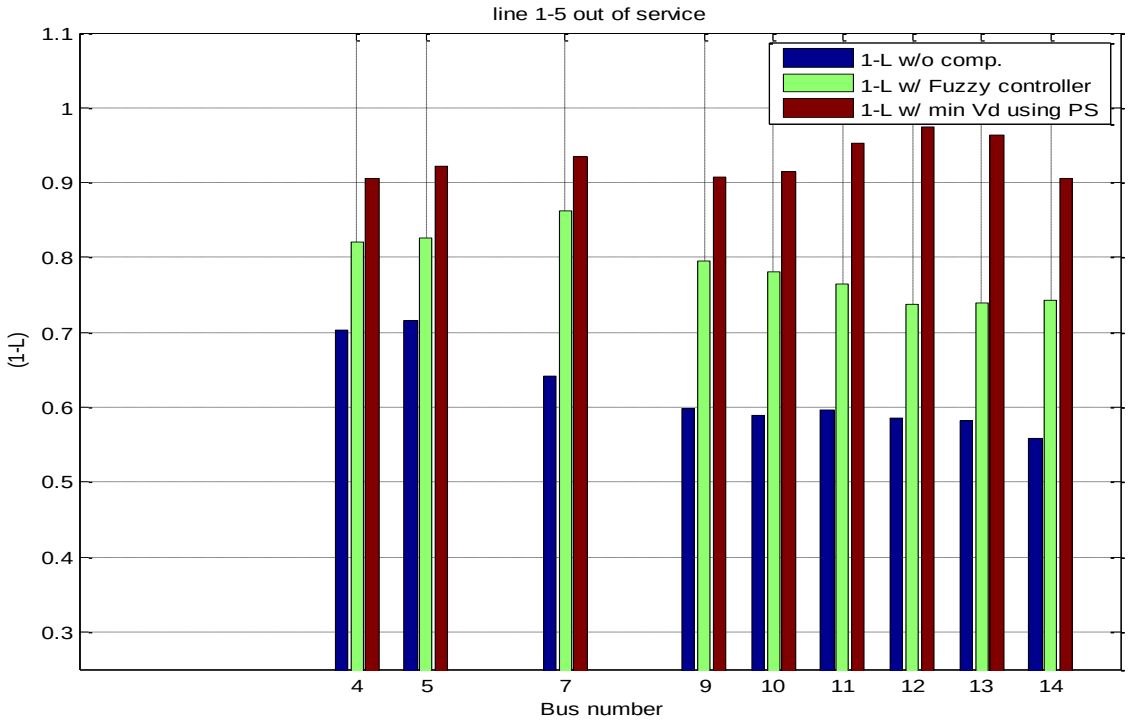

Figure 7.11: 1-L index at full load and line 1-5 out for the modified IEEE 14 bus

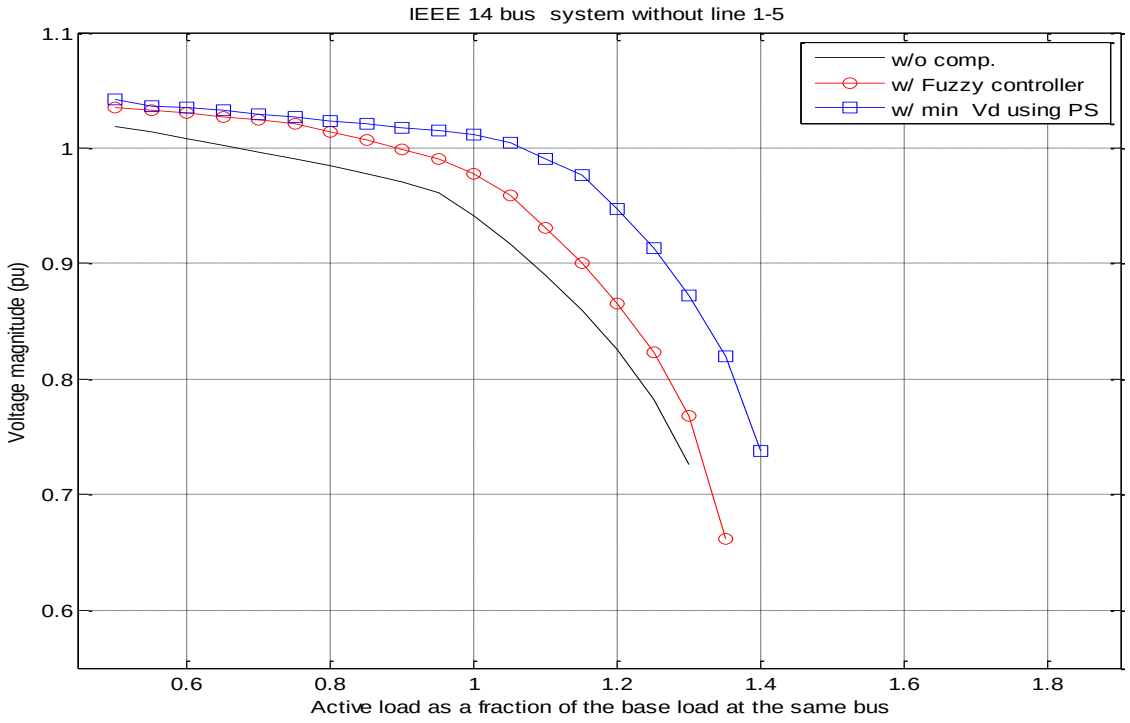

Figure 7.12: PV curves at bus 14 at full load and line 1-5 out for the modified IEEE 14 bus

7.7.3 Case 3: Modified IEEE 30 Bus System with Line 1-3 Out of Service

The complete description and data of the modified IEEE 30 system can be found in Appendix D. At full load with line 1-3 out of service the system has only one bus, bus number 30, which violates the permissible lower voltage limit as indicated in Figure (7.13). The voltage magnitude at this bus before any control action was 0.9412 pu. After compensation, the voltage magnitude at bus 30 improved to 0.9551 pu with fuzzy logic controller, and to 0.9845 pu using the objective function of minimum voltage deviation. Figure (7.13) shows the improvement in the voltage profile at all buses after making the required control actions using both methods.

The fuzzy logic controller in this case uses only one controller, the capacitor at bus 30, in order to remove the voltage violation at bus 30. On the other hand, the other method, minimum voltage deviation, uses 12 controllers to remove the voltage violation at bus 30. All the required adjustments for all controllers for both methods are indicated in Table (7.6).

Figure (7.14) indicates that bus number 30, most critical bus in the system, has the minimum value (0.8264) of the *1-L* indicator before taking any control action. This value

improved to be 0.8283 after adjusting the controllers using fuzzy logic controller, and to be 0.8376 with minimum voltage deviation method. It can be seen from the same figure that both methods are able to improve the voltage profile at all load buses. Also, the second method, minimum voltage deviation, causes more improvement in the *1-L* indicator. Figure (7.15) indicates that the two methods succeeded to increase the stability margin of the system and to remove the voltage violation at bus 30.

Table (7.7) indicates that the MSV improved from 0.1770 to 0.1773 with fuzzy logic controller. The MSV of the same case decreased to 0.1744 with minimum voltage deviation method. The real power losses are decreased from 5.77 MW to 5.74 MW with a percentage reduction of 0.52 %, and the reactive power losses are improved from 26.96 MVAR to 26.84 MVAR with a percentage reduction of 0.45 % using the fuzzy logic controller method. By using the method of minimum voltage deviation, the real and reactive power losses are reduced to 4.64 MW and 25.15 MVAR respectively. The corresponding percentage reductions are 19.58 % and 6.71 % respectively. The time taken to get the required control actions with Intel core i5 PC computer of 2.27GHz is 5.192 seconds with fuzzy logic controller, and 7.962 seconds with minimum voltage deviation method.

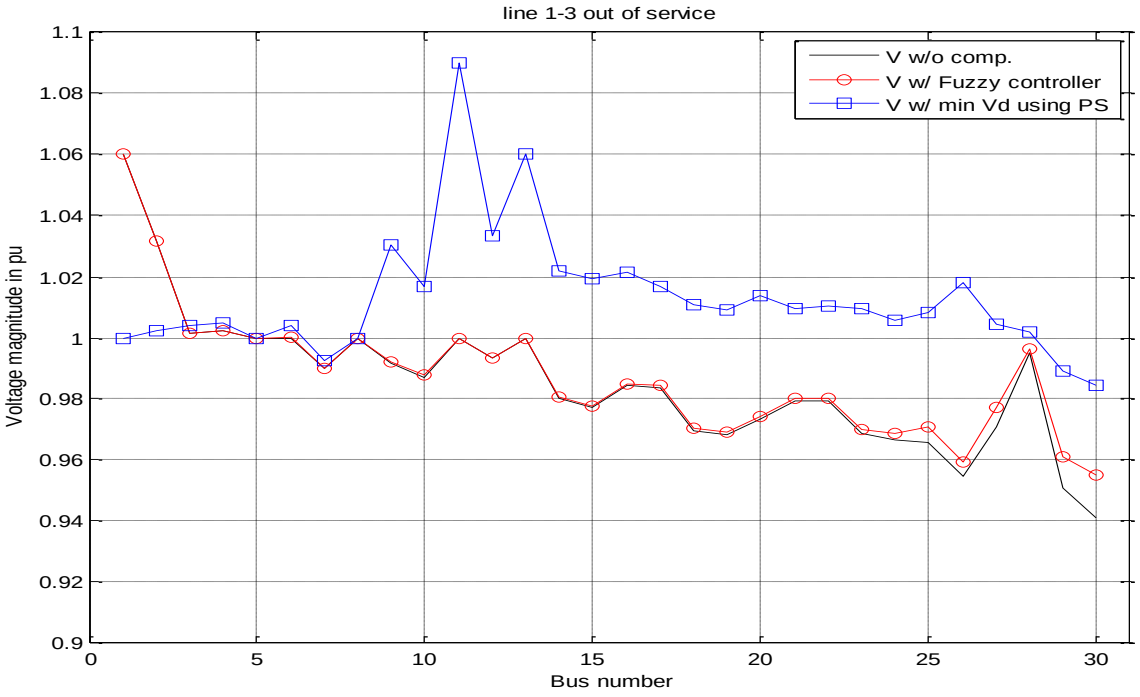

Figure 7.13: Voltage profile at full load and line 1-3 out for the modified IEEE 30 bus

Table 7.6: Change in controllers for IEEE 30 bus system at full load and w/o line 1-3

Algorithm / Controller name	Minimum control action	Minimum voltage deviations using PS
$\Delta t_{12\text{-}4}$	0	0
$\Delta t_{9\text{-}6}$	0	0
$\Delta t_{10\text{-}6}$	0	-0.06
$\Delta t_{27\text{-}28}$	0	0
ΔV_1	0	-0.06
ΔV_2	0	0
ΔV_5	0	0
ΔV_8	0	0
ΔV_{11}	0	0.09
ΔV_{13}	0	0.06
ΔQ_{c10}	0	-0.03
ΔQ_{c12}	0	0
ΔQ_{c15}	0	0.02
ΔQ_{c17}	0	0.02
ΔQ_{c20}	0	0.04
ΔQ_{c21}	0	-0.03
ΔQ_{c24}	0	0.02
ΔQ_{c26}	0	0.05
ΔQ_{c30}	0.02	0.02

Table 7.7: IEEE 30 bus system performance at full load and w/o line 1-3

Algorithm / Parameter	Without compensation	Fuzzy logic controller	Minimum voltage deviations using PS
Power losses	5.77 MW	5.74 MW	4.64 MW
Reactive power losses	26.96 MVAR	26.84 MVAR	25.15 MVAR
MSV	0.1770	0.1773	0.1744

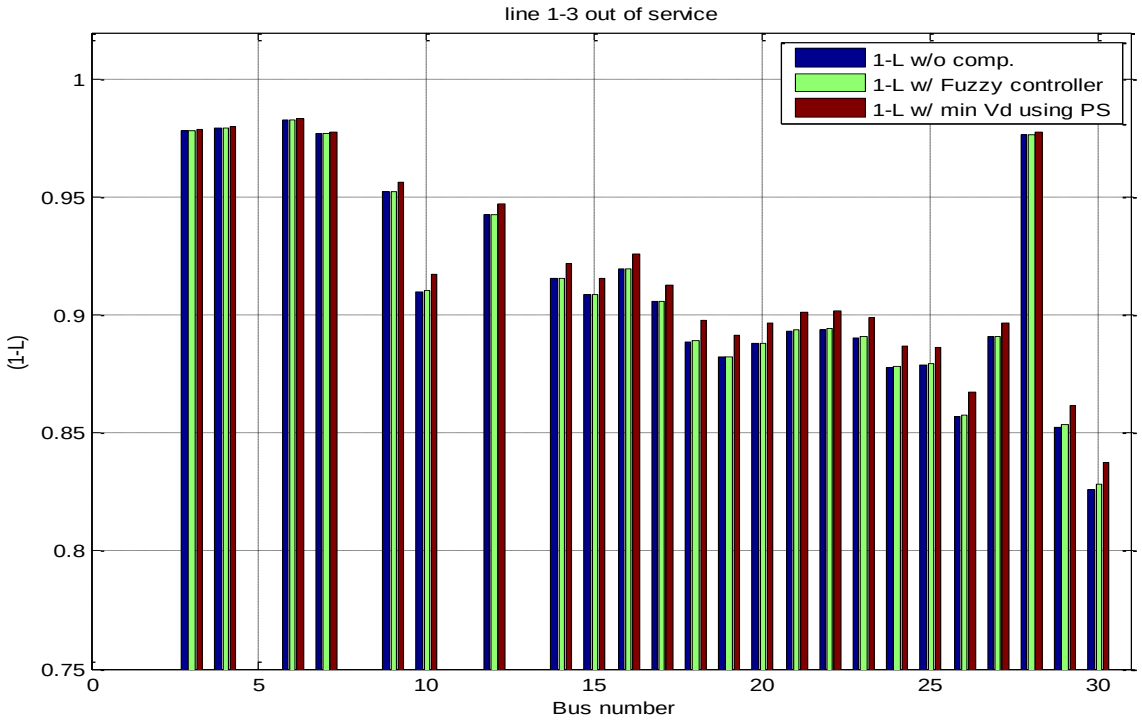

Figure 7.14 : *1-L* index at full load and line 1-3 out for the modified IEEE 30 bus

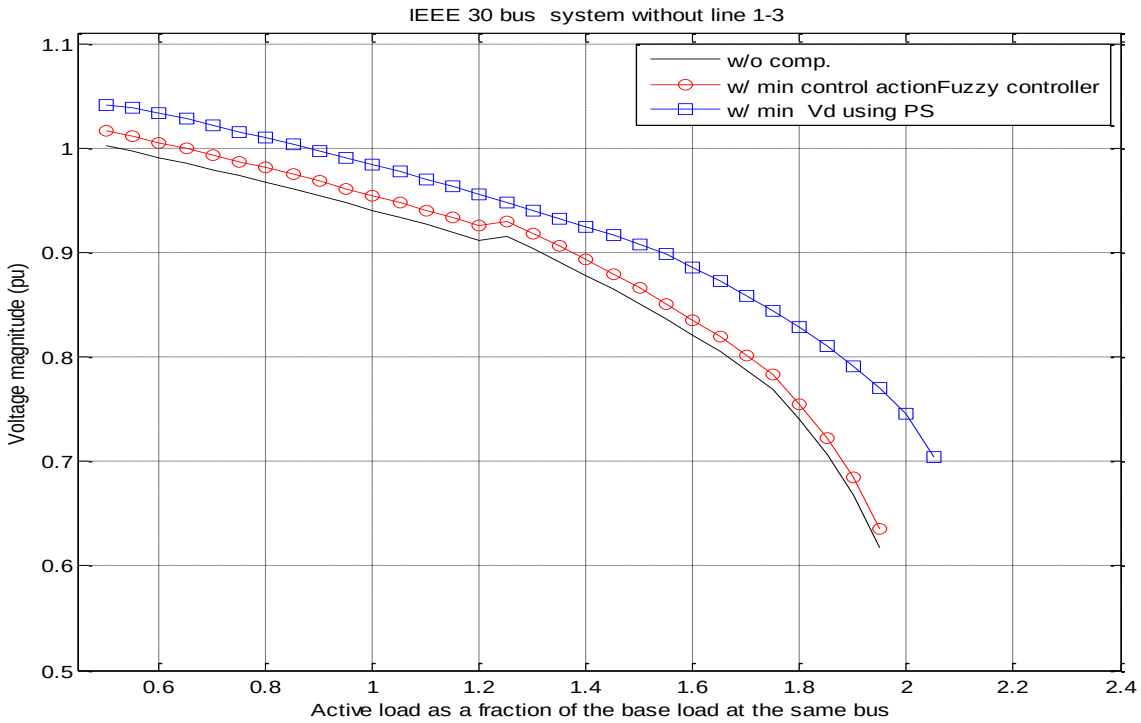

Figure 7.15: PV curves at bus 30 at full load and line 1-3 out for the modified IEEE 30 bus

7.7.4 Case 4: Modified IEEE 30 Bus System with Line 2-5 Out of Service

The modified IEEE 30 bus system at full load with line 2-5 out of service has only one bus, bus number 30, which violates the permissible lower voltage limit as shown in Figure (7.16). The voltage magnitude at this bus before any control action was 0.9460 pu. After making suitable control actions, the voltage magnitude at bus 30 improved to 0.9599 pu with fuzzy logic controller, and to 1.0008 pu using the objective function of minimum voltage deviation. As indicated in Figure (7.17), the voltage violation at bus 30 is removed and the overall voltage profile of the system is enhanced after making the required control actions using both methods.

The fuzzy logic controller in this case uses only one controller, the capacitor at bus 30, to remove the voltage violation at this bus. On the other hand, the other method, minimum voltage deviation, uses 12 controllers to remove the voltage violation at bus 30. All the required adjustments for all controllers for both methods are shown in Table (7.8).

Figure (7.18) shows that bus number 30, most critical bus in the system, has the minimum value (0.8298) of the *1-L* indicator before taking any control action. This value improved to be 0.8316 after adjusting the controllers using fuzzy logic controller, and to be 0.8403 with minimum voltage deviation method. It can be seen from the same figure that both methods are able to improve the voltage profile at all load buses. The second method, minimum voltage deviation, causes better improvement in the *1-L* indicator than the fuzzy logic method. As indicated in Figure (7.18), the two methods succeeded to increase the stability margin of the system and to remove the voltage violation at bus 30.

A review of Table (7.9) indicates that the MSV improved from 0.2180 to 0.2185 with fuzzy logic controller, and to 0.2210 with minimum voltage deviation method. The real power losses are decreased from 5.54 MW to 5.52 MW with a percentage reduction of 0.36 %, and the reactive power losses are improved from 26.39 MVAR to 26.28 MVAR with a percentage reduction of 0.42 % using the fuzzy logic controller method. When applying the method of minimum voltage deviation, the real and reactive power losses are reduced to 4.74 MW and 23.29 MVAR respectively. The corresponding percentage reductions are 14.44 % and 11.75 % respectively.

Table 7.8: Change in controllers for IEEE 30 bus system at full load and w/o line 2-5

Algorithm / Controller name	Fuzzy logic controller	Minimum voltage deviations using PS
Δt_{12-4}	0	0
Δt_{9-6}	0	0
Δt_{10-6}	0	0
Δt_{27-28}	0	0
ΔV_1	0	-0.02
ΔV_2	0	0
ΔV_5	0	0.03
ΔV_8	0	0
ΔV_{11}	0	0.02
ΔV_{13}	0	0.01
ΔQ_{c10}	0	0
ΔQ_{c12}	0	0.02
ΔQ_{c15}	0	0.04
ΔQ_{c17}	0	0.04
ΔQ_{c20}	0	0.03
ΔQ_{c21}	0	0.03
ΔQ_{c24}	0	0.04
ΔQ_{c26}	0	0.04
ΔQ_{c30}	0.02	0.04

Table 7.9: IEEE 30 bus system performance at full load and w/o line 2-5

Algorithm / Parameter	Without compensation	Fuzzy logic controller	Minimum voltage deviations using PS
Power losses	5.54 MW	5.52 MW	4.74 MW
Reactive power losses	26.39 MVAR	26.28 MVAR	23.29 MVAR
MSV	0.2180	0.2185	0.2210

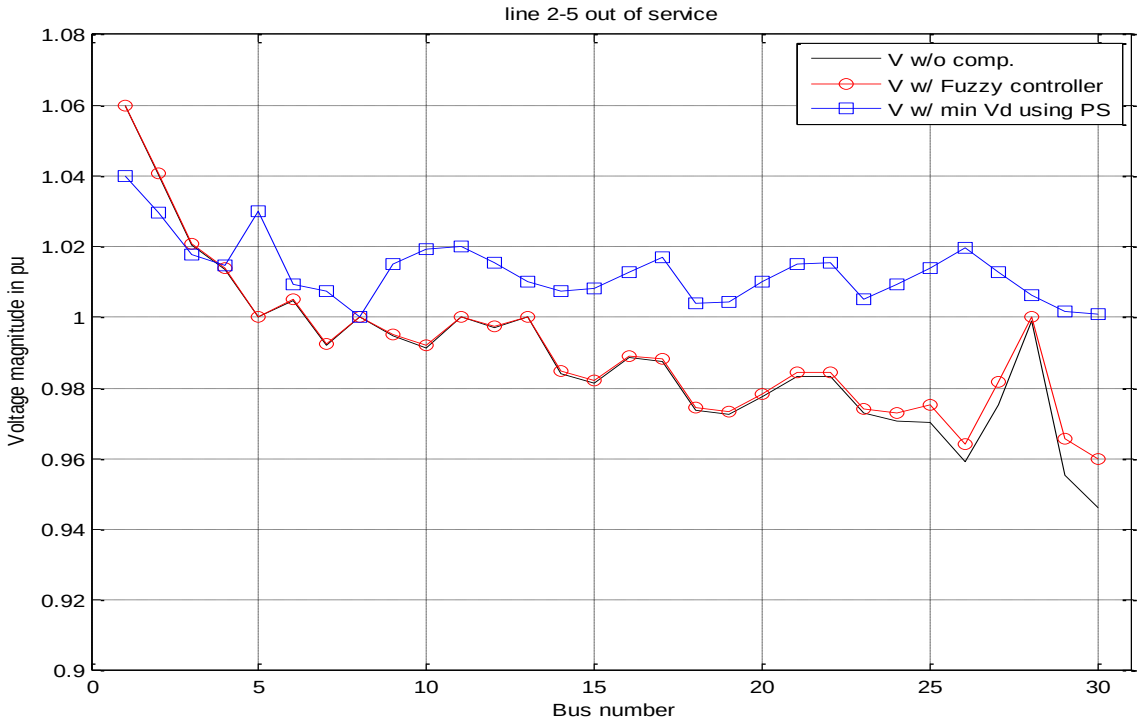

Figure 7.16: Voltage profile at full load and line 2-5 out for the modified IEEE 30 bus

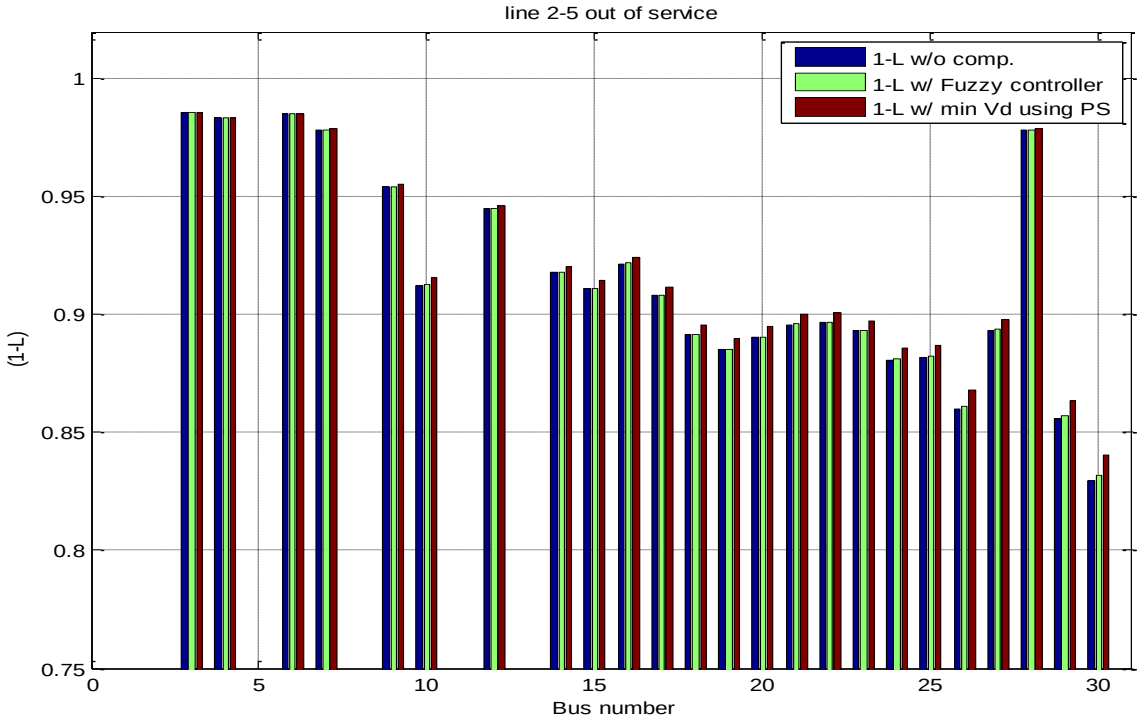

Figure 7.17: *1-L* index at full load and line 2-5 out for the modified IEEE 30 bus

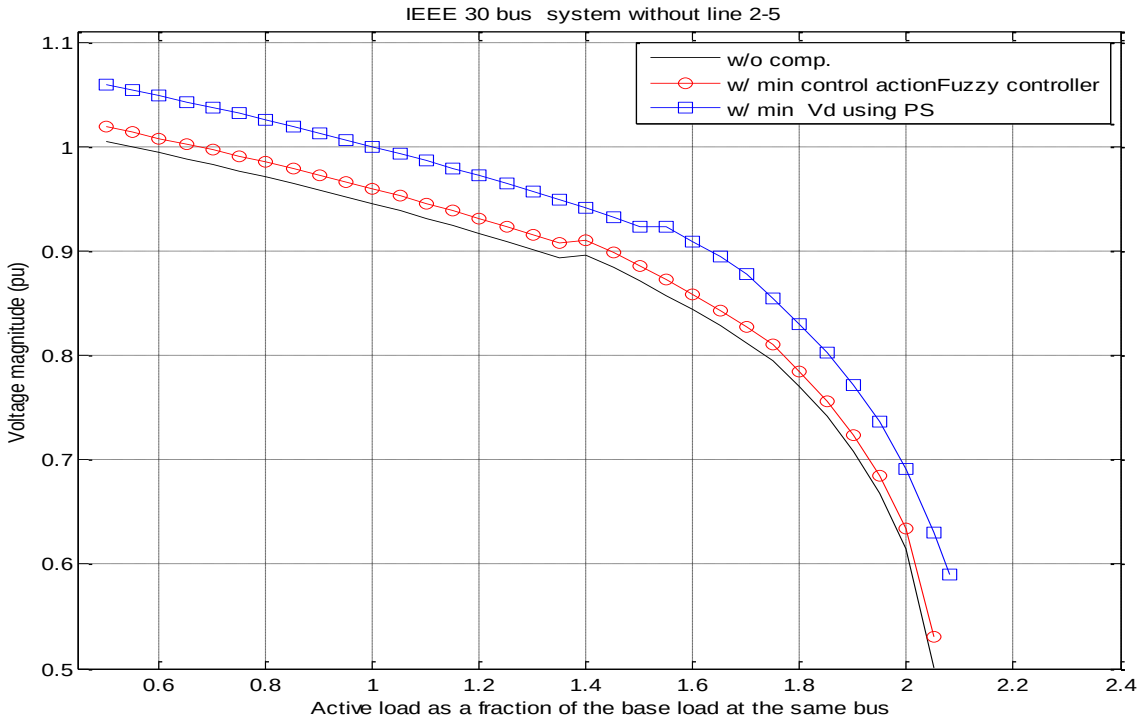

Figure 7.18: PV curves at bus 30 at full load and line 2-5 out for the modified IEEE 30 bus

7.8 Conclusions

Two different algorithms for further improving of the voltage profiles and decreasing the computational time have been presented in this chapter. The two algorithms consider all the available control variables in the system, i.e. ULTC transformers, generator excitation voltages, and the switchable shunt capacitors.

The first algorithm, Fuzzy logic controller, is used to improve the voltage profiles at all load buses after being subjected to any contingency and/or load change, to be within the pre-specified operating limits by using a smaller number of control actions. The results of the study cases show that this method is fast, reliable, and can improve the power system stability margin by using a smaller number of controllers. Thus, this method strongly suitable for on-line application to assist the ECC operators in making a reliable, and fast control decisions in order to improve the overall voltage profile. The membership function values of the inputs and output are dependent on the power system itself. Membership function values should be tuned and modified for each power system according to the permissible level of voltage variation. This can be done

by trying different values and/or shapes for the membership functions until getting acceptable decisions.

The second algorithm, PS-based algorithm, its objective function is to decrease the sum of the squares of voltage deviations at all load buses in the system (V_d). The results of the study cases illustrate that this method, in all cases, uses more controllers, and takes more time than the fuzzy logic controller algorithm. On the other hand, the stability margins resulted from PS-based method are better than those obtained from Fuzzy logic controller in most cases.

The initial point affects the final solution of PS Method. In these applications the best choice of the initial point is in the middle of the solution space

Chapter 8 Optimal Size of Switchable Shunt Capacitor Using GA

This chapter proposes the use of a GA-based optimal reactive power control, with the objective function selected to minimize the overall power losses, to identify the optimal size of a shunt capacitor necessary to improve the overall voltage profile of a power system under contingency operation. The location of the shunt capacitor is defined based on the critical bus or buses in the system, which can be identified as shown in Chapter 4. The proposed method is tested and validated on the 6 generator system used elsewhere in this work. Results indicate significant improvement in voltage stability margin, reduction in both active and reactive losses, in addition to moving all voltage magnitudes within limits. In this research, four different (N-1) contingency cases, which represent the most severe line outage cases in the system under study, are used in order to determine the optimal size of the desired capacitor.

8.1 Problem Formulation

Any change in power system topology after being subjected to contingency can cause a voltage violation. A permanent improvement in voltage security is essential to keep the power system secured. Optimal control of voltage and reactive power is a significant technique for voltage profile improvements of power system. By finding a set of adjustments to the control variables the operator can optimize a certain objective function, while satisfying the power system constraints for both dependent and control variables. Planning of reactive power compensation in a power system has to be comprehensive so as to maintain the voltages within the acceptable ranges under conditions of both light load, peak load conditions or after being subjected to contingency. During peak load conditions, the system may need capacitive reactive power support to maintain acceptable voltages at all buses, while the same system may experience over-voltages during light load conditions.

The objective of this chapter is to identify the optimal size of a shunt capacitor in order to get the system voltage profile back to be within limits after being subjected to contingency, while the best location is defined to be at the most critical bus in the system.

The network constraints include the upper and lower limits of the voltage magnitude at all load buses, the upper and lower limits of the reactive power for all the generators, and the

upper and lower limits of all the available controllers, which include generator terminal voltages, tap changing transformers, and switchable shunt capacitors.

8.2 Methodology

Consider a power system with *n* buses, with buses 1 to *g* as a generator buses, buses *g+1* to *n* as load buses, and the first generator is counted as the swing bus. The system has a number of tap changing transformers equal to t, and a number of buses with a switchable shunt capacitor equal to cap. By adjusting the controlling device at load bus *j*, the voltage improvement at bus *i* can be found by Equation (8.1) as:

$$\Delta V_i = S_{ij}.\Delta U_j \quad \text{for } i = g+1, g+2, \ldots, n \quad \text{and} \quad j = 1,2, \ldots, t + g + cap \tag{8.1}$$

where:

ΔV_i: is the voltage change at load bus *i*

ΔU_j: is the adjustment of the controlling device *j*

S_{ij}: is the sensitivity coefficient of *the controlling device j* on voltage at load bus *i*

The sensitivity matrix (S), is a matrix which relates the control variable and dependent variables as shown in Equation (6.51) repeated here as (8.2)

$$\begin{bmatrix} \Delta Q_1 \\ \vdots \\ \Delta Q_g \\ \Delta V_{g+1} \\ \vdots \\ \Delta V_{g+cap} \\ \Delta V_{g+cap+1} \\ \vdots \\ \Delta V_n \end{bmatrix} = [S] \begin{bmatrix} (\Delta t_{jk})_1 \\ \vdots \\ (\Delta t_{jk})_t \\ \Delta V_1 \\ \vdots \\ \Delta V_g \\ \Delta Q_{g+1} \\ \vdots \\ \Delta Q_{g+cap} \end{bmatrix} \tag{8.2}$$

The adjustment of the controlling devices is constrained with the upper and lower limits as:

$$\Delta U^{min} \leq \Delta U \leq \Delta U^{max} \tag{8.3}$$

where:

$$\Delta U = \left[(\Delta t_{jk})_1, \dots, (\Delta t_{jk})_t, \Delta V_1, \dots, \Delta V_g, \Delta Q_{g+1}, \dots, \Delta Q_{g+cap}\right]^t$$

$$\Delta U^{min} = \left[\Delta(t_{jk})_1^{min}, \dots, \Delta(t_{jk})_t^{min}, \Delta V_1^{min}, \dots, \Delta V_g^{min}, \Delta Q_{g+1}^{min}, \dots, \Delta Q_{g+cap}^{min}\right]^t$$

$$\Delta U^{max} = \left[\Delta(t_{jk})_1^{max}, \dots, \Delta(t_{jk})_t^{max}, \Delta V_1^{max}, \dots, \Delta V_g^{max}, \Delta Q_{g+1}^{max}, \dots, \Delta Q_{g+cap}^{max}\right]^t$$

The objective in this work is to keep the load bus voltage deviations within $\pm 5\%$ of the nominal voltage which is 1 pu i.e.,

$$0.95 \leq V_i \leq 1.05 \qquad \text{for } i = g+1, g+2, \dots, n \tag{8.4}$$

The objective function is to minimize power losses (P_l) of the power system according to the following equation:

$$P_l = \sum_{j=1}^{n} P_j \tag{8.5}$$

where:

n: is the total number of buses

P_j: is the active power injected at bus *j*

This method is used in order to get an optimal solution to the VAR control problem by applying the GA technique. After linearization, the objective function as mentioned before in the Chapter 6 is :

$$\Delta P_l = \begin{bmatrix} \frac{\partial P_l}{\partial (t_{jk})_1} & \cdots & \frac{\partial P_l}{\partial (t_{jk})_t} & \frac{\partial P_l}{\partial V_1} & \cdots & \frac{\partial P_l}{\partial V_g} & \frac{\partial P_l}{\partial Q_{g+1}} & \cdots & \frac{\partial P_l}{\partial Q_{g+cap}} \end{bmatrix} \begin{bmatrix} (\Delta t_{jk})_1 \\ \vdots \\ (\Delta t_{jk})_t \\ \Delta V_1 \\ \vdots \\ \Delta V_g \\ \Delta Q_{g+1} \\ \vdots \\ \Delta Q_{g+cap} \end{bmatrix} \tag{8.6}$$

where:

$(\Delta t_{jk})_1 \ldots, (\Delta t_{jk})_t,\ \Delta V_1, \ldots, \Delta V_g, \Delta Q_{g+1}, \ldots, \Delta Q_{g+cap}$ are the control variables

g: is the total number of generators

t: is the total number of tap changing transformer

cap: is the total number of switchable shunt capacitors

The complete solution process can be found in the Chapter 6, while the steps of the solution process of the optimal VAR control problem using minimum power losses (P_l) are given below.

1. Identify the most critical bus in the system under study.
2. Do (N-1) contingency.
3. Put a variable capacitor at the most critical bus in the system.
4. Perform a load flow solution.
5. Check the system performance and if it is necessary to improve the voltage profiles or to minimize the objective function or both, then proceed to Step 6, otherwise, go to Step 12.
6. Calculate the sensitivity matrix (S) relating the dependent variables, Δx, and the control variables, Δu as explained in Chapter 6.
7. Find the dependent variables' lower and upper limits, $\Delta x^{min}, \Delta x^{max}$ and the control variables' lower and upper limits, $\Delta u^{min}, \Delta u^{max}$ according to Equations (6.9) to (6.13) .
8. Calculate the coefficients of the objective function using the derivative of the objective function with respect to all the control variables, u, as indicated in the Chapter 6.

9. Solve the optimization problem by using the GA [117] to evaluate the required adjustments to the control variables including the added capacitor.
10. Update the values of the control variables using the output of the GA optimization technique such that $u^{new} = u^{old} + \Delta u$.
11. Perform a load flow solution after the adjustments in the control variables and go back to Step 5.
12. Repeat Steps 2 to 11 with different contingency case for all significant contingencies, then proceed to Step 13.
13. The largest value of the capacitor in all contingency cases is the required value of the capacitor.
14. stop

8.3 Results and Discussion

The proposed algorithms have been tested on the 6 generator system under contingency operation, the system data is given in Appendix A. The system at normal operation has active load of 506 MW, and reactive load of 195 MVAR while the active and reactive losses are 18.54 MW and -16.19 MVAR respectively. Results and analysis for some cases are indicated in the sections below.

8.3.1 Case 1: Line 1-8 Out of Service

With the line connecting buses 1 and 8 out of service at full load, the load flow results for this case, before compensation, show that there are five buses out of twenty one buses have voltage magnitudes below the minimum voltage limit. The minimum system voltage of 0.9403 pu is at bus number 21. The generated active and reactive power are 524.47 MW and 168.88 MVAR respectively. The swing bus generated 44.47 MW, and 46.83 MVAR. After applying the proposed algorithm to get all the voltages back to be within limits using the available control variables (six generators and the added capacitor at bus number 16), the minimum voltage improved to be 0.9989 pu at bus number 8. In this case, the generated active and reactive power are 525.79 MW and 189.91 MVAR respectively, while the swing bus generated 45.79 MW, and absorbed 4.18 MVAR. Table (8.1) indicates the change in system controllers. As indicated in Table (8.2), the MSV has been improved from 0.1065 to 0.1176, the power losses reduced from

19.79 MW to 18.47 MW with a percentage reduction of 6.67%. The reactive power generated by transmission lines changed from 5.09 MVAR to 18.96 MVAR with a percentage increase of 272.5%. Figure (8.1) shows the improvement in the voltage profile of the system after compensation, it also indicates that buses 15, 16, and 17 have almost the same voltage magnitude before and after compensation. Figure (8.2) shows the improvement in the system stability, where the *1-L* index at load buses increases or remains the same. It also indicates the improvement of *1-L* index at the most critical bus in the system (bus 16) to be 0.8127, with an increase of 0.0169. The P-V curves of Figure (8.3) also indicate the improvement in the system stability, by increasing the stability margin. So, these results indicate a significant improvement in the overall system performance by increasing system stability, reducing the active power losses, and also improving the voltage profiles, which reflects the success of the proposed optimization algorithm. Thus this case requires an added capacitor of 7 MVAR at bus number 16. Next we proceed to study other contingencies to see if they require a larger added capacitor.

Table 8.1: Change in controllers at full load with line 1-8 out of service

Algorithm / Controller name	Minimum power losses using GA
ΔV_1	0.05
ΔV_2	0.08
ΔV_3	0.06
ΔV_4	0.08
ΔV_5	-0.01
ΔV_6	0.01
ΔQ_{c16}	0.07

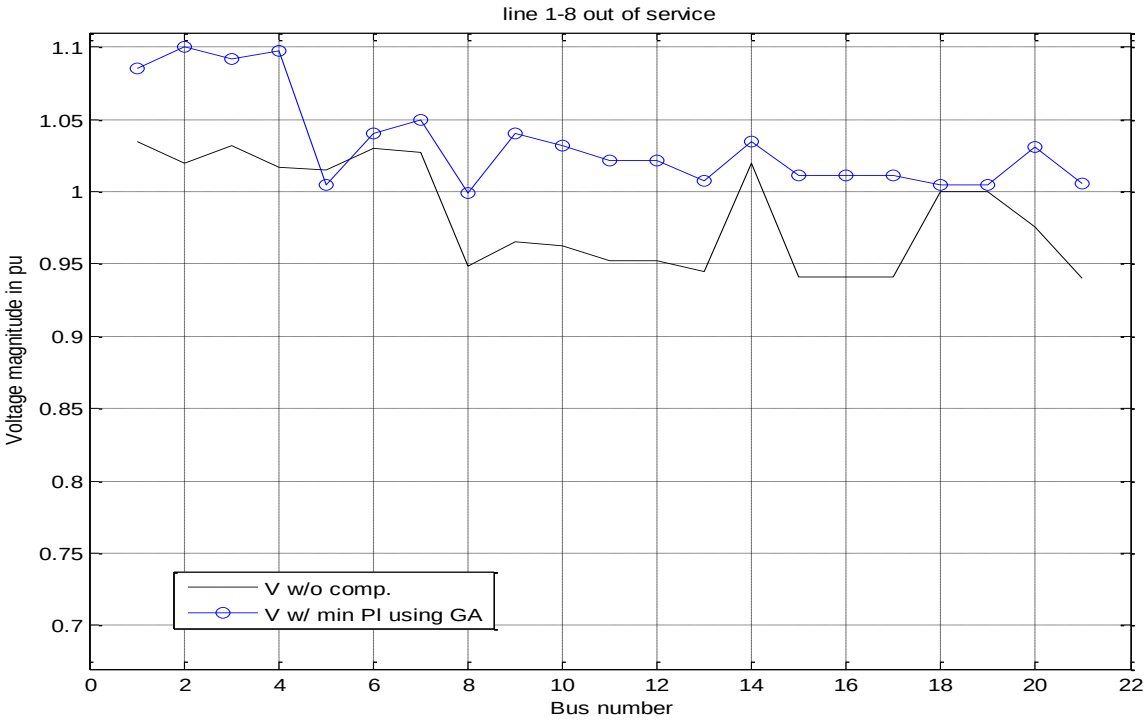

Figure 8.1: Voltage profile at full load with line 1-8 out of service

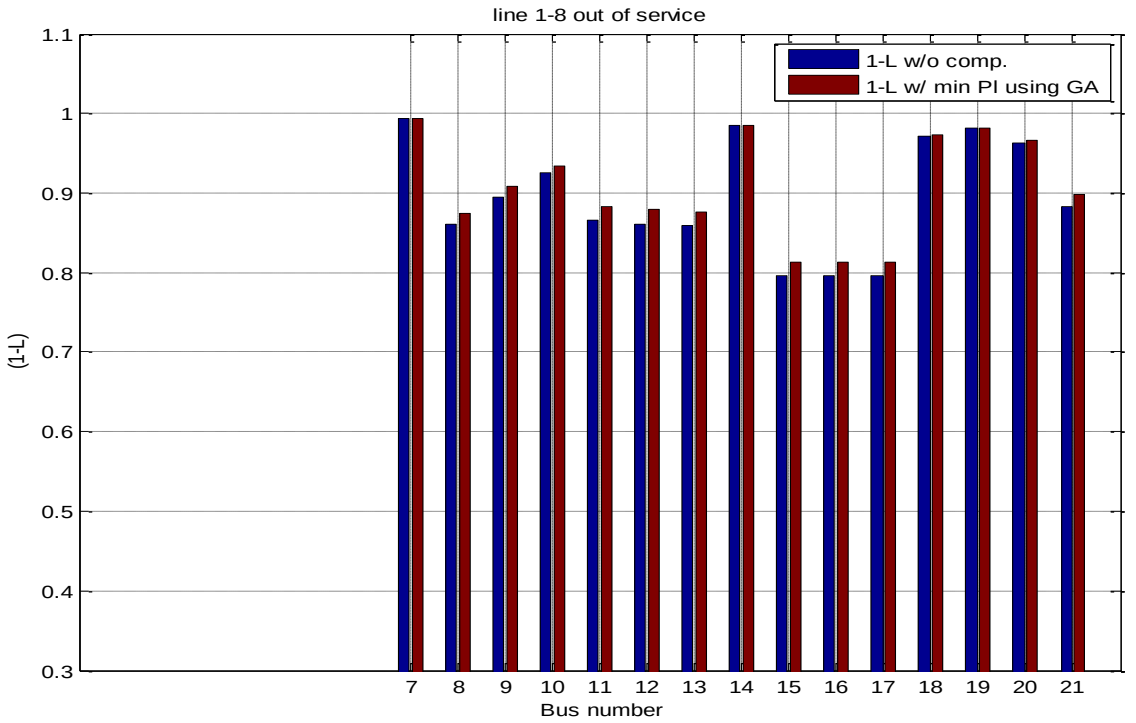

Figure 8.2: *1-L* index at full load with line 1-8 out of service

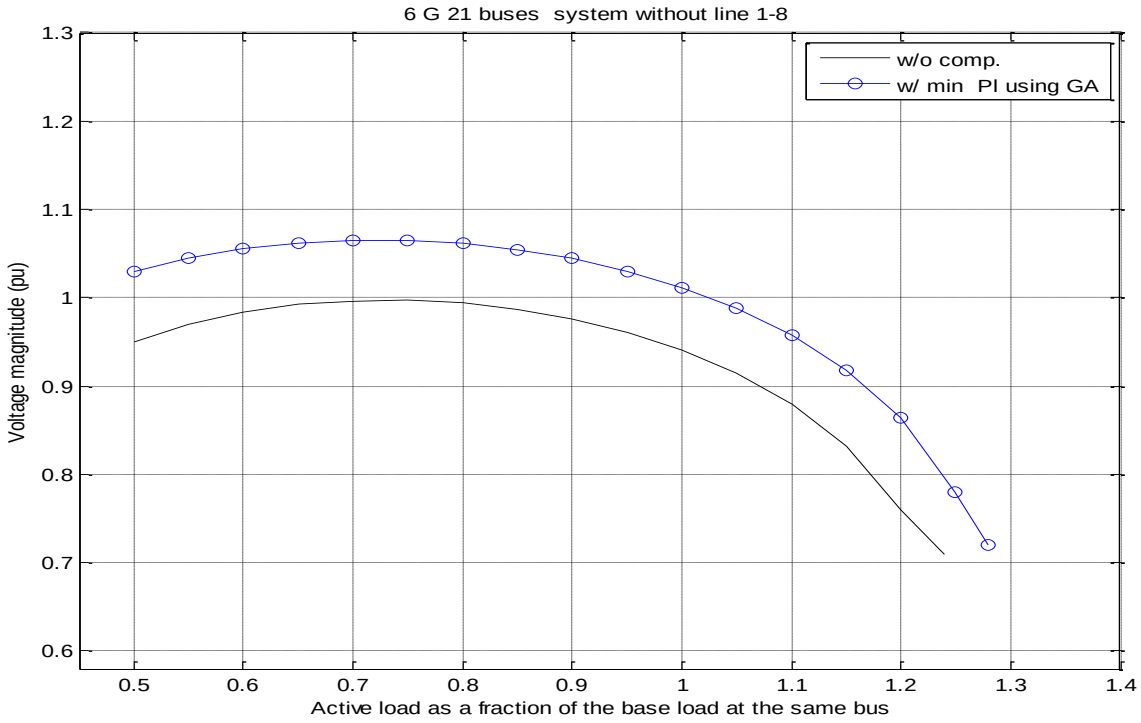

Figure 8.3: PV curves at bus 16 at full load with line 1-8 out of service

Table 8.2: System performance at full load with line 1-8 out of service

Algorithm / Parameter	Without compensation	Minimum power losses using GA
Power losses	19.79 MW	18.48 MW
Reactive power losses	-5.09 MVAR	-18.96 MVAR
MSV	0.1064	0.1176

8.3.2 Case 2: Line 8-13 Out of Service

With the line connecting buses 8 and 13 out of service at full load, the load flow results before compensation show that there are five buses out of twenty one buses with voltage magnitudes below the minimum voltage limit. The minimum voltage of 0.9379 pu is at bus number 21. The generated active and reactive power are 524.64 MW and 179.41 MVAR

respectively, while the swing bus generated 44.64 MW, and 48.22 MVAR. After applying the proposed algorithm to get all the voltages back within limits, the minimum voltage improved to be 0.9933 pu at bus number 20 and the generated active and reactive power are 523.01 MW and 159.09 MVAR respectively, while the swing bus generated 43.01 MW, and absorbed 0.85 MVAR. Table (8.3) indicates the change in system controllers. As indicated in Table (8.4), the MSV has been improved from 0.0659 to 0.0731, the power losses reduced from 18.64 MW to 17.01 MW with a percentage reduction of 8.74%, and the reactive power generated by transmission lines changed from 15.59 MVAR to 28.66 MVAR with a percentage increase of 83.84%. Figure (8.4) shows the improvement in the voltage profile of the system after compensation, it also indicates that buses 15, 16, and 17 have nearly the same voltage magnitude before and after compensation. Figure (8.5) shows the improvement in the system stability, showing the improvement of the *1-L* index at the most critical bus in the system to be 0.8171 with an increase of 0.0158. The P-V curves of Figure (8.6) also indicate the improvement in stability margin after adding a capacitor at bus number 16. The size of added capacitor is 7 MVAR.

Table 8.3: Change in controllers at full load with line 8-13 out of service

Algorithm / Controller name	Minimum power losses using GA
ΔV_1	0.01
ΔV_2	0.08
ΔV_3	0.06
ΔV_4	0.02
ΔV_5	-0.01
ΔV_6	0.02
ΔQ_{c16}	0.07

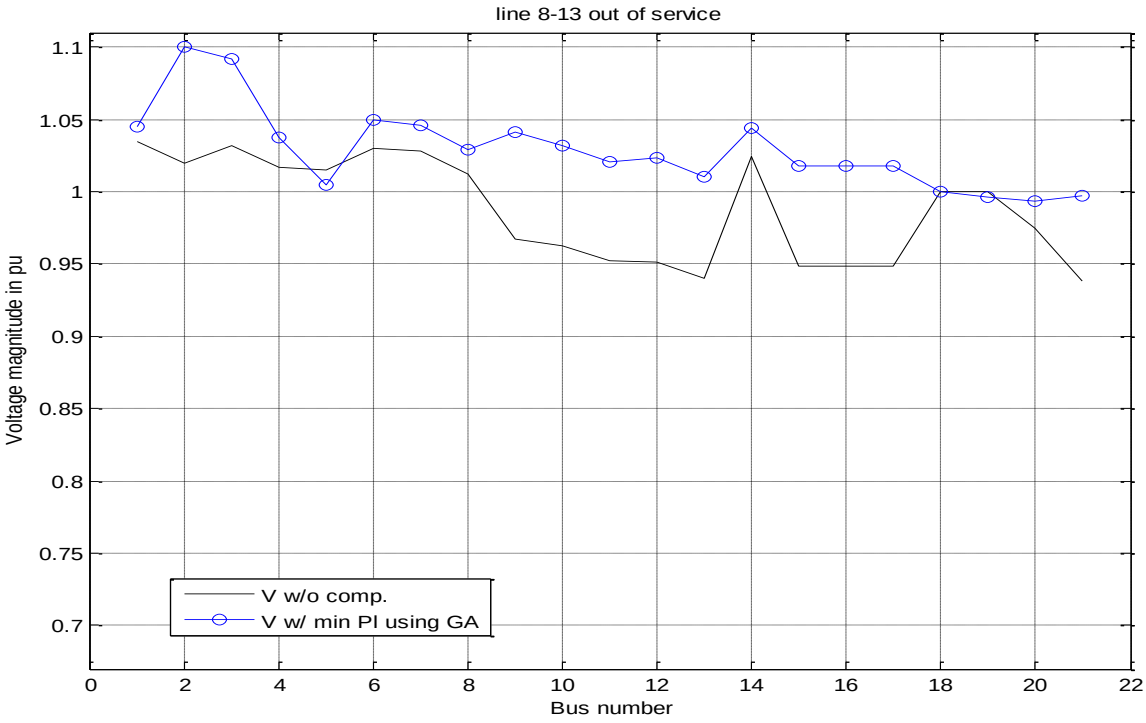

Figure 8.4: Voltage profile at full load with line 8-13 out of service

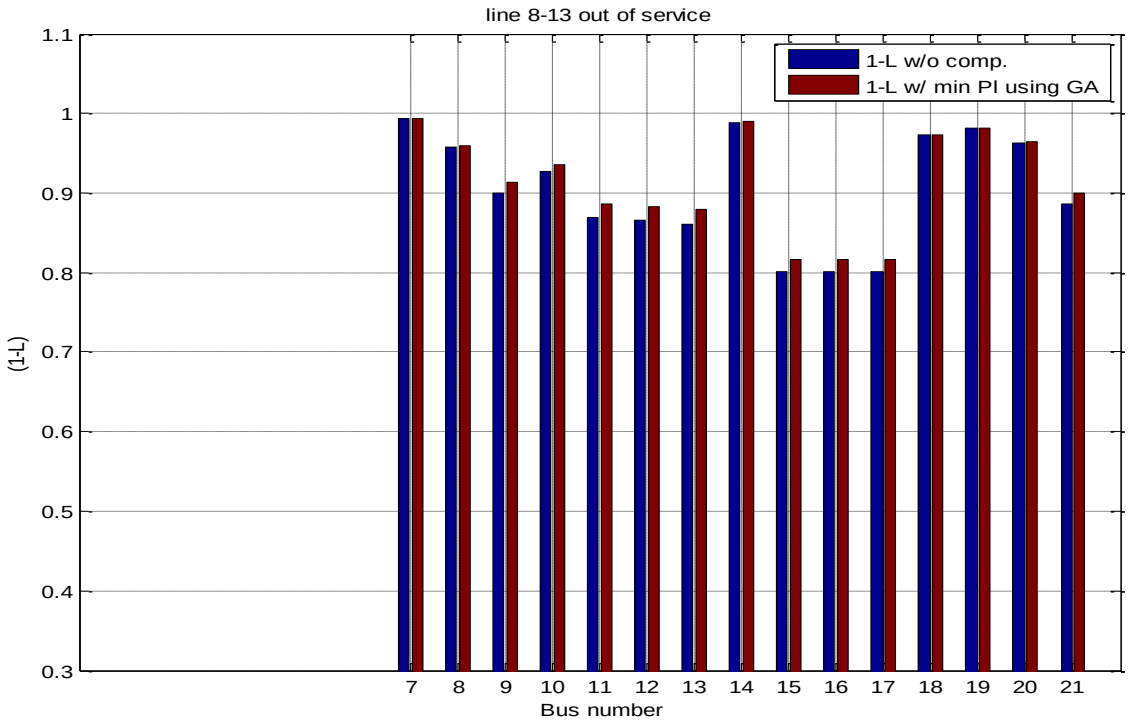

Figure 8.5: *1-L* index at full load with line 8-13 out of service

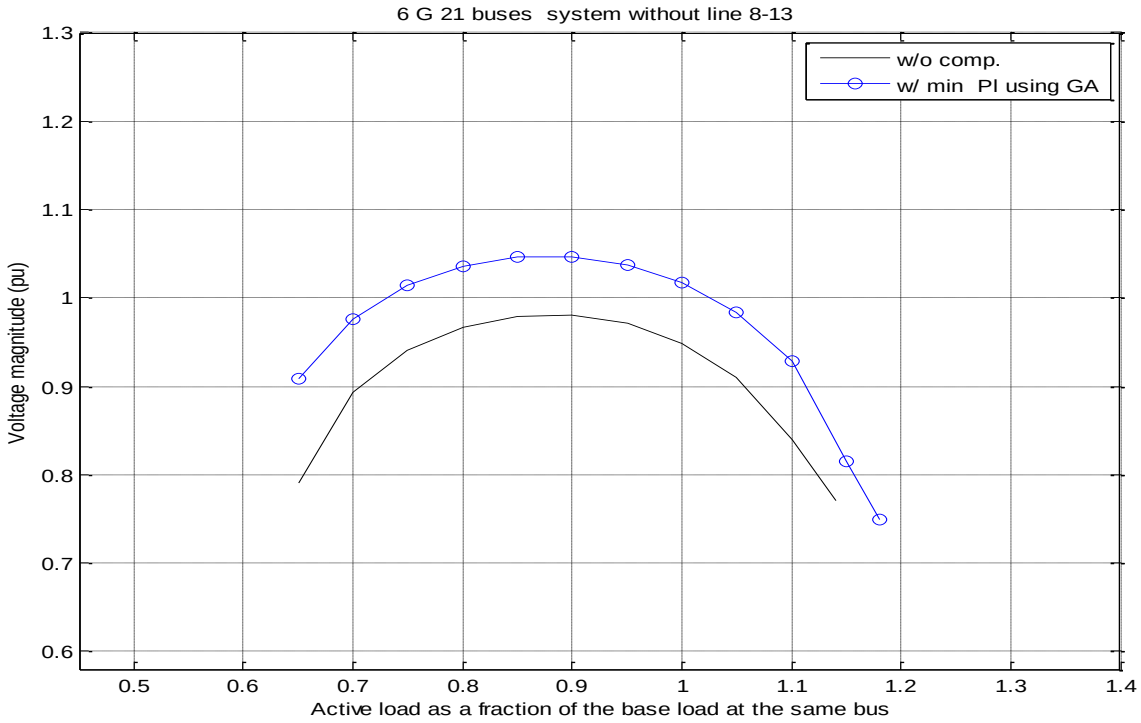

Figure 8.6: PV curves at bus 16 at full load with line 8-13 out of service

Table 8.4: System performance at full load with line 1-8 out of service

Algorithm / Parameter	Without compensation	Minimum power losses using GA
Power losses	18.64 MW	17.01 MW
Reactive power losses	-15.59 MVAR	-28.66 MVAR
MSV	0.0659	0.0731

8.3.3 Case 3: Line 14-16 Out of Service

With the line connecting buses 14 and 16 out of service at full load, there are four buses out of twenty one buses with voltage magnitudes below the minimum voltage limit, with a minimum voltage of 0.681 pu at bus number 16. The generated active and reactive power are 528.33 MW and 220.50 MVAR respectively, while the swing bus generates 48.33 MW, and 34.46 MVAR. After applying the proposed algorithm the minimum voltage improved to be 1.004

pu at bus number 21. The generated active and reactive power are 524.56 MW and 182.94 MVAR respectively, while the swing bus generated 44.56 MW, and absorbed 91.96 MVAR. Table (8.5) indicates the change in system controllers. As indicated in Table (8.6), the MSV has been improved from 0.0432 to 0.0896, the power losses reduced from 22.33 MW to 18.56 MW with a percentage reduction of 16.88%, and the reactive power losses improved from 25.5 MVAR to 4.2 MVAR with a percentage reduction of 83.53%. Figure (8.7) shows the improvement in the voltage profile of the system after compensation, Figure (8.8) shows the improvement of the *1-L* index at the most critical bus in the system to be 0.6585, with an increase of 0.2915. The P-V curves of Figure (8.9) also illustrate the improvement in the stability margin after adding a capacitor of 15 MVAR at bus number 16.

Table 8.5: Change in controllers at full load with line 14-16 out of service

Algorithm / Controller name	Minimum power losses using GA
ΔV_1	0.05
ΔV_2	0.04
ΔV_3	0.06
ΔV_4	0.08
ΔV_5	0.04
ΔV_6	0.01
ΔQ_{c16}	0.15

Table 8.6: System performance at full load with line 14-16 out of service

Algorithm / Parameter	Without compensation	Minimum power losses using GA
Power losses	22.33 MW	18.56 MW
Reactive power losses	25.50 MVAR	4.20 MVAR
MSV	0.0432	0.0896

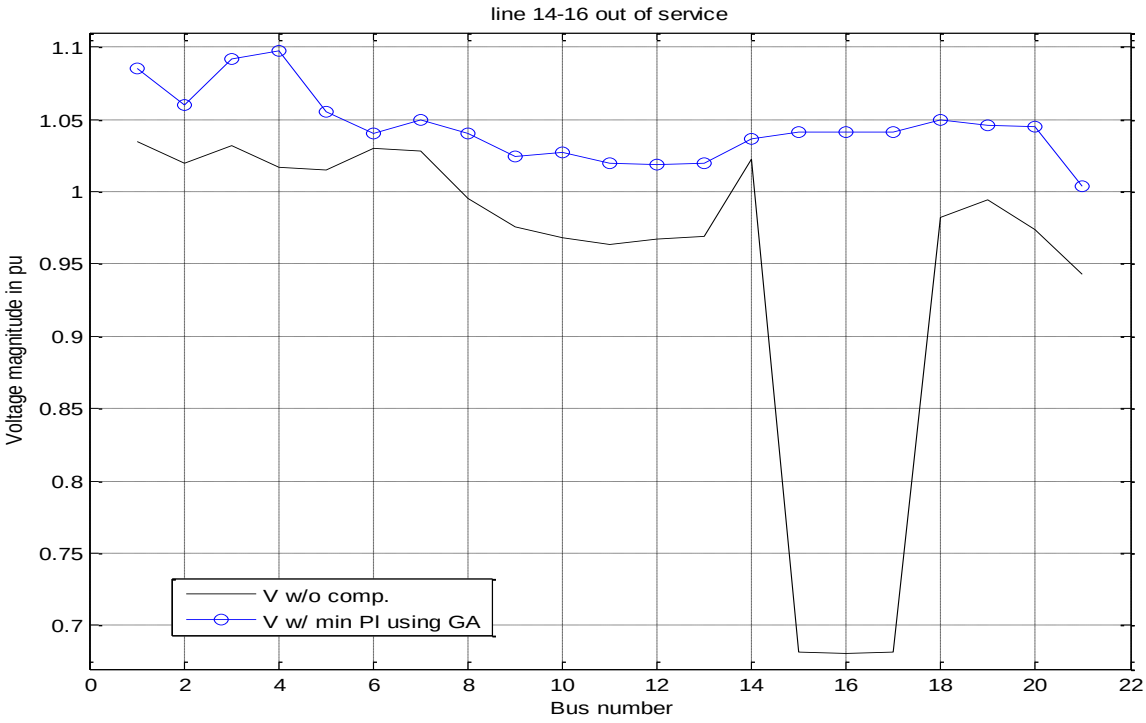

Figure 8.7: Voltage profile at full load with line 14-16 out of service

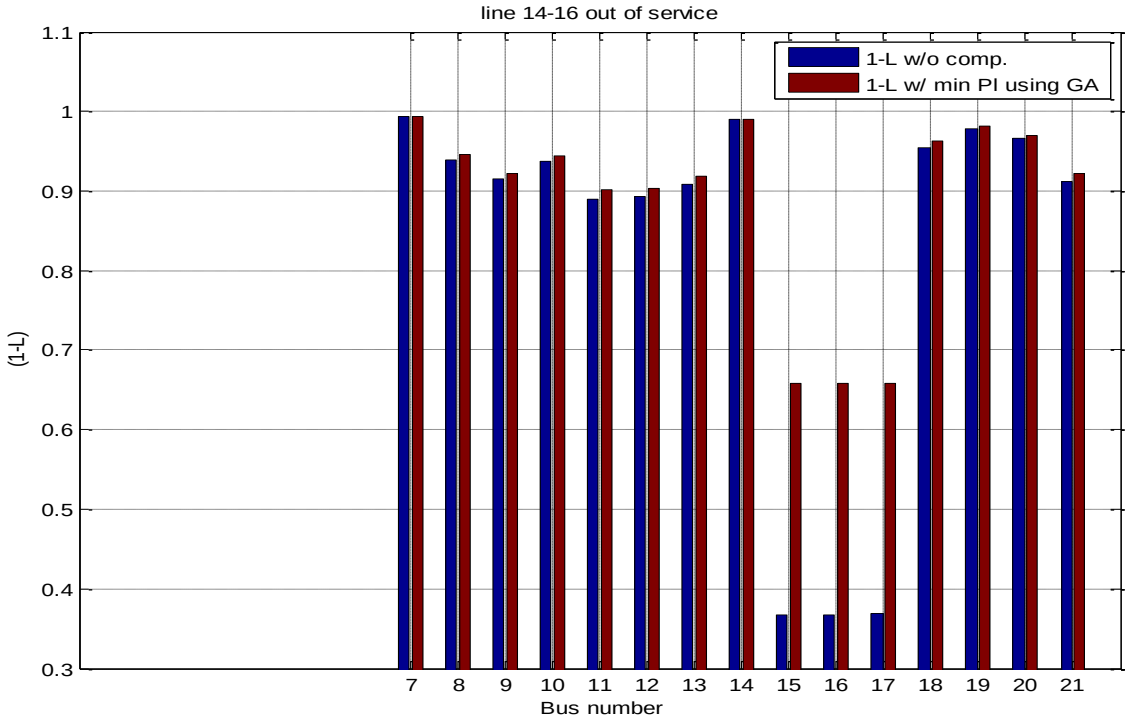

Figure 8.8: *1-L* index at full load with line 14-16 out of service

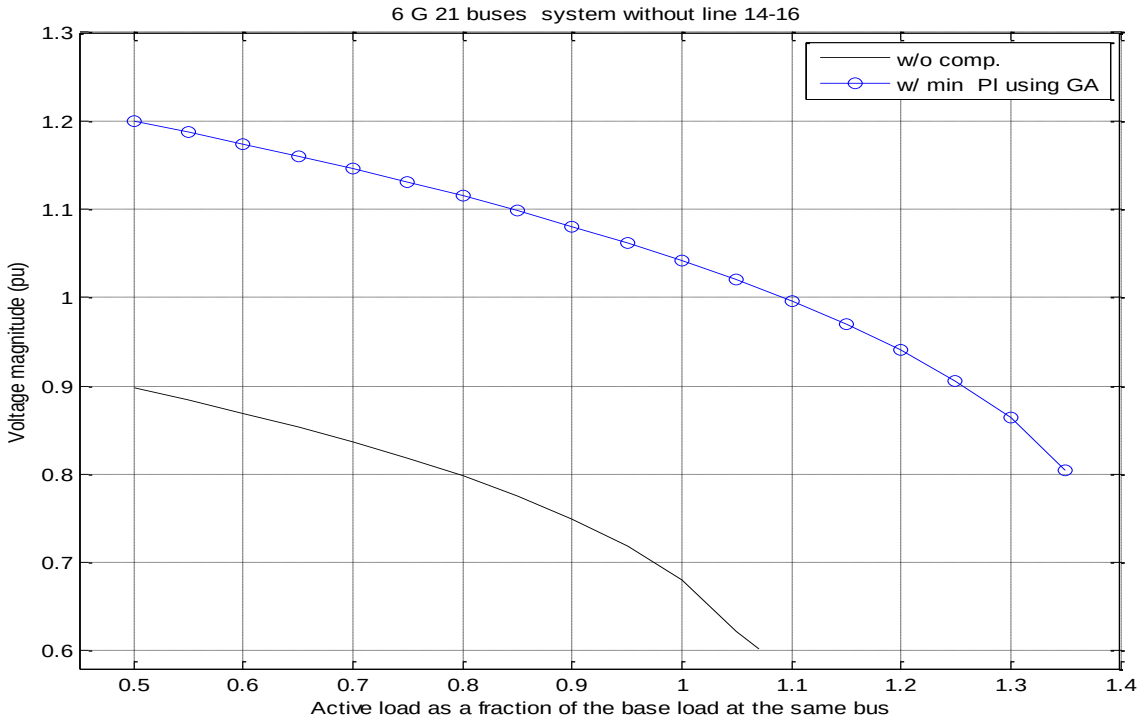

Figure 8.9: PV curves at bus 16 at full load with line 14-16 out of service

8.3.4 Case 4: Line 17-18 Out of Service

With the line connecting buses 14 and 16 out of service at full load, four buses out of twenty one buses have voltage magnitudes below the minimum voltage limit, with a minimum voltage of 0.7659 pu at buses number 15, and 17. The generated active and reactive power are 526.37 MW and 185.39 MVAR respectively, while the swing bus generated 46.37 MW, and 30.05 MVAR. After applying the proposed algorithm, the minimum voltage at bus number 10 improved to be 96.33 pu, and the generated active and reactive power are 525.17 MW and 167.12 MVAR respectively, while the swing bus generated active and reactive power of 45.17 MW, and 12.18 MVAR respectively. Table (8.7) indicates the change in system controllers. As indicated in Table (8.8), the MSV has been improved from 0.0407 to 0.0834, the power losses reduced from 20.37 MW to 19.17 MW with a percentage reduction of 5.89%, and the reactive power generated by the transmission lines increased from 9.91 MVAR to 18.39 MVAR with a percentage increase of 91.36%. Figure (8.10) shows the improvement in the voltage profile of the system after compensation. Figure (8.11) shows that the *1-L* index at the most critical bus in the system improved to be 0.5418, with an increase of 0.2342. The P-V curves of Figure (8.12)

also illustrate the improvement in the stability margin after putting a capacitor of 9 MVAR at bus number 16.

Table 8.7: Change in controllers at full load with line 17-18 out of service

Algorithm / Controller name	Minimum power losses using GA
ΔV_1	-0.01
ΔV_2	-0.01
ΔV_3	-0.01
ΔV_4	0.08
ΔV_5	0.04
ΔV_6	0.00
ΔQ_{c16}	0.09

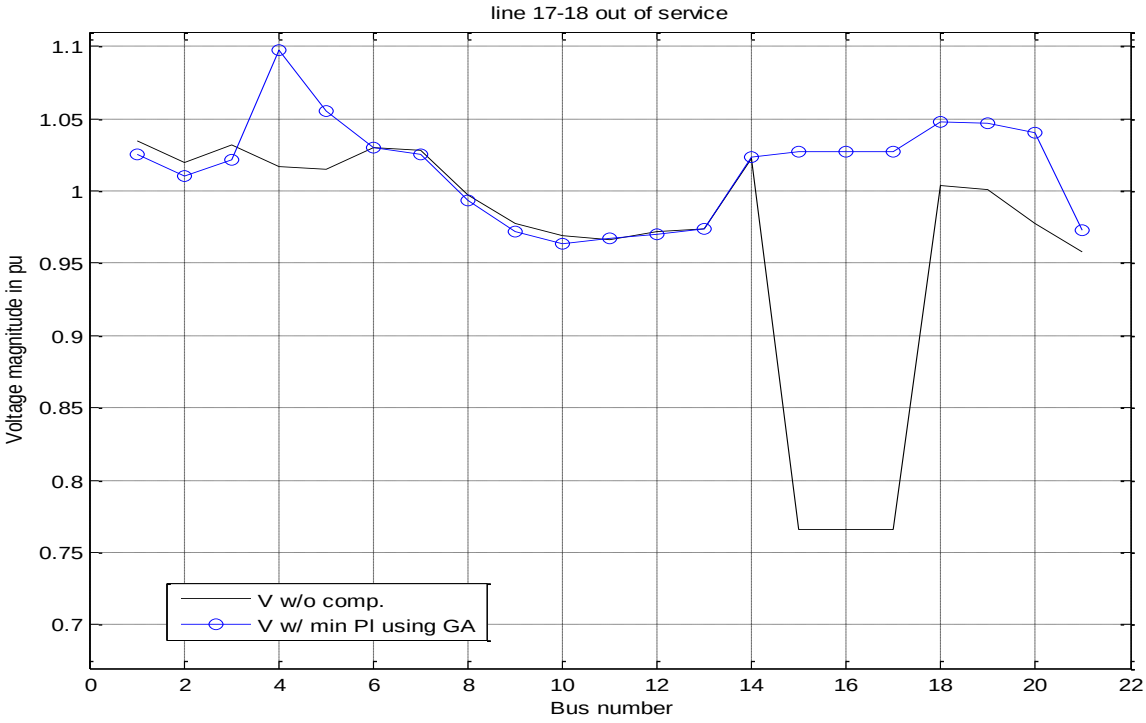

Figure 8.10: Voltage profile at full load with line 17-18 out of service

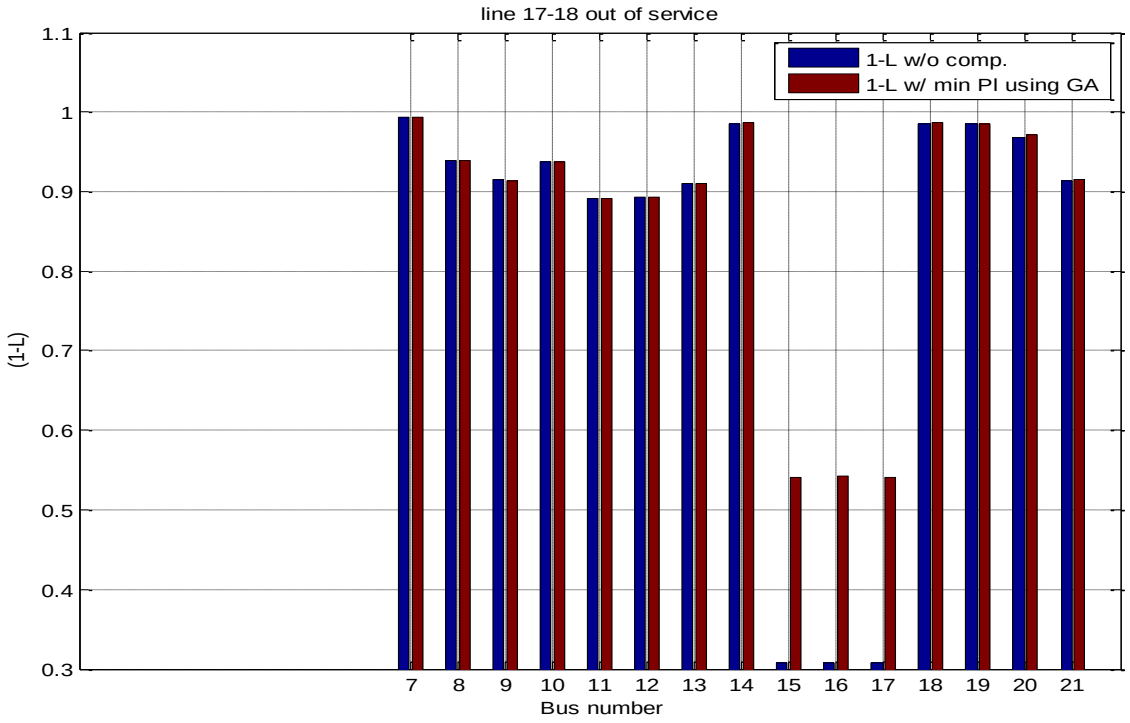

Figure 8.11: *1-L* index at full load with line 17-18 out of service

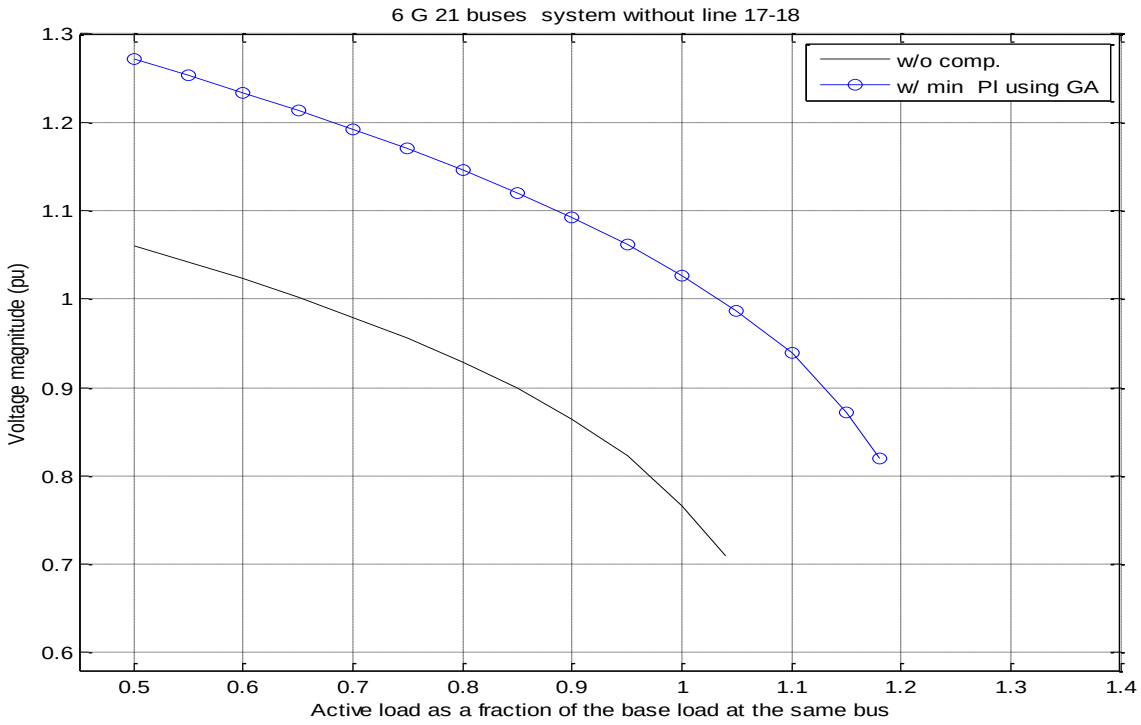

Figure 8.12: PV curves at bus 16 at full load with line 17-18 out of service

Table 8.8: System performance at full load with line 17-18 out of service

Algorithm / Parameter	Without compensation	Minimum power losses using GA
Power losses	20.37 MW	19.17 MW
Reactive power losses	-9.61 MVAR	-18.39 MVAR
MSV	0.0407	0.0834

8.4 Conclusion

A GA-based optimal reactive power control, with the objective function selected to minimize the overall power losses, is employed to calculate the optimal size of a shunt capacitor necessary to improve the overall voltage profile of a power system under contingency operation. The location of the shunt capacitor is defined based on the critical bus or buses in the system. Results indicate significant improvement in voltage stability margin, reduction in both active and reactive losses, in addition to moving all voltage magnitudes within limits

The transmission lines in three cases out of the four studied cases generate reactive power which helps in voltage improvement of the overall system.

From all the studied cases, the largest value of the reactive power generated by the installed capacitor at bus number 16 (most critical bus) is 15 MVAR at rated voltage. This means that the optimal size of the capacitor that should be installed in order to improve the system voltage profile and stability is a capacitor with 15 MVAR.

Chapter 9 Conclusions and Future Work

The aim of this research work is evaluate the usefulness of intelligent methods to aid in evaluation and control of modern power systems characterized by complex interconnections and stressed operating limits. The first part of this work has involved the design of artificial neural network techniques to evaluate the voltage profile of power systems and generate intelligent decisions regarding the status of the system from voltage instability prospective. The second part of this work has employed many techniques to provide the power system operators in energy control center with intelligent advice on the optimal dispatch and control of the available VAR sources: generator excitation systems, tap setting of under load tap setting transformers, and switchable shunt capacitors. The third part of this work has involved in the design of a genetic algorithm based tool to identify the optimal size of a shunt capacitor necessary to enhance the voltage profile of the system in case of being subjected to contingency.

9.1 Conclusions

The research has produced an extensive library of the effect of single level contingencies (N-1) on the static voltage stability of power systems. All these contingencies are ranked based on their impact on the voltage stability in order to reduce the number of contingencies out of all possible (N-1) contingencies that need to be considered for more voltage stability analysis. This library also includes a rank of all load buses according to their weakness.

An ANN approach is proposed to predict voltage collapse proximity. The proposed algorithm is fast, reliable, accurate, and strongly suitable for on-line application. In this work two different indicators, MSV and L-index, are used to predict the proximity of voltage collapse. A comparison between two different numbers of input features; all available inputs, and a reduced number of inputs based on feature selection technique, indicates that results of two networks are comparable, but networks based on a reduced number of inputs respond faster than networks based on all available inputs.

During emergency state, a fast, reliable, and accurate decision is required to get the system back into a secure normal state. So, the reduced number of input networks is more suitable for on-line implementation to help the power system operator take the suitable control action regarding the status of the system.

The adopted MVS ANN algorithm gives information about the status of the whole system without identifying the most critical bus in the system that may lead to voltage instability. On the other hand, the *L*-index ANN algorithm gives information about each load bus individually. This method helps in identifying the most critical bus in the system.

Many different algorithms for improving the voltage profiles and voltage stability of power systems have been presented in this research. All these algorithms consider all the available control variables in the system, i.e. ULTC transformer, generator excitation, and the shunt switchable capacitors. The objective of the first algorithm, minimizing the number of control actions, is to improve the voltage profiles of all load buses to be within the pre-specified limits with a minimum number of control actions after being subjected to any contingency and/or load change. Though this method is very fast and strongly suitable for on-line application, it does not guarantee the decreasing of system power losses in some cases.

GA-based methods with two different objective functions: minimizing the system active power losses (P_L), minimizing the sum of the squares of the voltage magnitude deviations at the load buses (V_d), are presented. The GA-based methods in all cases give better results than the first algorithm regarding the active and reactive power losses, but using more controllers, and also with longer computational times. Due to the fact that the GA-based algorithms started from a random initial point, the results of these methods depend on the selected random initial point. This fact makes these methods more suitable for off-line operation, like in the planning and operation of power system. Many runs are done in order to get the best results of the GA-based methods, because the GA-based method depends on a random initial point. It may be suitable to use the minimum number of controllers method on-line to find a fast solution to get the system back within acceptable operating limits. After that the GA -based methods can be applied off-line for more improvements in the system active and reactive losses.

A Fuzzy logic controller is added to the heuristic-sensitivity algorithm in order to decrease the computational time of this method. This method uses a smaller number of controllers compared to other optimal control methods. The results of the study cases show that this method is fast, reliable, and can improve the voltage profile of the power system by using a fewer number of controllers. Thus, this method is strongly suited for on-line application to assist the ECC operators in making a reliable and fast control decisions in order to improve the overall

system stability. The membership function values of the inputs and output are dependent on the power system itself. Membership functions should be determined for every power system.

An optimal reactive power control based on PS technique is used to decrease the sum of the squares of voltage deviations at all load buses in the system (V_d). A comparison of this algorithm with the Fuzzy logic one illustrates that this method, in all cases, uses more controllers, and takes more time than the fuzzy logic controller algorithm, but is still suitable for on-line applications. On the other hand, the stability margin resulted from PS-based method is better than that obtained from Fuzzy logic controller. The study cases indicate that the final solution of this method is strongly sensitive to the initial selected point.

A GA-based optimal reactive power control, with the objective function selected to minimize the overall power losses, is used to identify the optimal size of a shunt capacitor necessary to improve the overall voltage profile of a power system under contingency operation. The location of the shunt capacitor is defined based on the critical bus or buses in the system. Results indicate significant improvement in voltage stability margin, reduction in both active and reactive losses, in improvement of all voltage magnitudes to be within limits

9.2 Future Work

The following is a list of research activities that would be suitable for future work:

a. In this research an ANN approach is proposed to predict voltage collapse proximity. The proposed algorithm considered load increase simultaneously at all load buses, and at each single load bus separately. This work can be extended to consider load increase under contingency operation and other combinations of load increase.
b. The proposed optimal reactive power control methods did not consider generation rescheduling of the available generators. This work may be extended to consider the generation rescheduling as another control variable.
c. A Fuzzy logic controller has been proved to be effective in reducing the computational time required to get a set of controllers' adjustments. So application of Neuro- Fuzzy, Genetic Algorithm- based adaptive Fuzzy may be considered for further improvement.

d. The work that has been done in this research depended on steady state analysis. A similar approach can be implemented to consider the dynamics of the available devices, like generators, and FACTS.
e. The proposed work considers minimizing the active power losses, minimizing the sum of the square of voltage deviations at load buses, and minimizing the number of control actions. This work can be extended to consider other objective functions, like maximizing the voltage stability margin.
f. This work proposed the use of a shunt capacitor to enhance the voltage stability margin under contingency operation. This work can be extended to use micro grid (MG) technology, and or distributed generation (DG).
g. Implementation of the smart grid technology in the field of optimal reactive power and voltage control could be achieved by adding smart meters and using smart apparatus.
h. Other Artificial Intelligent techniques, like Particle swarm optimization, and the Bees Algorithm could be applied to solve the voltage and reactive power problem.

References

[1] Gregor Verbic and Ferdinand Gubina, "A new concept of voltage collapse protection based on local phasors," *IEEE Trans. on Power Delivery, Vol. 19, No. 2, pp .576-581, April 2004.*

[2] Sydulu Maheshwarapu, "New static ∝ - coefficients for reactive power planning in power systems," *TENCON '98. IEEE Region 10 International Conference on Global Connectivity in Energy, Computer, Communication and Control pp 518- 521, December 1998*

[3] Nidul Sinha, Loi Lei Lai and Palash Kumar Ghosh, "GA based algorithm for optimum allocation of reactive power under deregulated environment," *DRPT2008, Nanjing China pp. 926-932, April, 2008.*

[4] Omidi et al, "Voltage Stability Margin Improvement using Shunt Capacitors and Active and Reactive Power Management," *IEEE Electrical Power &Energy Conference, pp 1-5, 2009.*

[5] Bresesti et al, "Power system planning under uncertainty conditions. Criteria for transmission network flexibility evaluation," *IEEE Bologna power Tech. conference June 23th-26th Bologna Italy, 2003.*

[6] H.A. Gil, and E.L. da Silva, "A Reliable Approach for Solving the Transmission Network Expansion Planning Problem Using a Genetic Algorithm," *Electric Power System Research, 58, pp. 45–51, 2001*

[7] Z. Xu, Z.Y. Dong and K.P. Wong, "Transmission Planning in a Deregulated Environment," *IEE Proc.- Generation. Transmission, Distribution, 153, 3, pp. 326-334, May 2006*

[8] H. Sun and D.C. Yu, "A Multiple-objective Optimization Model of Transmission Enhancement Planning for Independent Transmission Company," *IEEE Power Engineer Society Summer Power Meeting, Seattle, WA, July, 2000*

[9] Aydogan Ozdemir and Chanan Singh, "Fuzzy logic based mw contingency ranking against masking problem," *Power Engineering Society Winter Meeting IEEE, Vol. 2, pp 504-509, 2001.*

[10] Shahidehpour et al, "Impact of security on power systems operation," *Proceedings of the IEEE, Vol. 93, No. 11, pp 2013-2025, November 2005*

[11] Z. Ruihua, D. Yumei, and L. Yuhong, "New Challenges to Power System Planning and Operation of Smart Grid Development in China," *International Conference on Power System Technology pp 1-8, October 2010.*

[12] Sidhu et al, "Protection Issues During System Restoration," *IEEE Trans. on Power Delivery Vol. 20, No. 1, pp 47-56, January 2005.*

[13] Prabha Kundur, Power system stability and control, *The EPRI Power System Engineering Series, McGraw-Hill,1994.*

[14] IEEE/CIGRE joint task force on stability terms and definitions, "Definition and classification of power system stability," *IEEE Trans. Power System, Vol. 19, No. 2, pp. 1387–1401, May 2004.*

[15] Mercede et al, "A framework to predict voltage collapse in power systems," *IEEE PEB Winter Power Meeting, New York, NY, 1988.*

[16] H. Mori, H. Tanaka, and J. Kanno, " A preconditioned fast de-coupled power flow method for contingency screening," *IEEE Trans. on Power Systems, Vol. 11, No. 1, pp. 357-36, February 1996.*

[17] G.C. Ejebe et al, " Methods for Contingency screening and ranking for Voltage Stability Analysis of Power System," *IEEE Trans. on Power Systems, Vol. 11, No. 1, pp. 350-356, February 1996.*

[18] Majid Poshtan, Parviz Rastgoufard, and Brij Singh, "Contingency ranking for voltage stability analysis of large-scale power systems," *Power System Conference and Exposition, Vol. 3, pp. 1506-1513, October 2004.*

[19] H.D. Chiang, C.S. Wang, and A.J. Flueck, "Look-ahead Voltage and Load Margin Contingency Selection Functions for Large-scale Power Systems," *IEEE Trans. Power Systems, Vol. 12, No.1, pp. 173-1 80, February 1997.*

[20] S. Greene, I. Dobson, and F.L. Alvarado, "Sensitivity of the Loading Margin to Voltage collapse with Respect to Arbitrary Parameters," *IEEE Tran. Power Systems, Vol. 12, No. 1, pp.* 262-272, *February 1997.*

[21] Wei Gu et al, "Improving large-disturbance stability through optimal bifurcation control and time domain simulations," *Electric Power Systems Research 78, pp. 337-345, 2008.*

[22] Ronnapa Paosateanpun et al, "The Line P-Q Curve for Steady-State Voltage Stability Analysis," *International Conference on Power System Technology, pp. 1-7, 2006.*

[23] R.D. Christe and S.N. Talukdar, "Expert systems for on-line security assessment a preliminary design," *IEEE Trans. on Power Systems, Vol.* 3**,** *pp. 654–659, 1988*.

[24] D.J. Sobajic and Y.H. Pao, "An artificial intelligence for power system contingency screening," *IEEE Trans. on Power Systems, Vol.* 3, *pp. 647–653, 1998.*

[25] D. Niebur and A.J. Germond, "Power system static security assessment using Kohonen neural network classifier," *IEEE Trans. on Power Systems, Vol.* ***7,*** *pp. 865–872, 1992.*

[26] D.J. Sobajic and Y.H. Pao, "Artificial neural-net based dynamic security assessment for electric power system," *IEEE Trans. on Power Systems Vol. 4, pp. 220–228, 1989.*

[27] T.S. Sidhu and L. Cui, "Contingency screening for steady analysis by using FFT and artificial neural network," *Trans. on Power Systems, Vol.* 15**,** pp. 421–426, 2000.

[28] S.J. Huang, "Static security assessment of a power system using query-based learning approaches with genetic enhancement," *IEE Proceeding of Generation, Transmission, Distribution*, Vol. 148, pp. 319–325, 2001.

[29] K.L. Lo et al, "Fast real power contingency ranking using counter propagation network," *IEEE Trans. on Power Systems, Vol.* 13, *pp. 1259–1264, 1998*.

[30] S. Chauhan, "Fast real power contingency ranking using counter propagation network: feature selection by neuro-fuzzy model," *Electric Power Systems Research, Vol. 73, No. 3, pp. 343-352, March 2005.*

[31] Nima Amjady, and Masoud Esmaili "Application of a New Sensitivity Analysis Framework for Voltage Contingency Ranking," *IEEE Trans. on Power Systems, Vol. 20, No. 2, , pp. 973-983, May 2005.*

[32] Ismail Musirin, Titik Khawa, and Abdul Rahman, "On-line voltage stability based contingency ranking using fast voltage stability index (FVSI)," *Transaction and Distribution Conference and Exhibition, Asia pacific, IEEE/ PES, pp 1118-1123, 2002.*

[33] F. Albuyeh, A. Bose, and B. Heath, "Reactive Power Considerations in Automatic Contingency Selection," *IEEE Trans. on Power Apparatus and Systems, Vol. 101, pp. 107-112, 1982.*

[34] G.C. Ejebe, H.P. Vanmeeteren, and B.F. Wollenberg, "Fast Contingency Screening and Evaluation for Voltage Security Analysis," *IEEE Trans. on Power Systems, Vol. 3, pp. 1582-1590, November 1988.*

[35] C.J. Fu and A. Bose, "Contingency ranking based on severity indices in dynamic security analysis," *IEEE Trans. on Power Systems, Vol. 14, pp. 980-985, August 1999.*

[36] Zarate et al, "Fast computation of voltage stability security margins using nonlinear programming techniques," *IEEE Trans. on Power System, Vol.21, pp. 19–27, 2006.*

[37] Z.W. Jia, J. Liu, and X.M. Xie "Study on Secondary Voltage Control Based on Multi-agent Particle Swarm Optimization Algorithm," *International Conference on Power System Technology, pp. 1-5, 2006.*

[38] N. Flatabo, R. Ognedal, and T. Carlsen, "Voltage stability condition in a power transmission system calculated by sensitivity methods," *IEEE Trans. Power System, Vol. 5, No. 4, pp. 1286–1293, November 1990.*

[39] G.K. Morison, B. Gao, and P. Kundur, "Voltage stability analysis using static and dynamic approaches," *IEEE Trans. on Power System, Vol. 8, No. 3, pp. 1159–1171, August 1993.*

[40] C.W. Taylor, Power System Stability, *The EPRI Power System Engineering Series McGraw-Hill, 1994*

[41] N. Flatabo et al, "A method for calculation of margins to voltage instability applied on the Norwegian system for maintaining required security level," *IEEE Trans. on Power System, Vol. 8, No. 3, pp. 920–928, August 1993.*

[42] T. Van Cutsem, C. Moisse, and R. Mailhot, "Determination of secure operating limits with respect to voltage collapse," *IEEE Trans. on Power System, Vol. 14, No. 1, pp. 327–335, Febuary 1999.*

[43] C. Cañizares, A.C.Z. Souza, and V. Quintana, "Comparison of performance indices for detection of proximity to voltage collapse," *IEEE Trans. on Power System, Vol. 11, No. 3, pp. 1441–1450, August 1996.*

[44] V. Ajjarapu, P. Lin, and S. Battula, "An optimal reactive power planning strategy against voltage collapse," *IEEE Trans. on Power System, Vol. 9, No. 2, pp. 906–917, May 1994.*

[45] D.J. Hill, P.A. Lof, and G. Anderson, "Analysis of longterm voltage stability," *Proceedings of the 10th Power System Computation Conference, Graz, Austria, pp. 1252-1259, August 1990.*

[46] A. Tiranuchit and R.J. Thomas, "A posturing strategy against voltage instabilities in electric power systems," *IEEE Trans. on Power Systems, Vol. 3, No. 1, pp. 87–93, 1988.*

[47] M. Begovic, and A.G. Phadke, "Control of voltage stability using sensitivity analysis," *IEEE Trans. on Power Systems, Vol*. 7, *No.1, pp. 114-123, 1992.*

[48] Venikov et al, "Estimation of electric power system steady-state stability in load flow calculations," *IEEE Trans. on Power Apparatus and Systems, Vol*. *PAS-94, No. 3pp. 1034-1041 , May/June 1975.*

[49] R.J. Thomas and A. Tiranuchit, "Voltage instabilities in electric power networks," *Proceedings of the 18th Southeastern Symposium on System Theory, Knoxville, Tennessee, pp. 359 – 363, April 1986.*

[50] P.A. Lof, G. Anderson, and D.J. Hill, "Voltage stability indices of stressed power systems," *IEEE Trans. on Power Systems, Vol*. 8, *No. 1, pp. 326-335, 1993*.

[51] B. Gao, G.K. Morison, and P. Kundur, "Voltage stability evaluation using modal analysis," *IEEE Trans. on Power Systems, Vol*. 7, *No. 4, pp.1529-1542, November 1992*.

[52] Muhammad Randhawa el al "Voltage stability assessment of a large power system," *Power and Energy Society General Meeting - Conversion and Delivery of Electrical Energy in the 21st Century, IEEE pp. 1-7, 2008.*

[53] F. Gubina, and B. Strmcnik, "Voltage collapse proximity index determination using voltage phasors approach," *IEEE Trans. on Power Systems, Vo*l. *10, No. 2, pp. 788-793, 1995.*

[54] A.M. Chebbo, M.R. Irving, and M.J.H. Stirling, "Voltage collapse proximity indicator: behaviour and implications," *Proceeding of IEE, Generation Transmission, Distribution, Vol*. *139, No. 3, pp. 241-252, May 1992.*

[55] A.R. Phadke, M. Fozdar, and K.R. Niazi, "A new technique for on-line monitoring of voltage stability margin using local signals," *Fifteenth National Power Systems Conference (NPSC), IIT Bombay, pp. 488-492, December 2008.*

[56] R.R. Zalapa and B.J. Cory, "Reactive reserve management," *Proceeding of IEE Gen. Trans. Distribution, Vol*. 142, *No. 1, pp.17-23, 1995.*

[57] Van Cutsem, "An approach to corrective control of voltage instability using simulation and sensitivity," *IEEE Trans. on power systems, Vol*. 10, *No. 2, pp. 616-622, 1995*.

[58] Muhammad Nizam, Azah Mohamed, and Aini Hussain, "Dynamic voltage collapse prediction in power systems using artificial neural network," *Proceeding of the international conference on Electrical Enginerring and Informatics, Institut Teknologi Bandung, Indonesia*, pp. 777-780, June 2007.

[59] M. La Scala, M. Trovato, and F. Torelli, "A neural network based method for voltage security monitoring," *IEEE Trans. on Power Systems, Vol. 11, No. 3, pp 1332–1341, 1996.*

[60] Jinquan Zhao et al, "A novel preventive control approach for mitigating voltage collapse," *Power Engineering Society General Meeting, IEEE, pp. 1-6, October 2006.*

[61] K. Iba et al, "Calculation of critical loading condition with nose curve using homotopy continuation method," *IEEE Trans. on Power Systems, Vol*. 6, *pp. 584-593, May 1991.*

[62] P. Kessel and H. Glavitsch, "Estimating the voltage stability of a power system," *IEEE Trans. on Power Delivery. Vol. PWRD-1 No. 3, pp. 346-354, July 1986.*

[63] V. Ajjarpu, C. Christy, "The Continuation Power Flow: A Tool for Steady State Voltage Stability Analysis," *IEEE Trans. on Power Systems, Vol.7, No. 1, pp. 416-423, February 1992.*

[64] C.A. Canizares, and F.L. Alvarado, "Point of collapse and continuation methods for large AC-DC systems," *IEEE Trans. on Power Systems, Vol.* 7, *No. 1, pp. 1-8, February 1993.*

[65] H.D. Chiang et al, "CPFLOW: A practical tool for tracing power system steady-state stationary behavior due to load and generation variations," *IEEE Trans. on Power Systems, Vol. 10, No. 2, pp. 623-634, May 1995.*

[66] Van Cutsem, "A method to compute reactive power margins with respect to voltage collapse," *IEEE Trans. on Power Systems, Vol*. 6, No. 1, pp. 145-156, February 1991.

[67] C. Rajagopalan et al, "Voltage collapse operating margin analysis using sensitivity techniques," *Proceedings Athens Power Tech 1993, Athens, Greece, pp. 332-336, September, 1993.*

[68] Antonio et al, "Increasing the lodability of power systems through optimal local control actions," *IEEE Trans. on Power Systems, Vol*.19, *No.1, February 2004.*

[69] Hsiao-Dong Chiang, and Rene Jean Jumeau, "Toward a practical performance index for predicting voltage collapse in electric power systems," *IEEE Trans. on Power Systems, Vol. 10, No. 2, pp. 584-592, May 1995.*

[70] Claudio A. Canizares, Antonio C.Z. de Souza, and Victor H. Quintana, "Comparison of performance indices for detection of proximity to voltage collapse," *IEEE Trans. on Power Systems, Vol. 11, No. 3, pp. 1441-1450, August 1996.*

[71] IEEE Committee Report, "Voltage stability of power systems: Concepts, analytical tools and industry experiences," *IEEE PES publication 90th 0358-2 PWR*

[72] North American Electric Reliability Council, "Survey of the voltage collapse phenomenon," *August 1991.*

[73] N. B. Bhatt, "August 14, 2003 US-Canada blackout," *presented at the IEEE/PES General Meeting, Denver, CO, 2004.*

[74] C.D. Vournas et al, "Analysis of a Voltage Instability Incident in the Greek Power System", *IEEE/PES Winter Meeting, Singapore, January 2000*

[75] Andersson et al, "Causes of the 2003 Major Grid Blackouts in North America and Europe, and Recommended Means to Improve System Dynamic Performance, " *IEEE Trans. on Power Systems, Vol. 20, No. 4, November 2005.*

[76] IEEE Power System Relaying Committee Report, Voltage collapse mitigation, December, 1996

[77] http://en.wikipedia.org/wiki/List_of_power_outages#cite_note-69

[78] IEEE Power System Relaying Committee Report, Summary of System Protection and Voltage stability, *Trans. on Power Delivery, Vol.* 10, *No. 2, April 1995.*

[79] Costas Vournas, "Technical Summary on the Athens and Southern Greece Blackout of July, 2004".

[80] Mansour et al, "SVC placement using critical modes of voltage instability," *IEEE Trans. on Power Systems, Vol. 9, No. 2, pp. 757-763, May 1994.*

[81] I. Dobson, et al., "Electric power transfer capability: Concepts, applications, sensitivity and uncertainty," *Power Systems Engineering Research Center PSerc, Vol.* 1, *No. 34, November 2001.*

[82] North American Electric Reliability Council, "Available transfer capability definitions and determination," *June 1996.*

[83] Parker et al, "Application of an optimization method for determining the reactive margin from voltage collapse in reactive power planning," *IEEE Trans. on Power Systems, Vol. 11, No. 3, pp. 1473-1481, August 1996,.*

[84] Claudio A. Canizares, and Zeno T. Faur, "Analysis of SVC and TCSC controllers in voltage collapse," *IEEE Trans. on power systems, Vol. 14, No. 1, pp. 158-165, February 1999.*

[85] C.D. Vournas, et al., "On-Line Voltage Security Assessment of the Hellenic Interconnected System," *IEEE Bologna Power Tech Conference, Bologna, Italy, June 23-26, 2003.*

[86] Miroslav M. Begovic, and Arun G. Phadke, "Dynamic simulation of voltage collapse," *IEEE Trans. on Power Systems, Vol*. 5, No. 4, *pp. 1529-1534, November 1990.*

[87] Leonard L. Grigsby, Power System Stability and Control, *CRS press, 2006.*

[88] T.K.P. Medicherla, R. Billinton, and M.S. Sachadev, "Generation rescheduling and load shedding to alleviate line over loads-analysis," *IEEE Trans. on Power Apparatus and Systems, Vol. 98, No. 12, pp .1876-1884, November, 1979.*

[89] T.K.P. Medicherla, R. Billinton, and M.S. Sachadev, "Generation rescheduling and load shedding to alleviate line overloads–system studies," *IEEE Trans. on Power Apparatus and Systems Vol. 100, No. 1, pp. 36-42, 1981.*

[90] G. Irisarri and A.M. Sasson, "An automatic contingency selection method for on-line security analysis," *IEEE Trans. on Power Apparatus and Systems, Vol. PAS-100, pp. 1838–1844, 1981.*

[91] A. Monticelli, M.V.F. Pereira, and S. Granville, "Security constrained optimal power flow with post contingency corrective rescheduling," *IEEE Trans. on Power Systems, Vol*. *PWRS-2, No.1, pp. 175-182, February 1987.*

[92] A. Mohamed, and G.B. Jasmon, "Realistic power system security algorithm," *Proceedings of IEE Generation, Transmission, Distribution, Vol. 135, No. 2, pp. 98-106, 1988.*

[93] Yong Zheng and N. Chowdhury, "Expansion of transmission systems in a deregulated environment," *IEEE Canadian Conference on Electrical and Computer Engineering, Vol. 4, pp. 1943- 1947, May, 2004.*

[94] A.A. Sallam and A.M. Khafaga, " Fuzzy expert system using load shedding for voltage instability control ," *Proceedings of the 2002 Large Engineering Systems Conference on Power Engineering, pp. 125-132, 2002.*

[95] G. Schnyder and H. Glavitsch, "Security enhancement using an optimal switching power flow," *IEEE Trans. on Power Systems, Vol*. 5, *No. 2, pp. 674-681 May,1990.*

[96] J. Yoshizawa et al, "An automatic knowledge acquisition method for switching sequences and its evaluation," *IEEE Trans. on Power Systems, Vol*. 9, No. 2, pp. 884-890, 1994.

[97] M.L. Baughman, and S.N. Siddiqi, "Real-time pricing of reactive power theory and case study results," *IEEE Trans. on power systems, Vol. PWRS-6, No. 1, pp. 23-29, February, 1991*.

[98] Milan Bjelorglic, Milan S. Calovic, and Borivoje S. Babic, "Application of Newton's optimal power flow in voltage/reactive power control," *IEEE Trans. on Power Systems, Vol. 5, No. 4, pp. 1447-1454, 1990.*

[99] K.R.C. Mamandur, "Emergency adjustments to VAR control variables to alleviate over-voltages, under-voltages and generator VAR limit violations," *IEEE Trans. on Power Apparatus and Systems, Vol. PAS-101, No. 5, pp. 1040-1047, May 1982.*

[100] D.S. Kirschen, H.P. Van Meeteren, "MW/voltage control in linear programming based optimal power flow," *IEEE Trans. on Power Systems, Vol. 3, No. 2, pp. 481- 489, May 1988.*

[101] O. Alsac et al, "Further developments in LP-based optimal power flow," *IEEE Trans. on Power Systems, Vol.* 5, *No. 3, pp. 697-711, August 1990.*

[102] Eric Hobson, "Network constrained reactive power control using linear programming," *IEEE Trans. on Power Apparatus and Systems, Vol. 99, No. 3, pp. 868-877,1980.*

[103] K.R.C. Mamandur and R.D. Chenoweth, "Optimal control of reactive power flow for improvements in voltage profiles and for real power loss minimization," *IEEE Transactions on Power Apparatus and Systems, vol. PAS-100, No. 7, pp. 3185-3194, July 1981.*

[104] S.A. Soman, K.Parthasarathy, and D. Thuharam, "Curtailed number and reduced controller movement optimization algorithms for real time voltage/reactive power control," *IEEE Trans. on Power Systems, Vol.9, No.4, pp. 2035-2040, November 1994.*

[105] Ching-Tzong Su and Chien-Tung Lin, "A new fuzzy control approach to voltage profile enhancement for power systems," *IEEE Trans. on Power Systems, Vol. 11, No. 3, pp. 1654-1659, August 1996.*

[106] Akbar Rahideh, M. Gitizadeh, and Abbas Rahideh, "Fuzzy logic in real time voltage/reactive power control in FARS regional electric network," *Electric Power Systems Research vol.76, no.11, pp 996–1002, July 2006.*

[107] Ching-Tzong Su and Chien-Tung Lin, "Fuzzy-based voltage/reactive power scheduling for voltage security improvement and loss reduction," *8th International Conference on Harmonics and Quality of Power ICHQP '98, jointly organized by IEEE/PES and NTUA, Athens, Greece, pp 48-53, October 14-16, I998.*

[108] J. Qiu and S.M. Shahidehpour, "A new approach for minimizing power losses and improving voltage profile," *IEEE Trans. On Power Systems, Vol.* 2, No. 2, pp. 287-295, *May 1987.*

[109] T.V. Menezes et al, "MVAR management on the pre-dispatch problem for improving voltage stability margin," *IEE of Proceeding Geneneration, Transmission, Distribution, Vol*. 151*, No. 6, pp. 665-672, November 2004.*

[110] Yong-jun Zhang and Zhen Ren, "Optimal reactive power dispatch considering costs of adjusting the control devices," *IEEE Trans. on Power Systems, Vol*. 20, No. 3*, pp. 1349-1356, August 2005.*

[111] William et al, "A rule based approach to decentralized voltage control," *IEEE Trans. on Power Systems, Vol. 5, No. 2, pp 643-651, May 1990.*

[112] Kevin Tonsovic, "A fuzzy linear programming approach to the reactive power/voltage control problem," *IEEE Trans. on power systems, Vol.7, No.1, pp.287-293, February 1992.*

[113] G.R.M. Da Costa, "Modified Newton method for reactive dispatching," Int. *Journal of Electrical Power and Energy Systems, Vol. 24, pp. 815-819, 2002.*

[114] Alessandro et al., "A Knowledge-based system for supervision and control of regional voltage profile and security," *IEEE Trans. on Power Systems, Vol.20, No.4, pp 400-407, February.2005.*

[115] A. Ghafouri, M.R. Zolghadri, and M. Ehsan, "Power system stability improvement using self-tuning fuzzy logic controlled STATCOM," *Eurocon 2007, International Conference on "Computer as a tool" Warsaw, September, 2007.*

[116] L.Robert, B. Grzegors, and W. Magdalena, "Application of voltage control area to determine reactive power requirements," *Modern Electric Power Systems 2010, Wrolaw, Poland 2010.*

[117] The Mathworks Inc., 2004–2010 Global Optimization Toolbox™ 3 User's Guide for using in MALAB

[118] Qiuxia Yu et al, "Adaptability evaluation of transmission network planning under deregulation," *Universities Power Engineering Conference, 2007. UPEC 2007. 42nd International pp. 53-56, 4-6 September 2007*

[119] http://www.intelligrid.info/IntelliGrid_Architecture/Use_Cases/TO_Contingency_ Analysis_ Baseline.htm

[120] Joe Chow, Graham Rogers Power System Toolbox Version 3.0 User's Guide

[121] J.B. Ward and H.W. Hale, "Digital Computer Solution of Power-Flow Problems," *Trans of the AIEE, Vol. 75, III, pp. 398-404, 1956.*

[122] http://www.ee.washington.edu/research/pstca/

[123] The Mathworks Inc., 2007 Neural Network Toolbox™ 6 User's Guide for using in MALAB.

[124] M. Tarafdar Haque and A.M. Kashtiban, "Application of neural networks in power systems; A review," *World Academy of Science, Engineering and Technology 6 2005, pp 53-57, 2005.*

[125] H.W. Dommel, and W.F. Tinney, "Optimal power flow solutions," *IEEE Trans. on Power Apparatus and Systems, Vol. 87, pp. 1866-1876, 1968,.*

[126] K.Y. Lee, Y.M. Park, and J.L. Ortiz, "A united approach to real and reactive power dispatch," *IEEE Transaction on Apparatus and Systems, Vol. 104, pp.1147-1153, 1985.*

[127] J.A. Momoh, M.E. El-Hawary and R. Adapa, "A review of selected optimal power flow literature to 1993 Part I: Nonlinear and quadratic programming approachesI," *IEEE Transaction on Power Systems, Vol. 14, No. 1, pp. 96-111, February 1999.*

[128] H.H. Happ, "Optimal Power Dispatch," *IEEE Transaction on Power Apparatus and Systems, Vol. 93, pp. 820-830, 1974.*

[129] Mohamed E. El-hawary, Electric Power Applications of Fuzzy Systems, IEEE press

[130] http://www.seattlerobotics.org/encoder/mar98/fuz/fl_part1.html

[131] http://www.seattlerobotics.org/encoder/mar98/fuz/fl_part2.html

[132] The MathWorks, Inc., 1995–2010 Fuzzy Logic Toolbox™ 2 User's Guide for using in MALAB.

[133] http://www.seattlerobotics.org/encoder/mar98/fuz/fl_part4.html

Appendix A 6 Generator System

The following tables present the data used in the analysis of 6 generator system.

Table A.1: Bus data

Bus number	Voltage magnitude (pu)	Voltage angle	Pg (pu)	Qg (pu)	Pl (pu)	Ql (pu)	Shunt Conductance (pu)	Shunt susceptance (pu)	Bus type	Max voltage Limit (pu)	Min voltage Limit (pu)
1	1.035	0.0	1.4	0.0	0.0	0.0	0.0	0.0	1	1.1	1.0
2	1.020	0.0	1.3	0.0	0.65	0.25	0.0	0.0	2	1.1	1.0
3	1.032	0.0	1.1	0.0	0.14	0.04	0.0	0.0	2	1.1	1.0
4	1.017	0.0	1.0	0.0	0.08	0.02	0.0	0.0	2	1.1	1.0
5	1.015	0.0	0.5	0.0	0.92	0.33	0.0	0.0	2	1.1	1.0
6	1.030	0.0	0.9	0.0	0.20	0.04	0.0	0.0	2	1.1	1.0
7	1.000	0.0	0.0	0.0	0.17	0.09	0.0	0.0	3	1.05	0.95
8	1.000	0.0	0.0	0.0	0.37	0.21	0.0	0.0	3	1.05	0.95
9	1.000	0.0	0.0	0.0	0.52	0.13	0.0	0.0	3	1.05	0.95
10	1.000	0.0	0.0	0.0	0.09	0.01	0.0	0.0	3	1.05	0.95
11	1.000	0.0	0.0	0.0	0.30	0.14	0.0	0.0	3	1.05	0.95
12	1.000	0.0	0.0	0.0	0.32	007	0.0	0.0	3	1.05	0.95
13	1.000	0.0	0.0	0.0	0.08	0.05	0.0	0.0	3	1.05	0.95
14	1.000	0.0	0.0	0.0	0.44	0.25	0.0	0.0	3	1.05	0.95
15	1.000	0.0	0.0	0.0	0.07	0.03	0.0	0.0	3	1.05	0.95
16	1.000	0.0	0.0	0.0	0.12	0.05	0.0	0.0	3	1.05	0.95
17	1.000	0.0	0.0	0.0	0.00	0.00	0.0	0.0	3	1.05	0.95
18	1.000	0.0	0.0	0.0	0.04	0.02	0.0	0.0	3	1.05	0.95
19	1.000	0.0	0.0	0.0	0.33	0.11	0.0	0.0	3	1.05	0.95
20	1.000	0.0	0.0	0.0	0.19	0.10	0.0	0.0	3	1.05	0.95
21	1.000	0.0	0.0	0.0	0.03	0.01	0.0	0.0	3	1.05	0.95

Table A.2: Line data

From Bus #	To Bus #	Resistance (pu)	Reactance (pu)	Total Line Charging (pu)
1	7	0.01938	0.5917	0.05640
1	8	0.01403	0.12304	0.04460
2	9	0.04699	0.09797	0.03190
8	9	0.25811	1.17632	0.03870
9	10	0.05695	0.37388	0.04700
3	10	0.06701	0.17103	0.04730
10	11	0.01335	0.24211	0.01640
9	12	0.03181	0.08450	0.00216
9	11	0.09498	0.29890	0.00428
11	12	0.05291	0.25581	0.02111
8	13	0.01615	0.13027	0.00070
8	14	0.02711	0.27038	0.03137
12	13	0.08205	0.09207	0.09913
11	21	0.22092	0.19988	0.00037
13	21	0.00393	0.24802	0.02515
20	21	0.00110	0.40970	0.00112
4	20	0.05950	0.09960	0.00346
4	19	0.31770	0.99500	0.00188
19	20	0.02960	0.16410	0.00302
5	19	0.00370	0.03740	0.04080
18	19	0.00380	0.11950	0.00000
5	18	0.03060	0.27540	0.01300
17	18	0.40680	1.21670	0.00030
7	14	0.02550	0.06250	0.02800
6	7	0.01430	0.03520	0.00161
6	14	0.00640	0.01570	0.01027
14	16	0.60530	1.50640	0.20009
15	16	0.00090	0.00220	0.00004
15	17	0.00030	0.00140	0.00003
16	17	0.00660	0.01640	0.00028

Table A.3: Generators VAR limits

Generator Bus Number	Lower limit (pu)	Upper limit (pu)
1	-10.0	10.0
2	-0.5	1.0
3	-0.5	1.0
4	-0.5	1.0
5	-0.5	1.0
6	-0.5	1.0

Appendix B Ward and Hale Power System

The following figure represents the single line diagram for Ward and Hale system. In addition, there are five tables present the data used in the analysis of Ward and Hale system.

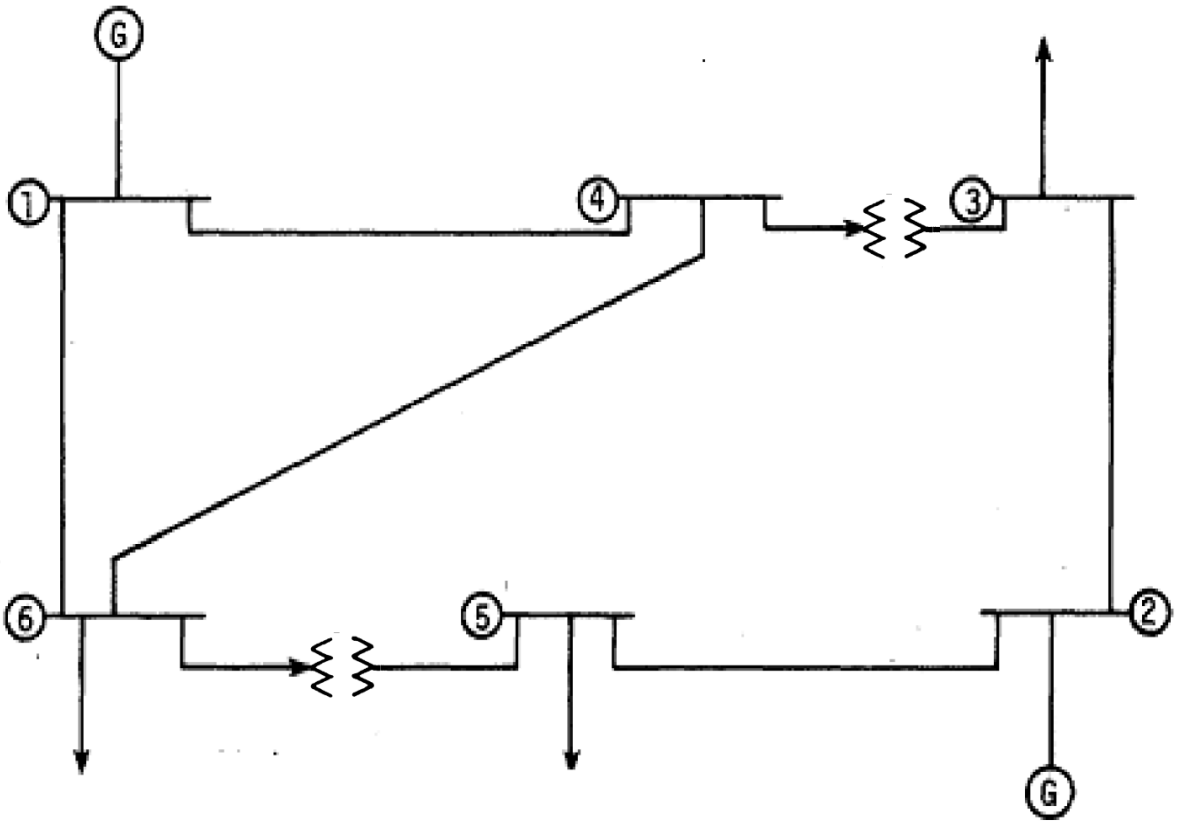

Figure B.1: Single line Diagram for Ward and Hale system

Table B.1: Bus data

Bus number	Voltage magnitude (pu)	Voltage angle	Pg (pu)	Qg (pu)	Pl (pu)	Ql (pu)	Shunt Conductance (pu) (pu)	Shunt Suseptance (pu)	Bus type	Max voltage Limit (pu)	Min voltage Limit (pu)
1	1.050	0.0	0.0	0.0	0.00	0.00	0.0	0.0	1	1.1	1.0
2	1.000	0.0	0.5	0.0	0.00	0.00	0.0	0.0	2	1.1	1.0
3	1.000	0.0	0.0	0.0	0.55	0.13	0.0	0.0	3	1.05	0.95
4	1.000	0.0	0.0	0.0	0.00	0.00	0.0	0.01	3	1.05	0.95
5	1.000	0.0	0.0	0.0	0.30	0.18	0.0	0.0	3	1.05	0.95
6	1.000	0.0	0.0	0.0	0.50	0.05	0.0	0.01	3	1.05	0.95

Table B.2: Line data

From Bus #	To Bus #	Resistance (pu)	Reactance (pu)	Total Line Charging (pu)
1	6	0.123	0.512	0.05640
1	4	0.080	0.370	0.04460
4	6	0.097	0.407	0.03190
6	5	0.000	0.300	0.03870
5	2	0.282	0.640	0.04700
2	3	0.723	1.050	0.04730
4	3	0.000	0.133	0.01640

Table B.3: Generators VAR limits

Generator Bus Number	Lower limit (pu)	Upper limit (pu)
1	-0.2	1.0
2	-0.2	1.0

Table B.4: Transformer tap setting

From Bus Number	To Bus Number	Initial Tap setting	Lower limit	Upper limit
6	5	1.02	0.9	1.1
4	7	1.10	0.9	1.1

Table B.5: Capacitors range

Generator Bus Number	Initial value (pu)	Lower limit (pu)	Upper limit (pu)
4	0.01	0.0	0.05
6	0.01	0.0	0.06

Appendix C Modified IEEE 14 Bus System

The following figure represents the single line diagram for the modified IEEE 14 bus system. In addition, there are five tables present the data used in the analysis for the same system.

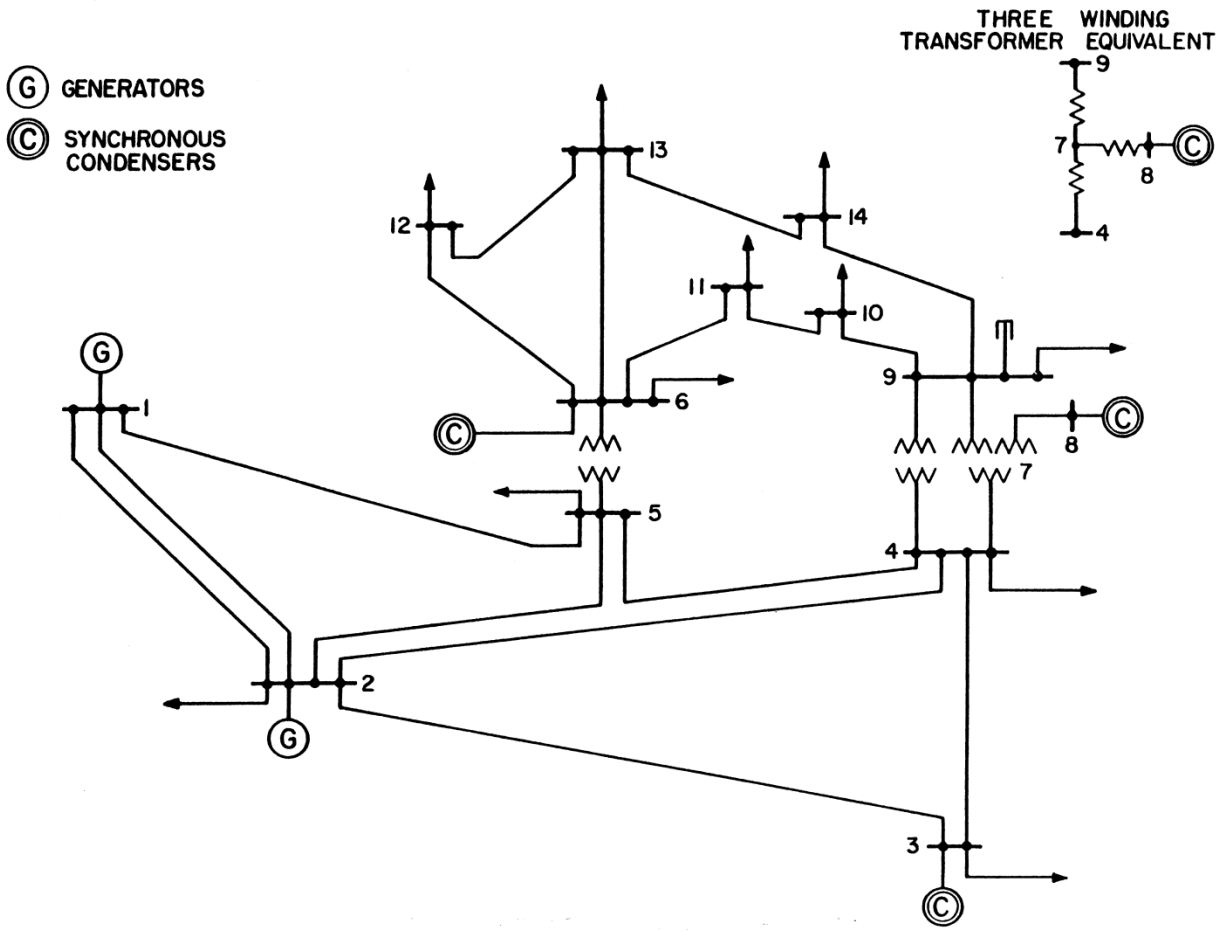

Figure C.1: Single line diagram for IEEE 14 bus system

Table C.1: Bus data

Bus number	Voltage magnitude (pu)	Voltage angle	Pg (pu)	Qg (pu)	Pl (pu)	Ql (pu)	Shunt Conductance (pu) (pu)	Shunt Susebtance (pu) (pu)	Bus type	Max voltage Limit (pu)	Min voltage Limit (pu)
1	1.060	0.00	0.0	0.0	0.00	0.00	0.0	0.0	1	1.1	1.0
2	1.045	-4.98	0.4	0.0	0.217	0.127	0.0	0.0	2	1.1	1.0
3	1.010	-12.72	0.0	0.0	0.942	0.190	0.0	0.0	2	1.1	1.0
4	1.019	-10.33	0.0	0.0	0.478	-0.039	0.0	0.0	3	1.05	0.95
5	1.020	-8.78	0.0	0.0	0.076	0.016	0.0	0.0	3	1.05	0.95
6	1.050	-14.22	0.	0.0	0.112	0.075	0.0	0.0	2	1.1	1.0
7	1.062	-13.37	0.0	0.0	0.000	0.000	0.0	0.0	3	1.05	0.95
8	1.060	-13.36	0.0	0.0	0.000	0.000	0.0	0.0	2	1.1	1.0
9	1.056	-14.94	0.0	0.0	0.295	0.166	0.0	0.05	3	1.05	0.95
10	1.051	-15.10	0.0	0.0	0.090	0.058	0.0	0.0	3	1.05	0.95
11	1.057	-14.79	0.0	0.0	0.035	0.018	0.0	0.0	3	1.05	0.95
12	1.055	-15.07	0.0	0.0	0.061	0.016	0.0	0.0	3	1.05	0.95
13	1.050	-15.16	0.0	0.0	0.135	0.058	0.0	0.0	3	1.05	0.95
14	1.036	-16.04	0.0	0.0	0.149	0.050	0.0	0.0	3	1.05	0.95

Table C.2: Generators VAR limits

Generator Bus Number	Lower limit (pu)	Upper limit (pu)
1	-10.0	10.0
2	-0.40	0.50
3	0.00	0.40
6	-0.06	0.24
8	-0.06	0.24

Table C.3: Capacitor range

Capacitor Bus Number	Initial value (pu)	Lower limit (pu)	Upper limit (pu)
9	0.05	0.0	0.25

Table C.4: Line data

From Bus #	To Bus #	Resistance (pu)	Reactance (pu)	Total Line Charging (pu)
1	2	0.01938	0.05917	0.0528
1	5	0.05403	0.22304	0.0492
7	8	0.0	0.17615	0.0
6	5	0.0	0.25202	0.0
6	11	0.09498	0.19890	0.0
6	12	0.12291	0.25581	0.0
6	13	0.06615	0.13027	0.0
2	3	0.04699	0.19797	0.0438
3	4	0.06701	0.17103	0.0128
2	4	0.05811	0.17632	0.0340
2	5	0.05695	0.17388	0.0346
4	5	0.01335	0.04211	0.0
4	7	0.0	0.20912	0.0
4	9	0.0	0.55618	0.0
7	9	0.0	0.11001	0.0
9	10	0.03181	0.08450	0.0
9	14	0.12711	0.27038	0.0
10	11	0.08205	0.19207	0.0
12	13	0.22092	0.19988	0.0
13	14	0.17093	0.34802	0.0

Table C.5: Transformer tap setting

From Bus Number	To Bus Number	Initial Tap setting	Lower limit	Upper limit
6	5	0.95	0.9	1.1
4	7	0.98	0.9	1.1
4	9	0.97	0.9	1.1

Appendix D Modified IEEE 30 Bus System

The following figure represents the single line diagram for the modified IEEE 30 bus system. In addition, there are five tables present the data used in the analysis for the same system.

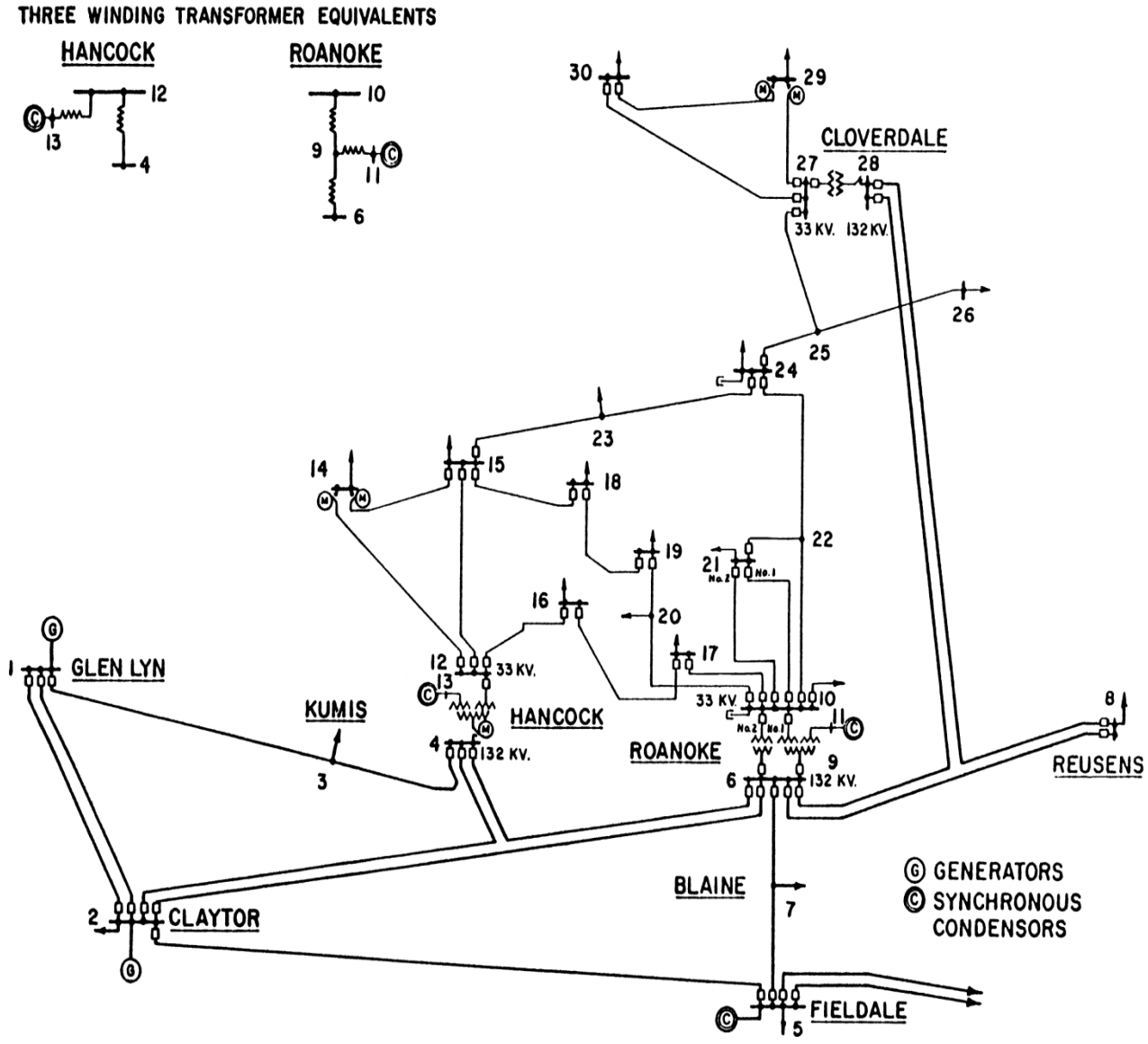

Figure D.1: Single line diagram for IEEE 30 bus system

Table D.1: Bus data

Bus number	Voltage magnitude (pu)	Voltage angle	Pg (pu)	Qg (pu)	Pl (pu)	Ql (pu)	Shunt Conductance (pu) (pu)	Shunt susceptance (pu)	Bus type	Max voltage Limit (pu)	Min voltage Limit (pu)
1	1.06	0.0	0.0	0.0	0.0	0.0	0.0	0.0	1	1.1	1.0
2	1.00	0.0	1.108	0.0	0.024	0.012	0.0	0.0	2	1.1	1.0
3	1.00	0.0	0.0	0.0	0.024	0.012	0.0	0.0	3	1.05	0.95
4	1.00	0.0	0.0	0.0	0.076	0.038	0.0	0.0	3	1.05	0.95
5	1.00	0.0	1.300	0.0	0.942	0.190	0.0	0.0	2	1.1	1.0
6	1.00	0.0	0.0	0.0	0.0	0.0	0.0	0.0	3	1.05	0.95
7	1.00	0.0	0.0	0.0	0.228	0.109	0.0	0.0	3	1.05	0.95
8	1.00	0.0	0.175	0.0	0.30	0.30	0.0	0.0	2	1.1	1.0
9	1.00	0.0	0.0	0.0	0.0	0.0	0.0	0.0	3	1.05	0.95
10	1.00	0.0	0.0	0.0	0.058	0.035	0.0	0.10	3	1.05	0.95
11	1.00	0.0	0.525	0.0	0.0	0.0	0.0	0.0	2	1.1	1.0
12	1.00	0.0	0.0	0.0	0.112	0.075	0.0	0.07	3	1.05	0.95
13	1.00	0.0	0.525	0.0	0.0	0.0	0.0	0.0	2	1.1	1.0
14	1.00	0.0	0.0	0.0	0.062	0.016	0.0	0.0	3	1.05	0.95
15	1.00	0.0	0.0	0.0	0.082	0.050	0.0	0.05	3	1.05	0.95
16	1.00	0.0	0.0	0.0	0.035	0.018	0.0	0.0	3	1.05	0.95
17	1.00	0.0	0.0	0.0	0.090	0.058	0.0	0.05	3	1.05	0.95
18	1.00	0.0	0.0	0.0	0.032	0.009	0.0	0.0	3	1.05	0.95
19	1.00	0.0	0.0	0.0	0.095	0.034	0.0	0.0	3	1.05	0.95
20	1.00	0.0	0.0	0.0	0.022	0.011	0.0	0.03	3	1.05	0.95
21	1.00	0.0	0.0	0.0	0.175	0.112	0.0	0.10	3	1.05	0.95
22	1.00	0.0	0.0	0.0	0.0	0.0	0.0	0.0	3	1.05	0.95
23	1.00	0.0	0.0	0.0	0.032	0.016	0.0	0.0	3	1.05	0.95
24	1.00	0.0	0.0	0.0	0.087	0.067	0.0	0.05	3	1.05	0.95
25	1.00	0.0	0.0	0.0	0.0	0.0	0.0	0.0	3	1.05	0.95
26	1.00	0.0	0.0	0.0	0.035	0.023	0.0	0.02	3	1.05	0.95

27	1.00	0.0	0.0	0.0	0.0	0.0	0.0	0.0	3	1.05	0.95
28	1.00	0.0	0.0	0.0	0.0	0.0	0.0	0.0	3	1.05	0.95
29	1.00	0.0	0.0	0.0	0.024	0.012	0.0	0.0	3	1.05	0.95
30	1.00	0.0	0.0	0.0	0.106	0.053	0.0	0.05	3	1.05	0.95

Table D.2: Generators VAR limits

Generator Bus Number	Lower limit (pu)	Upper limit (pu)
1	-0.3	1.0
2	-0.3	1.0
5	-0.25	0.8
8	-0.25	0.8
11	-0.2	0.8
13	-0.2	0.8

Table D.3: Transformer tap setting

From Bus Number	To Bus Number	Initial Tap setting	Lower limit	Upper limit
12	4	1.0	0.9	1.1
9	6	1.0	0.9	1.1
10	6	1.0	0.9	1.1
27	28	1.0	0.9	1.1

Table D.4: Capacitor range

Capacitor Bus Number	Initial value (pu)	Lower limit (pu)	Upper limit (pu)
10	0.10	0.0	0.25
12	0.07	0.0	0.25
15	0.05	0.0	0.25
17	0.05	0.0	0.25
20	0.03	0.0	0.25
21	0.10	0.0	0.25
24	0.05	0.0	0.25
26	0.02	0.0	0.25
30	0.05	0.0	0.25

Table D.5: Line data

From Bus #	To Bus #	Resistance (pu)	Reactance (pu)	Total Line Charging (pu)
1	2	0.0192	0.0575	0.0
1	3	0.0452	0.1852	0.0
2	4	0.0570	0.1737	0.0
2	5	0.0472	0.1983	0.0
2	6	0.0581	0.1763	0.0
3	4	0.0132	0.0379	0.0
4	6	0.0119	0.0414	0.0
12	4	0.0128	0.2560	0.0
5	7	0.0460	0.1160	0.0
6	7	0.0267	0.0820	0.0
6	8	0.0120	0.0420	0.0
9	6	0.0104	0.2080	0.0
10	6	0.0278	0.5560	0.0
6	28	0.0169	0.0599	0.0
8	28	0.0636	0.2000	0.0

9	10	0.0055	0.1100	0.0
9	11	0.0104	0.2080	0.0
10	17	0.0324	0.0845	0.0
10	20	0.0936	0.2090	0.0
10	21	0.0348	0.0749	0.0
10	22	0.0727	0.1499	0.0
12	13	0.0070	0.1400	0.0
12	14	0.1231	0.2559	0.0
12	15	0.0662	0.1304	0.0
12	16	0.0945	0.1987	0.0
14	15	0.2210	0.1997	0.0
15	18	0.1070	0.2185	0.0
15	23	0.1000	0.2020	0.0
16	17	0.0824	0.1932	0.0
18	19	0.0639	0.1292	0.0
19	20	0.0340	0.0680	0.0
21	22	0.0116	0.0236	0.0
22	24	0.1150	0.1790	0.0
23	24	0.1320	0.2700	0.0
24	25	0.1885	0.3292	0.0
25	26	0.2544	0.3800	0.0
25	27	0.1093	0.2087	0.0
27	28	0.0198	0.3960	0.0
27	29	0.2198	0.4153	0.0
27	30	0.3202	0.6027	0.0
29	30	0.2399	0.4533	0.0